Monascus ruber ICMP 15220 fermentation for the production of pigments

A thesis presented in partial fulfilment of the requirements for the degree of
Doctor of Philosophy in Bioprocess Engineering
at Massey University, New Zealand

FARHAN BINTI MOHD SAID

2010

Abstract

Edible pigments of *Monascus* species have an established history of use in certain Asiatic foods. This work focused on development and optimization of production of the red pigments of *Monascus ruber* ICMP 15220. This particular *Monascus* strain had not been previously investigated.

Suitable media compositions for growth and pigment production were first evaluated on agar plates. Media that contained glucose and monosodium glutamate (MSG) as carbon and nitrogen sources, respectively, were found to be most suitable for red colour production and became the basis for further studies. Both submerged culture and solid-state fermentations were assessed for pigment production.

In submerged culture, a fully defined medium with 10 g L^{-1} glucose and a carbon to nitrogen mass ratio of 9 : 1 at 30^{o}C proved to be the most productive for the target red pigments. This medium used MSG as the nitrogen source. Attempts were made to replace MSG with less expensive inorganic nitrogen sources, but no suitable replacement was found. Biomass and pigment productivity were evaluated on a variety of carbon sources, but ethanol was confirmed to be best.

Solid-state fermentation on steamed rice proved to be remarkably more productive for the target pigment than the submerged fermentation. Solid-state fermentation did not require supplemental nitrogen to attain a high productivity. The C : N ratio for attaining the peak pigment productivity in solid-state culture proved to be entirely different from the value that had been found to be optimal in submerged culture. In view of its superior characteristics, the solid-state fermentation was optimized in packed-bed bioreactors. A central composite experimental design was used for the optimization that focused on the initial moisture content of the substrate and aeration rate in the bed as the main operation parameters. In 18 cm deep packed beds of steamed rice, the optimal fermentation conditions were at 30^{o}C, an initial moisture content of 70%, and aeration with humidified air (97 – 99% relative humidity) at a flow rate of 0.14 L/min.

In all cases, the production of pigments was growth associated. Under optimal conditions in the packed-bed bioreactor, the red pigment productivity was nearly 3.4×10^{4}-fold greater than in the best case submerged culture. The stability of the pigments produced under the various conditions was characterized with respect to ambient light, pH, and heat.

Acknowledgements

Alhamdulillah, millions of thanks to the God the Almighty because only with His pure blessing and mercy, this project managed to be accomplished successfully. It was impossible to complete this thesis without the help and support of the good and kind people around me. It is a great pleasure to express my appreciation to all of them in this acknowledgement, in which they are worth a special mention.

First and foremost, I would like to thank my beloved husband, Sulaiman, for his incessant support, sacrifice, and utmost patience throughout the years. He dedicated his time, lent me his hands and legs, and relieved my sadness and sorrow. Many thanks also to my family in Malaysia, mama, baba, mak, abah, sisters, and brother who gave their continuous support, encouragement, and prayers from far-away.

I most gratefully acknowledge my principal supervisor, Professor Yusuf Chisti for his supervision, advice and guidance from the very early stage of the research until the thesis writing phase. Without him this thesis would not have been possible. His input and ideas contributed to the success of the research. I hope to continue our collaboration in my future career as an academic.

I would like to record my gratitude to Professor John Brooks, my co-supervisor, for his advice and comments, which were also very helpful in completing this study.

I would also like to acknowledge the Ministry of Higher Education, Malaysia, for the financial support. Without their sponsorship, it would have been impossible for me to be in New Zealand, to pursue my PhD studies. Not to be forgotten is the help and support from my employer, University Malaysia Pahang, Malaysia, especially the academic staff of the Faculty of Chemical Engineering and Natural Resources.

I am grateful to Massey University, especially the School of Engineering and Advanced Technology (SEAT), for providing me a platform to further enhance my knowledge and technical experience. I spent nearly four years at SEAT. There were ups

and downs, but the School's staff were always helpful in accommodating and meeting their students' needs. For this I thank them so much.

I am also very grateful to all the technical staff of Massey University Microlaboratory; Ann-Marie Jackson, John Edwards, John Sykes, Weiping Liu, Judy Collins, and others for the technical support. They all tried very hard to accommodate my research needs in the laboratory throughout this work.

Furthermore, I would like to thank all Malaysian friends in Palmerston North, New Zealand, for the sincere and close friendship. Throughout the years, we all lived and worked together, provided help and expertise to each other, despite our different specializations and disciplines. The friendship among us made life in New Zealand a lot easier and like being in our home country.

My special thanks also go to other friends, Pattamawadee Tananchai, Tiyaporn Luangpipat, Sadia Tahir, and others for the help, support, and knowledge sharing. Different cultures never became a barrier for us to get close with each other and work together from the day we met.

Finally, I would like to give my sincere appreciation to everybody who was involved directly or indirectly in the realization of this thesis, on which I could not mention personally one by one.

Table of Contents

List of Figures

List of Tables

Abbreviations

sp.	Species
Kr	Radial growth rate
M.	*Monascus*
L*	Lightness
a*	+a* = red; -a* = green
b*	+b* = yellow; -b* = blue
h^O	Hue angle
C*	Chroma
C : N	Carbon to nitrogen ratio
Rpm	Rotation per minute
DNA	Deoxyribonucleic acid
RNA	Ribonucleic acid
NMR	Nuclear magnetic resonance
IMC	Initial moisture content
TLC	Thin layer chromatography
UV	Ultraviolet
R_f	Retention factor
Aw	Water activity
SSC	Solid-state cultivation
$Y_{P/X}$	Yield of product on biomass
$Y_{X/S}$	Yield of biomass on substrate
Cf	Conversion factor
Df	Dilution factor
μ_{max}	Maximum specific growth rate
T	Time
AU	Absorbance unit
X_{max}	Maximum biomass concnetration
r_{BM}	Rate of biomass production
r_P	Specific rate of product formation
Cdw	Cell dry weight

Pr	Productivity
w/w	Weight per weight
vol/vol	Volume per volume
SS	Sum of squares
DF	Degrees of freedom
MS	Mean square
CV	Coefficient of variation
R^2	Coefficient of determination

CHAPTER 1

Introduction

Natural colorants are in great demand particularly for use in foods and drinks. In 2007, the market for natural food colorants was valued at US $465 million USD, an increased of 4.6% from the year 2004 (Mapari *et al.*, 2010).

Natural pigments and colorants are extracted from plants, animals, and microorganisms. Production of pigments using microorganisms has a certain advantage over the other sources as microorganisms can be grown rapidly under highly controlled conditions. This results in a high productivity of the pigment (Carvalho *et al.*, 2007; Kim *et al.*, 1999). Many microorganisms have the ability to produce pigments, including species of the genera *Monascus*, *Paecilomyces*, *Serratia*, *Cordyceps*, *Streptomyces*, and *Penicillium* (Gunasekaran and Poorniammal, 2008). *Monascus* species have attracted special attention as they produce edible pigments of different colours (Francis, 1987; Hajjaj *et al.*, 2000a; Hamdi *et al.*, 1997; Mak *et al.*, 1990; Yang *et al.*, 2005; Yongsmith *et al.*, 1994). Among the *Monascus* pigments, the red pigments are of particular interest because red is an often desired food colour. Also, true red natural pigments that are suitable for use in foods are difficult to obtain.

Members of the genus *Monascus* are filamentous fungi. Production of *Monascus* red pigment by submerged culture (Hajjaj *et al.*, 2000a; Hesseltine, 1965; Lin, 1973; Lin and Demain, 1994; McHan and Johnson, 1970) and solid-state culture (Carvalho *et al.*, 2006; Chen and Johns, 1993; Chiu *et al.*, 2006; Han and Mudgett, 1992; Hesseltine, 1965; Lotong and Suwanarit, 1990; Rosenblitt *et al.*, 2000; Teng and Feldheim, 2000) has been widely studied. Commercial submerged culture processes have been developed, but *Monascus* fermentations are generally performed in solid-state culture.

This thesis is focused on a systematic assessment of the production of red pigment by *Monascus ruber* ICMP 15220, a strain that has not been previously studied. First, this fungus is characterized for pigment production. The information gained is used to develop optimal pigment production in submerged culture, with an emphasis on the nutritional requirements, particularly the carbon and nitrogen sources. Pigment production is then developed in solid-state culture in Erlenmeyer flasks and packed-bed bioreactors. The best production scenarios for the various culture methods are assessed in terms of production kinetics. In view of its superior performance, the pigment production is optimized in a packed-bed bioreactor. Attempts are made to purify the red pigment of *Monascus ruber* ICMP 15220 for possible use as a quantification standard. Stability characteristics of the crude pigments are evaluated.

CHAPTER 2

Literature Review

2.1 General aspects

Use of *Monascus* pigments originated in China. *Monascus* pigmented rice known as angkak or red mould rice has been used in Asian countries for centuries (Hesseltine, 1965). *Monascus* pigments are used as food colorants and flavouring agents. While much of the fermented rice is produced by cottage producers, industrial type commercial production has become established in Japan (known as beni-koji), Taiwan, Thailand, Indonesia, and the Philippines (Downham and Collins, 2000; Dufosse *et al.*, 2005; Erdogrul and Azirak, 2005; Lin *et al.*, 2008; Wissgott and Bortlik, 1996). In addition, *Monascus* pigmented food is said to improve digestion and cardiovascular health. Some *Monascus* strains are known to produce lovastatin, a powerful agent for lowering blood cholesterol.

Nearly 58 *Monascus* strains have been collected in the American Type Culture Collection (ATCC). Based on the taxonomy established by Hawksworth and Pitt (1983), most of these strains have been classified as *Monascus pilosus*, *Monascus ruber*, and *Monascus purpureus*.

2.2 *Monascus* species and uses of *Monascus* pigments

The genus *Monascus* belongs to the class *Ascomycetes* and the family *Monascaceae* (Hoog *et al.*, 2004; Juzlova *et al.*, 1996; Pitt and Hocking, 1997). The genus *Monascus* is generally divided into 6 species: *M. pilosus*, *M. purpureus*, *M. ruber*, *M. floridanus*, *M. pallens*, and *M. sanguineus* (Martinkova and Patakova, 1999; Pattanagul *et al.*, 2007). The species can be differentiated by their ability to produce secondary polyketide metabolites. Some of the species produce strong yellow, orange, or red colours, while others have very little pigmentation (Juzlova *et al.*, 1996; Martinkova and Patakova, 1999). *Monascus* is a homothallic fungus which can reproduce both sexually and asexually (Hawksworth and Pitt, 1983).

Monascus fungi are able to produce various potentially useful metabolites including both primary metabolites (i.e. ethyl alcohol, acids, esters, and other flavoring compounds) and secondary metabolites (i.e. pigments, lovastatin (monacolin), and antimicrobial agents) (Hsu *et al.*, 2002; Kono and Himeno, 1999).

The main use of *Monascus* is for pigment production. These pigments are used as natural colorants in various food products such as imitation crabmeat, soybean products, jellies, milk, and ice cream. In addition, *Monascus* red pigment can also be used to substitute nitrites in fermented meat and sausages (Chen and Johns, 1993; Fabre *et al.*, 1993). *Monascus* is used to produce the health product lovastatin (monacolin K), which helps control the hyperlipidemia disease and is useful in lowering the blood cholesterol level (Akihisa *et al.*, 2005; Endo, 1979). Some *Monascus* strains produce the antibiotic substance Monascidin A that inhibits the growth of bacteria of the genera *Bacillus*, *Streptococcus*, and *Pseudomonas* (Wong and Bau, 1977). Production of the various *Monascus* secondary metabolites is dependent on the culture conditions.

2.3 *Monascus ruber*

Ruber is Latin for red (Erdogrul and Azirak, 2005). *Monascus ruber* is a producer of a strong red pigment and other metabolites. On potato dextrose agar (PDA), the most common medium used for culturing, *Monascus ruber* forms a flat colony on the petri dish. Initially, a white mycelium is formed within 1 to 2 days of inoculation and then the colour turns to orange and red as the colony grows, with the development of cleistotechia and aleurioconidia (Carvalho *et al.*, 2003; Pitt and Hocking, 1997). Based on microscopic observations, the cleisthothecia have a round shape with a diameter of 30 to 60 µm. The fungus is able to grow from 15 to 18^{o}C (minimum) to around a temperature of 45^{o}C (maximum) (Pitt and Hocking, 1997). However, the optimal temperature is 30^{o}C (Hoog *et al.*, 2004). The pigments produced vary with the cultivation conditions.

2.4 Fermentation conditions

For a profitable production of pigments, the culture medium and the environmental factors must be such as to maximize productivity, i.e. the amount of pigment produced per unit bioreactor volume per unit time.

2.4.1 Medium composition

Selection of a suitable medium composition is essential to developing a successful fermentation process. The medium composition influences both the final biomass yield and the growth rate. The carbon and nitrogen sources used are known to influence *Monascus* pigment production (Chen and Johns, 1993; Lin and Demain, 1991; Wong *et al.*, 1981).

2.4.1.1 Carbon source

The carbon source generally provides the energy for growth and secondary metabolism. It also provides the carbon for making the various cell structures, organic chemicals, and metabolites. As a heterotrophic microorganism, *Monascus ruber* can utilize a wide range of carbon sources for growth. The type and concentration of the carbon source are known to directly affect the growth of *Monascus* sp. (Lee *et al.*, 2007). The most commonly used carbon sources for *Monascus* species are glucose, maltose, and starch. Most studies suggest glucose to be a superior carbon source for pigment production (Broder and Koehler, 1980; Lin and Demain, 1991; Martin and Edward, 1990; Yoshimura *et al.*, 1975) but other evidence suggests that ethanol and sucrose may be superior to glucose for pigment production as they reduce growth rate compared to glucose and this results in higher biomass specific pigments production (Juzlova *et al.*, 1996; Santerre *et al.*, 1995). Some of the discrepancies in the reported results may be due to the different *Monascus* strain used by different researchers. Compared to the above noted carbon sources, i.e. lactose, fructose, and xylose have been found to be inferior for growth and pigment production (Lin, 1973; Lin and Demain, 1991).

Concentration of glucose in the fermentation medium influences the amount of biomass produced and the biomass specific yields of pigments. For *Monascus* fermentations, Juzlova *et al.* (1996) suggested that the glucose concentration should be kept at < 20 g L^{-1} so as to prevent the Crabtree effect that supposedly occurs at a concentration of > 20 g L^{-1}. The Crabtree effect involves a shift in metabolism from aerobic to partly anaerobic even though plenty of oxygen may be available (Carvalho *et al.*, 2003; Chen and Johns, 1994). Crabtree effect tends to reduce growth rate and pigment synthesis. It may also lead to production of ethanol. In some cases, a relatively low glucose concentration in submerged culture has been associated with an initial production of ethanol, which is later used for biomass and pigments production (Hamdi *et al.*, 1996). This may have been due to insufficient aeration in the fermentation process.

Certain other studies have used maltose as the carbon source. In presence of peptones, a high concentration of maltose (50 g L^{-1}) enhanced the production of the red pigment 3-folds compared to the use of a high concentration of glucose (> 20 g L^{-1})

(Chen and Johns, 1994). All of the above suggests a strain specific behaviour of *Monascus* in relation to the optimal carbon source for growth and pigment production.

Complex carbon sources such as starch have also been investigated for possible use in producing *Monascus* pigments in submerged culture (Lee *et al.*, 1995). Difficulties were encountered mainly because of the viscous rheology of starch solutions. Poor oxygen mass transfer as a consequence of high viscosity of the medium resulted in relatively low final concentration of the biomass and pigments (Lee *et al.*, 1995; Lee *et al.*, 1994). Thus, the use of crude starch in submerged culture fermentation does not seem to be a viable option for this fermentation.

Complex carbon sources such as rice have been found to be quite suitable when used in solid-state culture of *Monascus* (Lin, 1973; Teng and Feldheim, 2001; Tseng *et al.*, 2000).

2.4.1.2 Nitrogen source

A source of nitrogen is essential for growth of most microorganisms. Nitrogen comprises approximately 10% of dry weight of fungi (Pirt, 1985). The type of nitrogen source influences growth, sporulation, and the type of pigments produced by *Monascus* sp. The consumption of different nitrogen sources produces different pH profiles in uncontrolled fermentations, and this also affects the pattern of growth and pigment production (Martinkova and Patakova, 1999; Wong *et al.*, 1981). In traditional processes of angkak production using rice as the substrate, further supplementation with a nitrogen source is unnecessary as the rice itself has 5 to 8% of proteins (Carvalho *et al.*, 2003). If other low nitrogen substrates are used, supplementation with nitrogen may be required to stimulate growth and pigment production.

Organic nitrogen sources such as monosodium glutamate (MSG), peptone, and some amino acids (i.e. methanproline and azetidinecarboxylic acid) have been reported to stimulate *Monascus* growth and pigment production, especially the production of the red and yellow pigments (Chen and Johns, 1993; Chen and Johns, 1994; Cho *et al.*, 2002;

Gunasekaran and Poorniammal, 2008; Juzlova *et al.*, 1996; Lin, 1991; Yongsmith *et al.*, 1993). Use of yeast extract as an organic nitrogen source was reported to stimulate conidiation and biomass growth but not pigment production (Juzlova *et al.*, 1996).

The use of inorganic nitrogen sources such as ammonium and nitrates also stimulates cell growth and promotes pigment production. Addition of ammonium chloride to the medium was reported to promote the production of orange pigments as the acidification of the medium likely weakened the reaction of the orange pigments (rubropunctatine and monascorubrine) with amine groups and consequent transformation to the red pigment (Juzlova *et al.*, 1996; Martinkova and Patakova, 1999). Use of sodium nitrate in the medium is said to limit growth and pigment yield (Juzlova *et al.*, 1996). The medium must provide sufficient nitrogen in a suitable form to promote both growth and pigment production.

2.4.1.3 Trace metals

Trace metals such as zinc, manganese, iron, magnesium, and phosphorus have been reported to profoundly influence the secondary metabolism of *Monascus* fungi. Too high a concentration of trace metals can have a negative effect especially on pigment formation.

Influence of zinc on *Monascus* growth and pigmentation has been extensively discussed in the literature (Bau and Wong, 1979; Johnson and McHan, 1975; McHan and Johnson, 1970). Zinc is essential for fungal growth at low concentrations but becomes toxic at higher concentrations. The growth of *Monascus purpureus* was enhanced by increasing the zinc concentration in the medium from 0.5 µg L^{-1} to 800 µg L^{-1} (McHan and Johnson, 1970). Zinc concentration of 800 µg L^{-1} appeared to be the optimum for growth and pigment formation. For other fungi, the optimal zinc concentration has been reported to range from 1 to 500 µg L^{-1}, or 0.001 to 0.5 ppm (Cochrane, 1958).

Phosphorus is another essential element for living organisms, as it is needed to produce phospholipids and other essential biochemicals. An absence of potassium phosphate in the medium has been reported to adversely affect the red pigment production by *Monascus pilosus* (Lin *et al.*, 2007). A limited supply of phosphate however stimulated biomass and pigment production (Lin, 1991).

Potassium chloride concentration of between 3 mM and 63 mM was found to not affect cell growth and pigment production (Lin, 1991), but the pigment production declined at < 3 mM potassium chloride (Lin and Demain, 1991). Similarly, the level of magnesium has proven to be important for fungal growth (Lin and Demain, 1991). A magnesium sulphate concentration of < 2 mM was found to limit the biomass growth and pigment production.

2.4.2 Environmental factors

In addition to the composition of the culture medium, the fermentation conditions also significantly influence growth and pigment production by *Monascus* as discussed in the following sections.

2.4.2.1 pH

Unless the pH is controlled, the pH profile during cultivation depends significantly on the nitrogen source and to a lesser extent on the carbon source used. The ideal pH range for pigment production is from pH 4.0 to pH 7.0, and the pH for growth range from pH 2.5 to pH 8.0 (Yongsmith *et al.*, 1993). The control of pH at a constant value during cultivation has not proved beneficial in *Monascus* fermentation (Yoshimura *et al.*, 1975). Usually only the initial pH value is adjusted to a suitable level depending on the carbon and nitrogen sources used.

According to Chen and Johns (1993), *Monascus* grows better at a low pH (pH 4.0). However, the changes in pH in the medium significantly affect pigment production. Usually, at low pH values, the pigments produced are mainly the yellow pigments. At higher pH values, the red pigments tend to dominate. At pH 4.0, stimulation of the yellow pigment (ankaflavine) production depresses the production of orange and red pigments (Yongsmith *et al.*, 1993). The production of yellow pigments has been found to increase with increasing pH until pH 5.5. Above this value, red pigment production exceeds that of the yellow pigment. Relatively high pH values (pH > 7.0) are associated with the transformation of the orange pigments to red pigments (Mak *et al.*, 1990).

In a typical submerged fermentation of *Monascus,* the pH tends to become alkaline and this promotes the red pigment development specially in the later stages of fermentation.

2.4.2.2 Temperature

Temperature affects the rates of biochemical reactions therefore affects the rates of biomass growth and product formation (Pirt, 1985). However, growth and metabolite production may respond differently to the temperature changes (Pirt, 1985; Shuler and Kargi, 2002). Optimal temperature for growth of *Monascus* species is broad. Depending on species, the optimal temperature could vary from 25 to 37^{o}C (Carvalho *et al.*, 2005; Lin, 1991; Shepherd, 1977). For different species, the pigment production may respond differently to changes in temperature and other cultivation conditions. In some cases, a high temperature has promoted pigment production (Carvalho *et al.*, 2005).

Temperature is readily controlled in submerged culture but can be difficult to control in solid-state culture in which the solid substrate is not generally mixed.

2.4.2.3 Aeration

Monascus is an obligate aerobe and therefore requires a sufficiency of oxygen to grow rapidly. Under limiting oxygen conditions growth is slowed (Carvalho *et al.*, 2003). Growth and secondary metabolism of *Monascus ruber* are significantly affected by the aeration and agitation conditions (Hajjaj *et al.*, 1999). Agitation can also enhance the uniformity of the growth environment (Braun and Vechtlifshitz, 1991).

A limiting oxygen environment leads to an increasing production of ethanol, a lower biomass yield, and consequently a low pigment yield (Han and Mudgett, 1992; Lee *et al.*, 1994; Pastrana *et al.*, 1995). A high concentration of oxygen also suppresses the production of aflatoxins (Shih and Marth, 1974). Although, in the presence of excessive oxygen, metabolites such as L-maltose, succinate, and dicarboxylic acid, may be produced and this reduces the production of pigments (Lin *et al.*, 2008). Excessive agitation can damage *Monascus* mycelia and reduce the growth rate (Lee *et al.*, 1995).

Owing to the essential requirement of aeration, submerged fermentation by *Monascus* can only be carried out in shaken flasks or in well stirred and aerated fermenters (Juzlova, 1994). In solid-state culture of *Monascus purpureus*, pigment production in packed-bed bioreactors has been found to improve with improved aeration (Han and Mudgett, 1992).

2.5 Fermentation techniques for pigment production

Both submerged culture and solid-state culture have been used to produce *Monascus* pigments. These two fermentation methods are quite different as discussed in the following sections.

2.5.1 Submerged culture

Although the traditional angkak production is by solid-state culture, the submerged culture fermentation of *Monascus* has been extensively studied. The interest in submerged culture is driven by its ease of operation and an excellent controllability (Chen and Johns, 1994; Lee *et al.*, 2001). Submerged culture produces lower pigment yields than solid-state culture, but this has actually driven the apparently unsuccessful attempts to match in the submerged culture the level of production of the solid-state fermentation.

The conventional stirred tank is the most commonly used type of fermentor for *Monascus.* Most of the focus has been on the relatively simple batch fermentation. A variety of carbon sources have been used including simple sugars (i.e. glucose, sucrose) and complex substrate such as rice powder and starch (Ahn *et al.*, 2006; Kim *et al.*, 2002; Lee *et al.*, 1995). In a few cases, agricultural waste has been used as substrate for submerged culture (i.e. grape waste, cassava decanter wastewater) (Phoolphundh *et al.*, 2007; Silveira *et al.*, 2008; Wongwicharn *et al.*, 2006). A nitrogen source is always required in defined media and supplemental nitrogen is generally added also to nitrogen poor complex media. Trace metals are generally added and the initial pH is usually adjusted to approximately 6.5 prior to sterilization. The medium is inoculated with a seed culture, which has been pre-cultured from a suspension of spores. Aeration and agitation are used to provide oxygen and ensure homogeneity of the culture environment.

Typically, a laboratory batch fermentation of *Monascus* in submerged culture takes 8 to 9 days, including the 2 to 4 days used for preparing the seed culture. In submerged fermentations of mycelial fungi such as *Monascus*, the viscosity of the broth increases with growth and this adversely affects productivity (Ahn *et al.*, 2006) as oxygen supply generally become limiting (Kim *et al.*, 2002). Short branched mycelia and small pellets may be produced at later stages of a *Monascus* fermentation. This results in an improved oxygen supply and pigment productivity (Ahn *et al.*, 2006; Kim *et al.*, 2002). The viscosity of the fermentation broth depends both on the biomass concentration and on the growth morphology. Morphology in turn is affected by the fermentation conditions (i.e. agitation intensity) and the nutrients used (Metz and Kossen, 1977).

2.5.2 Solid-state culture

Solid-state fermentation of *Monascus* for anka, angkak, or Chinese red rice has been known for more than 1500 years (Martinkova and Patakova, 1999; Pandey, 1994).

The Chinese traditional process uses bamboo trays for the fermentation. Initially, the rice is soaked for 6 to 8 h, then cooked and inoculated with *Monascus*. Inoculated rice is then spread in a 5 to 6 cm deep layer on a round bamboo tray. The trays are stacked in shelves and incubated at room temperature. During the fermentation, the rice is occasionally mixed by hand to remove the heat produced and aerate the culture. To maintain the proper moisture content during incubation, each tray is taken out and briefly soaked in water. This process is repeated at least three times during the fermentation. The fermentation is continued for about 6 to 7 days, and the fermented rice is dried at 45^{o}C for one day (Chiu *et al.*, 2006). The dried fermented rice is ground to a mash form and used as a colorant. Similar methods are used in the Philippines and Taiwan for *Monascus* production (Martinkova and Patakova, 1999).

The traditional solid-state culture in trays is not easily scaled up because it is laborious and the trays take up a lot of space. Also, the traditional method is prone to contamination and the quality of the product can be inconsistent from batch to batch. Not withstanding its problems, the solid-state culture has a higher pigment productivity than submerged culture (Carvalho *et al.*, 2006; Evans and Wang, 1984; Lin, 1973; Soccol and Vandenberghe, 2003) and is relatively inexpensive (Carvalho *et al.*, 2006; Holker and Lenz, 2005; Pandey, 2003). The low pigment productivity of submerged culture is associated with product inhibition of the fermentation. In submerged culture, the relatively hydrophobic pigments remain mostly within the mycelium and this suppresses their further production by feed back inhibition. In solid-state cultivation, the pigments continuously diffuse from the mycelium to the surface of the rice grain and into the grain and this reduce product inhibition. Table 2.1 is a summary of advantages and disadvantages of solid-state cultivation.

Table 2.1: Potential advantages and disadvantages of solid-state culture

Advantages	Disadvantages
Higher yield and productivity compared to submerged culture.	Insufficient substrate mixing results heterogeneity.
Minimum water requirement, hence a reduced possibility of bacterial contamination.	Poor control of the process parameters (i.e. moisture, nutrients, temperature, etc).
Low cost substrate (i.e. agricultural by-product) can be used.	Heat build up due to poor heat transfer in the substrate.
Simpler technology than submerged culture.	Difficult to scale up.
Lower cost and energy demand.	
Solid-state culture simulates the natural habitat of fungi such as *Monascus*	

Static flasks, packed bed columns (Carvalho *et al.*, 2006; Han and Mudgett, 1992; Rosenblitt *et al.*, 2000), rotating drum fermentors (Carvalho *et al.*, 2006), and open trays (Lee *et al.*, 2002) have been used in studies of solid-state *Monascus* fermentation. Studies in static flasks have been useful in identifying the supplemental nutrient requirement for rice, the inoculum size, and suitable initial moisture content (Lee *et al.*, 2002; Yongsmith *et al.*, 2000). Unconventional substrates have included corn meal, coconut residue, peanut meal, soybean meal, jackfruit seed, wheat bran, and grape waste (Babitha *et al.*, 2006, 2007b; Nimnoi and Lumyong, 2009; Silveira *et al.*, 2008). Studies in more sophisticated reactors (i.e. bed columns, trays, drum reactors) have generally focussed on the effects of aeration and agitation (Carvalho *et al.*, 2006; Eduardo *et al.*, 2007; Han and Mudgett, 1992).

No in depth systematic study of solid-state culture of *Monascus* in packed-bed bioreactors has focused on the specific strain of interest here and on the interactive effects of various environmental conditions on the fermentation.

2.6 Principles of solid-state cultivation

2.6.1 Introduction

Solid-state fermentation is a process of growing microorganisms, mostly fungi, on or within particles, or other solid substrates, in the absence or near absence of free water. The substrate must of course contain enough moisture to assure microbial growth and metabolism (Couto and Sanroman, 2006; Mitchell and Lonsane, 1992; Perez-Guerra *et al.*, 2003; Prabhakar *et al.*, 2005; Singhania *et al.*, 2009; Viniegra-Gonzalez, 1996; Young *et al.*, 1983). Although, many microorganisms are able to grow on a solid substrate in presence of sufficient water, only fungi typically thrive in the low-water environment of a solid substrates fermentation (Couto and Sanroman, 2006; Pandey, 1992, 2003; Pandey *et al.*, 2000; Raimbault, 1998; Young *et al.*, 1983). Unlike most other microorganisms, fungal mycelia can grow into the substrate particles.

Although solid-state culture has been used for centuries in the preparation of traditional foods, the microbiological and biochemical process involved are poorly understood. The environment of a solid-state fermentation is akin to the natural habitat of microorganisms. The general aspects of solid-state fermentations have been extensively reviewed (Barrios-Gonzalez *et al.*, 2005; Couto and Sanroman, 2006; Mitchell and Lonsane, 1992; Pandey, 2003; Pandey *et al.*, 2000; Prabhakar *et al.*, 2005; Raimbault, 1998; Singhania *et al.*, 2009).

The following sections discuss some of the major factors that are important for solid-state culture involving fungi.

2.6.2 Spore germination and fungal growth

The pattern of growth of filamentous fungi in submerged culture is generally not the same as in solid-state culture. Typically, the growth in solid-state culture is more complex compared to submerged culture. In submerged culture, the fungi grow by extending the hyphae which then break off due to turbulence or agitation. In solid-state culture, the growth is by extension of hyphae to eventually cover the entire surface of the static solid substrate and a penetration of the substrate. In solid-state growth, the structure of the hyphal mat is retained and the nutrients are not uniformly available. The rate of growth depends on the substrate properties (Young *et al.*, 1983).

The hyphal mode of growth and the ability of fungi to thrive at a relatively low water activity (Aw) offers them a major advantage over bacteria and yeasts (Mitchell and Lonsane, 1992). The density of the growing mycelial mass depends on the amount of nutrients available in the solid substrate (Bull and Trinci, 1977). The ability of the mycelium to penetrate the substrate particles may improve accessibility to nutrients (Mitchell and Lonsane, 1992).

2.6.3 Substrates

The choice and preparation of the substrate can significantly affect a solid-state culture process. The substrates used are usually products of agriculture or by-product of the agro-industry. The substrates are generally insoluble in water and are made of digestible macromolecules (i.e. starch, cellulose, protein) (Manpreet *et al.*, 2005; Mitchell *et al.*, 1992a; Raimbault, 1998). Growth is controlled often by the ability of the fungus to digest the substrate. Not all substrates are digested equally easily. For example, the lignocellulosic substrate (i.e. wheat straw, wheat bran, sugar-beet pulp) are more difficult to digest than starches (Durand *et al.*, 1988; Hoogschagen *et al.*, 2001; Zadrazil and Puniya, 1995). A majority of solid-state fermentations use starchy material as substrate. Some examples of starchy substrate that are commonly used are rice, cassava, and sweet potato (Dalla Santa *et al.*, 2004; Prado *et al.*, 2004; Rosenblitt *et al.*, 2000). Substrates

may need to be supplemented with other nutrients to achieve the desired fermentation or enhance metabolite production.

In addition to its chemical properties, the physical form of the substrate (i.e. particle size, shape, porosity, consistency) may affect its utility in a solid-state fermentation. Particle size and shape appear to be the most significant factors that influence the substrate consumption (Manpreet *et al.*, 2005; Mitchell *et al.*, 1992a). Particle size and shape affect microbial growth by influencing oxygen supply and the removal of carbon dioxide. The ratio of the surface area to the volume of the particle, which relates to the particle size and shape, may influence the depth of hyphae penetration in a static bed of solids. If a fungus has a poor hyphae penetration of the substrate particles, it may be necessary to increase the surface area to volume ratio of the substrate particles in order to improve their utilization. Particle size affects the packing density and the void fraction in the bed. Generally a loosely packed-bed of a high porosity is wanted to enhance diffusion of oxygen.

2.6.4 Biomass determination in solid-state cultivation

A determination of the biomass amount is essential for characterizing microbial growth in detail. In a solid-state cultivation, the biomass is difficult to measure directly as it is nearly impossible to separate the mycelium from the fermenting substrate. Nevertheless, the quantity of the produced biomass can be determined indirectly. The relevant methods are reviewed in this section.

2.6.4.1 Metabolic activity of biomass

2.6.4.1.1 Respiratory metabolism

During a fungal fermentation process, oxygen is consumed and carbon dioxide is produced due to respiration. The respiration rate is directly proportional to the amount of active biomass present and can be used for its estimation (Raimbault, 1998). This method does not measure any accumulated but inactive biomass and is not commonly used.

2.6.4.2 Biomass components

Any unique constituent of the biomass that is stable and present in a fixed proportion to the biomass, can be used to estimate it (Mitchell, 1992). The biomass components that could be used for its estimation are reviewed in this section.

2.6.4.2.1 Protein and nitrogen content

Protein is a readily measured cellular components for biomass estimation (Raimbault, 1998). Determination of soluble protein has been used to estimate the biomass of *Aspergillus niger* (Favela-Torres *et al.*, 1998; Raimbault and Alazard, 1980), but this method is believed to be unreliable for use in solid-state cultivation (Mitchell, 1989). For example, the substrate may often contain some protein that may be consumed during fungal growth.

2.6.4.2.2 Deoxyribonucleic acid (DNA)

DNA measurement has been used to estimate biomass production by *Aspergillus oryzae* on rice (Bajracharya and Mudgett, 1980). At early stage of fermentation, the DNA contents were high and slowly decreased towards the end of the fermentation. The method had to be adjusted for the DNA content in the rice. The biomass production was estimated by correlating the measured DNA content of the solid-state culture to a biomass concentration using a DNA to biomass ratio that had been determined in submerged culture on a dissolved substrate (Mitchell, 1992; Raimbault, 1998). This method is not reliable if the substrate contains nucleic acids.

2.6.4.2.3 Glucosamine

Chitin (poly-N-acetylglucosamine), a polymer of glucosamine, is an essential component of fungal cell walls (Abd-Aziz *et al.*, 2008; Desgranges *et al.*, 1991a; Roche *et al.*, 1993). Hydrolysis of chitin produces glucosamine that can be measured and correlated to the biomass content. Glucosamine measurement is widely claimed to be a good indicator for fungal growth (Abd-Aziz *et al.*, 2008; Zheng and Shetty, 1998).

Glucosamine measurements during biomass growth on a soluble substrate in submerged culture are used for calibration. The accuracy of biomass estimation depends on the consistency of the conversion factor (*cf*), which relates the biomass dry weight to the measured glucosamine (Nilsson and Bjurman, 1998; Sharma *et al.*, 1977). The conversion factor must be experimentally established and should not vary much during the course of a batch fermentation.

2.6.4.2.4 Ergoesterol

Ergosterol is the major sterol in fungal cell membrane. It is commonly used to determine the fungal biomass in soils (Carvalho *et al.*, 2006; Mitchell, 1992; Raimbault, 1998). Contents of ergosterol and glucosamine in fungal biomass are generally well correlated. However, in some cases at least, ergosterol measurements may not reliably indicate the biomass content. For example, for *Beauveria bassiana* the ratio of ergosterol to biomass varied during growth and between media (Desgranges *et al.*, 1991a).

2.6.5 Environmental factors

In addition to the nature of the substrate, environmental factors profoundly affect growth and product formation in a solid-state fermentation where they can be impossible to control as well as in a submerged culture. The relevant environmental factors are reviewed in this section.

2.6.5.1 Temperature

Temperature has a substantial direct impact on growth, spore germination, and product formation. In solid-state fermentation the metabolic heat production ranges from 100 to 300 kJ/kg of cell mass (Prior and Preez, 1992). Inadequate heat removal inevitably leads to a rise in substrate temperature. Porous solid substrates are poor conductors of heat (Ghildyal *et al.*, 1994; GutierrezRojas *et al.*, 1996; Saucedo-Castaneda *et al.*, 1990; Stuart *et al.*, 1999) and therefore the heat generated is not easily dissipated. The maximum temperature attained in the fermenting mass depends on the substrate being metabolized and the supply of oxygen (i.e. particle size, substrate porosity, depth of the substrate) (Gervais and Molin, 2003; Raghavarao *et al.*, 2003; Raimbault, 1998).

In traditional solid-state fermentation, the temperature is controlled to a limited extent by using a low depth of substrate, occasional mixing with hand, and by carrying out the fermentation in a cool place. More advanced methods typically rely on forced aeration of the substrate beds with conditioned air. Forced aeration may remove more than 80% of heat produced (Manpreet *et al.*, 2005), but high aeration rates may cause a loss of moisture and a reduced water activity of the substrate. Dry air is more effective for cooling (evaporative cooling) but humidified air is generally used to minimize water loss. Some water loss occurs even if water saturated air is used (Raghavarao *et al.*, 2003).

2.6.5.2 Initial moisture content

In solid-state culture, moisture content of the substrate has a substantial influence on growth and metabolite production (Pandey, 1992, 2003). Too high a moisture content may reduce substrate porosity and mass transfer of oxygen. While too low a moisture content results in a reduced accessibility of nutrients to the fungus (Babitha *et al.*, 2007b; Pandey, 2003). In most cases, fungal growth requires a moisture content in the range of 30-75% (w/w). In contrast, bacterial culture requires more than 75% (w/w) moisture in the substrate (Gautam *et al.*, 2002; Perez-Guerra *et al.*, 2003).

For pigment production by *Monascus*, different strains have been reported to have their own optimum initial moisture content. Lotong and Suwanarit (1990) reported that at a high initial moisture content of 43%, *Monascus* sp. NP1 rapidly released glucose from the starch, which in turn inhibited pigment production. While at a low moisture content of 32%, the hydrolysis of starch to glucose was too slow and this too decreased pigment production. However, *Monascus* strains generally tend to require a moisture content in the range of 40-50% (w/w) for optimal growth (Johns and Stuart, 1991; Juzlova, 1994).

2.6.5.3 Water activity

Water activity (Aw) is the ratio of the vapour pressure of water in a system to the vapour pressure of pure water at the same temperature (Manpreet *et al.*, 2005; Raimbault, 1998). Water activity is the same as the relative humidity divided by 100. Aw of pure water is 1.00 and it decreases with the addition of solutes. Water activity is a measure of the water that is actually available to microorganisms for growth in a substrate. Water activity significantly affects growth and product formation (Gervais and Molin, 2003).

Fungi and yeasts can grow at a relatively low water activity in the range of 0.6-0.9. In contrast, bacteria require higher water activity values for growth (Manpreet *et al.*, 2005). Most fungi can grow at Aw in a range of 0.8 to 0.9 (Raimbault, 1998). A decrease in water activity during a fermentation will adversely affect biomass growth (Liu and Tzeng, 1999) and product formation.

2.6.5.4 Aeration

In solid-state culture, aeration is used to supply oxygen, remove carbon dioxide that is produced by metabolism, and control the substrate temperature (Durand *et al.*, 1988; Gervais and Molin, 2003). *Monascus* fermentation is quite sensitive to aeration and pigment production is reduced by accumulation of excess carbon dioxide (Han and Mudgett, 1992; Teng and Feldheim, 2000). Secondary metabolism of *Monascus* is influenced by oxygen as the *Monascus* pigments and other secondary metabolites contain significant oxygen in their structures (Turner, 1971).

Aeration rate should not be excessive or moisture loss from the substrate will adversely affect the fermentation (Anisha *et al.*, 2010; Carvalho *et al.*, 2006; Lee *et al.*, 2002; Weber *et al.*, 2002). Moisture loss can be reduced by using air at > 90% relative humidity for aeration (Oriol *et al.*, 1988; Stuart and Mitchell, 2003).

2.6.6 Reactors

A solid-state fermentation bioreactor is designed to provide the desired environment for the fermentation while limiting contamination. Bioreactor may be sterilized initially but are not generally operated aseptically. The bioreactors used are generally less complex than the ones used in submerged culture. Four major types of bioreactors are used (Durand, 2003; Mitchell *et al.*, 2006). These are the tray bioreactor, the packed bed bioreactor, the rotating drum bioreactor, and the mechanically mixed bioreactor. These are briefly explained in the following sections.

2.6.6.1 Tray bioreactor

The tray bioreactor is the simplest type of fermentor and has been used traditionally for centuries (Martinkova and Patakova, 1999). Typically, a tray is rectangular and made of wood, metal, or plastic. Inoculated trays are stacked on one another and left in a humid area with good ventilation. Tray bioreactors are typically operated in an open environment. Trays are open at the top and have a perforated bottom, in order to improve diffusion of oxygen. The substrate is spread on the tray in a layer that typically ranges in depth from 5 to 15 cm (Krishna, 2005). The substrate may be occasionally mixed manually. Because of a limited depth, tray bioreactors require a large area and are labour intensive. In addition, they are easily contaminated (Mitchell *et al.*, 2006; Mitchell *et al.*, 1992b).

2.6.6.2 Packed-bed bioreactor

Packed-bed bioreactor is an adaptation of the tray bioreactor in which a static bed of substrate is supported on a perforated base plate. Typically, a packed-bed bioreactor consists of a cylindrical column that is operated as a closed system for control of contamination. The substrate is packed to a higher depth than in the tray fermentor and humid air is forced through the base plate to provide oxygen and cool the bed (Mitchell *et al.*, 1992b).

Because of its relative simplicity and other advantages, the packed-bed bioreactor has attracted much attention (Carvalho *et al.*, 2006; Fanaei and Vaziri, 2009; Mazutti *et al.*, 2010a; Mitchell *et al.*, 1992b; Mitchell *et al.*, 2003; Mitchell and Von Meien, 2000; Najafpour *et al.*, 2009; Weber *et al.*, 2002). Shojaosadati and Babaeipour (2002) discussed the effects of aeration rate, bed height, particle size, and initial moisture content on citric acid production by *Aspergillus niger* in a solid-state packed-bed bioreactor. Mazutti *et al.* (2010c) reported on the effects of inlet air temperature and volumetric flow rate on the inulinase production by *Kluyveromyces marxianus* NRRL Y-7571 in a packed-bed. Assamoi *et al.* (2008) and Alani *et al.* (2009) examined the impact of inoculum size, bed loading, aeration rate, and initial moisture content on xylanase production by *Penicillium canescens* 10–10c and mycophenolic acid production by *Penicillium brevicompactum* ATCC 16024, respectively.

Although packed-bed bioreactors have been examined for various solid-state fermentation, only three studies appear to have been done on the genus *Monascus* (Carvalho *et al.*, 2006; Han and Mudgett, 1992; Rosenblitt *et al.*, 2000). Two of these studies focused on *Monascus purpureus* (Han and Mudgett, 1992; Rosenblitt *et al.*, 2000) and the one focused on an identified *Monascus* strain (Carvalho *et al.*, 2006). None of these studies attempted a rigorous comparison of the solid-state fermentation with the submerged mode of culture. No attempts were made to optimize the culture media and operationl regimes.

2.6.6.3 Rotating drum bioreactor

A rotating drum bioreactor consists of a horizontal cylindrical drum supported on rollers. The drum is partly filled with the substrates and inoculated. Aeration is provided through the headspace (Mitchell *et al.*, 2006). The drum is rotated slowly to gently mix the substrate. Agitation improves mixing and mass transfer and reduces the heterogeneity of the substrate, hence producing a fairly uniform microbial growth (Lonsane *et al.*, 1985). Rotation can damage mycelia (Mitchell *et al.*, 1992b) and agglomeration of substrate can pose problems.

2.6.6.4 Mechanically mixed bioreactor

The mechanically mixed bioreactor is equivalent to a packed-bed bioreactor installed with an agitator (Mitchell *et al.*, 2006). The agitator is inserted from the top and is run slowly continuously or intermittently. Forced aeration is provided from the bottom of the bed. Agitation may not always be suitable as it tears the mycelial structure of fungi.

2.6.6.5 Fluidized bed bioreactor

Fluidized bed bioreactor consists of a relatively tall column in which the air flow from the perforated base is sufficiently high that the substrate particles are fluidized (Mitchell *et al.*, 2006). A fluidized bed allows good mass and heat transfer, but moist solids can be difficult to fluidize because of agglomeration. Because of design complexities and difficult operation, fluidized beds are not commonly used for solid-state fermentation.

2.6.7 Challenges in solid-state culture

Although solid-state culture has certain advantages over submerged culture, its consistent operation is a challenge. A direct estimation of the biomass concentration in solid-state culture is essentially impossible and the heterogeneity of the substrate poses other problems. Biomass must be determined indirectly as previously discussed (Abd-Aziz *et al.*, 2008; Zheng and Shetty, 1998). Heterogeneity of the fermenting mass means that in a large bioreactor a point sample may not at all be representative. Therefore, multiple large samples may be required to satisfactorily characterize the overall bioreactor performance.

2.7 Secondary metabolite production

Secondary metabolites are compounds that are not essential to microbial survival. Pigments of *Monascus* species are secondary metabolites (Dufosse *et al.*, 2005; Johns and Stuart, 1991). Lovastatin, a cholesterol lowering agent, is another secondary metabolite of *Monascus* species (Pattanagul *et al.*, 2007).

2.7.1 Pigments from *Monascus*

Monascus generally is able to produce at least six polyketide pigment structures which can be classified into three major groups. The pigments groups are a mixture of orange (rubropunctatine ($C_{21}H_{22}O_5$), monascorubrine ($C_{23}H_{26}O_5$)), red (rubropunctamine ($C_{21}H_{23}NO_4$), monascorubramine ($C_{23}H_{27}NO_4$)), and yellow (monascine ($C_{21}H_{26}O_5$), ankaflavine ($C_{23}H_{30}O_5$)) (Chen *et al.*, 1971; Fielding *et al.*, 1961; Hadfield *et al.*, 1967; Kuromo *et al.*, 1963; Sabater-Vilar *et al.*, 1999; Su and Huang, 1980). The molecular structures of the pigments are shown in Figure 2.1.

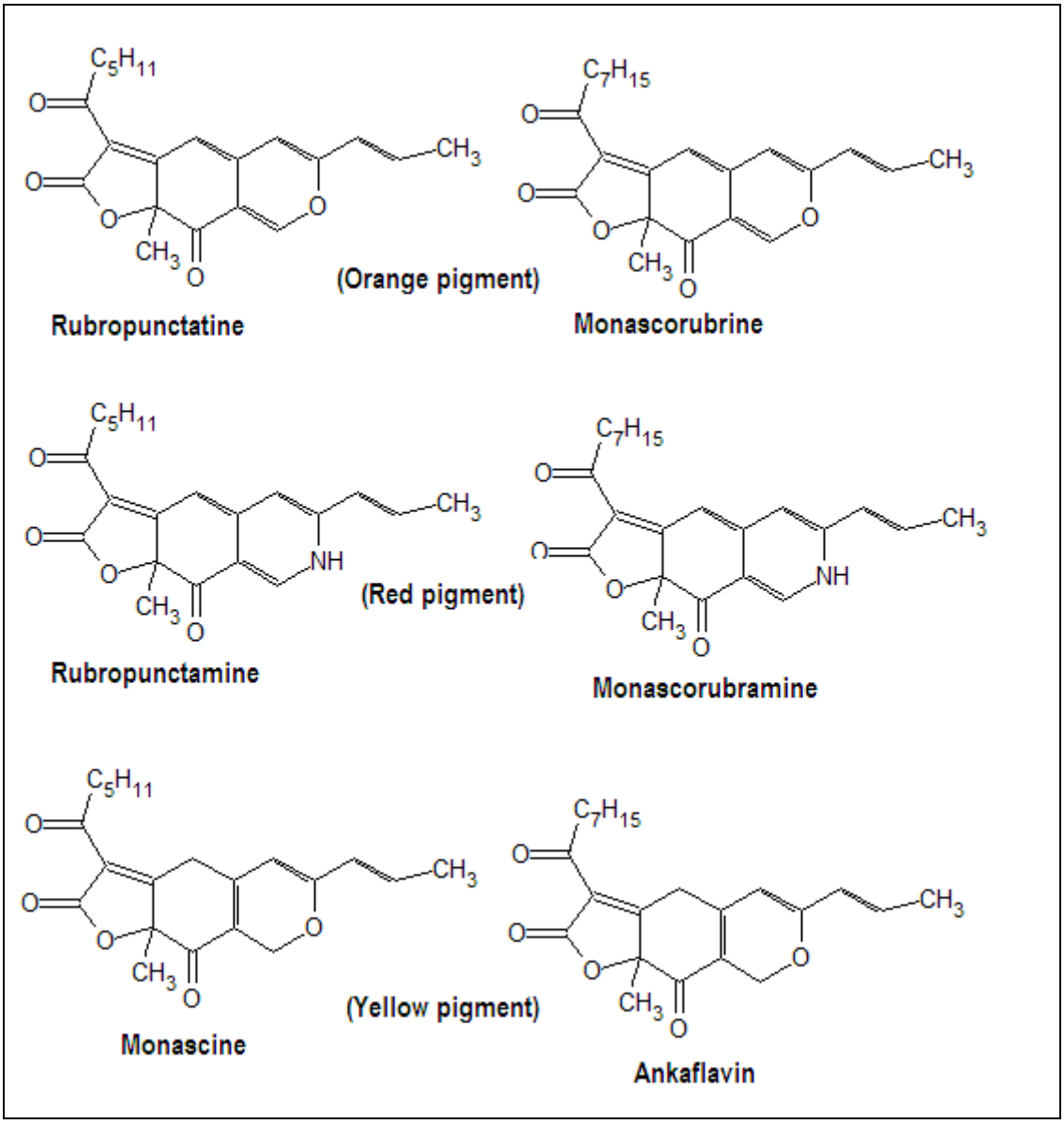

Figure 2.1: *Monascus* sp. pigments

(Adapted from Sweeny *et al.* (1981) and Dufosse *et al.* (2005))

Monascus pigments of similar colours differ only in the length of the aliphatic chain linked to the carbonyl function (Teng and Feldheim, 1998) (Figure 2.1). All pigments can be produced in both submerged and solid state culture, but production characteristics may differ depending on the nutrient type and culture conditions (Juzlova *et al.*, 1996; Patakova-Juzlova *et al.*, 1998).

The orange pigments (monascorubrine and rubropunctatine) are produced by the multienzyme complex of polyketide synthase in the cytosol, from acetyl coenzyme A (Hopwood and Sherman, 1990; Robinson, 1991). Orange pigments (rubropunctatine and monascorubrine) are azaphilones that readily react with ammonia and methylamine. The strong tendency of the orange pigments to react with primary amino group (Juzlova *et al.*, 1996; Lin, 1991) of amino acids leads to the production of water soluble red pigments, monascorubramine ($C_{23}H_{27}NO_4$) and rubropunctamine ($C_{21}H_{23}NO_4$) (Blanc *et al.*, 1994; Francis, 1987; Juzlova *et al.*, 1996; Lin *et al.*, 1992). The amino group could be from amino acids, peptides, or proteins. The water soluble red pigments are said to be more stable to heat, light, and pH changes (Tezuka and Kashino, 1979).

The yellow pigments, ankaflavine ($C_{23}H_{30}O_5$) and monascine ($C_{21}H_{26}O_5$), are produced by chemical oxidation of the orange pigments (Juzlova *et al.*, 1996; Yongsmith *et al.*, 1993). The yellow pigments cannot react with NH-groups to produce the related amine; therefore, only the orange pigments are able to form the red pigments (Fielding *et al.*, 1961).

It is generally difficult to purify pigments that are produced by solid-state cultures because of the complexity of the pigment mixture, the similarity of their structure, and contamination with the substrate material. In submerged culture, the nature of pigments produced depends on the initial pH; depending on pH the production might lean towards the yellow or the red pigments. In submerged culture, the pigments are produced in the cell bound state and remain in the cells because they have low solubility in water. Ordinarily, pigments produced in the cell bound state are more sensitive to heat, unstable to the acidic pH ($pH \leq 4$), alkaline pH ($pH \geq 10$), and fade with exposure to light (Hajjaj *et al.*, 2000a; Hajjaj *et al.*, 1997; Hamdi *et al.*, 1997; Mak *et al.*, 1990; Wong and Koehler, 1983; Yongsmith *et al.*, 1994). Because the red pigments are water soluble and more stable than the other pigments they are preferred as colorants.

2.7.2 Lovastatin

In addition to the pigments, some strains of *Monascus* produce another important metabolite known as lovastatin, Mevinolin, or Monacolin K. Lovastatin and its semisynthetic derivatives are used as powerful agents for reducing blood cholesterol in medical practice (Pattanagul *et al.*, 2007).

Lovastatin occurs in its open hydroxyl acid form and the lactone form (Figure 2.2). In submerged culture, the major form of lovastatin is the open hydroxyl acid form. The ratio of the acid form to the lactone form differs depending on the *Monascus* strain, the pH, the culture medium (Xu *et al.*, 2005), the temperature, and the initial moisture content of the substrate.

Lovastatin production is said to be higher in solid-state culture compared to submerged culture. This is likely because lovastatin inhibits its own synthesis as observed in other fungi (Casas Lopez *et al.*, 2004). In solid-state culture, the lovastatin produced is absorbed in the rice grain. In submerged culture, a lot of it remains in the mycelium and this might inhibit further synthesis.

Most of the lovastatin producing strains of *Monascus* are found to produce relatively low levels of the compound (Juzlova *et al.*, 1996; Martinkova *et al.*, 1995).

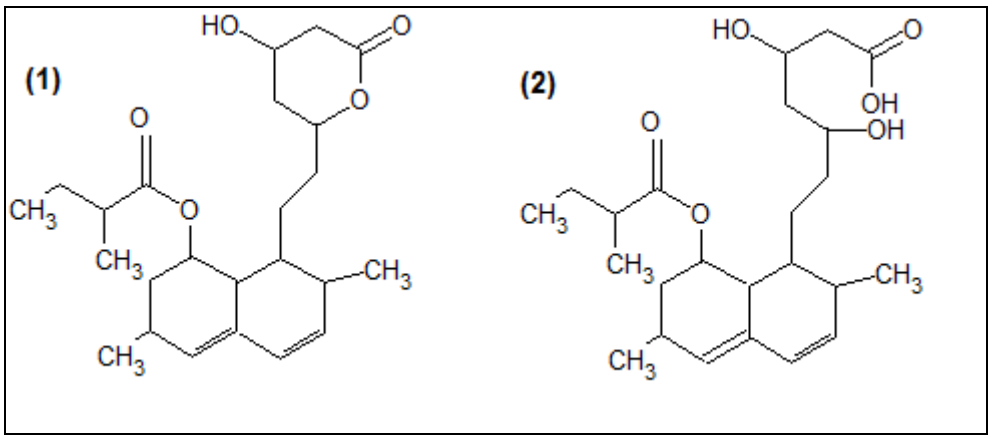

Figure 2.2: Lovastatin: (1) lactone form; (2) open hydroxyl acid form.

CHAPTER 3

Research Methodology

3.1 Introduction

This chapter describes the materials and methods used in the experimental work.

The preliminary experimental work focused on determining the suitable media for pigment production by *Monascus ruber* ICMP 15220 as this strain had not been previously reported in the literature. The aim of the work was to identify media for optimal production of pigments particularly the red pigment. Both submerged and solid-state culture methods were investigated. The experimental work was divided into three parts:

1. Initial experiments were done on agar plates. Ten different media compositions were used to examine their effect on the production of red pigment and the growth of *Monascus ruber*. The media compositions were selected using as a basis the culture media that have been reported for *Monascus* species. The pigment production and the fungal growth were measured.

2. The second part of the study was done in a submerged culture. A few media compositions were selected based on work in part 1 and used in submerged culture. In submerged batch cultures, the concentration of glucose was varied for a fixed ratio of carbon to nitrogen. This was done to determine the highest acceptable concentration of glucose. In a different series of experiments, the carbon to nitrogen ratio was varied but the concentration of glucose remained fixed (based on the initial work on glucose concentration). Upon establishing the highest acceptable concentration of glucose and a suitable carbon to nitrogen ratio, further experiments were done by shifting the organic nitrogen source in the media to various inorganic nitrogen sources and

replacing glucose in the media with other carbon sources. The pigment production, biomass growth, pH changes, and glucose consumption were measured during the course of the fermentations.

3. The third and the major part of the experimental work focused on solid-state fermentation. Effects of the operational factors such as depth of the substrate bed in a packed-bed bioreactor, the initial moisture content of the substrate and the aeration rate of humidified air (relative humidity of 97-99%) were examined on the pigment production and biomass growth. Preliminary experimental work on solid-state fermentations was done in Erlenmeyer flasks. Effects of different initial moisture content of the substrate and the nitrogen sources were examined to see how the results might compare with similar data obtained in submerged culture.

Extensive experimental work was carried out in packed-bed solid state bioreactors. Effects of various forced aeration rates on pigment production were examined. Statistically designed (Design Expert; Stat-Ease, Inc, Version 6.0.8 and Statistica, Version 5.5) experiments were used to asses the combined effects of the initial moisture contents and forced aeration rates on the pigment production and biomass growth.

In addition to the above, the purification of the red pigment produced by submerged culture was attempted and the stability of the pigment in a dissolved form under various conditions was studied.

3.2 Materials

3.2.1 Microorganism and conservation

Monascus ruber ICMP 15220 strain used in the experiments was purchased from Landcare Research New Zealand. ICMP, or International Collection of Microorganisms from Plants, is a major international collection that is a part of the New Zealand Reference Culture Collection. It is managed by Landcare Research, New Zealand. This fungus had been isolated from a palm kernel in Auckland, New Zealand, and identified as *Monascus ruber* Tieghem according to the taxonomy proposed by Hawksworth and Pitt (1983). The microorganism was maintained on Potato Dextrose Agar (PDA) plates and slants at 4^{o}C and sub cultured once every month.

3.2.2 Chemicals

All chemicals used for the fermentation and analytical work are identified in Table 3.1.

Table 3.1: Chemicals and manufactures

Name	Formula	Grade	Manufacturer
Acetic acid	CH_3COOH	A.R.	Labserve Biolab, BIOLAB Australia Limited
Acetylacetone	$C_5H_80_2$	A.R.	BDH Prolabo, VWR International, England
Agar			Merck, E. Merck, Germany
Ammonium chloride	NH_4Cl	A.R.	Labserve Biolab, BIOLAB Australia Limited
Ammonium nitrate	$(NH_4)NO_3$	A.R.	BDH Prolabo, VWR International, England
Ammonium sulphate	$(NH_4)_2SO_4$	A.R.	Scharlau, Scharlau Chemie, Spain
Calcium chloride	CaCl	A.R.	BDH Prolabo, VWR International, England
Chloroform	$CHCl_3$	A.R.	Labserve Biolab, BIOLAB Australia Limited
Di-potassium hydrogen phosphate	K_2HPO_4	A.R.	Labserve Biolab, BIOLAB Australia Limited
Ethanol	C_2H_5OH	A.R.	UNIVAR, AJAX Finechem Pty Ltd., New Zealand
Ferrous sulphate	$FeSO_4$	A.R.	BDH Prolabo, VWR International, England
Ferrous sulphate-7-hydrate	$FeSO_47H_2O$	A.R.	BDH Prolabo, VWR International, England
Glucose	$C_6H_{12}O_6$	A.R.	Fisher Scientific, UK Limited
Glycerine	$C_3H_5(OH)_3$	A.R.	Labserve Biolab, BIOLAB Australia Limited
Hydrochloric acid	HCl	A.R.	JT Baker, Mallinckrodt Baker Inc., USA
Magnesium sulphate-7-hydrate	$MgSO_47H_2O$	A.R.	Labserve Biolab, BIOLAB Australia Limited
Malt extract			Merck, E. Merck, Germany
Manganese sulphate	$MnSO_4H_2O$	A.R.	BDH Prolabo, VWR International, England
Meat extract			Merck, E. Merck, Germany

Name	Formula	Grade	Manufacturer
Methanol	CH_3OH	A.R.	Merck, E. Merck, Germany
Monosodium glutamate (MSG)	$C_5H_8NNaO_4$		The Three Mac Co. Ltd., New Zealand
N -acetyl-D-glucosamine	$C_8H_{15}NO_6$		Sigma, Sigma Chemical Co., USA
Ortophosphorc acid	H_3PO_4	A.R.	UNIVAR, AJAX Chemicals Co., Australia
p-Dimethylaminobenzaldehyde	$C_9H_{11}NO$	A.R.	BDH Prolabo, VWR International, England
Peptone from soymeal (papain digested)			Merck, E. Merck, Germany
Potassium chloride	KCl	A.R.	JT Baker, Mallinckrodt Baker Inc., USA
Potassium di-hydrogen phosphate	KH_2PO_4	A.R.	BDH Prolabo, VWR International, England
Potassium nitrate	KNO_3	A.R.	BDH Prolabo, VWR International, England
Potassium sulphate	K_2SO_4	A.R.	BDH Prolabo, VWR International, England
Potato Dextrose Agar			Difco TM, Dickson and Company Sparks, USA
Rice powder			Toops, New Zealand
Sodium bicarbonate	Na_2CO_3	A.R.	BDH Prolabo, VWR International, England
Sodium chloride	NaCl	A.R.	BDH Prolabo, VWR International, England
Sodium hydroxide	NaOH	A.R.	BDH Prolabo, VWR International, England
Sodium nitrate	$NaNO_3$	A.R.	BDH Prolabo, VWR International, England
Sulphuric acid	H_2SO_4	A.R.	BDH Prolabo, VWR International, England
Yeast extract			Merck, E. Merck, Germany
Zinc sulphate-7-hydrate	$ZnSO_47H_2O$	A.R.	BDH Prolabo, VWR International, England

Note: A.R. is an analytical reagent

3.3 Fermentations

3.3.1 Agar plate cultures

3.3.1.1 Agar medium

Ten different media compositions were used in preliminary studies on agar plates to examine their effect on growth and production of the red pigment. The choice of media was based on compositions published previously for submerged culture of *Monascus* species (Al-Sarrani and El-Naggar, 2006; ATCC, 2007; Blanc *et al.*, 1994; Carels and Shepherd, 1975; Chang *et al.*, 2002; Hajjaj *et al.*, 2000b; Hajjaj *et al.*, 1997; Hamano *et al.*, 2005; Orozco and Kilikian, 2008; Xu *et al.*, 2005). The media compositions A to J used are shown in Table 3.2.

Table 3.2: Media compositions for agar plate cultures

Component	**Media compositions (g L^{-1} of deionized water)**									
	A	**B**	**C**	**D**	**E**	**F**	**G**	**H**	**I**	**J**
Potato Dextrose Agar (PDA)	39									
Glucose		10	10	20	20		110	40	30	5
Ethanol						15.78				
Rice powder							30		20	
Glycerine							30		63	
MSG			7.6	5		5				5
Meat extract		3								
Peptone from soymeal (papain digested)		5			10		9		8	
Yeast extract			1		5				10	
$NaNO_3$								3	2	
$MgSO_4 7H_2O$			4.8	0.5		0.5	1	0.05	1	0.5
KH_2PO_4			1.5	5		5		0.1	1	5
K_2HPO_4			1.5	5		5				5
$ZnSO_4 7H_2O$			0.01	0.01		0.01		0.008		0.01
NaCl			0.4							

Component	Media compositions (g L^{-1} of deionized water)									
	A	**B**	**C**	**D**	**E**	**F**	**G**	**H**	**I**	**J**
$FeSO_4$			0.01							
$FeSO_47H_2O$				0.01		0.5		0.001		0.01
$CaCl_2$				0.1		0.5				0.1
$MnSO_4H_2O$				0.03		0.03		0.003		0.03
KNO_3							2			
KCl										
Acetic acid									3.67	
pH		5.5	5.5	6.5 with H_3PO_4		6.5	5	6.5	5	6.5 with H_3PO_4
Agar		15	15	15	15	15	15	15	15	15
Reference	ATCC (2007)	Orozco & Kilikian (2008)	Hamano *et al.* (2005)	Hajjaj *et al.* (1997)	Carels & Shepherd (1975)	Blanc *et al.* (1994)	Chang *et al.* (2002)	Al-Sarrani & El-Naggar (2006)	Xu *et al.* (2005)	Hajjaj *et al.* (2000b)

Note: The pH was adjusted with 1 N HCl, unless otherwise stated

3.3.1.2 Cultivation method

The aseptic stock cultures were maintained on Potato Dextrose Agar (PDA). Spores of *Monascus ruber* ICMP 15220 strain were prepared by growing on PDA plates for 7 days in the dark at 30^{o}C. Then, 1 mm × 1 mm mat of spores from the PDA were inoculated in triplicate at the centers of ten agar plates of different media (30 plates). The inoculated plates were incubated in the dark at 30^{o}C for 7 days.

The sterile agar plates had been made as follows: ingredients of media A to J (Table 3.2) were dissolved in 1 L of deionized water and autoclaved (121^{o}C, 15 min). After the mixture had cooled to approximately 50^{o}C, 15 to 20 mL of it was aseptically poured into sterile clear plastic disposable Petri dish plates (approximately 85 mm in diameter). The agar plates were then allowed to cool and set at room temperature. Any excess plates were stored in the cold room (4^{o}C) by stacking upside down to prevent any condensation from dripping onto the agar surface.

3.3.2 Submerged culture

3.3.2.1 Culture media

3.3.2.1.1 Inoculum media

Inoculum for submerged culture was grown in a medium that contained (g L^{-1}): yeast extract (3.0); malt extract (3.0); peptone from soymeal (5.0); and glucose (20.0) (Lin *et al.*, 1992). The medium was autoclaved at 121^{o}C for 15 min.

3.3.2.1.2 Production media

Based on results of the agar plate experiments, two media compositions were selected for further study in submerged culture. There were media D and J (Table 3.2), but without the agar.

The media D and J differed only in their concentration of glucose. This resulted in different carbon to nitrogen mass ratio of 23 to 1 (medium D) and 9 to 1 (medium J). The medium composition J resulted in better pigment production as discussed elsewhere in the thesis.

Initially, medium J was used to identify the optimal temperature for red pigment production. The submerged cultures were exposed to three different incubation temperatures of 25^{o}C, 30^{o}C, and 45^{o}C, separately for 48 h. At the end of the fermentation, the entire flasks were filtered using qualitative filter paper (Grade 4, Whatman Schleicher & Schuel, Whatman International Ltd., England) and the supernatant was subjected to UV visible spectrophotometer wavelength scans from 300 to 750 nm (Ultrospec 2000, Pharmacia Biotech, England) to measure absorption spectra.

Then, using a fixed C : N ratio of 9 : 1, as per medium J (Table 3.2), different concentrations of glucose 0.5, 1.0, 1.5, 2.0 and 2.5% (g/100 mL) were evaluated in submerged cultures while the concentrations of all the other components remained fixed in the medium.

Because a high concentration of glucose can reduce the water activity, a series of submerged culture runs were carried out with the glucose concentration fixed at 1.0% and C : N mole ratios of 6 : 1, 9 : 1, 14 : 1 and 20 : 1. All other components remained fixed in the medium as described for medium J (Table 3.2).

After having identified the optimal carbon to nitrogen ratio and the optimal concentration of glucose for pigment production, different nitrogen sources (monosodium glutamate, MSG; sodium nitrate, $NaNO_3$; ammonium chloride, NH_4Cl; ammonium nitrate, NH_4NO_3; ammonium sulfate, $(NH_4)_2SO_4$) were investigated. In all cases, the

glucose concentration was fixed at 1.0% and the C : N ratio was maintained at 9 : 1, the value that had proved best for pigment production.

In separate experiments, glucose was replaced with other carbon sources (maltose, ethanol). The nitrogen source (MSG) was fixed. In all cases, the MSG concentration was fixed at 1.0% and the C : N ratio was maintained at 9 : 1.

All submerged culture experiments were done in triplicate.

3.3.2.2 Cultivation method

3.3.2.2.1 Inoculum preparation

Monascus ruber ICMP 15220 was grown on Potato Dextrose Agar (PDA) slants in the dark at 30^{o}C for 7 days. Spores and hyphae were scraped off from the agar slant using a Pasteur pipette and suspended in 5 mL of sterilized deionized water at room temperature. This suspension was adjusted with sterilized deionized water in order to get approximately 10^{7} spores mL^{-1}. The spore number was counted using a haemacytometer slide (0.1 mm depth, 1/400 mm^{2}; Improved Neubauer, Boeco, Germany). The adjusted spore suspension was used to inoculate 100 mL (5%, vol/vol inoculum size) of a pre-inoculum medium contained in a 500 mL Erlenmeyer flask. The Erlenmeyer flask was incubated on a rotary shaker (Orbital Incubator, Watson Victor Ltd., New Zealand) in the dark at 30^{o}C, 250 rpm, for 4 days (Lin *et al.*, 1992).

3.3.2.2.2 Inoculation and cultivation

A 2 L Erlenmeyer flask containing 900 mL of the production medium was inoculated with 100 mL (10%, vol/vol) of the pre inoculum culture and incubated in the dark at 30^{o}C, 250 rpm (Orbital Incubator, Watson Victor Ltd., New Zealand), for 144 h unless otherwise mentioned.

3.3.3 Solid-state culture

3.3.3.1 Substrate preparation

Polished long grain rice (Sun Rice, premium white long grain rice, Ricegrowers Limited, NSW, Australia) was purchased locally. The experimental work was done initially in Erlenmeyer flasks before proceeding to the glass packed-bed columns.

3.3.3.1.1 Studies in Erlenmeyer flasks

For experiment in Erlenmeyer flasks, 20 g of rice was placed in a 200 mL Erlenmeyer flask and deionized water (5.5 mL, 10.6 mL, 19.7 mL, 40.0 mL or 50.3 mL) was added to achieve an initial moisture content of approximately 35%, 45%, 56%, 70%, or 75% (g water per 100 g wet substrate) in different flasks. A solution of zinc sulfate ($ZnSO_4 7H_2O$) (2 mL, 0.128 M) was added to each flask. The rice was then allowed to soak at 30^{o}C for 1 h. The flasks containing soaked rice were then covered with two layers of aluminum foil to prevent moisture loss and autoclaved at 121^{o}C for 15 min.

In a separate experiment, three individual Erlenmeyer flasks (200 mL) containing 30 g of rice substrate each, were supplemented with additional nitrogen sources (5.49 g of sodium nitrate ($NaNO_3$), 2.58 g ammonium nitrate (NH_4NO_3), 20.58 g monosodium glutamate (MSG) in separate flasks) prior to soaking (30^{o}C, 1 h) in deionized water and 3 mL of 0.128 M $ZnSO_4 7H_2O$. Deionized water was added to attain an initial moisture content of 45%. The C : N mass ratio was 9 : 1 in all cases, or comparable to the value identified to be optimal in submerged culture.

3.3.3.1.2 Packed-bed experiments

A series of packed-bed bioreactors operated in parallel were used in these experiments. The reactors were set up as shown in Figure 3.1. The dissembled and assembled reactors are shown in Figures 3.2 and 3.3, respectively.

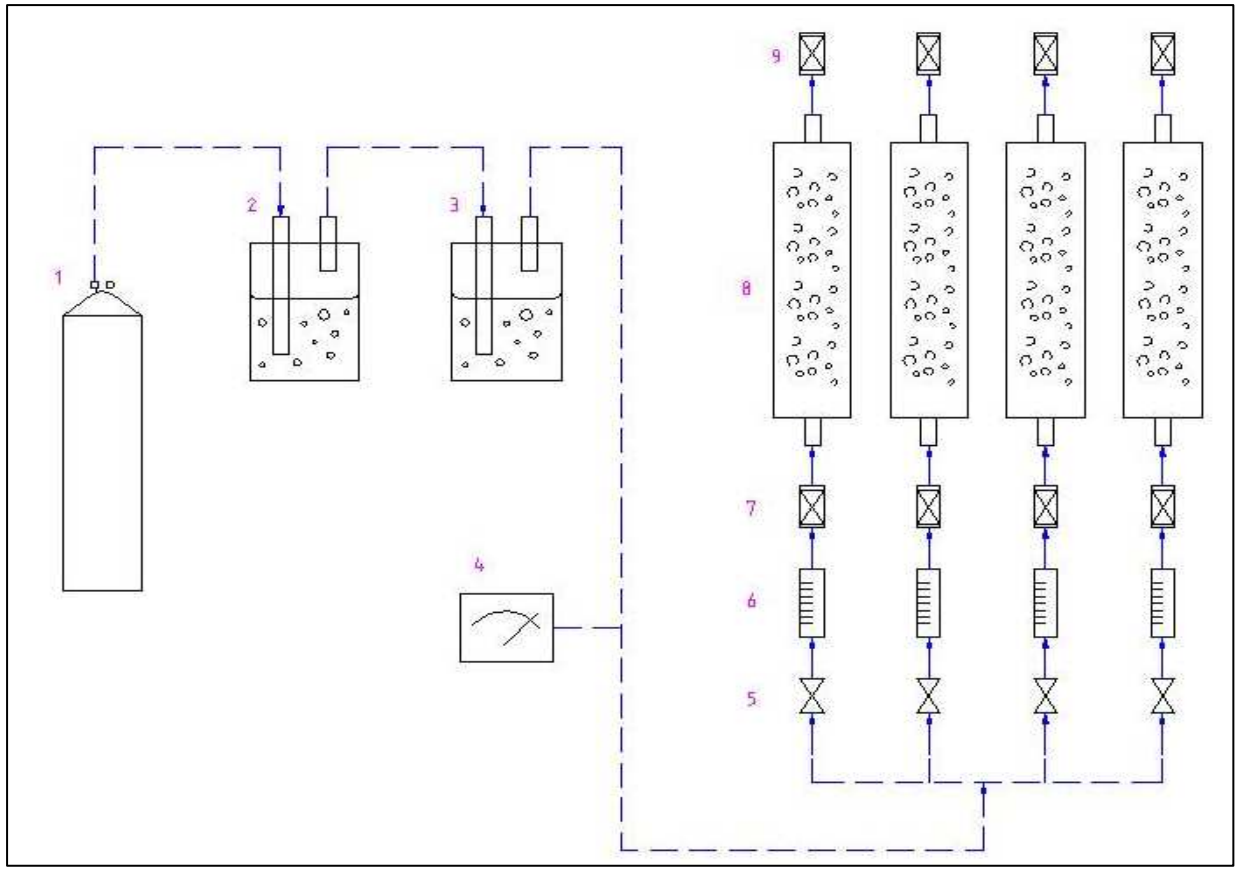

No	Description
1	Compressed dry air cylinder
2	Humidification in distilled water
3	Saturated K_2SO_4
4	Humidity sensor
5	Valves
6	Rotameters
7	Sterile filters (0.22 μm)
8	Packed-bed column
9	Sterile filters (0.22 μm)

Figure 3.1: Schematic diagram of the packed bed system

a)

b)

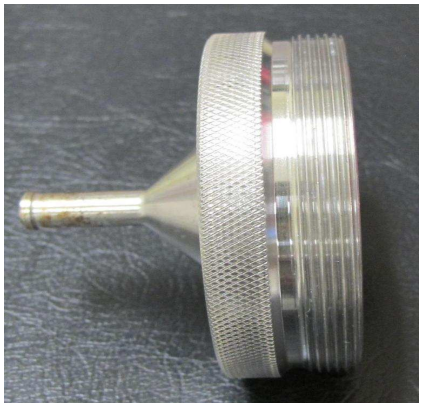

c)

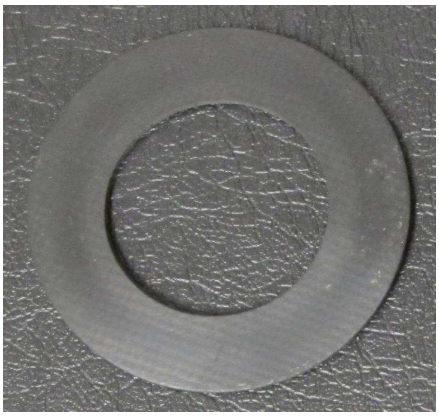

d)

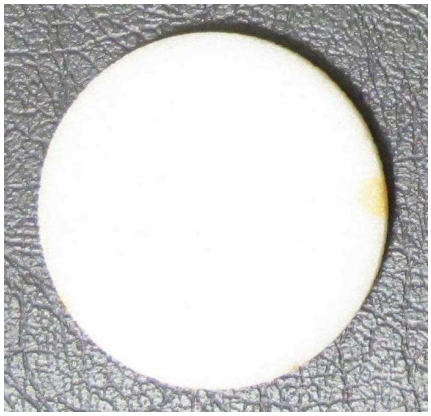

e)

f)

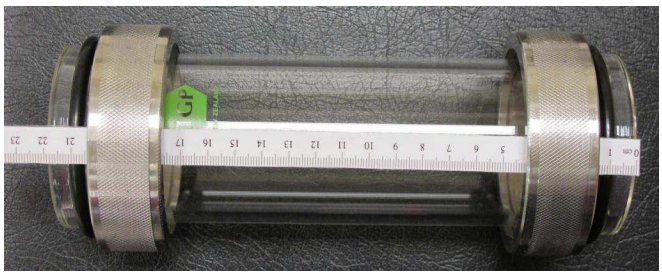

Figure 3.2: Dissembled packed-bed column.

a) lid of the column; b) lid of the column from a different angle; c) washer of the column; d) glass filter; e) ring nut for attaching a to f; f) the column

Figure 3.3: Packed-bed columns for solid-state cultivation

The rice substrate for each bed was prepared as follows: 120 g of rice was placed in a 500 mL beaker and 132 mL of deionized water was added to achieve the required initial moisture content of approximately 54 - 57% (g water per 100 g wet substrate). 12 mL of 0.128 M $ZnSO_4 7H_2O$ was added to the rice. The rice was allowed to soak at 30°C for 1 h and then the beaker was covered with two layers of aluminum foil and autoclaved at 121°C for 15 min. The assembled reactors were autoclaved separately at 121^{o}C for 25 min prior to use.

After the steamed rice had cooled to room temperature, the rice was inoculated with 12 mL of a 10^7 spore mL^{-1} inoculumn. The inoculumn was mixed well with rice in an aseptic manner. The inoculated rice was then filled into the reactors aseptically using sterilized spatula and spoon. Inoculated rice beds with an initial moisture content of approximately 54-57% were aerated from the bottom of the column (0.052 m diameter, 0.22 m height) at various constant aeration rates of 0.05, 0.2, 0.5, 1.0, and 2.0 L min^{-1} using humidified air with a relative humidity (RH) of 97–99% (Figure 3.1). RH was controlled by passing the compressed air through distilled water and then a saturated potassium sulfate (K_2SO_4) solution prior to entry in the reactors (Han and Mudgett, 1992) (Figure 3.1). RH was measured by a hygrometer (GonDo Humidity Transmitter TRH

301, Bell Technology Limited, New Zealand). The schematic diagram of the packed bed system is shown in Figure 3.1.

In a separate experiment, rice with different initial moisture content of approximately 45%, 57.5%, and 70% was used in the beds. This was prepared by mixing rice (130, 120, and 110 g) with an appropriate amount of deionized water in 500 mL beakers. $ZnSO_4 7H_2O$ solution (1 mL per 10 g rice; 0.128 M) was added to each beaker. The rice was then soaked (1 h) and autoclaved (121^{o}C, 15 min). Separately autoclaved glass columns were aseptically filled with rice to a height of 0.18 m.

3.3.3.2 Experimental design

The investigation of the combined effects of the initial moisture content of rice and the aeration rate in the bed, on pigment production and biomass growth used an experimental design that was established with the Design Expert (Stat-Ease, Inc, Version 6.0.8) and Statistica Packages (Version 5.5, 1999; Tulsa OK, USA). Various initial moisture contents of the substrate (approximately 45%, 57.5%, and 70%) were treated with various aeration rates of 0.05, 0.125, and 0.2 L min^{-1}. The combination of the two variables for the experimental runs is shown in Table 3.3.

Table 3.3: Experimental design for the effects of initial moisture content and aeration rate

Run	Factors	
	Initial moisture content (%)	Aeration rate (L min^{-1})
1	57.5	0.2
2	45	0.05
3	57.5	0.125
4	45	0.125
5	57.5	0.125
6	70	0.2
7	70	0.05
8	57.5	0.05
9	70	0.125
10	45	0.2

The sterilized beds were filled to the required depth with rice and operated in accordance with the cultivation protocol discussed in Section 3.3.3.3. Sterilized thermocouples were positioned at different bed depths of 1.5, 4.5, 7.5, 10.5, 13.5, and 16.5 cm to record the bed temperature using a multichannel temperature data logger (Agilent 34970A, Data Acquisition/ Switch unit, Malaysia). The air entering the columns was sterilized by filtration through 0.2 μm air filters (Midisart 2000, Sartorius Stedim Biotech, Germany).

3.3.3.3 Cultivation method

3.3.3.3.1 Inoculum preparation

Monascus ruber ICMP 15220 was grown on Potato Dextrose Agar (PDA) slants as noted in Section 3.3.2.2.1, to produce a standardized spore suspension (approximately 10^7 spores mL^{-1}). This standardized suspension was used as the inoculum.

3.3.3.3.2 Inoculation and cultivation

The steamed and cooled rice (room temperature) was inoculated aseptically with 1 mL spore suspension per 10 g of rice. The inoculated rice was mixed aseptically. 110 g (dry weight) of inoculated steamed rice was then placed in a packed bed reactor (0.052 m internal diameter, 0.18 m bed height) for cultivation (Figure 3.3). The bioreactor columns were covered with aluminium foil (to maintain darkness), and incubated at 30^oC for 18 days unless otherwise mentioned. At the end of the fermentation, the entire packed-bed of substrate was removed from the column as a plug and was carefully cut into six slices of equal height.

3.4 Assay methods

3.4.1 Agar plates culture

3.4.1.1 Colony diameter

The diameter of the fungal colonies on agar plates was measured with a ruler from one side of the colony to the other through its center. Measurements were made at intervals of approximately 24 h. Several measurements were made at any given time and the values were averaged. A linear regression line of a colony radius (Carvalho *et al.*, 2005) against time plot was used to obtain the growth rate (mm day^{-1}).

3.4.1.2 Colour

A CIE (Commission International de I' Eclairage) L* a* b* colour system (McGuire, 1992) was used for colour determinations on agar plates culture. Coloration was determined with a Chroma meter (Minolta, CR-200, Japan), which measured the spectrum of the reflected light and converted it into a set of colour coordinates (L*, a*, and b*) values. These coordinates were represented in a three dimensional space that contained all the colours, the CIELAB colour space (1976) (Fabre *et al.*, 1993). The value of L* represented "lightness", which equaled 0 for black and 100 for white; the a* axis showed the amount of red (+) or green (-), while the b* axis showed the amount of yellow (+) or blue (-). The colorimeter had an 8 mm diameter of a viewing area and was calibrated before each use with a standard tile (1864-721 Konica Minolta Sensing, INC, Japan) that had the colour coordinates of L* = 95.49, a* = -0.11, and b* = 2.420. Measurements were made in triplicate at the center of growth of the colony.

3.4.2 Submerged culture

3.4.2.1 Biomass (dry cell weight)

Biomass concentration was determined by filtering the culture broth (30 mL) through a pre-weighed Whatman glass microfiber filter disc Grade GF/C (pore size 1.2 µm, Whatman Schleicher & Schuel, Whatman International Ltd., England). The filter paper was washed twice with distilled water (30 mL) and dried at 80^{o}C in an oven (Watvic incubator, Clayson Laboratory Appratus, New Zealand) for 24 h (Lin and Demain, 1991).

The dry samples were cooled to room temperature in a desiccator for 2 h and then weighed. Biomass was determined by gravimetric analysis. The biomass concentration was calculated using the following equation:

$$\text{Biomass}\left(g\ L^{-1}\right)=\left(\frac{\left(\begin{array}{c}\text{weight of dried sample}\\ \text{on filter paper}\end{array}-\begin{array}{c}\text{weight of empty}\\ \text{filter paper}\end{array}\right)(g)}{\text{volume of culture broth }(L)}\right) \qquad \text{Equation 3.1}$$

3.4.2.2 pH

The pH of the culture broth was measured immediately after sampling by using a calibrated pH meter (Orion pH meter, Watson Victor Ltd., New Zealand) (Dominguez-Espinosa and Webb, 2003).

3.4.2.3 Pigment extraction and analysis

3.4.2.3.1 Extracellular pigment

Pigment concentration was determined by spectrophotometry. A 10 mL sample of culture broth was filtered using qualitative filter paper (Grade 4, Whatman Schleicher & Schuel, Whatman International Ltd., England) and washed (2 × 10 mL) with distilled water. The washed mycelia were kept aside for measuring the intracellular pigment. The filtrate was made up to 50 mL with distilled water and then measured on a UV visible spectrophotometer (Ultrospec 2000, Pharmacia Biotech, England) at 400, 470, and 500 nm for yellow, orange, and red pigments, respectively (Carels and Shepherd, 1977; Johns and Stuart, 1991; Lin *et al.*, 1992; Orozco and Kilikian, 2008). If necessary, the filtrate was further diluted with distilled water to ensure that the absorbance reading was ≤ 0.9. The uninoculated medium was used as the blank. The pigment absorbance was then calculated by multiplying the measured absorbance by the dilution factor (*df*). The pigment production was estimated using the equation:

Absorbance of extracellular pigment:

$$(AU_{Total\ extra}) = AU_{extra} \times \left(\frac{50\ mL}{10\ mL} \right) \times df \qquad \text{.....Equation 3.2}$$

where, *df* is the dilution factor and AU_{extra} is the absorbance of the diluted sample.

3.4.2.3.2 Intracellular pigment

The freshly harvested washed mycelia from the above step (Section 3.4.2.3.1) were scraped off the filter paper with a spatula and transferred to a 150 mL Erlenmeyer flask and 10 mL of 95% ethanol was added. The suspension was allowed to stand at 30^{o}C for 12 h (Lin and Demain, 1991; Tseng *et al.*, 2000). The supernatant was then recovered by centrifugation (Himac CR 22GII, Hitachi Koki Company Limited, Japan) at 10 000 *g*, 10 min. The absorbance of the suspension was measured at 500, 470, and 400 nm using a UV visible spectrophotometer to determine red, orange, and yellow pigments, respectively (Chen and Johns, 1993; Lin and Iizuka, 1982; Lin and Demain, 1991). If necessary, the supernatant was diluted with 95% ethanol to ensure that the absorbance reading was ≤ 0.9. The pigment absorbance was calculated as follows.

Absorbance of intracellular pigment $(AU_{Total\ intra}) = AU_{intra} \times df$ ……Equation 3.3

where, AU_{intra} is the absorbance unit of the diluted supernatant and *df* is the dilution factor.

The total absorbance unit (*AU*) of the culture broth was conducted as follows:

Total absorbance unit $(AU) = AU_{Total\ extra} + AU_{Total\ intra}$ ……Equation 3.4

The $AU_{Total\ extra}$ and $AU_{Total\ intra}$ values were from Equation 3.2 and Equation 3.3, respectively.

3.4.2.4 Glucose determination

Glucose was estimated spectrophotometrically by the dinitrosalicylic acid (DNS) method (Miller, 1959; Ishiaku *et al.*, 2002; Sinegani and Emtiazi, 2006). A 3 mL sample of the culture filtrate was mixed with 3 mL of DNS reagent and then heated in a boiling water bath for 15 minutes. Then 1 mL of Rochelle salt (40% (g/100 mL)) potassium sodium tartrate in deionized water) solution was added to stabilize the colour. Subsequently, the mixture was cooled to room temperature in a cold water bath and the absorbance was recorded at 575 nm. The measurements were against a blank that was made by replacing the culture filtrate in the above procedure with deionized water.

The DNS reagent (g L^{-1}) consisted of 10.0 g dinitrosalicylic acid (DNS), 2.0 g phenol, 0.5 g sodium sulphite, and 10.0 g sodium hydroxide dissolved in 1 L of deionized water (Miller, 1959).

A glucose standard curve (Figure 3.3) was prepared by analyzing the various dilutions (0, 0.06, 0.09, 0.11, 0.14, 0.17 mg/mL) of a standard aqueous glucose solution. The glucose content of the samples was calculated as follows:

$$\text{Glucose content } (g\ L^{-1}) = \frac{Abs_{575}}{0.0049} \times \frac{\text{total volume of mixture}}{\text{sample volume } (mL)} \times df \times 10^{-3} \quad \ldots\ldots \text{Equation 3.5}$$

where, *df* is the dilution factor

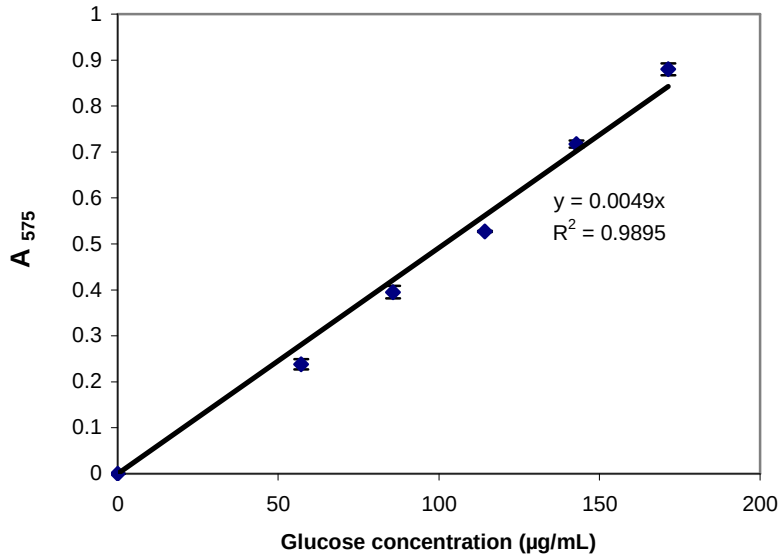

Figure 3.4: Calibration curve for glucose

3.4.2.5 Red pigment stability

Effects of light, pH, and temperature on stability of the red pigment were assessed.

The submerged culture broth was filtered through the Whatman glass microfiber filter (Grade GF/C, Whatman Schleicher & Schuel, Whatman International Ltd., England) to separate the mycelia and the supernatant. The filtrate was again filtered using a sterile filter (0.45 µm; Minisart, Sartorius stedim Biotech, Germany) to remove any microbial contamination. To asses the stability of the red pigment under standard laboratory lightning, four screw capped sterile Pyrex tubes (25 mL) were aseptically filled separately with 10 mL of the sterile filtrated sample. The tubes were stored at room temperature (approximately 25^{o}C) for 168 h. Two of the tubes were covered with aluminum foil and used as controls. Time zero pigment absorbance was recorded in each tube against distilled water as a reference.

In a separate experiment, to investigate the effect of pH on stability, the sterile filtrated sample was subjected to different pH values: neutral (pH 7), acidic (pH 4), and alkaline (pH 10) for 8 h in sterile Pyrex tubes covered with aluminum foil. All tubes were held at room temperature (approximately 25^{o}C). The various pH values were attained by adding a few drops of either 0.5 M HCl or 0.5 M NaOH.

To investigate the effect of temperature on stability, sterile filtrated samples were separately subjected to different temperatures of: 70^{o}C for 8 h, boiling water bath for 1 min, and autoclave conditions (121^{o}C for 15 min).

For stability measurements on pigments produced by solid-state culture, 2.0 g of freeze-dried fermented solids sample in a Erlenmeyer flask was extracted with 200 mL 95% ethanol for 2 h at 180 rpm, then centrifuged at 10 000 *g* for 10 min to remove the suspended solids. As described for the submerged culture sample, the extracted ethanol solution was sterile filtered and dispensed in sterile Pyrex tubes. Two tubes containing 10 mL of extracted ethanol solution were stored (at room temperature) under standard laboratory lightning for measuring the stability towards light. Another two tubes were stored covered with aluminum foil for a comparison. Time zero pigment absorbance was recorded for all tubes against a blank of 95% ethanol.

For pH stability measurements, the extracted ethanol solution was subjected to different pH values of neutral (pH 7), acidic (pH 4), and alkaline (pH 10) for 8 h in sterile Pyrex tubes covered with aluminum foil. All tubes were held at room temperature (approximately 25^{o}C). The pH was adjusted as previously specified.

For measuring stability to temperature, the extracted sterile ethanol solution was separately subjected to different temperatures of 70^{o}C for 8 h, boiling water bath for 1 min, and autoclave conditions (121^{o}C for 15 min), in sealed tubes.

In all cases, two tubes were subjected to each condition. The red pigment was measured spectrophotometrically as explained in Section 3.4.2.3.1.

3.4.2.6 Pigment purification

3.4.2.6.1 Column chromatography

The mycelium was separated from the culture broth by filtration with qualitative filter paper (Grade 4, Whatman Schleicher & Schuel, Whatman International Ltd., England). The filtrate and the mycelia were then separately freeze dried at -80^{o}C for 24 h (Telstar CRYODOS-80 Freeze dryer, Spain). 0.5 g of freeze dried filtrate and mycelia powder samples were extracted in Erlenmeyer flask with 20 mL of ethanol (95%) at 180 rpm, 30^{o}C for 24 h. The sample suspension was then sonicated in a sonicator bath (Bandelin Sonorex, 230 V 50/60 Hz, Germany) for 15 min followed by centrifugation (Ependorf Centrifuge 5702, Global Science, Germany) at 3000 *g* for 10 min. The samples were then filtered through the glass filter (Millipore glass filter, Millipore Corporate, USA) to remove the suspended solids and transferred to pre-weighed round-bottom flasks and evaporated to dryness under vacuum in a rotary evaporator (Rotavapor R110, Buchi Laboratories, Switzerland). The resulting solids were then dissolved in 2 mL of chloroform:methanol (50:50, vol/vol) and applied to pre-packed Solid Phase Extraction (SPE) chromatographic columns (Altech silica 2000 mg, Grace Davison Discovery Science, United States), separately.

Prior to the sample application, the pre-packed chromatographic columns had been washed with chloroform (20 mL). After application of the samples, the columns were first eluted with 100 mL of chloroform:methanol (90:10, vol/vol) to elute the less polar products. Then the columns were eluted with 300 mL of chloroform:methanol (50:50, vol/vol) (Blanc *et al.*, 1994) to recover the more polar compounds.

The fractions from the columns were collected in pre-weighed round bottomed flasks and evaporated under vacuum to dryness to obtain the purified pigments (Yongsmith *et al.*, 1994). The recovered solids in the flasks were then re-weighed. The recovered solids were dissolved in 2.5 mL of 95% ethanol and measured in a scanning UV visible spectrophotometer (Spectrophotometer U-200, Hitachi, Japan) at a wavelength range of 350 to 650 nm. Ethanol (95%) was used as the blank and measured in the same wavelength range. This provided the UV spectra of the various pigments.

3.4.2.6.2 Thin layer chromatography (TLC)

Individual pigments isolated from the various fractions of column chromatography and the crude extracts used in column chromatography were further analyzed by preparative thin layer chromatography (TLC Silica gel 60, 20 × 20 cm, Merck KGaA, Germany). Initially, the preparative TLC plate was marked with a pencil for the start and finishing lines. These marks were used to guide the plate development.

Then, approximately 100 µL (1 mg/mL for purified pigment, 3 mg/mL for crude sample) of the sample was carefully applied to the preparative-TLC plate using a 10 µL pipette tip with intermediate drying by a hair dryer. The development solvent system of chloroform: methanol: water (65:25:4, vol/vol) (Blanc *et al.*, 1994) was carefully poured into the flat-bottomed (20 × 20 cm) chamber. The spotted TLC plate was then placed vertically in the solvent filled chamber. The plate was developed for approximately 90 min or until the solvent front reached the finishing line.

For the purified pigment sample, the red spot obtained was scrapped off, dissolved in 95% ethanol, and measured using a scanning UV visible spectrophotometer (Spectrophotometer U-200, Hitachi, Japan) at a wavelength range of 380 to 650 nm. Ethanol (95%) was used as the blank.

For the crude samples, the pigments separated into various spots and the retention factor (R_f) values of these were calculated as follows:

$$R_f = \frac{\text{distance traveled by the component } (mm)}{\text{distance traveled by the solvent front } (mm)} \qquad \text{……..Equation 3.6}$$

3.4.3 Solid-state culture

3.4.3.1 Biomass (dry cell weight)

The biomass growth in solid-state culture was estimated by determining the *N*-acetyl-D-glucosamine released by the acid hydrolysis of the chitin which is present in the cell wall of fungi (Sakurai *et al.*, 1977).

Fermented solids were freeze dried (Telstar CRYODOS-80 Freeze dryer, Spain) at -80^{o}C for 24 h and milled (for 2-3 min) to a fine powder with a grinder (Breville, Model CG 2B, Australia) at room temperature for further tests. The powder was stored at -20^{o}C for further analysis.

0.5 g of dried fermented solids powder was mixed with 2 mL of 60% (vol/vol) sulfuric acid and the mixture was kept at 25^{o}C for 24 h (Roopesh *et al.*, 2006). Then the mixture was diluted with distilled water to make a 1 N solution of sulfuric acid and autoclaved at 121^{o}C for 1 h. The mixture was cooled to room temperature and neutralized with 5 N NaOH to pH 7 and the final volume was made up to 60 mL with deionized water. The diluted solution was filtered through a 0.45 µm filter (Minisart RC15, Sartorius Stedim Biotech, Germany). 1 mL of filtered diluted solution was mixed with 1 mL of acetyl acetone reagent (2% (vol/vol) of acetyl acetone in 1 N sodium bicarbonate (Na_2CO_3)). The acetyl acetone reagent was freshly prepared as it was stable only for 2-3 h at 18^{o}C (Rondle and Morgan, 1955).

The mixture was then held in a boiling water bath for 20 min. After cooling to room temperature, ethanol 95% (6 mL) was added followed by 1 mL of Ehrlich reagent (2.67% (w/v) of p-dimethylaminobenzaldehyde (Merck) in 1:1 mixture of ethanol and concentrated hydrochloric acid) (Swift, 1973). The mixture was incubated in a water bath (Grant GD100, Grant Instruments Cambridge Limited, England) at 65^{o}C for 10 min. After cooling, the optical density was read at 530 nm against the reagent blank using UV visible spectrophotometer (Ultrospec 2000, Pharmacia Biotech, England). The reagent blank had been prepared using the above procedure but with the fermented solids being replaced with unfermented rice.

N-acetyl-D-glucosamine was used as the standard (Babitha *et al.*, 2007a; Babitha *et al.*, 2007b). *N*-acetyl-D-glucosamine standard curve (Figure 3.5) was prepared by analyzing various dilutions (22, 44, 66, 88 and 111 µg mL^{-1}) of a standard aqueous solution. The standard curve was used to convert the measured absorbance of the sample to *N*-acetyl-D-glucosamine content. Thus, 1 mL of standard solution (various dilutions) was mixed with 1 mL of acetyl acetone reagent. The mixture was then incubated in a boiling water bath for 20 min and left to cool to room temperature. Then 6 mL of ethanol was added followed by 1 mL of Ehrlich reagent. The mixture was then incubated at 65^{o}C for 10 min. After cooling, the optical density was read at 530 nm as described earlier.

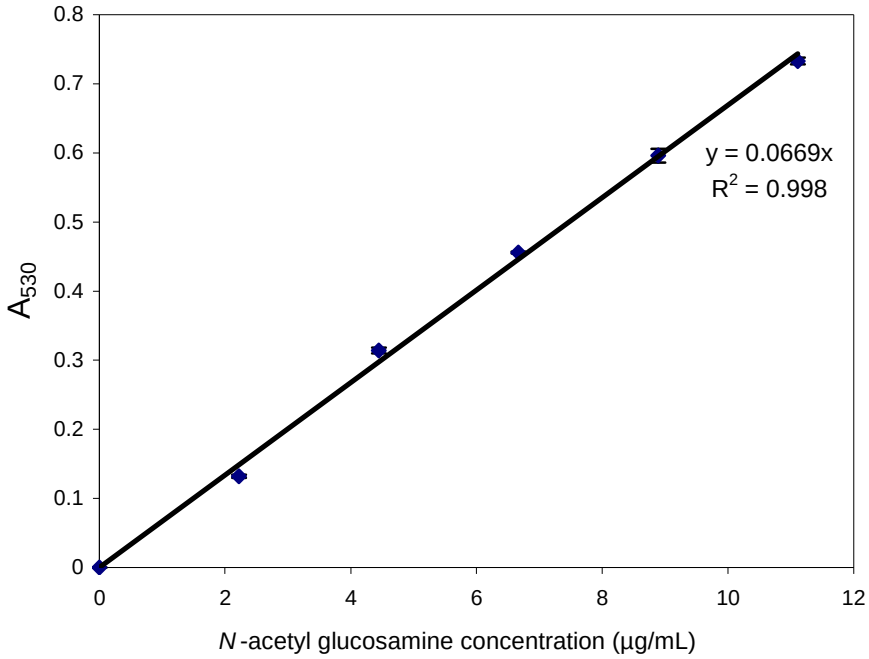

Figure 3.5: Calibration curve for *N*-acetyl-D-glucosamine

The biomass content of samples was calculated as follows:

$$\text{Biomass}\left(mg\,cell\,dry\ \ weight / g\,dry\,matter\right) =$$

$$\frac{Abs_{530}}{0.0669} \times \frac{\text{total volume of mixture}\left(mL\right)}{\text{sample volume}\left(mL\right)} \times \frac{60\,mL}{0.5\,g} \times df \times 10^{-3} \times \frac{1}{cf} \quad \text{...Equation 3.7}$$

where, Abs_{530} is absorbance at 530 nm, df is the dilution factor and cf is the conversion factor of experimentally determined ratio of glucosamine to cell dry weight (mg mg^{-1}).

3.4.3.2 pH

Two grams of fresh moist fermented mass was thoroughly mixed with 5 mL of distilled water using a vortex mixer for 1 min and the pH of the resulting suspension was measured using a calibrated pH meter (Orion pH meter, Watson Victor Ltd., New Zealand) (Han and Mudgett, 1992).

3.4.3.3 Pigment extraction and analysis

0.5 g of freeze dried powdered fermented solids (Section 3.4.3.1) was extracted with 20 mL of 95% ethanol in an incubator shaker (InforsHT, Multitron, Infors AG, Germany) for 2 h at 180 rpm in an Erlenmeyer flask. The extract was then centrifuged at 10 000 *g* for 10 min to remove suspended solids. The supernatant was analyzed by a spectrophotometer using a 95% ethanol blank (Chiu and Poon, 1993; Johns and Stuart, 1991; Lin *et al.*, 1992). Pigment concentration was measured using a double beam spectrophotometer (Ultrospec 2000, Pharmacia Biotech, England) at 400, 470 and 500 nm for yellow, orange, and red pigments, respectively, taking into consideration the dilution factor of the sample (Carvalho *et al.*, 2003; Chiu and Poon, 1993). The results were expressed as absorbance unit (AU) per gram of dried solids (Lin and Iizuka, 1982):

Total absorbance of pigment $(AU\ g^{-1}) = Abs \times \frac{20}{0.5} \times df$ ……Equation 3.8

For measurement in the packed-bed bioreactor, the overall or averaged pigment production was calculated as:

$$\left(AU\ g^{-1}\right) = \frac{\left(AU\ g^{-1}\right)_{level\,1} + \left(AU\ g^{-1}\right)_{level\,2} + ... + \left(AU\ g^{-1}\right)_{level\,6}}{6}$$ .....Equation 3.9

The $AU\ g^{-1}{}_{level\ 1,}$ $AU\ g^{-1}{}_{level\ 2}$ to $AU\ g^{-1}{}_{level\ 6}$ were from Equation 3.8.

3.4.3.4 Moisture content

The moisture content of the fermented solids (1 g) was determined by heating the accurately weighed fresh samples in a hot air oven (Contherm Digital series oven, Contherm Scientific Company, New Zealand) at 105^{o}C for 24 h. The weight was again measured after cooling the samples to room temperature in a desiccator (Johns and Stuart, 1991; Yongsmith *et al.*, 2000). The moisture content (wet basis) was calculated as follows:

$$\text{Moisture content}(\%) = 100\% \times \left(\frac{\left(\begin{matrix} \text{wet weight} \\ \text{of the solids} \end{matrix} - \text{dry weight} \right)(g)}{\text{wet weight of the solids}(g)} \right) \quad \ldots\ldots \text{Equation 3.10}$$

3.4.3.5 Temperature

Temperature profile in the packed-bed bioreactor during fermentation was determined using a multichannel temperature data logger (Agilent 34970A, Data Acquisition/ Switch unit, Malaysia) and sterilized thermocouples placed at the bed depths of 1.5, 4.5, 7.5, 10.5, 13.5, and 16.5 cm.

3.4.3.6 Water activity

The water activity (a_w) of fermented solids was determined at room temperature using a Aqualab water activity meter (Decagon Devices, Model CX-2, Pullman, Washington, USA). The equipment was calibrated with saturated salt solutions in the a_w range of interest (Decagon Devices, Model CX-2 Manual). Each measurement was done in duplicate. Under these conditions the accuracy of the measurement was ± 0.003 a_w.

3.4.3.7 Carbon and nitrogen

The total amount of carbon and nitrogen in the long grain rice substrate was determined by the Leco CNS 2000 analyser (Model 602 600 200, USA). One gram of dried long grain rice was milled with a grinder (Breville, Model CG 2B, Australia) to a fine powder and then analyzed for carbon and nitrogen. The carbon was determined by infrared detection of carbon dioxide produced by combustion of the rice powder. Nitrogen was determined by thermal conductivity measurements on the combustion gasses. The data obtained was used for calculating the ratio carbon to nitrogen of the rice.

CHAPTER 4

Results and Discussion

4.1 General characterization of growth and pigment production on agar plates

4.1.1 Introduction

The ability of *Monascus* sp. to produce secondary metabolite and edible pigments is well known (Fabre *et al.*, 1993; Juzlova *et al.*, 1996). *Monascus ruber* ICMP 15220 has not been previously studied for growth and pigment production. As *Monascus* strains differ in their metabolic profiles, the amount of colour produced, and the tone of colour, a characterization of the ICMP 15220 strain was necessary. As the composition of the growth medium plays an important role in any fermentation process (Stanbury and Whitaker, 1984) and mycelial fungi grow on solid substrate in natural habitats (Prosser and Tough, 1991), fungal growth and pigment production were first characterized on agar plates. Agar plates are commonly used for preliminary characterization of microorganisms (Pirt, 1985).

The study on agar plates aimed to identify suitable media for growth and pigment production with a focus on the red pigment. Ten different media compositions were randomly selected from the literature on the other *Monascus* strains to examine for growth and pigment production of *Monascus ruber* ICMP 15220.

Growth was characterized by measurements of the colony diameter at different times to calculate the colony radial growth rate (Kr). The pigment coloration intensity was recorded by using a colorimeter (Section 3.4.1.2).

4.1.2 Effect of different media compositions on growth

The growth profiles were observed for a period of 7 days. Measurements were made daily in triplicate.

Figure 4.1 and Figure 4.2 show the colony diameter and radius at different times on media compositions A to J (Table 3.2). From the figures, growth occurred on all the media. The colony radial growth rates calculated from Figure 4.2 are summarized in Table 4.1. Growth on medium G was the most rapid. On this medium, the fungal colony attained a diameter of 55 mm at day 7 (Figure 4.1). The colony radial growth rate was 0.200 mm h^{-1} (Table 4.1). Medium I was the second best in terms of the ability to support growth (Figure 4.1). Media B, C, D, and J (Figure 4.1) had nearly comparable abilities to support growth. In terms of radial growth rate, the worst medium (i.e. medium H) was only 52% as capable as the best medium (i.e. Medium G).

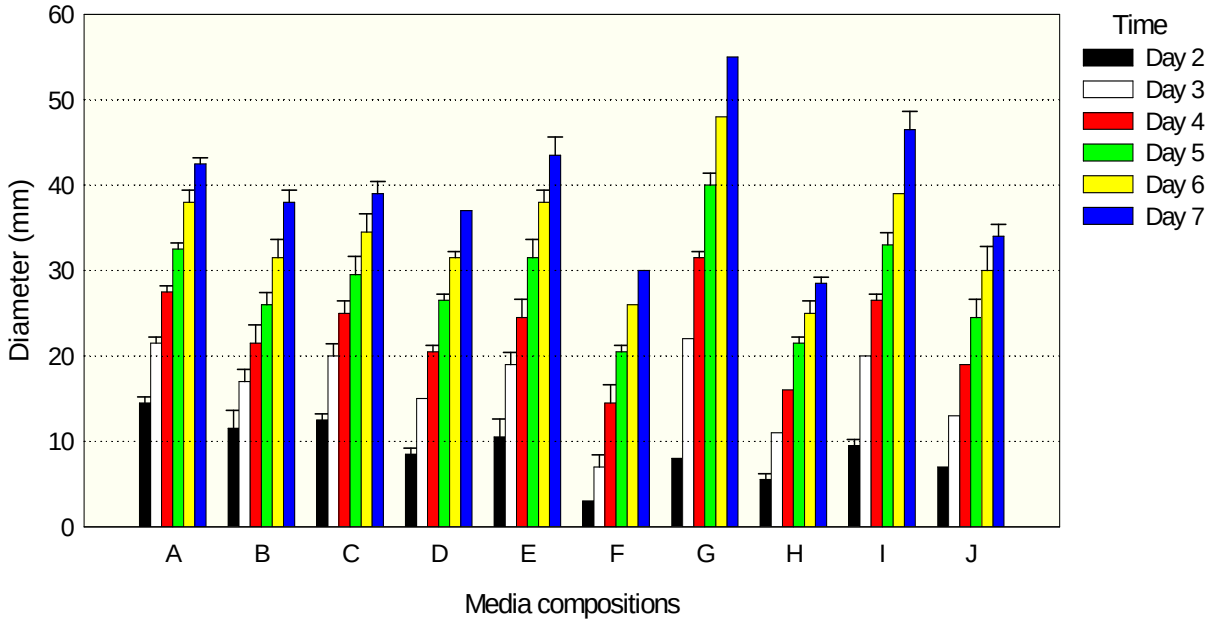

Figure 4.1: Growth profiles of *M. ruber* ICMP 15220 on different media

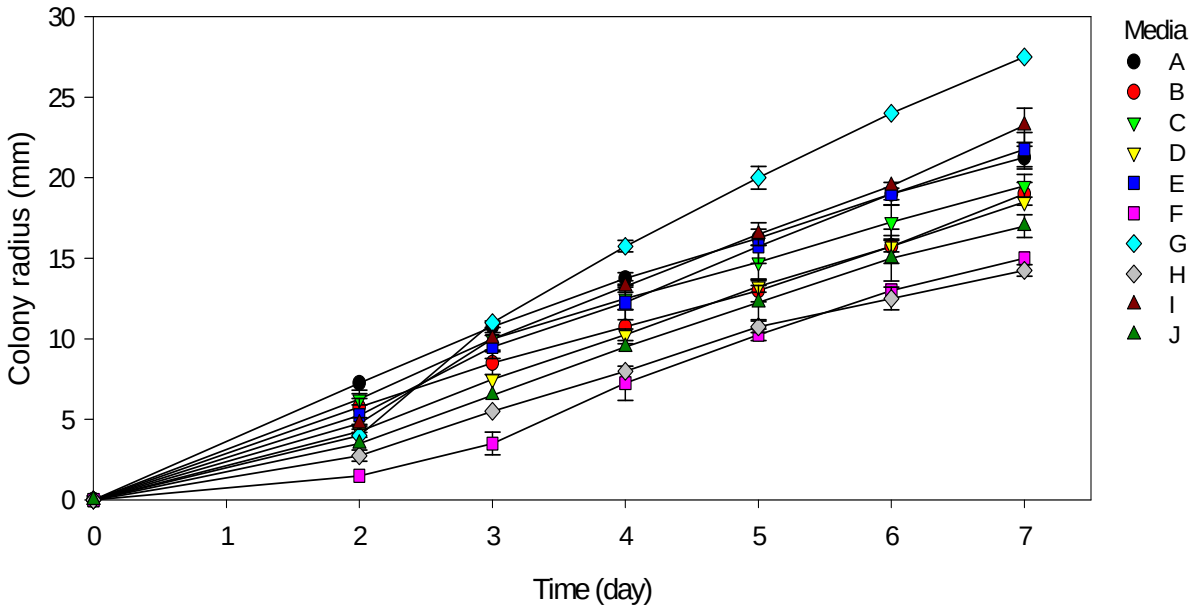

Figure 4.2: Colony radius on different media

Table 4.1: Radial growth rate on different media

Media compositions	Colony radial growth rate (Kr, mm/h)[a]
A	$(120.8 \pm 2.9) \times 10^{-3}$
B	$(108.7 \pm 0.2) \times 10^{-3}$
C	$(113.3 \pm 5.4) \times 10^{-3}$
D	$(110.3 \pm 0.7) \times 10^{-3}$
E	$(130.2 \pm 1.5) \times 10^{-3}$
F	$(104.2 \pm 0.0) \times 10^{-3}$
G	$(200.0 \pm 2.9) \times 10^{-3}$
H	$(103.1 \pm 4.4) \times 10^{-3}$
I	$(132.3 \pm 1.5) \times 10^{-3}$
J	$(110.4 \pm 2.9) \times 10^{-3}$

[a] Average and standard deviation of triplicate measurements

4.1.3 Effect of different media compositions on colour production

Pigment production by *Monascus ruber* on different media on agar plates was quantified using a colorimetric instrument (chroma meter). Chroma meter is a compact portable instrument that measures light reflected from an object's surface in terms of the three primary colours of red, green, and blue (Mapari *et al.*, 2006; Ozkan *et al.*, 2003). This instrument responds to light and colour in a similar manner as the human eye (Anonymous, 1993). Each of the primary colours is characterized in terms of three elements of hue angle, chroma value, and value of lightness.

Measurements were made by using the Minolta CR-200 Chroma meter with the CIE (Commission International de I' Eclairage) L* a* b* colour system (McGuire, 1992), as explained in the Section 3.4.1.2. Responses were read using the CIE L* a* b* colour chart (Figure 4.3) on the three-dimensional coordinate system shown in Figure 4.4. As in Figure 4.4, coordinates a* and b*, that are perpendicular to the L* axis, describe colour using four directions of +a* red at 0^o, +b* yellow at 90^o, -a* green at 180^o, and –b* blue at 270^o. While, the hue angle, h^o, measured around the wheel, shows the direction of the colour, red, yellow, blue, or green. Chroma or C* (Figure 4.4), measures the saturation or purity of the colour. The longer the C* distance, the more saturated is the colour.

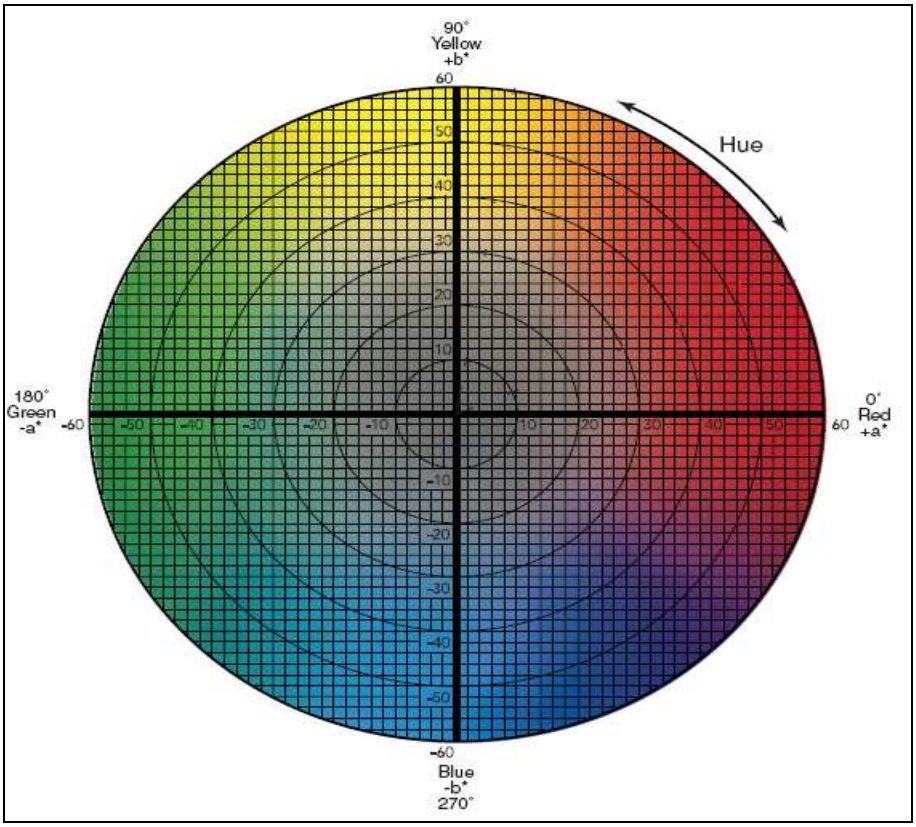

Figure 4.3: CIE L*a*b* colour chart

(Adapted from Anonymous, 2007)

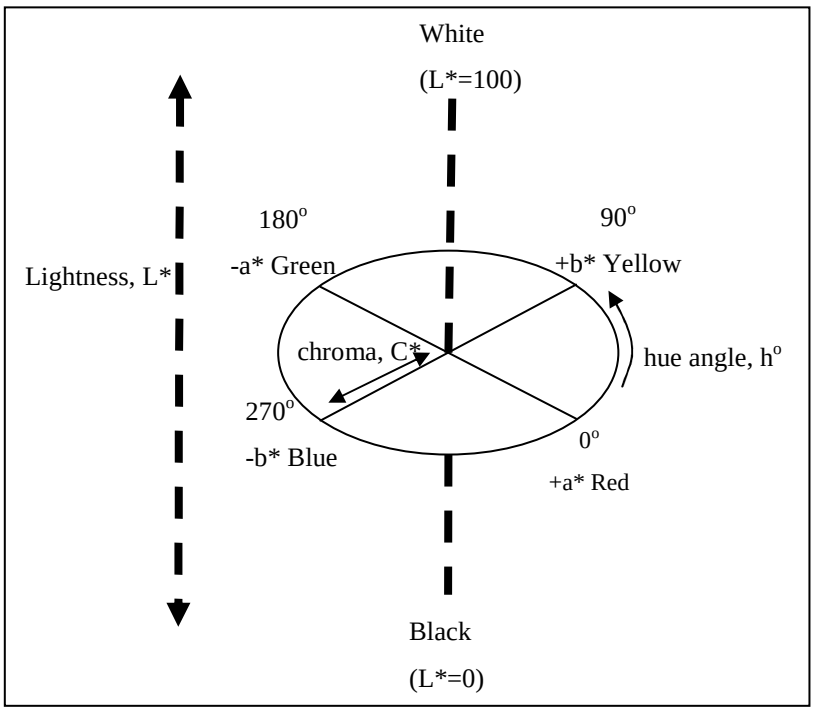

Figure 4.4: CIE L* a* b* colour system represented in three-dimensional coordinates

Time variation of lightness (L*), a*, and b* values on different media are shown in Figures 4.5, 4.6, and 4.7, respectively. The various media produced distinct patterns of variation of L*, a*, and b*. The L* value on all of the media declined with the incubation time (Figure 4.5), except for the medium J. The L* value profiles suggest that the pigmentation became more intense with time. Only in medium J, the L* value slightly increased after day 5, suggesting a reducing intensity of pigmentation (Figure 4.5).

At the end of fermentation (day 7), the colour in medium J had the highest value of a* (Figure 4.6), which meant the reddest colour of all the colonies. For medium J, the redness was high from day 4. Media D and C also gave high values of a* at 25.41 and 23.43 at day 7, respectively. Media D, F, and H showed a peak of a* value at day 6 and a subsequent decline.

The time variation of b* values, an indicator of yellowness, was similar for media C and J (Figure 4.7). For media D, F, and H there were clear peaks in the b* value profiles, but for all the other media, the b* value declined with time.

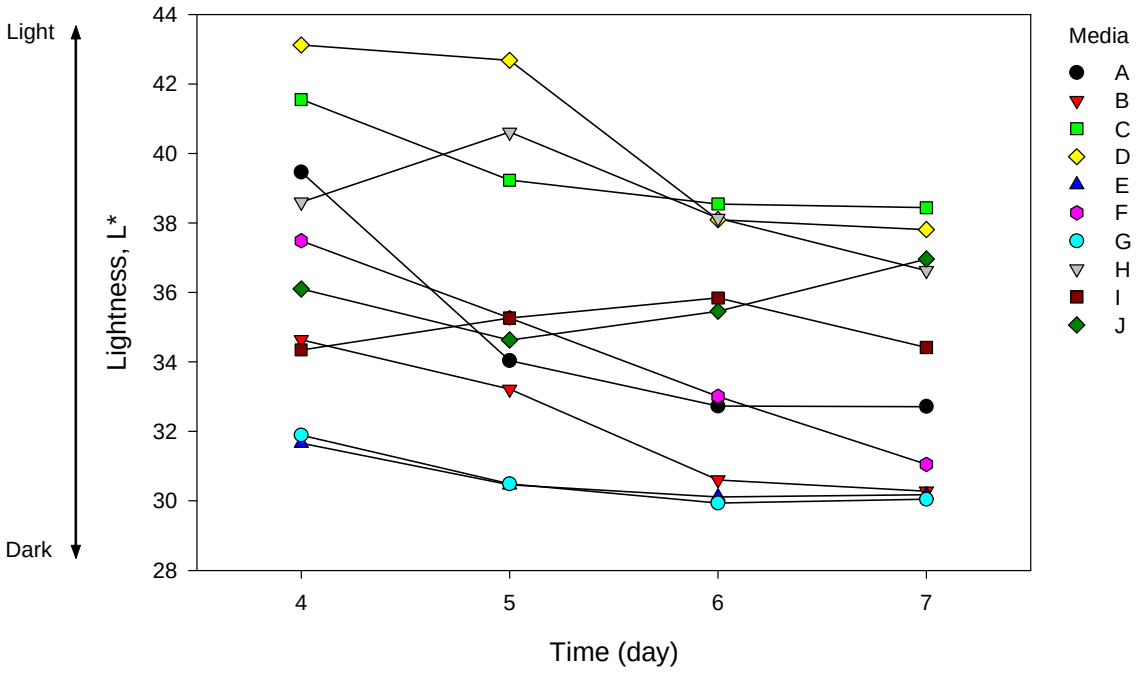

Figure 4.5: Time variation of the lightness (L*) value on different media compositions

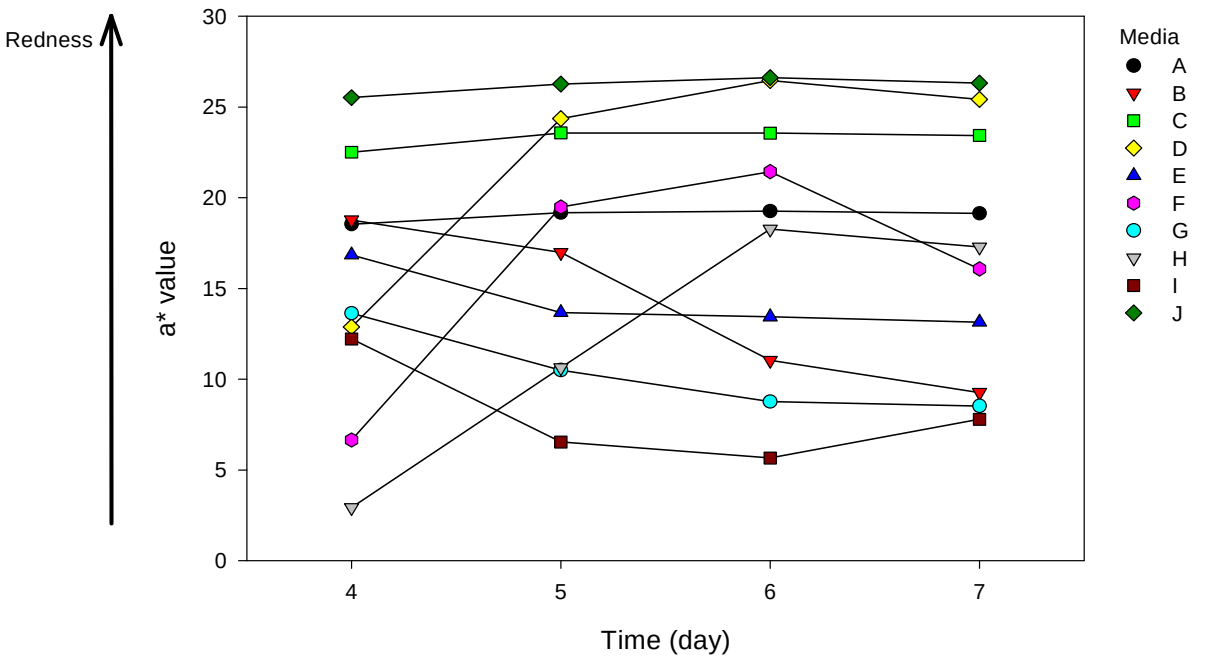

Figure 4.6: Time variation of a* value on different media compositions

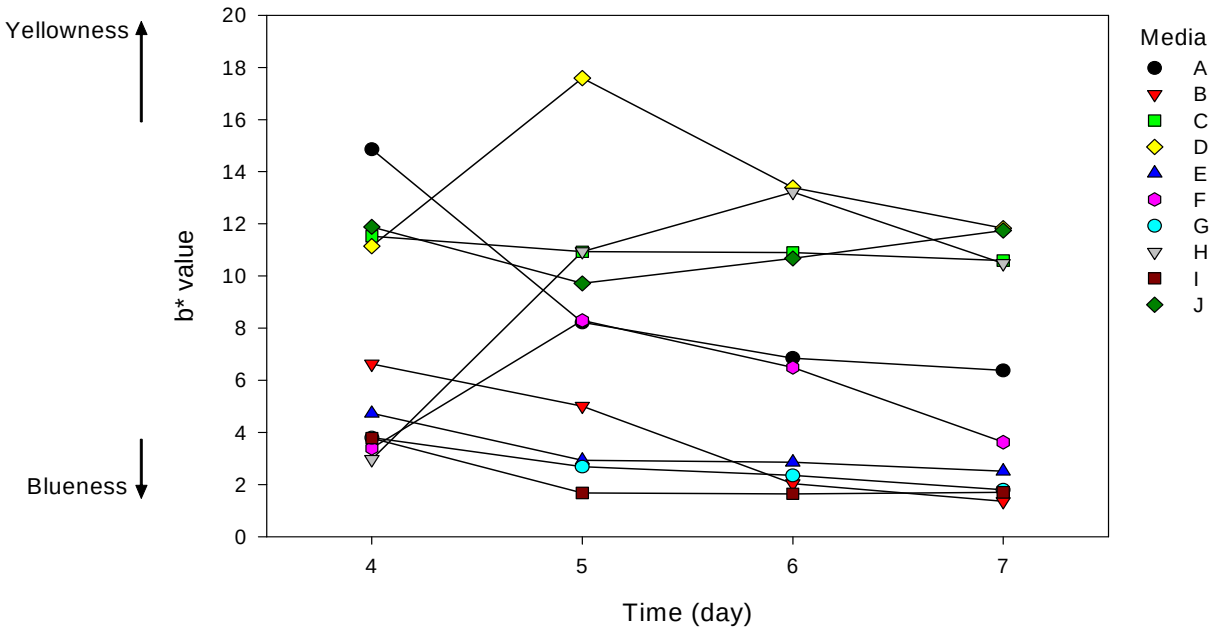

Figure 4.7: Time variation of b* value on different media compositions

The L*, a*, and b* measurements were generally quite reproducible as shown in Table 4.2. Table 4.2 also shows the calculated hue angles (h^o) and the chroma value (C*) of the colours produced by the fungus on different media near the end (day 6) of the fermentation. For the various media, the L* values varied in the range of 29 to 39 (Table 4.2). The a* and b* values were always positive. The a* values ranged from 5 to 27, whereas the b* values ranged from 1 to 14.

Table 4.2: L*, a*, b*, h^o, and C* colour values of fungal colony on different media compositions on day 6

Media composition	L*	a*	b*	Hue angle, h^o ($\tan^{-1}$ (b*/a*))	Chroma, C*
A	32.73 ± 0.16	19.26 ± 0.01	6.85 ± 0.24	19.58	20.44
B	30.61 ± 0.05	11.03 ± 1.46	2.03 ± 0.35	10.43	11.22
C	38.55 ± 2.88	23.56 ± 0.45	10.90 ± 1.78	24.83	25.95
D	38.10 ± 0.47	26.45 ± 0.81	13.39 ± 0.76	26.85	29.65
E	30.12 ± 0.06	13.44 ± 0.36	2.86 ± 0.06	12.00	13.74
F	33.01 ± 0.89	21.44 ± 1.32	6.49 ± 1.29	16.83	22.39
G	29.94 ± 0.79	8.76 ± 0.23	2.35 ± 0.09	14.99	9.07
H	38.14 ± 0.23	18.26 ± 0.64	13.22 ± 1.14	35.89	22.54
I	35.84 ± 0.92	5.66 ± 0.83	1.64 ± 0.38	16.17	5.89
J	35.46 ± 0.40	26.62 ± 0.93	10.67 ± 1.02	21.85	28.67

Values are average and standard deviation of triplicate measurements

The fungal colony pigment characterization for the various media are shown in Figure 4.8 based on the coloration scheme of Figure 4.3. The hue angles (h^o) and the chroma value (C*) varied as in Table 4.2. Coloration on medium D had the highest chroma value of 29.65 (Table 4.2 and Figure 4.8), or the most intense colour (McGuire, 1992), closely followed by medium J with a C* value of 28.67. The hue angles for media D and J were 26.85^o and 21.85^o, respectively. The observed hue angles (Figure 4.8) were within the 0-60^o range reported for pigment of other *Monascus* species (Jung *et al.*, 2003; Jung *et al.*, 2005; Mapari *et al.*, 2006). The hue angle refers to the direction of the colour, a lower degree indicates a colour trend towards redness.

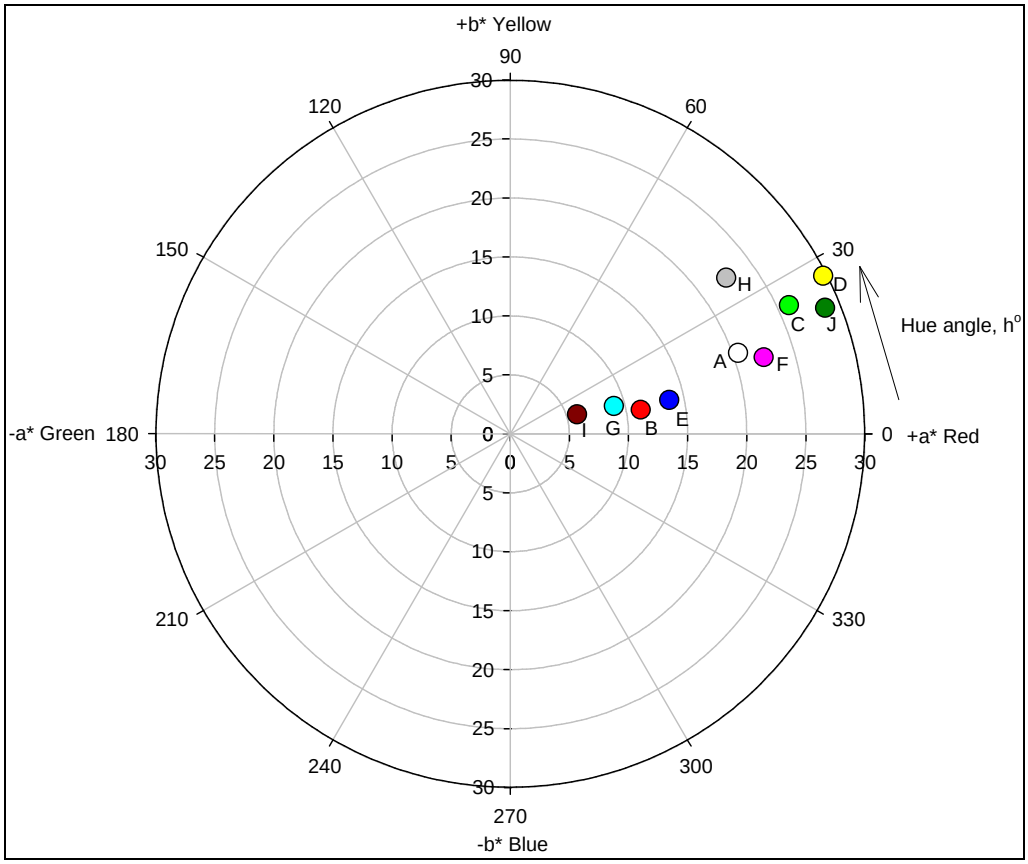

Figure 4.8: Polar scatter plot of the pigment hue angles and chromas for different media compositions at an L* value of 34.25 ± 3.42 on day 6.
The letters A to J denote the various media (Table 3.2)

In view of the low C* values ranging from 5 to 14, the colours produced on media E, B, G, and I were relatively dull or grey (Table 4.2 and Figure 4.8) compared to colours produced on the other media.

Figure 4.9 shows the growth morphology of *M. ruber* ICMP 15220 on the media J, D, and A on day 2, 5 and 7. These media were selected for comparison in Figure 4.9, as medium J was the best for red pigment production, followed by medium D, while medium A has been the most commonly used medium in the literature on *Monascus* species. Observations showed that the fungal colonies (Figure 4.9) were generally circular. Aerial development of the colonies began at day 2 (Figure 4.9). The mycelia were initially white in colour (day 2) and then turned to a reddish colour as they aged. Red coloration beyond the borders of some of the colonies (Figure 4.9) suggests that the pigment produced by the mycelia diffused outward faster than the radial growth of the

colony (i.e. medium J). A similar behaviour was seen on medium D, except that the mycelia turned to slightly orange colour as they aged. Medium A (PDA), which is most commonly used in the literature, clearly supported reasonably good growth but not the best development of the red colour based on quantitative measurements with the chroma meter at the center of the colony.

Media	Fungal colony morphology		
	Day 2	Day 5	Day 7
J (a)	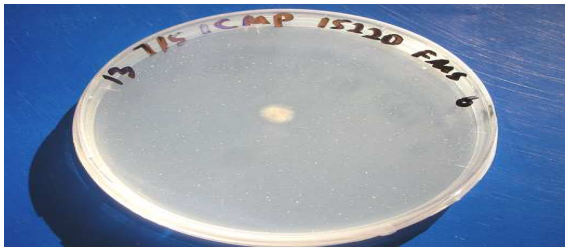	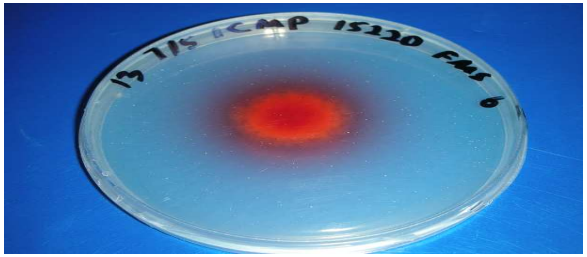	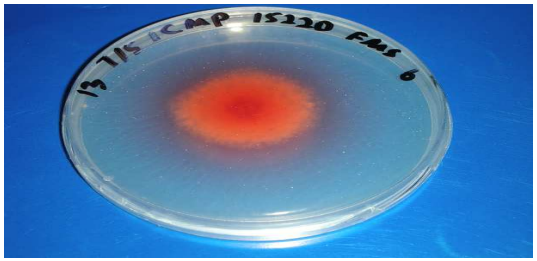
D (b)	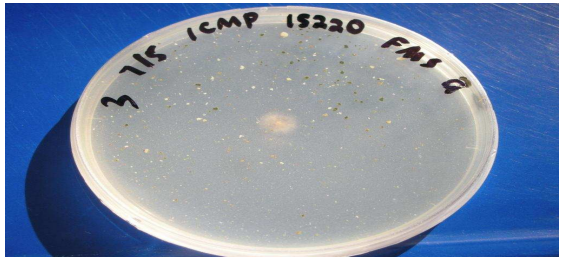	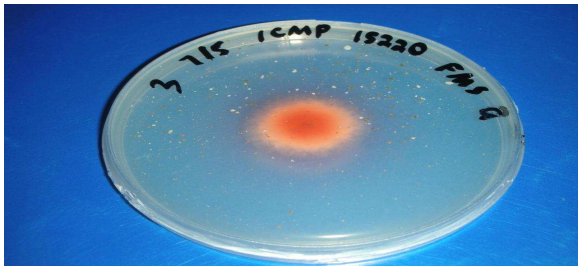	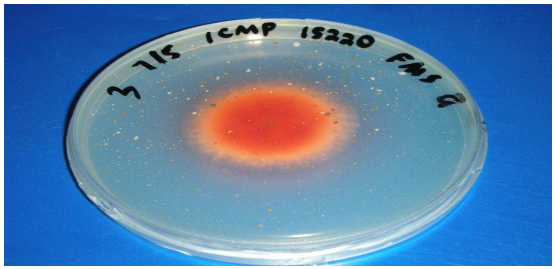
A (c)	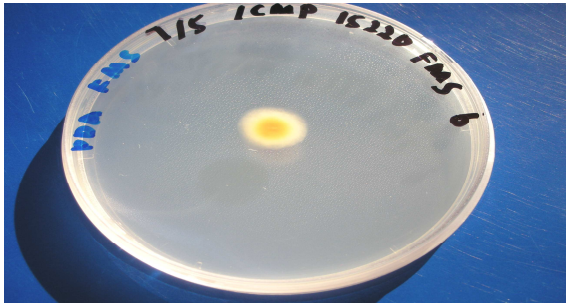	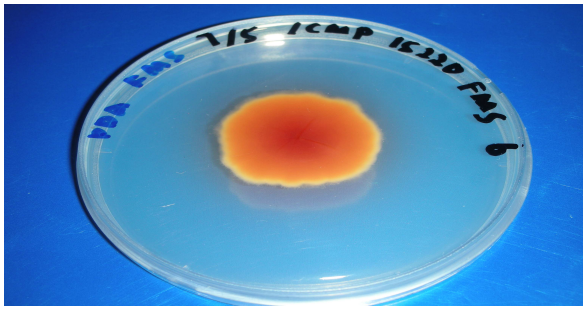	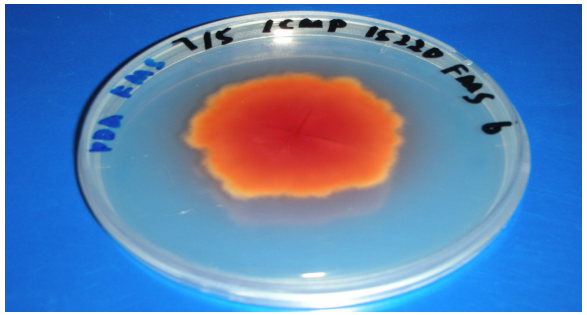

Figure 4.9: *Monascus ruber* ICMP 15220 colony morphology and pigmentation on media compositions J, D, and A at day 2, 5 and 7.

4.1.4 Discussion

All the media compositions tested supported fungal growth (Figure 4.1) and pigment production (Figure 4.8), but to varying extents. Medium G afforded the most rapid growth (Kr value of 0.200 mm h^{-1}) and the largest final colony diameter (55 mm). The next best medium in terms of growth was medium I. Both media G and I were relatively rich in the amount of carbon sources. Both contained rice powder, which probably promoted the growth development, as has been previously reported for solid-state fermentation of *Monascus* on rice (Lin, 1973; Teng and Feldheim, 2001). Medium G was by far the richest in glucose compared to the other media. Based on the medium constituents, medium G also had a much higher C : N ratio than medium I. Irrespective of the medium, the increase in colony radius was linear with time as previously reported for the fungus *Sclerotium rolfsii* (Farina *et al.*, 1997) and other *Monascus* strains (Carvalho *et al.*, 2005; Rasheva *et al.*, 1997-1998) growing on agar plates. Media that supported the most rapid growth were unfortunately not the best in terms of pigment production.

Media D and J appeared to be best for red pigment development. The red colour produced in these media was the most intense with the C* values of 29.65 (medium D) and 28.67 (medium J) and hue angles of 26.85^{o} (medium D) and 21.85^{o} (medium J). Media G and I, which appeared to be the most favourable for rapid growth, had the least purity of red colour. The red colour developed was relatively dull and grey with lower C* values of 9.07 (medium G) and 5.89 (medium I) as illustrated in Figure 4.8. Media D and J had much lower C : N ratios than the media G and I.

Media that contained monosodium glutamate (MSG) as the sole or mixed nitrogen source (i.e. media D, J, C, and F) produced greater intensity of red colour as shown in Figure 4.8. The complex structure of organic nitrogen source (i.e. MSG) and the possibility of the nitrogen regulation of the red colour production, led to the better red colour production. Use of ethanol as the main carbon source in combination with MSG reduced the purity of the red colour (medium F). Under this condition, the red colour produced was less intense compared to the use of glucose as the main carbon source (i.e. media D, J, and C). This was consistent with the literature claims of glucose being a superior substrate for pigment production by *Monascus* species (Juzlova *et al.*, 1994; Lin

et al., 1992) and MSG being the most favourable nitrogen source for development of red pigments (Lin, 1973). Medium H with sodium nitrate as the sole nitrogen source gave a relatively slow colony radial growth rate but was good for red-orange pigment production (Figure 4.8).

Trace elements are known to have important effects on secondary metabolism (Weinberg, 1989). In this study, all media that contained Zn^{2+} (i.e. media C, D, F, and J) (Figure 4.8) favoured red pigment production but not rapid growth (Figure 4.1), indicating the importance of Zn^{2+} for red colour production. However, high concentration of Zn^{2+} in the medium can retard the colour production by *Monascus ruber*, due to the toxicity (Bau and Wong, 1979). These results were consistent with other studies. For example, the growth of *Monascus purpureus* has been claimed to be inhibited by zinc sulphate that promoted pigment production (Bau and Wong, 1979; Johnson and McHan, 1975; Wong, 1982).

Medium A (PDA) is a commonly used medium for maintaining *Monascus* species (ATCC, 2007), but it did not promote red pigment development as well as the media that contained MSG. The radial growth rate on medium A (2.90 mm day^{-1}) was comparable to values reported for *Monascus purpureus* NRRL 2897 (3.0 mm day^{-1}) and *Monascus purpureus* LPB 31 (3.1 mm day^{-1}) grown on PDA (Carvalho *et al.*, 2005).

The initial pH of the medium can also affect growth and pigment production. Table 3.2 and Table 4.1 show that a relatively low initial pH of 5.0 favoured colony growth in media G and I. While, high initial pH (i.e. pH 6.5) favoured red colour production (i.e. media D, J, F, and H). This phenomenon possibly occurred due to the transformation of the orange colour to the red colour at high initial pH (Mak *et al.*, 1990). Low initial pH of 5.5 and 4.0 have been reported to also promote growth of *Monascus purpureus* (Chen and Johns, 1993; Lee *et al.*, 2001).

Based on the above preliminary screening work, the suitable media for producing red pigment using *Monascus ruber* ICMP 1520 were media J and D. These media compositions became the basis of further studies of pigment production in submerged culture.

4.2 Development of a chemically defined medium for *M. ruber* submerged culture

4.2.1 Introduction

Submerged fermentation for producing secondary metabolites of various *Monascus* species has been extensively studied (Chen and Johns, 1993; Juzlova *et al.*, 1994; Lin, 1973; Lin and Suen, 1973; Lin and Demain, 1991; Makhmur Ahmad *et al.*, 2009). Effects of the medium composition, temperature, pH, and aeration in submerged fermentation have been investigated (Carels and Shepherd, 1977; Hajjaj *et al.*, 2000a; Juzlova *et al.*, 1994; Lin and Demain, 1991). Composition of culture medium is known to affect pigment production in *Monascus* species (Carels and Shepherd, 1979). The interest in submerged culture is because it is easy to control and provides a uniform distribution of nutrients.

No prior work exists on submerged fermentation of *Monascus ruber* ICMP 15220. As the optimal carbon and nitrogen sources are strain dependant (Lin, 1973; Lin and Demain, 1993; Lin *et al.*, 1992; Yoshimura *et al.*, 1975), development of a chemically defined medium for producing a high yield of red pigment in submerged culture of *Monascus ruber* ICMP15220 was examined. Based on the earlier described studies on agar plates (Section 4.1), media D and J were selected as starting points for developing a suitable submerged culture medium.

4.2.2 Fungal growth in submerged culture

Media D and J had identical constituents but in different concentrations. Medium D was richer in glucose compared to medium J. Consequently the C : N ratio for the media was substantially different at 23 to 1 (medium D) and 9 to 1 (medium J). Batch submerged fermentations were conducted under identical conditions (Section 3.3.2.2.2). The inoculum used was approximately the same as described in Section 3.3.2.2.1. The cultures were grown for 140 h and samples were taken at intervals of 12 h. Pigments

concentrations, biomass cell dry weight, pH, and glucose concentration were determined as described in Section 3.4.2.

The time course of the fermentation in media D and J is shown in Figures 4.10 to 4.13. In medium D there was a pronounced lag phase for the first 36 h after inoculation. The lag was followed by exponential growth, stationary, and decline phases (Figure 4.10). During exponential growth, the maximum specific growth rate (μ_{max}) was 0.036 h^{-1} (Table 4.3). The maximum cell biomass concentration was obtained at 96 h. Nearly all glucose had been consumed by 72 h of fermentation, and this was the likely cause of a slowed growth (Figure 4.10). The red and orange pigments were produced throughout the fermentation in a growth-associated manner (Figure 4.11). Production of the yellow pigment was not apparently growth-associated (Figure 4.11). The pH was not constant and it increased from 6.5 to 7.0. The pH changes in the medium were probably the cause of transformation of the orange pigment to the red pigment (Mak *et al.*, 1990). The transformation from orange to red happened because of the reaction with NH_2 group of MSG (Lin and Demain, 1994; Silveira *et al.*, 2008).

In medium J, the lag phase was significantly shorter (Figure 4.12) than in medium D (Figure 4.10). During exponential growth, the maximum specific growth rate (μ_{max}) was 0.040 h^{-1}, or a little higher than in medium D. The maximum biomass concentration was lower at 4.3 g L^{-1}. Nearly all glucose was used up by 36 h because of a lower level of initial glucose than in medium D. Subsequently, the cell growth began to slow. The patterns of the production profiles of the red, orange, and yellow pigments (Figure 4.13) were comparable to the profiles in medium D (Figure 4.11), as discussed above. Similarly, the pH profile (Figure 4.12) was comparable to that of medium D (Figure 4.11).

Both media appeared to favour production of red and orange pigments, but not the yellow pigment.

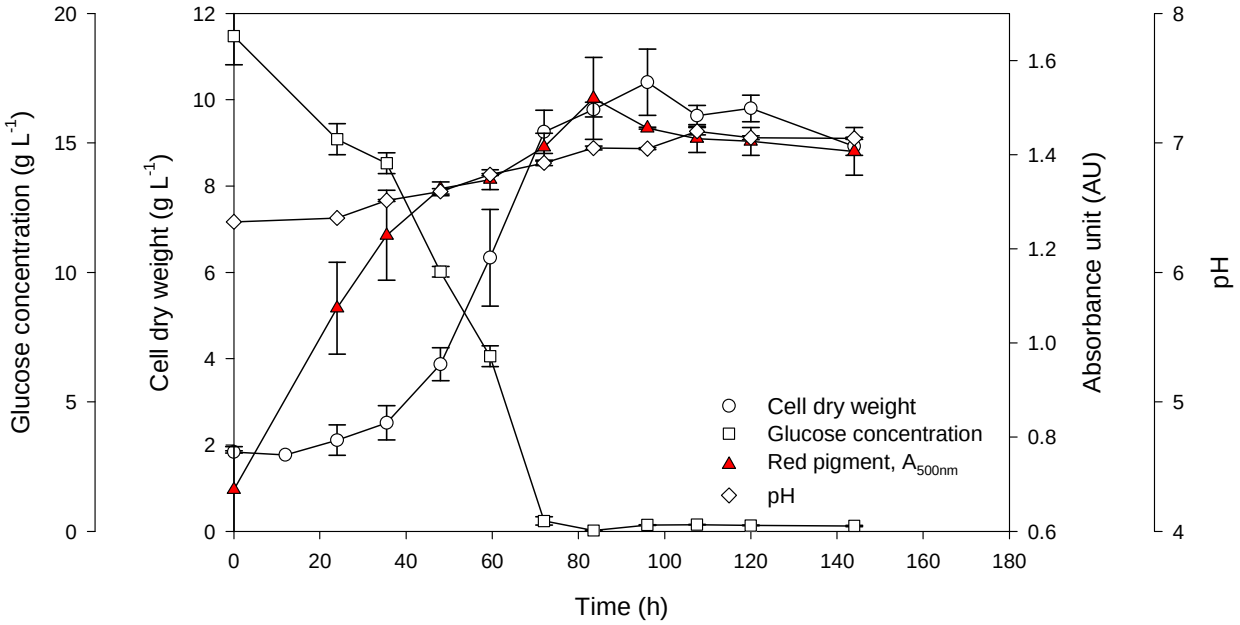

Figure 4.10: Fermentation time course for *Monascus ruber* growing on medium D

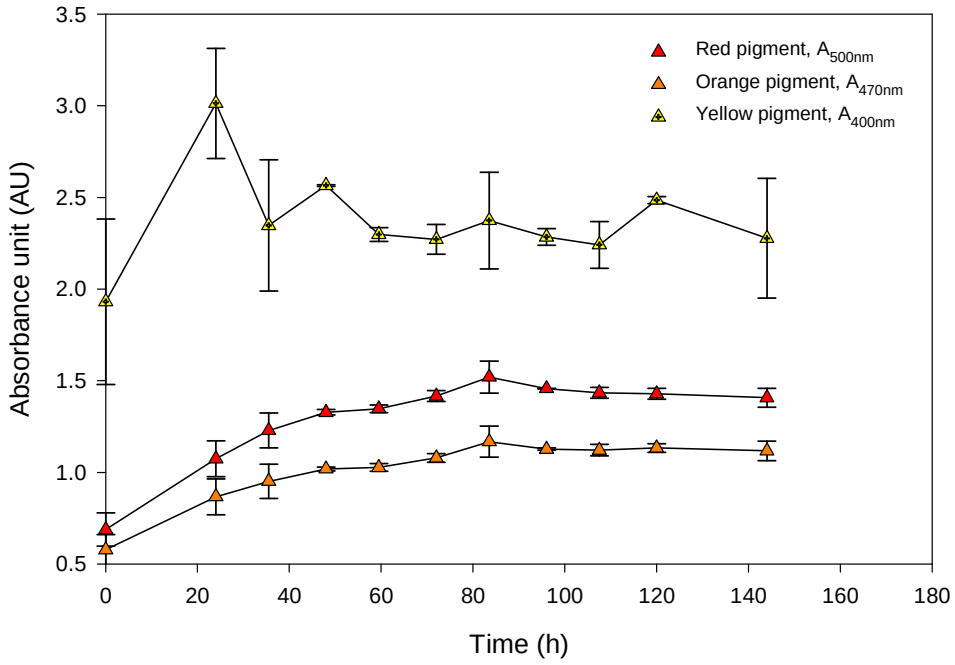

Figure 4.11: Pigments concentration profile during fermentation on medium D

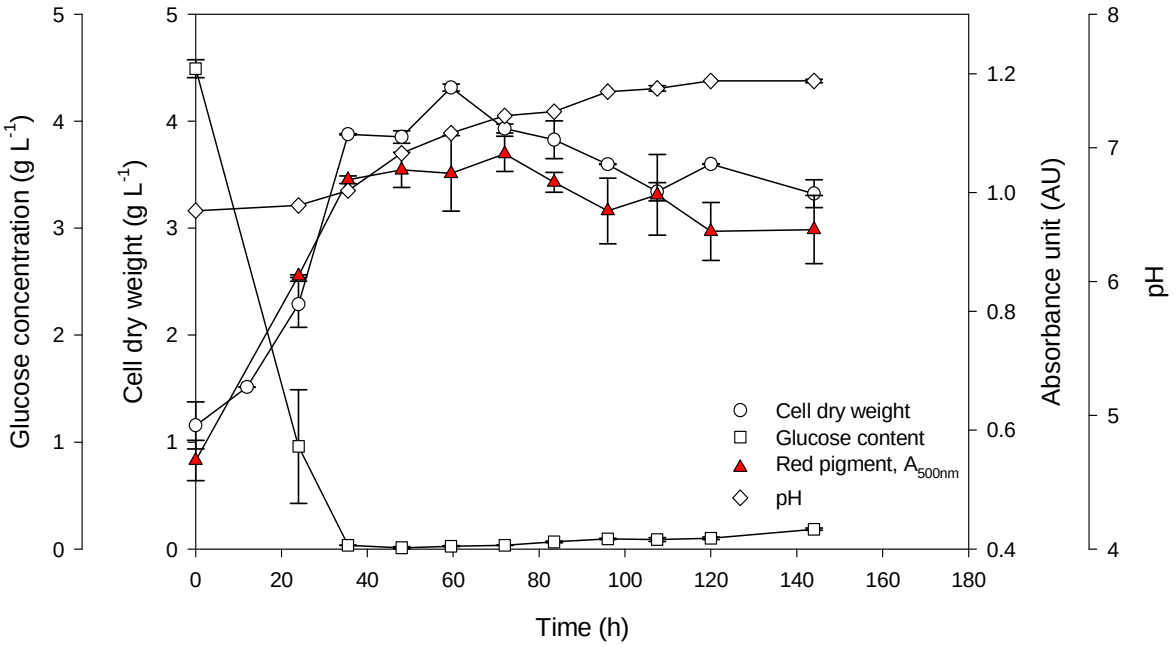

Figure 4.12: Fermentation time course for *Monascus ruber* growing on medium J

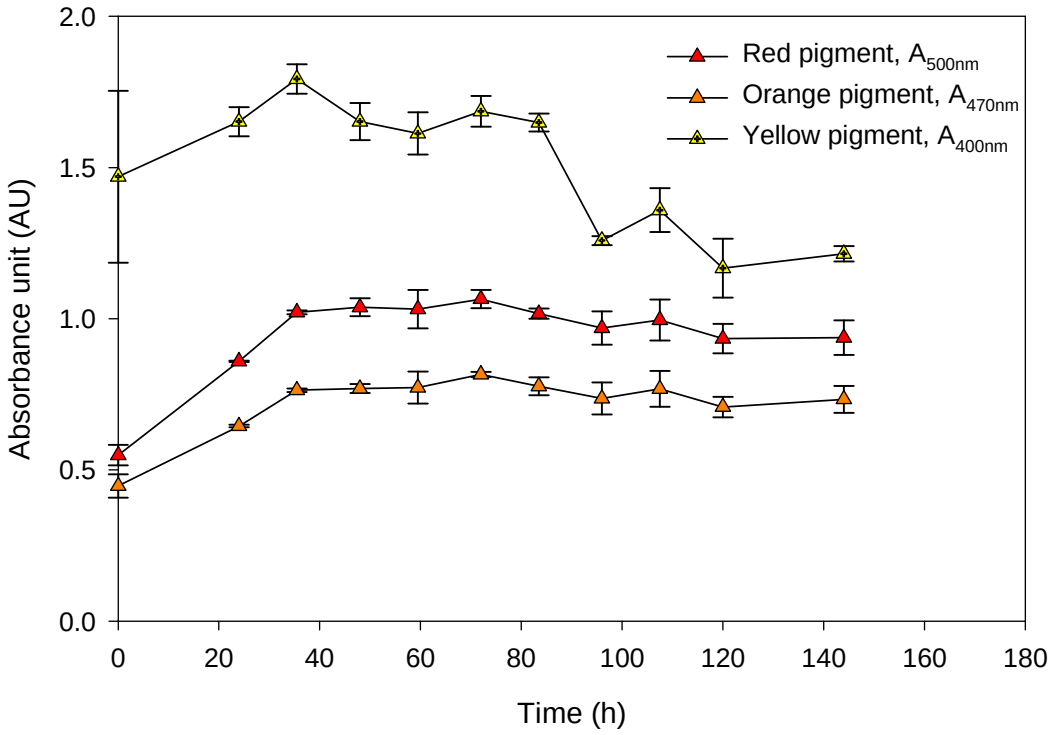

Figure 4.13: Pigments concentration profile during fermentation on medium J

The various kinetic parameters for the fermentation in media D and J are shown in Table 4.3. From the data, the medium D, which contained more glucose (20 g L^{-1}) produced a 41.5% higher concentration of biomass compared to medium J (Table 4.3); however, the biomass yield on glucose was significantly greater in medium J. Medium J also afforded a higher yield of red pigment on biomass than did medium D. It was apparent that biomass production was affected by the carbon source (i.e. glucose 20 g L^{-1} (medium D) produced higher biomass compared to medium J (glucose 5 g L^{-1})). In contrast, the red pigment production was affected by the ratio of C : N (i.e. high ratio of C : N (medium D) produced lower pigment production).

Table 4.3: Kinetic parameters, yields and productivity of red pigment on media D and J

Medium	C : N ratio	μ_{max} (h^{-1})	X_{max} (g L^{-1})	$Y_{X/S}$ (g g^{-1})	Pr (AU L^{-1} h^{-1})	$Y_{P/X}$ (AU g^{-1})
D	23.6 : 1	0.036	10.4	0.51	0.010	10.48
J	9.1 : 1	0.040	4.3	0.71	0.013	17.36

X – biomass; P – red pigment; S - glucose

In both media, the fermentation was complete by 120 h and there was no advantage to further prolonging the batch culture. As medium J afforded a higher pigment yield on substrate, it was selected for further investigation in submerged culture with a fermentation time of 120 h. In keeping with the objective of the study, further investigation focused only on the production of red pigment.

4.2.3 Effect of temperature

Fermentation temperature profoundly affects growth and product development. Furthermore, the optimal temperature for growth may be different from that for product formation (Shuler and Kargi, 2002). Generally, the optimal temperature for growth of *Monascus* species has ranged between 25-37^{o}C, depending on the strain (Lin, 1991). An experiment was conducted to determine the optimal temperature for red pigment production by *Monascus ruber* ICMP 15220 in submerged culture.

Incubation temperatures of 25^{o}C, 30^{o}C, and 40^{o}C were used separately in submerged culture (Section 3.4.2) using medium J, which had been earlier identified to favour pigment production (Section 4.2.2). Fermentations were run for 48 h, as red pigment concentration reached a maximum value by this time in earlier experiments (Figure 4.13). At 48 h, absorption spectra of the filtered fermentation broth were generated over a wavelength range of 300 to 750 nm. Figure 4.14 depicts the absorption spectra. In all cases, the spectra had maximum absorption at wavelengths of 400 and 500 nm, corresponding to yellow and red pigments, respectively. The maximum absorbance at 500 nm (red pigment) was attained at the incubation temperature of 30^{o}C. The absorbance (500 nm) values at incubation temperatures of 25^{o}C and 40^{o}C were 30.5% and 26.2%, respectively, of the value at 30^{o}C. Temperatures of 30^{o}C and 25^{o}C appeared to favour preferential production of red pigment relative to the yellow pigment, but at elevated temperature (i.e. 40^{o}C), the red pigment was degraded and yellow pigment was produced preferentially (Babitha *et al.*, 2007a; Carvalho *et al.*, 2005).

In view of these results, the optimal temperature for red pigment production by *Monascus ruber* ICMP 15220 was 30^{o}C. This incubation temperature was used for all further investigations in submerged culture.

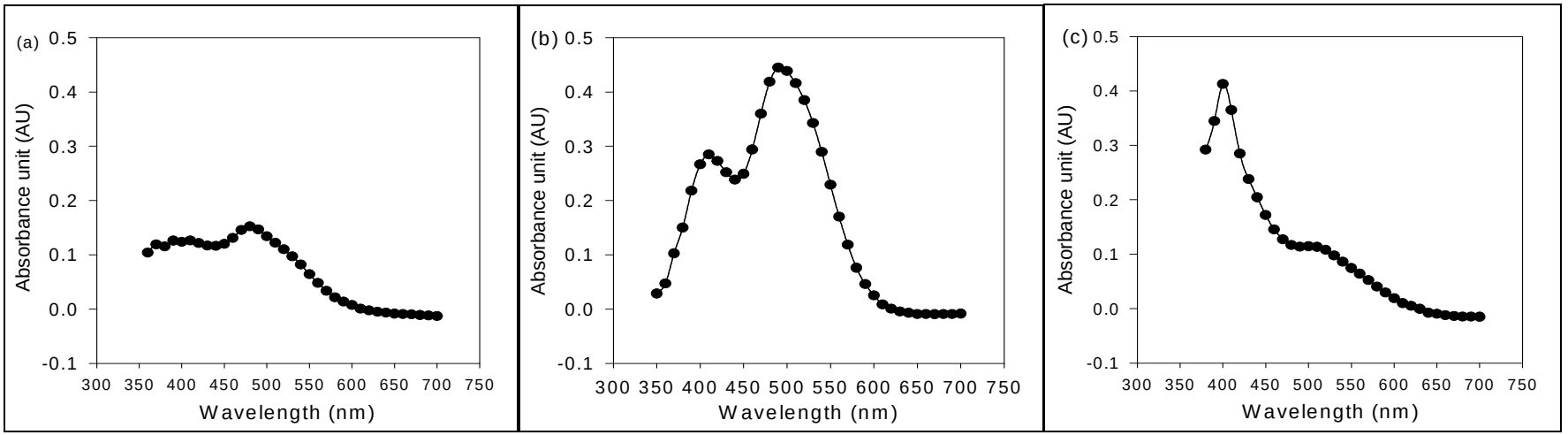

Figure 4.14: Absorption spectra of the extracellular pigment produced by *Monascus ruber* at different incubation temperatures.

(a) 25^{o}C, (b) 30^{o}C, (c) 40^{o}C

4.2.4 Effect of initial glucose concentration on red pigment production

As discussed in Section 4.2.2, medium J with a C : N ratio of 9 to 1 appeared to be the most favourable for red pigment production in submerged culture. The initial glucose concentration in medium J was relatively low at 5 g L^{-1}. According to some earlier studies (Wong *et al.*, 1981), elevated level of glucose induced pigment production in *Monascus* species. Therefore, the effect of the initial glucose concentration was investigated in such a way that the C : N ratio remained at 9 : 1. A range of 0.5 to 2.5% (g/100 mL) initial glucose concentrations was investigated. The initial glucose concentrations were 0.5, 1.0, 1.5, 2.0, and 2.5%, corresponding to 5.0, 10.0, 15.0, 20.0, and 25.0 g L^{-1}. The concentration of monosodium glutamate (MSG), the nitrogen source in medium J, was adjusted to keep the C : N ratio at 9 : 1. The MSG concentrations were 5.0, 10.0, 15.0, 20.0, and 25.0 g L^{-1}, for the initial glucose levels of 0.5, 1.0, 1.5, 2.0, and 2.5%, respectively. The fermentations were run for 120 h at 30^{o}C, in keeping with earlier findings (Section 4.2.2 and Section 4.2.3).

Increasing initial glucose concentration did not affect the growth rate much, but allowed growth to occur for a longer period (Figure 4.15). The final biomass concentration increased progressively with increasing initial glucose concentration. Increasing initial concentration of glucose increased the time for complete exhaustion of glucose (Figure 4.16). For instance, for 2.5% initial glucose, it took approximately 72 h to consume 97.6% of glucose. In contrast, with 0.5% initial glucose concentration, 99.7% of glucose had been consumed by approximately 48 h of fermentation (Figure 4.16 and Table 4.4). The general shape of the pH profiles (Figure 4.17) was not affected by changes in initial glucose concentration. The pH-value increased as the biomass concentration increased and the rate of pH increase was faster during rapid growth.

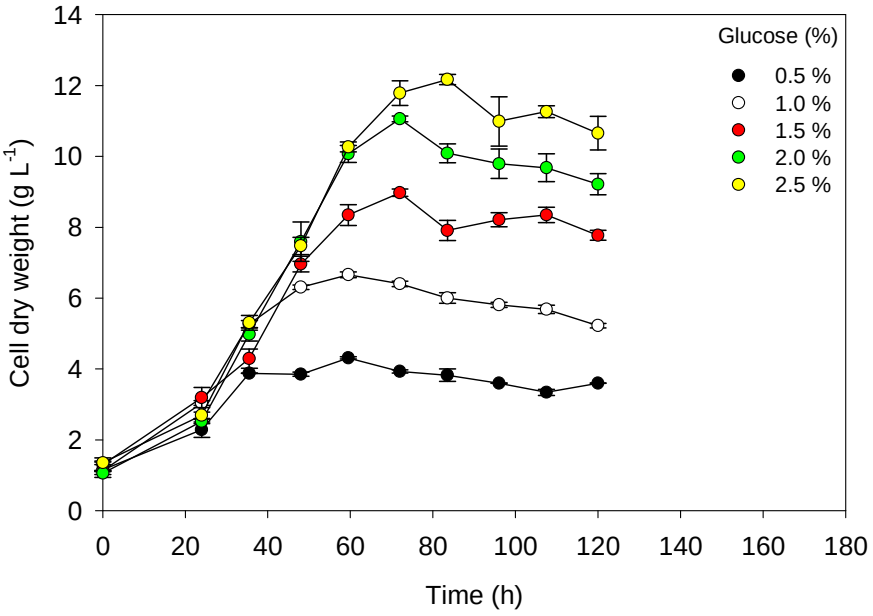

Figure 4.15: Effect of initial glucose concentration on the biomass cell dry weight

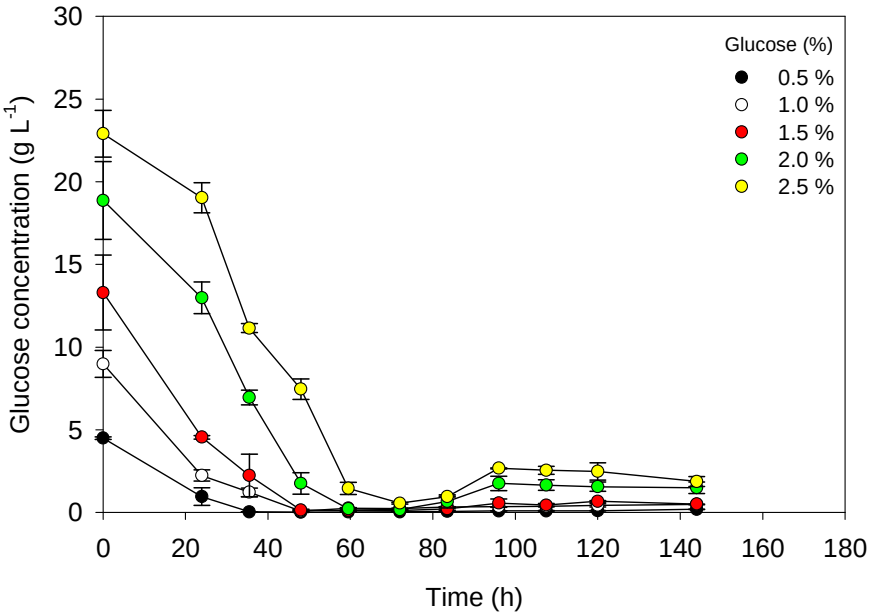

Figure 4.16: Effect of initial glucose concentration on the glucose consumption

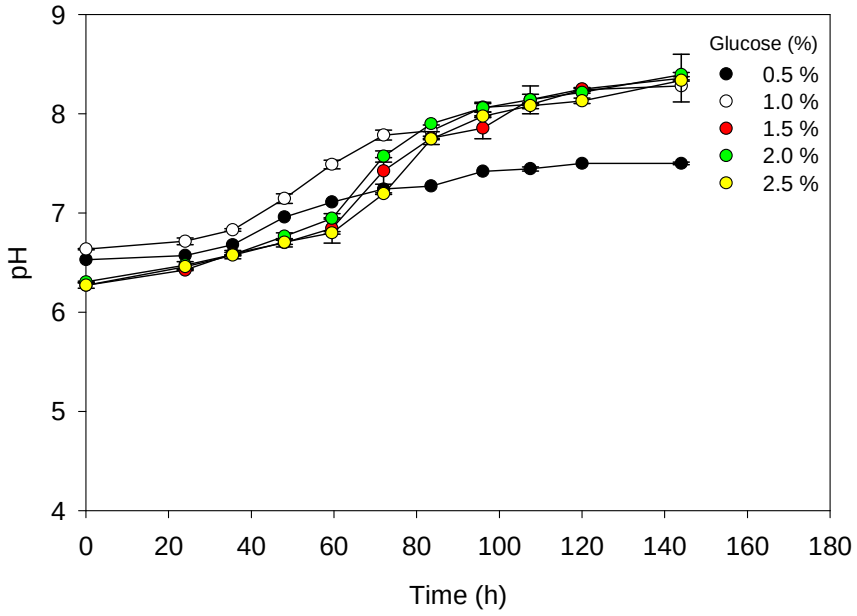

Figure 4.17: Effect of initial glucose concentration on the pH

The effect of initial glucose concentration on the red pigment production is shown in Figure 4.18. In all cases, the pigment production appeared to be growth associated. A glucose concentration of 1.0 to 1.5% was clearly best for pigment production (Figure 4.18). Lower and higher levels of initial glucose had a marked adverse effect on pigment production. This was probably due to the excessive biomass growth at high initial glucose concentration suppressed pigment production. Lack of carbon (i.e. at low initial glucose concentration) also inhibited the activity of metabolite production (i.e. pigment production) (Wong *et al.*, 1981).

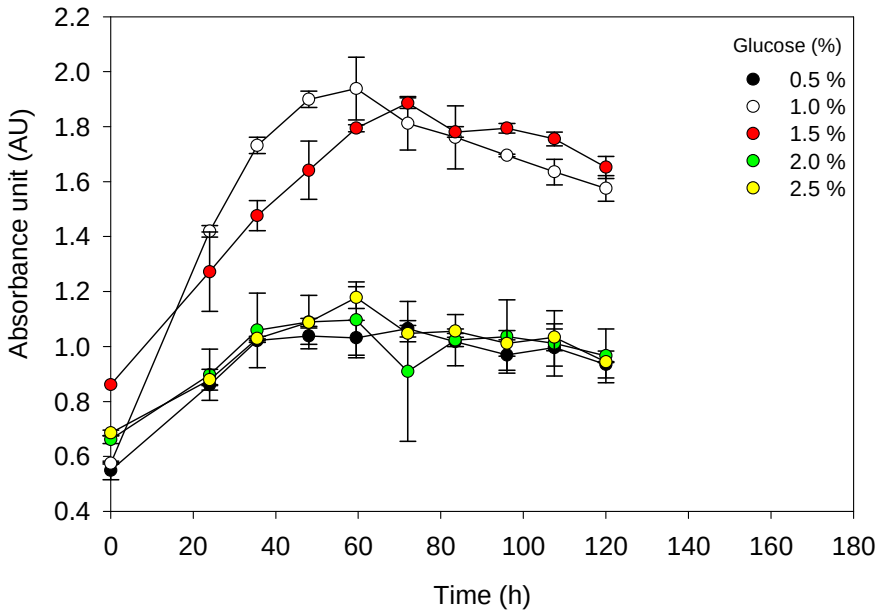

Figure 4.18: Effect of initial glucose concentration on the red pigment production

The kinetic parameters of the fermentations at various initial glucose levels are summarized in Table 4.4. The highest value of the maximum specific growth rate (μ_{max}) occurred at a glucose concentration of 1.0%. The μ_{max} decreased as the initial glucose concentration increased beyond 1.0%. This was likely an effect of osmotic pressure (Kim *et al.*, 1997). Osmotic pressure increases with increasing concentration of glucose and this reduces water availability for microbial growth. A glucose concentration of 1.0% that was most favourable for growth also afforded the highest concentration and productivity of the red pigment (Table 4.4).

Table 4.4: Fermentation parameters for different initial glucose concentrations

Initial glucose concentration (%)	μ_{max} (h^{-1})	X_{max} (g L^{-1})	$Y_{X/S}$ (g g^{-1})	Pr (AU L^{-1} h^{-1})	$Y_{P/X}$ (AU g^{-1})	Glucose utilization (%)
0.5	0.040	4.3	0.71	0.013	17.36	99.7 (48 h)
1.0	0.043	6.7	0.63	0.023	24.65	99.1 (48 h)
1.5	0.034	9.0	0.58	0.014	13.36	99.1 (72 h)
2.0	0.029	11.1	0.54	0.009	5.67	99.1 (72 h)
2.5	0.028	12.2	0.49	0.008	5.53	97.6 (72 h)

X – biomass; P – red pigment; S - glucose

In view of these results, all subsequent work in submerged culture used an initial glucose concentration of 1.0%, or 10 g L^{-1}. This medium had an initial MSG concentration of 10 g L^{-1} so that the C : N mass ratio remained unchanged at 9 : 1.

4.2.5 Effect of carbon to nitrogen ratio

Carbon to nitrogen ratio has been found to influence pigment production in certain *Monascus* species (Wong *et al.*, 1981) as well as other fungi (Mao *et al.*, 2005). Therefore, using the modified medium J (Section 4.2.4) as the basis, the influence of carbon to nitrogen ratio (C : N) on production of the red pigment and biomass was investigated in submerged culture.

In all experiments, the initial glucose concentration remained fixed at 1.0%, or 10 g L^{-1} (Section 4.2.4). The following C : N ratios were tested: 6 : 1, 9 : 1, 14 : 1, and 20 : 1. The C : N ratio was modified by varying the concentration of monosodium glutamate (MSG), the sole nitrogen source in the medium. Other components in the medium and the initial pH remained fixed as in the reference medium (medium J, Table 3.2). Batch fermentations were run for 120 h, 30^{o}C, and an agitation rate of 250 rpm.

The biomass, red pigment, and pH profiles of the fermentations are shown in Figure 4.19, Figure 4.20, and Figure 4.21, respectively. A C : N ratio of 9 : 1 was clearly best for maximizing the biomass concentration and productivity (Figure 4.19). Too high a C : N ratio suppressed growth. Pigment concentration generally peaked to coincide with the peak biomass concentration and declined after growth had ceased (Figure 4.20). This again confirmed the growth associated nature of the red pigment production. As for biomass concentration, a C : N ratio of 9 : 1 maximized production of the red pigment. Higher and lower values of C : N ratios adversely affected the production of red pigment relative to the data obtained at the C : N ratio of 9 : 1. It showed that, high amount of nitrogen (i.e. MSG as the nitrogen source with the C : N ratio of 6 : 1) in the medium, might be inhibitory for metabolite production and retarded the red pigment. While, less nitrogen (i.e. C : N ratio of 20 : 1) might change the regulation of nitrogen uptake and metabolism, due to a deficiency of NH_2 group. Thus, these two conditions restricted the formation of red pigment.

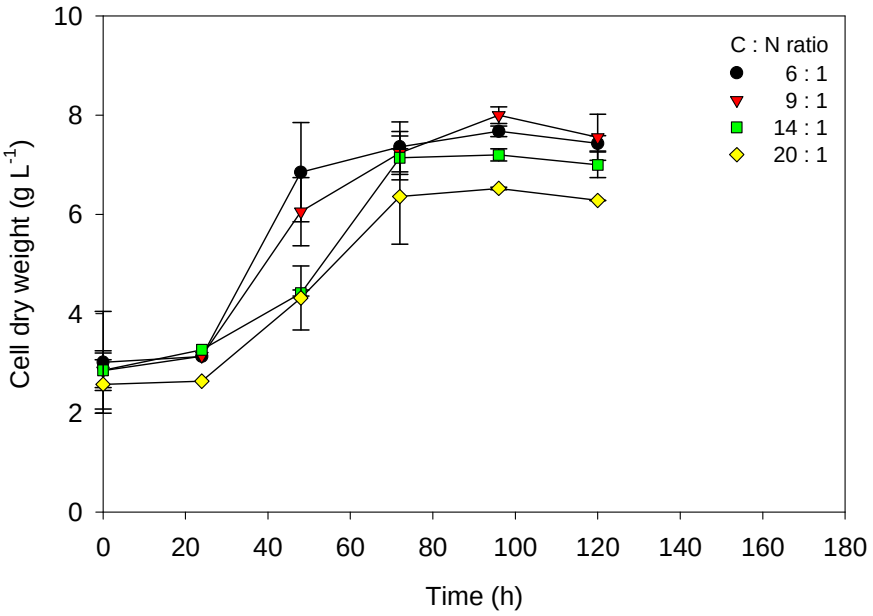

Figure 4.19: Effect of C : N ratio on the biomass growth

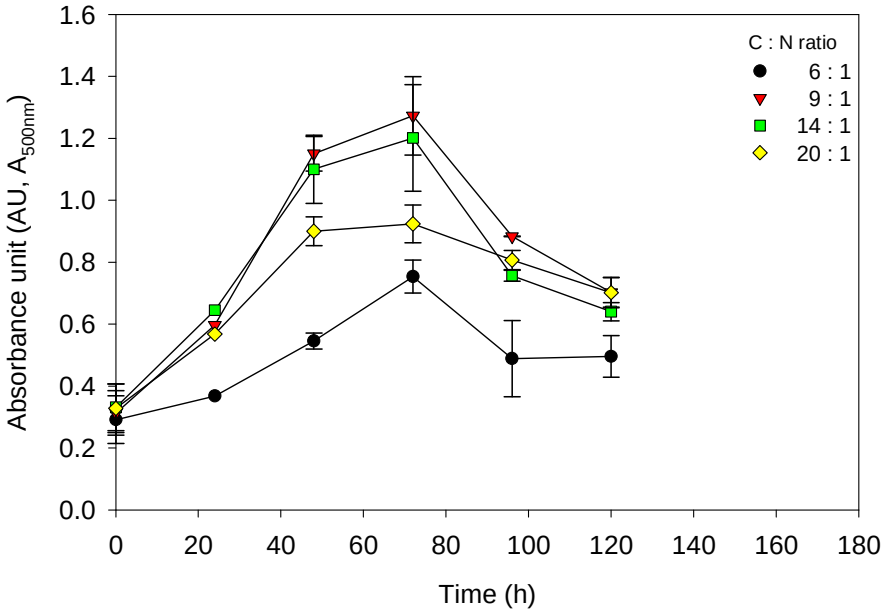

Figure 4.20: Effect of C : N ratio on red pigment production

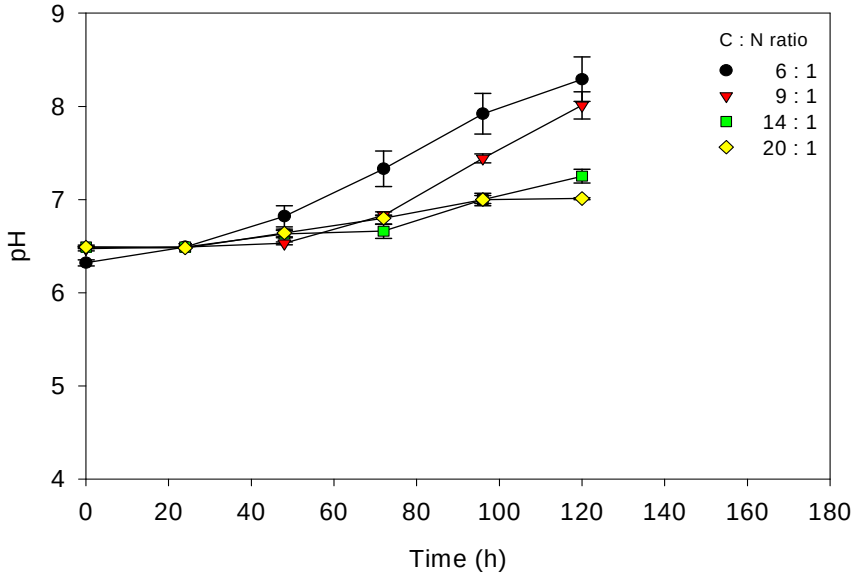

Figure 4.21: Effect of C : N ratio on the pH

The C : N ratio influenced the pH profile noticeably (Figure 4.21). Relatively high values of C : N ratio reduced the characteristic rise in pH of this fermentation. Both the productivity of the red pigment (Figure 4.22) and its yield on biomass (Figure 4.23) were maximum at a C : N ratio of 9 : 1.

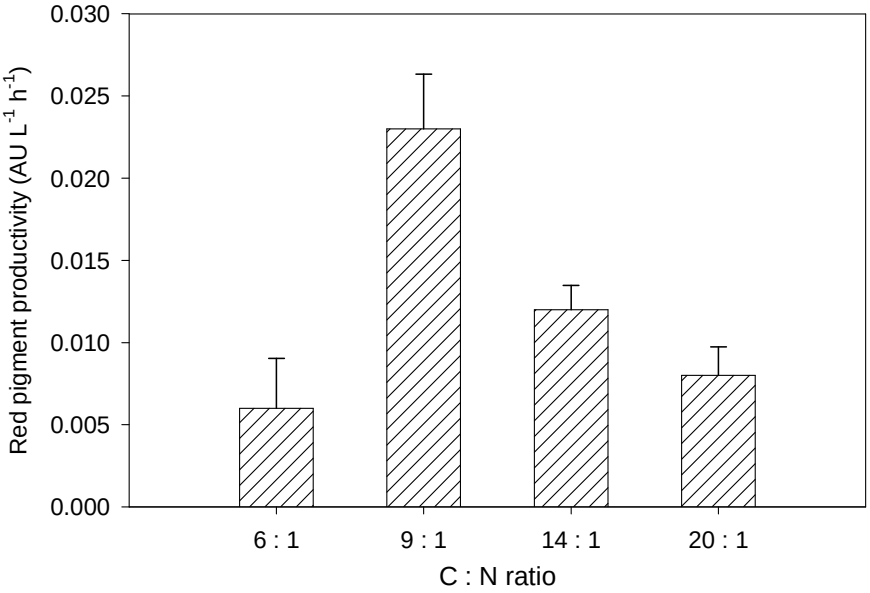

Figure 4.22: Effect of C : N ratio on red pigment productivity

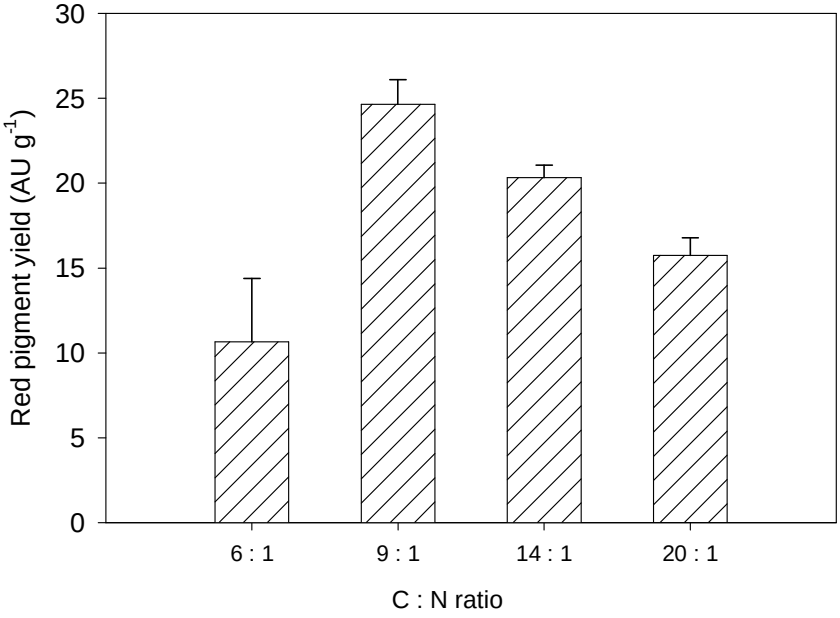

Figure 4.23: Effect of C : N ratio on yield of red pigment on biomass

In conclusion, a C : N ratio of 9 : 1 was optimal for producing the red pigment by submerged culture using glucose and MSG as carbon and nitrogen sources, respectively.

4.2.6 Effect of the nitrogen source

Microorganisms require nitrogen to produce protein, DNA, RNA, and other compounds. Typically, 10 to 14% (w/w) of microbial cell dry weight is nitrogen (Pirt, 1985; Shuler and Kargi, 2002). Most microorganisms can use nitrogen containing organic compounds and inorganic salts as nitrogen sources, but the type of nitrogen source can influence growth characteristic and production of metabolites.

Generally, organic nitrogen sources such as yeast extract, urea, monosodium glutamate (MSG), and peptone are expensive compared to inorganic nitrogen sources such as ammonium salts and nitrates. Therefore, attempts were made to replace monosodium glutamate (MSG) with inexpensive inorganic salts as a nitrogen source to reduce the cost of production of the red pigments. The following inorganic nitrogen sources were investigated in separate experiments: sodium nitrate ($NaNO_3$), ammonium chloride (NH_4Cl), ammonium nitrate (NH_4NO_3), and ammonium sulphate ($(NH_4)_2SO_4$). Control experiments used MSG as the nitrogen source. All experiments were carried out with a fixed initial glucose concentration of 1.0%, or 10.0 g L^{-1} (Section 4.2.4) and a fixed C : N ratio of 9 : 1 (Section 4.2.5), as per earlier findings. The other components in the medium and the initial pH remained fixed as for the reference medium (medium J, Table 3.2). Fermentations were run for 120 h at 30^{o}C and an agitation rate of 250 rpm.

The effect of nitrogen source on the biomass growth profile, pigment production profile, and pH profile are shown in Figure 4.24, Figure 4.25, and Figure 4.26, respectively. All nitrogen sources supported growth (Figure 4.24), but MSG was a far superior nitrogen source compared to the inorganic salts. The biomass production profiles obtained with $(NH_4)_2SO_4$, $NaNO_3$, NH_4NO_3 were quite similar (Figure 4.24). A distinct lag phase of little growth was observed when inorganic salts were the nitrogen source (Figure 4.24).

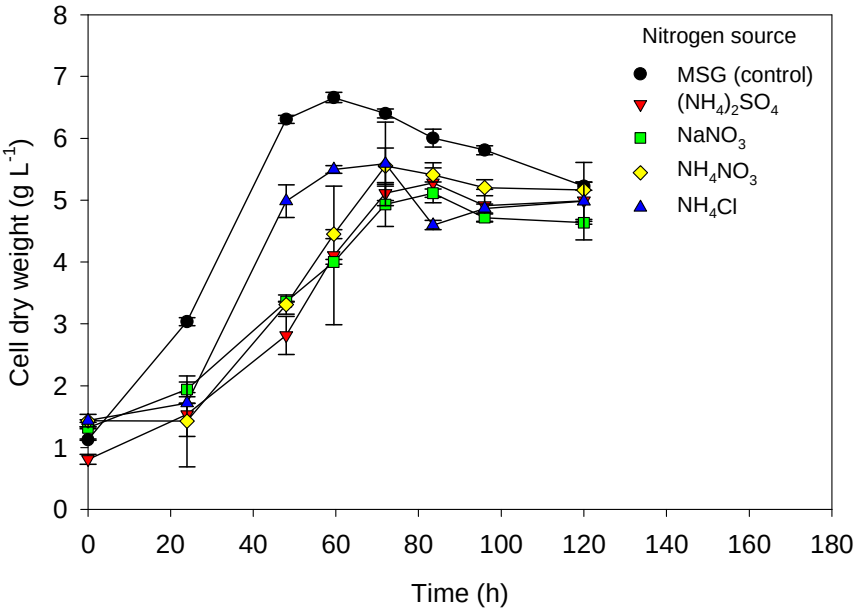

Figure 4.24: Effect of nitrogen source on biomass growth

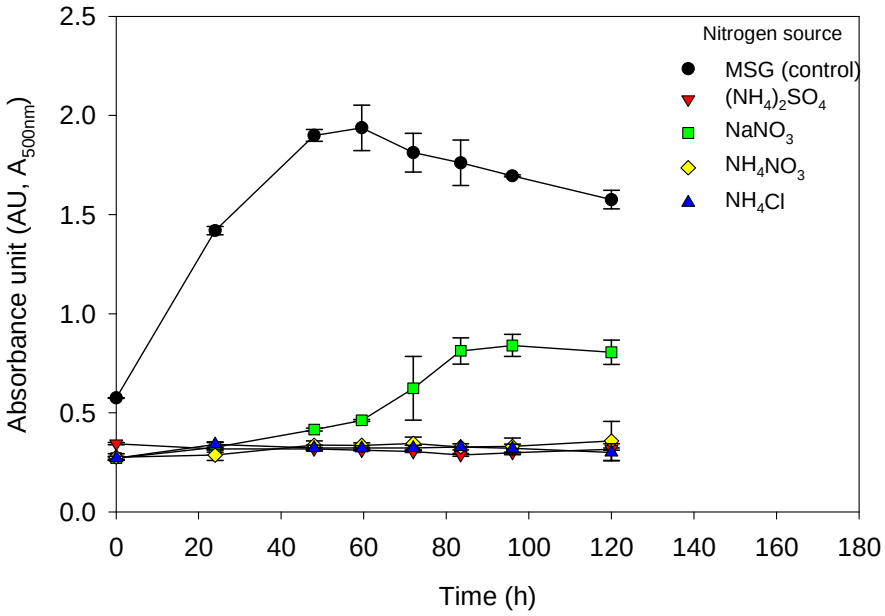

Figure 4.25: Effect of nitrogen source on red pigment production

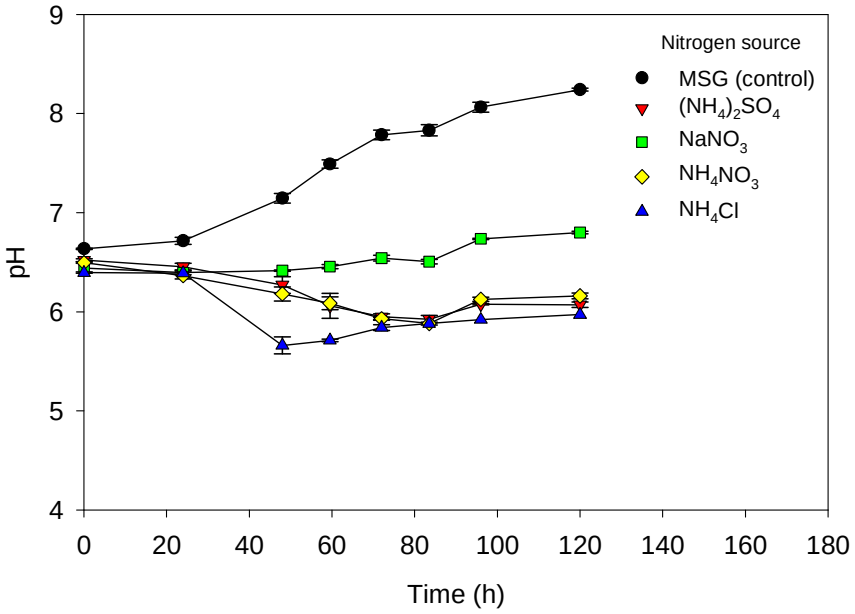

Figure 4.26: Effect of nitrogen source on pH

Among the inorganic nitrogen sources, only $NaNO_3$ promoted red pigment production (Figure 4.25), but not as well as the organic nitrogen source, MSG. MSG afforded a greater pigment yield on biomass (Figure 4.27) and pigment productivity (Figure 4.28) than the inorganic nitrogen sources. This result was in agreement with reports on other *Monascus* strains (Jiang *et al.*, 2005; Lee *et al.*, 2001; Lin and Demain, 1991; Silveira *et al.*, 2008).

Unlike with MSG, the use of inorganic nitrogen sources that contained NH_4^+ always produced an initial decline in the pH-value followed by some recovery, but the pH (Figure 4.26) always remained acidic. With $NaNO_3$, the only inorganic nitrogen source that did not contain NH_4^+, the pH remained relatively stable and close to the initial pH (Figure 4.26). Only with MSG did the pH-value continually rise to become alkaline. The rising of pH (i.e. final pH above 6) during fermentation may contribute to the conversion of orange to the red pigment (Wong *et al.*, 1981). Figure 4.26 suggests that the pH profile and the nitrogen source are interdependent but pH control was no used as it would have been impractical to apply in packed beds that were later found to be best for this

fermentation. Submerged cultures of *Monascus* do not generally use pH control (Martinkova and Patakova, 1999; Wong *et al*., 1981).

The initial acidification observed with the use of NH_4^+ containing salt is explicable as follows: cells first take up the NH_4^+ ion, incorporate it in proteins as NH_3^+ and reject the H^+ that causes acidification (Chisti, 1999b). Once all the NH_4^+ has been used, nitrate (NO_3^-) is used as the nitrogen source. Nitrate is a less preferred nitrogen source because it must be reduced in an energy requiring processed before being used in building cellular proteins. During nitrate consumption, the pH rises and NO_3^- is reduced to NH_3 for incorporation into proteins and hydroxyl iron (OH^-) are released (Lambers *et al.*, 2008).

Figure 4.27 and Figure 4.28 summarize the effect of nitrogen sources on the yield of red pigment and productivity, respectively. The figures clearly demonstrate that among the inorganic nitrogen sources used, the maximum yield of red pigment (Figure 4.27) and productivity (Figure 4.28) observed was with $NaNO_3$. Compared to the use of organic nitrogen source (i.e. MSG), the yield of red pigment and its productivity were only 57.74% and 26.09%, respectively, with the best inorganic nitrogen source.

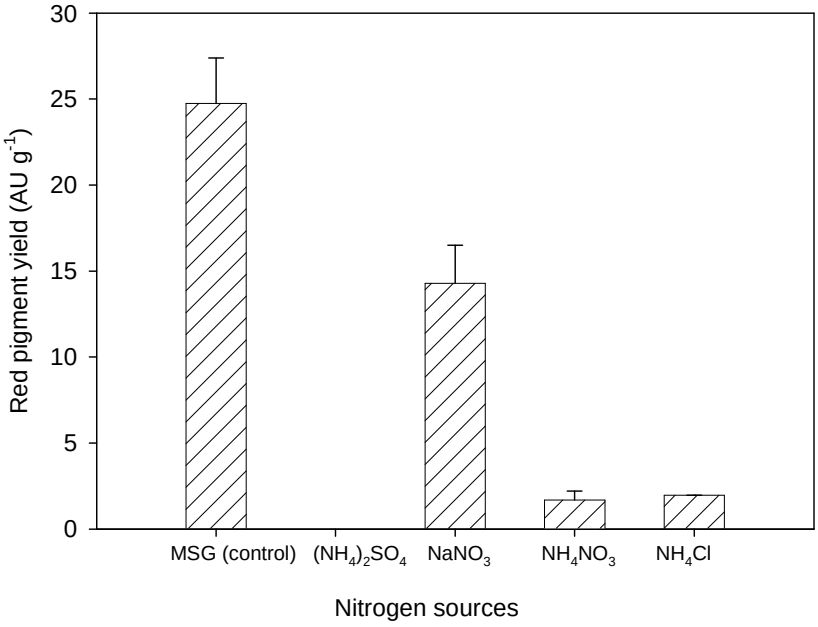

Figure 4.27: Effect of nitrogen source on red pigment yield on biomass

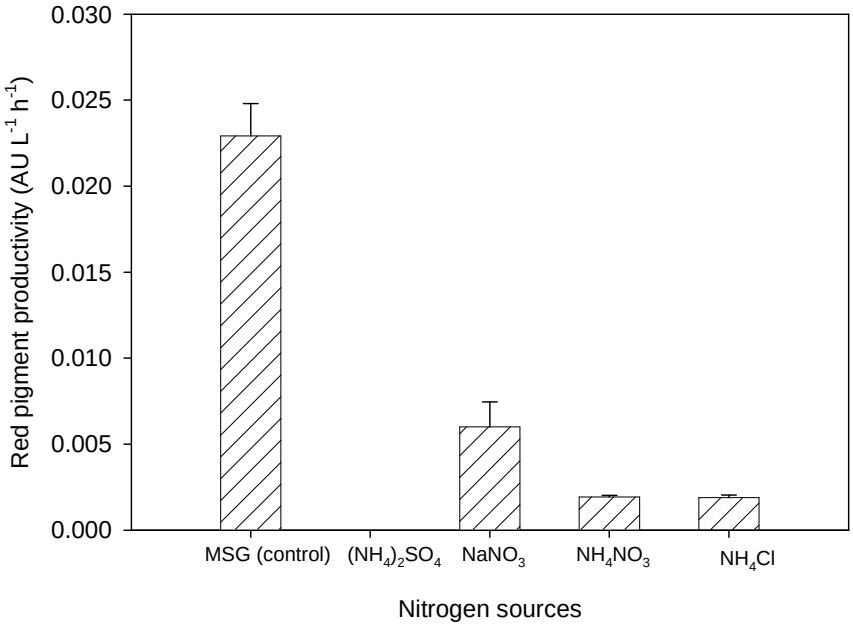

Figure 4.28: Effect of nitrogen source on red pigment productivity

In conclusion, none of the common inorganic salts could effectively substitute for MSG as the nitrogen source. Thus, MSG was retained as the nitrogen source in the subsequent work.

4.2.7 Effect of carbon source

The type of the carbon source can also affect the production of *Monascus* pigments in at least some species (Chen and Johns, 1993; Juzlova *et al.*, 1996; Lin, 1973; Lin and Demain, 1991). Considering this, the effect of the carbon source on fermentation of *Monascus ruber* ICMP 15220 was examined. In addition to glucose, maltose and ethanol were assessed separately in submerged culture. Maltose and ethanol were used because in studies with *Monascus pupureus* they had been found to be relatively good for producing red pigments (Chen and Johns, 1994; Juzlova *et al.*, 1994). Fermentation on glucose were used as controls.

All fermentations were carried out with MSG as the nitrogen source at a fixed concentration of 10 g L^{-1} (Section 4.2.4). A sufficient amount of the selected carbon source was added to achieve a C : N ratio of 9 : 1 as per earlier findings (Section 4.2.5). All the other components in the medium and the initial pH remained fixed as in the reference medium (Medium J, Table 3.2). The fermentations were run for 120 h at 30^{o}C and an agitation speed of 250 rpm.

The effects of the carbon source on the biomass growth profile, pigment production, and the pH profile are shown in Figure 4.29, Figure 4.30, and Figure 4.31, respectively. Biomass growth on glucose was the most rapid. Maltose afforded a little higher biomass concentration than glucose, but the maximum biomass concentrations attained on the three carbon sources were fairly similar (Figure 4.29).

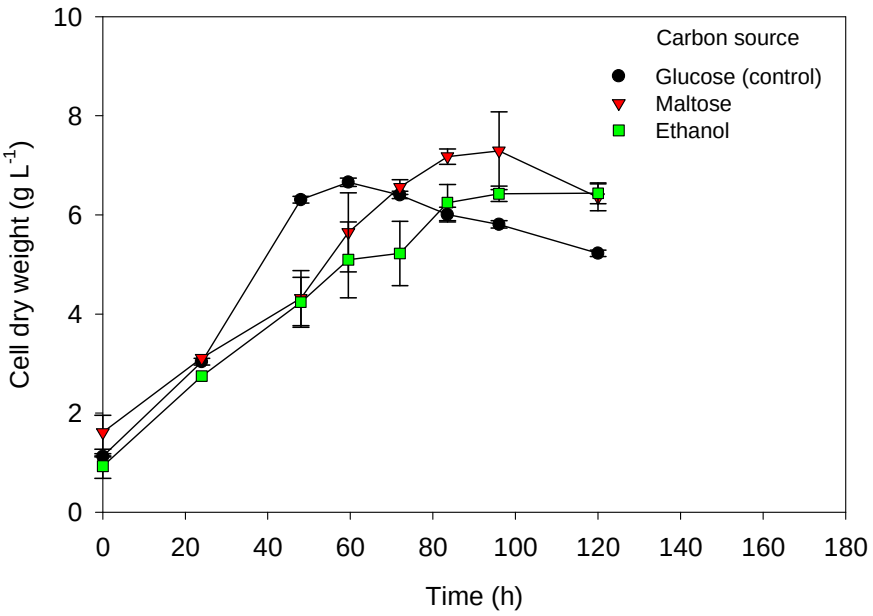

Figure 4.29: Effect of the carbon source on biomass growth

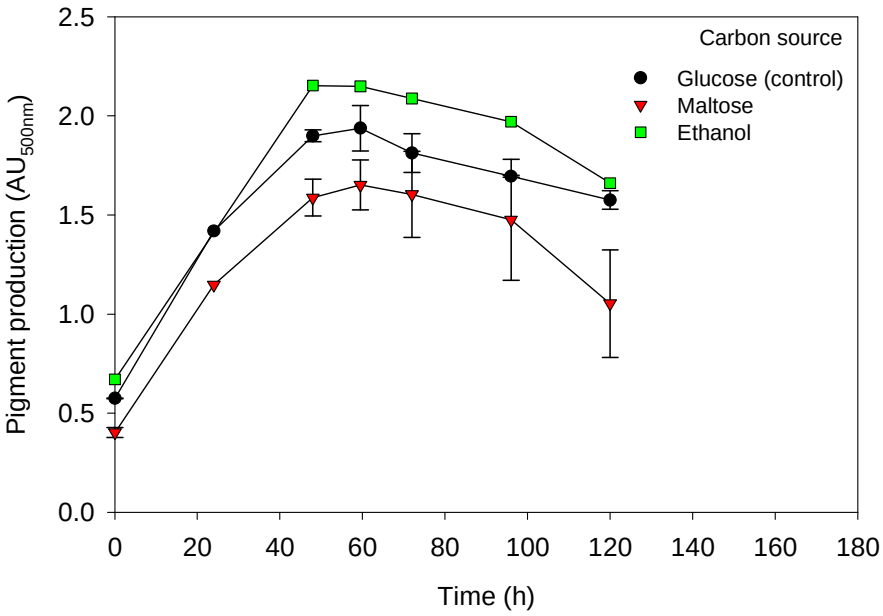

Figure 4.30: Effect of the carbon source on red pigment production

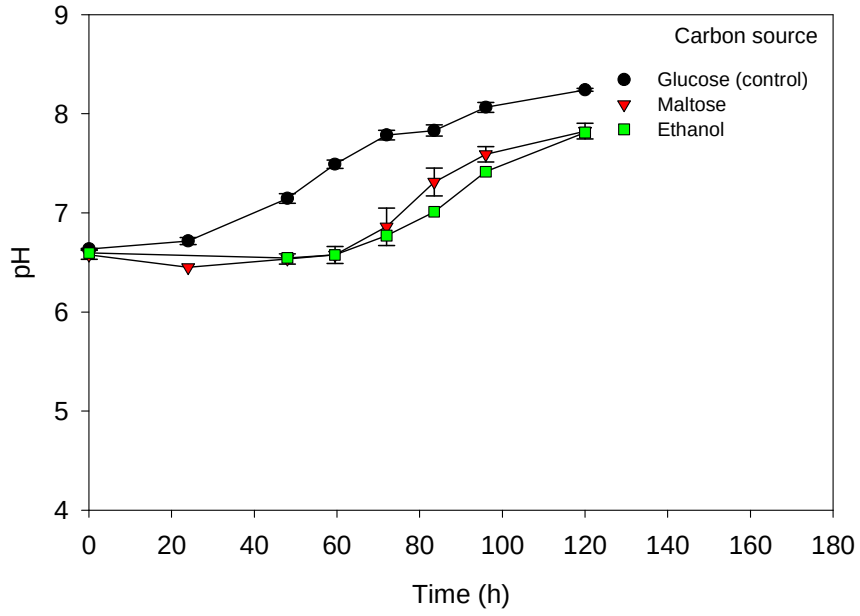

Figure 4.31: Effect of the carbon sources on the pH

Ethanol proved to be best for pigment production (Figure 4.30). Glucose was a little less effective than ethanol for pigment production, but was better than maltose (Figure 4.30). The higher pigment production on ethanol might have been slowed due to a biomass growth (Figure 4.29) without reducing the final biomass concentration relative to the other carbon sources. The results were consistent with reports for other *Monascus* strains (Hamdi *et al.*, 1997; Juzlova *et al.*, 1996; Yoshimura *et al.*, 1975). The pH profiles were similar for all carbon sources (Figure 4.31), but the pH increase was more rapid on glucose, which also afforded most rapid growth.

The effects of the carbon source on the red pigment productivity and specific rate of production are shown in Figure 4.32 and Figure 4.33, respectively. Ethanol afforded a higher productivity than other carbon sources. Pigment productivity on ethanol was 1.3-fold higher than on glucose. Productivity on glucose and maltose were comparable (Figure 4.32). The specific rate of red pigment was fairly similar for both glucose and ethanol (Figure 4.33).

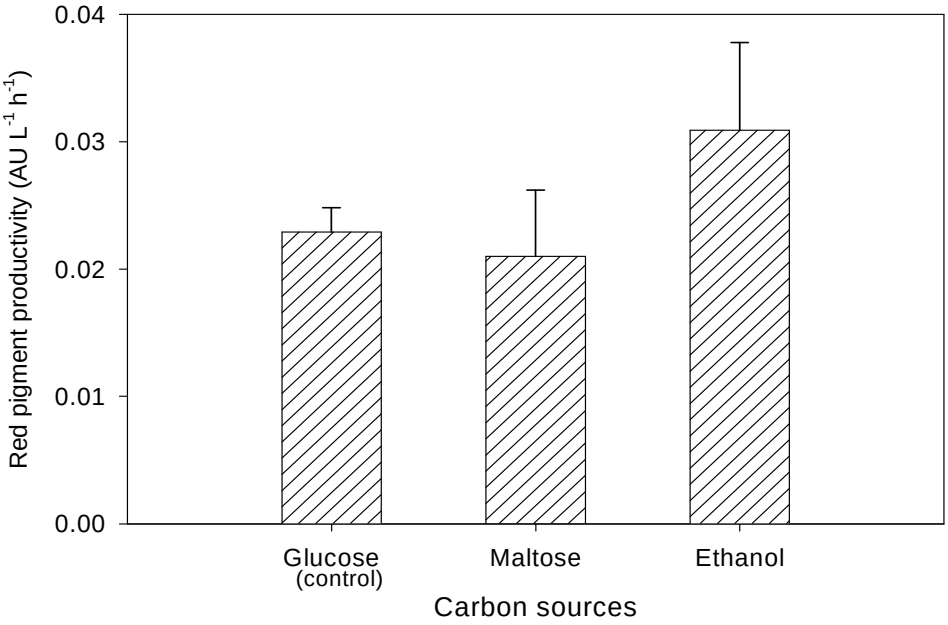

Figure 4.32: Effect of the carbon source on red pigment productivity

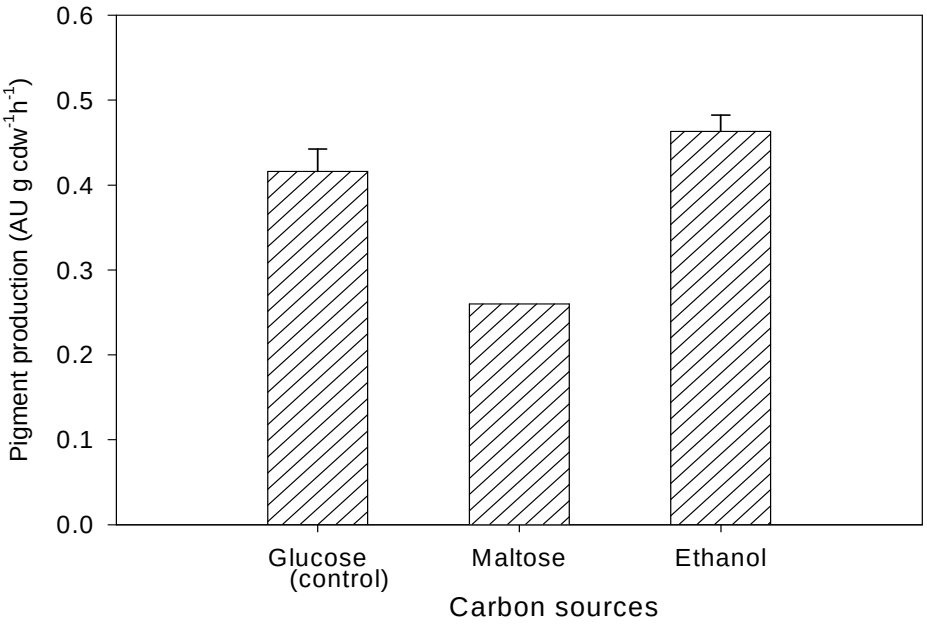

Figure 4.33: Effect of the carbon sources on specific rate of red pigment production

4.2.8 Summary

All the carbon and nitrogen sources tested supported fungal growth and development of certain pigments. The nitrogen sources that contained NH_4^+ proved to be quite unsatisfactory for development of the red pigment. MSG proved to be the best nitrogen source for producing the red pigment in submerged culture. Pigment production appeared to be growth associated, as also reported for other *Monascus* strains (Hajjaj *et al.*, 2000b; Phoolphundh *et al.*, 2007). A C : N ratio of 9 : 1 proved best for growth and pigment development. The most suitable concentration of glucose proved to be 10 g L^{-1}. At this concentration, and a C : N ratio of 9 : 1, using MSG as the nitrogen source, the batch fermentation was completed within 120 h. An incubation temperature of 30^{o}C appeared to be the most favourable for attaining a high yield of the red pigment. A higher temperature of 40^{o}C promoted preferential development of the yellow pigment. These results were consistent with the published reports for the other *Monascus* strains (Babitha *et al.*, 2007a; Carvalho *et al.*, 2005; Chatterjee *et al.*, 2009).

4.3 Production of red pigment by solid-state fermentation

4.3.1 Introduction

For comparison with submerged fermentation (Section 4.2), red pigment production in solid-state cultivation (SSC) was investigated. First, the suitable conditions for producing a high yield of red pigment in SSC needed to be identified. For this purpose, SSC was carried out in Erlenmeyer flasks. The carbon to nitrogen ratio in the solid substrate was determined. Growth and pigment production kinetics were characterized. Effects of changes in C : N ratio by supplementing the substrate with nitrogen sources were examined. The effect of initial moisture content on pigment and biomass production was elucidated. Data obtained in Erlenmeyer flasks were used as a basis for further studies in packed-bed bioreactors.

4.3.2 Properties of the solid substrate

Sunlong Premium long grain rice purchased from a local market was used as the substrate for SSC (see Section 3.3.3.1). Rice has been widely used as substrate in SSC because is generally nutritionally satisfactory (Johns and Stuart, 1991; Lee *et al.*, 2002; Sakurai *et al.*, 1977; Vidyalakshmi *et al.*, 2009; Yongsmith *et al.*, 2000), and produces a sufficiently porous bed that allows a good penetration of oxygen. Rice is also widely used in traditional Asiatic fermentations involving *Monascus* species.

In submerged fermentations (Section 4.2.5), the ratio of carbon to nitrogen was found to affect growth and red pigment production by *Monascus ruber*. Therefore, C : N ratio was expected to affect also the solid-state fermentation. For controlling the C : N ratio, its basal value in the substrate had to be determined. A sample (1.0 g) of ground rice was used in this determination (see Section 3.4.3.7). The results are shown in Table 4.5. Thus, the ratio of carbon to nitrogen in the rice was 30.2 : 1, by weight. Table 4.6 shows

the nutritional information of the Sunlong Premium long grain rice provided by the manufacturer.

Table 4.5: Composition of Sunlong Premium long grain rice

Constituents	Content (g /100 g weight)
Moisture	10.83
Carbon	39.30[a] or 44.07[b]
Nitrogen	1.30[a] or 1.46[b]
Crude protein	8.69[c]

[a] wet basis

[b] dry basis

[c] Nitrogen to protein conversion factor = 5.95

Table 4.6: Nutritional information of Sunlong Premium long grain rice

Constituents	Content (g /100 g weight)
Fat, total	< 1
-saturated	< 1
-trans	< 1
-polyunsaturated	< 1
-monounsaturated	< 1
Cholesterol	0
Carbohydrate	79
-sugars	< 1
Dietary fibre	< 1
Sodium	$< 5 \times 10^{-3}$
Potassium	94×10^{-3}

Note: Information given by the manufacturer of Sunlong Premium long grain rice

4.3.3 Biomass estimation in solid-state culture

In solid-state culture (SSC), direct measurement of biomass concentration is almost impossible, as the mycelium is impossible to separate from the substrate (Raimbault, 1998; Sakurai *et al.*, 1977; Scotti *et al.*, 2001; Singhania *et al.*, 2009; Terebiznik and Pilosof, 1999). Thus, an indirect method was used to estimate the biomass concentration in the fermenting substrate. The method was based on measuring the glucosamine content of the fermenting solids (Desgranges *et al.*, 1991b; Desgranges *et al.*, 1991a; Raimbault, 1998; Roche *et al.*, 1993). Glucosamine content were converted to a biomass concentration using a conversion factor (*cf*) that related the fungal glucosamine to the cell dry weight. The relevant conversion factor had been measured in a submerged fermentation that used only dissolved substrates.

Thus, a set of submerged fermentations were carried out under conditions that were comparable to that of the solid-state culture, especially in terms of the ratio of C : N and the trace elements added. In the submerged cultures, 10.0 g L^{-1} of glucose was used as the carbon source. Nitrogen was provided using NH_4NO_3. The C : N ratio of the liquid medium was 30 : 1. $ZnSO_47H_2O$ was added to the liquid medium at the same mass ratio of $ZnSO_47H_2O$ to carbon as used in SSC (Section 3.3.3.1.1). The liquid medium was inoculated with 10% (vol/vol) inoculum (Section 3.3.2.2.2). The fermentation was ran in shake flasks, for 168 h at 30^oC in the dark at an agitation rate of 250 rpm. Each 2 L flask contained 1 L of broth. The duplicate 20 mL broth samples were taken at intervals of 24 h. Mycelial cell dry weight and glucosamine content of the fermentation broth were determined as described in Section 3.4.2. The data is shown in Figure 4.34.

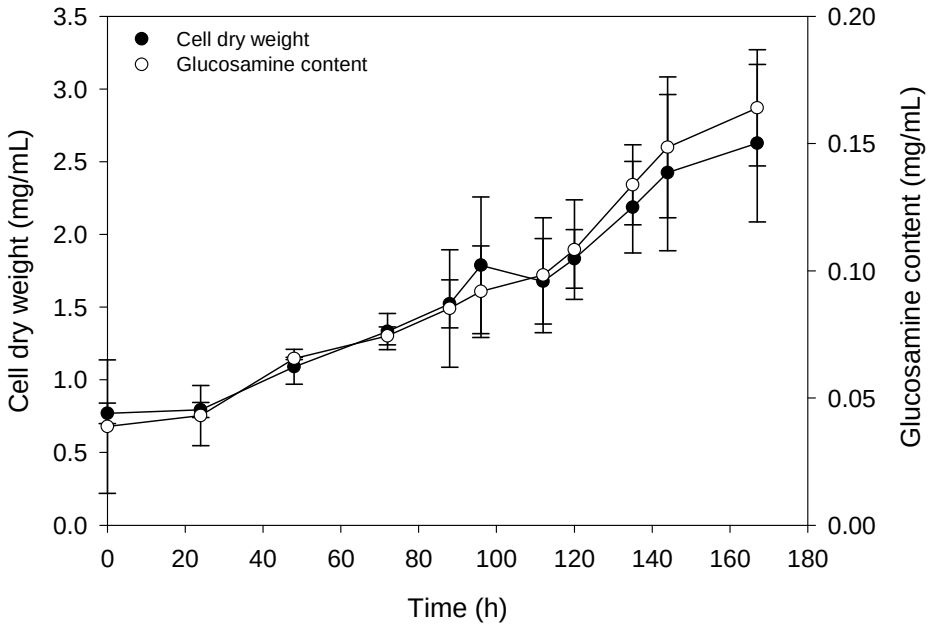

Figure 4.34: Fungal biomass dry weight and glucosamine content of submerged culture

The glucosamine content of the submerged culture broth increased in near direct proportion to the mycelial cell dry weight concentration in the broth. Using the data in Figure 4.34, a linear relationship was established between the glucosamine content of the biomass and the cell dry weight, as shown in Figure 4.35. The coefficient of determination (R^2) of the regression line in Figure 4.35 was 0.9832. The equation of the line in Figure 4.35 was:

$$G\ (mg) = 0.0591\ X\ (mg) \quad \text{..... Equation 4.1}$$

In Equation 4.1, G is the quantity of glucosamine (mg) and X is the biomass dry weight (mg). Equation 4.1 was used for estimating the biomass concentration in SSC from the measured glucosamine content. A conversion factor (*cf)* of 5.91×10^{-2} mg glucosamine/mg cell dry weight was obtained. Thus, the glucosamine content correlated well with the cell dry weight of *Monascus ruber*. These results suggest that the measured glucosamine level can be used confidently to estimate the biomass concentration in SSC.

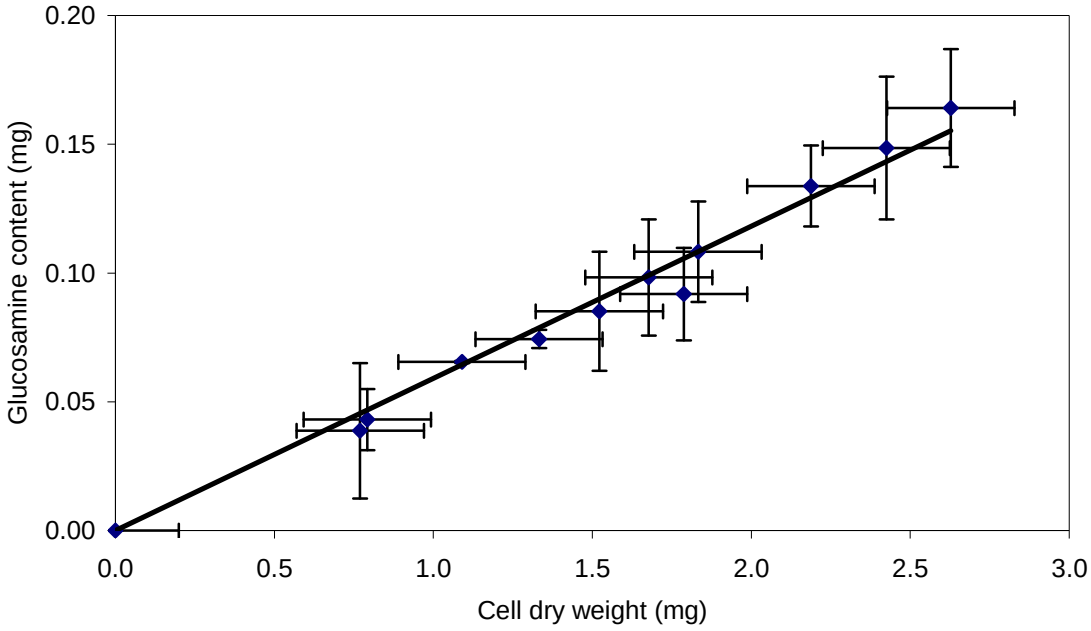

Figure 4.35: Relationship between glucosamine content and cell dry weight in submerged culture

4.3.4 Fungal growth in Erlenmeyer flasks

SSC were initially assessed in Erlenmeyer flasks. Long grain rice (20 g) with an initial moisture content of 53% (w/w) was sterilized in each Erlenmeyer flask (200 mL). Once the substrate had cooled to room temperature, it was inoculated with 10^6 spores per g rice, and grown in the dark at 30^{o}C, as described in Section 3.3.3.3.2. The cultures were grown for 18 days. Two Erlenmeyer flasks were periodically harvested for duplicate analyses. Pigments concentrations, biomass cell dry weight, pH, and the final moisture content were determined as described in Section 3.4.3.

Figure 4.36 and Figure 4.37 depict the fermentation profile in SSC. The biomass growth profile in Figure 4.36 is consistent with the expected pattern of a lag phase, followed by exponential growth, a stationary phase, and a decline phase. The maximum biomass concentration of 125.9 mg cell dry weight/g dry matter was attained on day 14. Production of the pigments began on day 2 and pigment concentration progressively increased until day 14, coinciding with the biomass peak concentration. The peak

concentrations of the various pigments were 328.1, 440.0, and 453.2 AU/g dry matter, for red, orange, and yellow pigments, respectively. The results suggest that the production of pigments was generally growth associated.

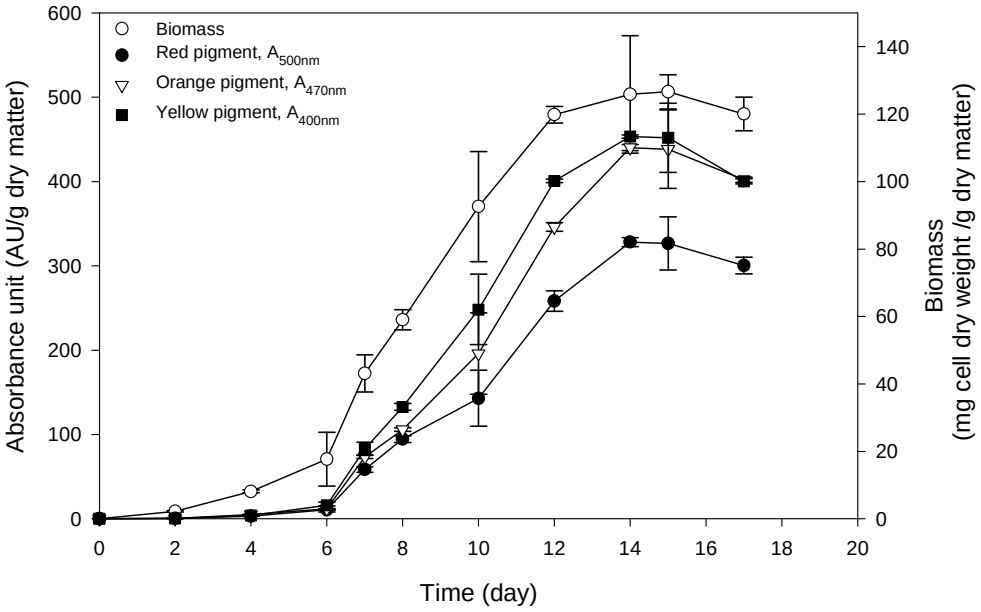

Figure 4.36: Fermentation time profile of *Monascus ruber* in Erlenmeyer flasks

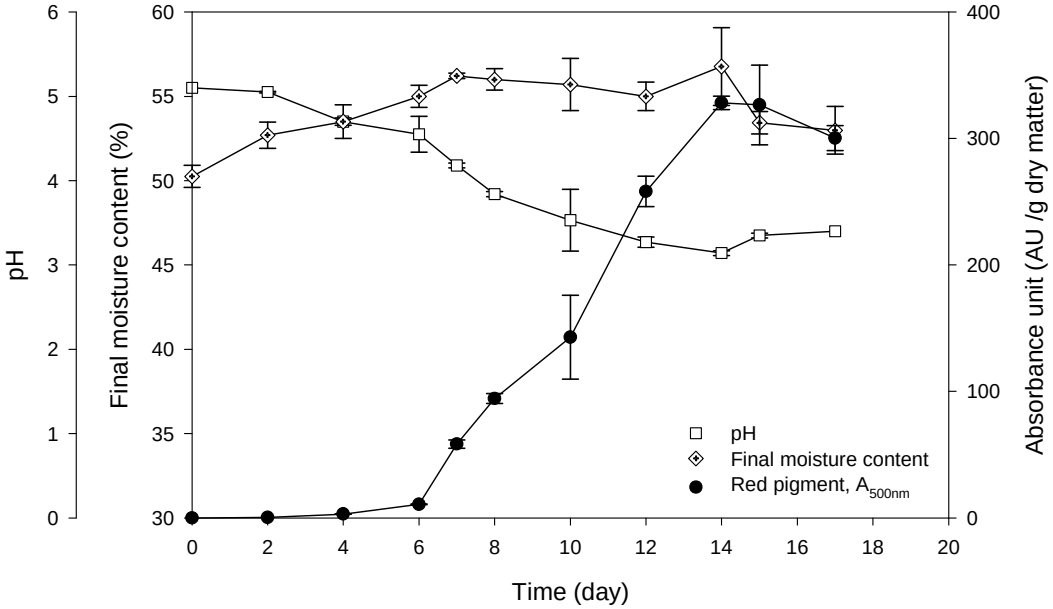

Figure 4.37: Fermentation time profile of pH, final moisture content, and the red pigment concentration

The final moisture content increased with biomass growth (Figure 4.37) to up to 56.8% on day 14 and then gradually dropped. This was because during the growth phase, water vapour was produced as a consequence of oxidation of the substrate and the removal of the water by evaporation in the headspace of the flask was insufficient to prevent a rise in the moisture content. Once growth had ceased, the rate of water removal to the flask headspace exceeded the rate of moisture generation and there was some drying of the fermenting solids. The pH-value gradually declined from 5.1 to 3.1 at day 14 and then remained stable. The pH dropped presumably due to the production of H^+ as a consequence of consumption of ammonium (NH_4^+), which is incorporated in biomass proteins as $– NH_2$.

The following kinetic parameters were calculated:

Pigment productivity,

$$\mathrm{Pr} = \frac{\left(\left(AU\ g^{-1}\right)_2 - \left(AU\ g^{-1}\right)_1\right)}{\left(t_2 - t_1\right)}\ \text{(AU/g dry matter h)} \quad \text{.....Equation 4.2}$$

(Based on dry weight of fermented solid)

Rate of fungal biomass production,

$$r_{BM} = \frac{\left(X_2 - X_1\right)}{\left(t_2 - t_1\right)} \qquad \text{(mg dry cell weight/g dry matter h)} \quad \text{.....Equation 4.3}$$

(Based on dry weight of fermented solid)

Yield of product on biomass,

$$Y_{P/X} = \frac{((AU\ g^{-1})_2 - (AU\ g^{-1})_1)}{(X_2 - X_1)} \qquad \text{(AU/mg dry cell weight)} \qquad \text{...Equation 4.4}$$

Specific growth rate,

$$\frac{\mathrm{dX}}{\mathrm{dt}} = \mu\ X \quad ; \quad X_t = X_o e^{\mu t}$$

$$InX_t = \ln X_o + \mu t \quad ; \quad \mu = \ln(\frac{X_t}{X_o})(\frac{1}{t}) \qquad (\mathrm{h}^{-1}) \text{..... Equation 4.5}$$

Specific rate of product formation,

$$r_P = \frac{dP}{dt} = Y_{P/X}\frac{dX}{dt} \quad \text{(AU/mg cell dry weight h)} \quad \text{.....Equation 4.6}$$

The time profile of the above parameters are shown in Figures 4.38 to 4.40.

The specific growth rate attained a maximum value of 0.022 h^{-1} approximately at day 7 and declined afterwards. The biomass production rate attained a maximum at day 12 with a value of 0.42 mg dry cell weight/g dry matter h, and declined steadily thereafter. Similar patterns were observed for the productivity of the pigments; all the pigments attained their maximum productivity values at day 14. The values obtained for the pigments productivity were 0.98, 1.31, and 1.35 AU/g dry matter h, for red, orange, and yellow pigments, respectively (Figure 4.38).

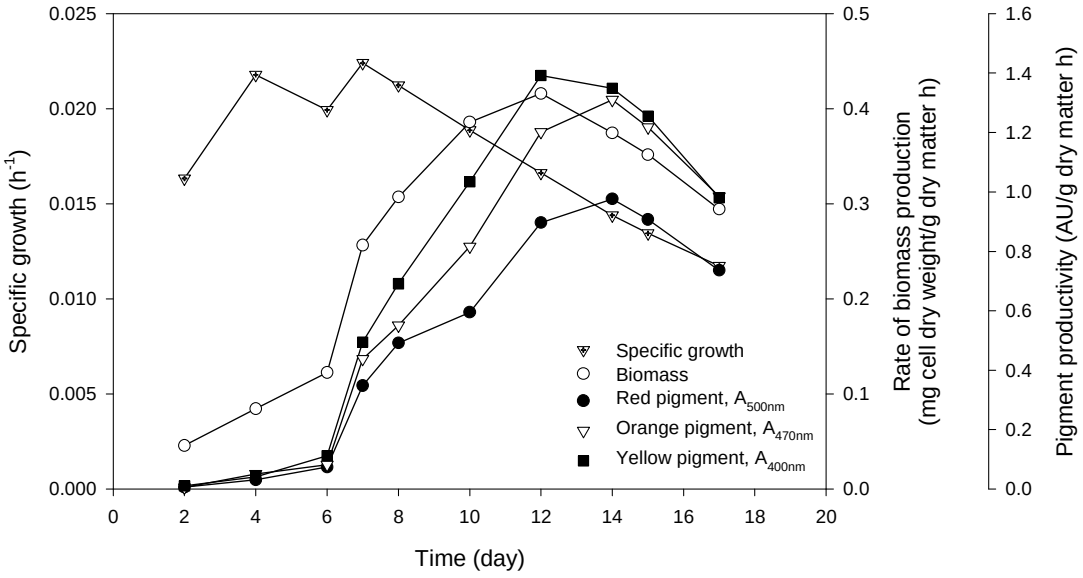

Figure 4.38: Specific growth, biomass production rate and pigments productivity in Erlenmeyer flasks

Figure 4.39 and Figure 4.40 depict the profile of yields of pigments on biomass and the rate of product formation. The productivity patterns for the red, orange, and yellow pigments were similar. The maximum yield of pigments occurred approximately on day 14, with values of 2607.4, 3496.5, and 3606.9 AU/g dry cell weight, for red, orange, and yellow pigments, respectively. The maximum specific rates of pigment production occurred on day 8. The values were 8.3, 9.3, and 11.7 AU/g cell dry weight h, for red, orange, and yellow pigments, respectively.

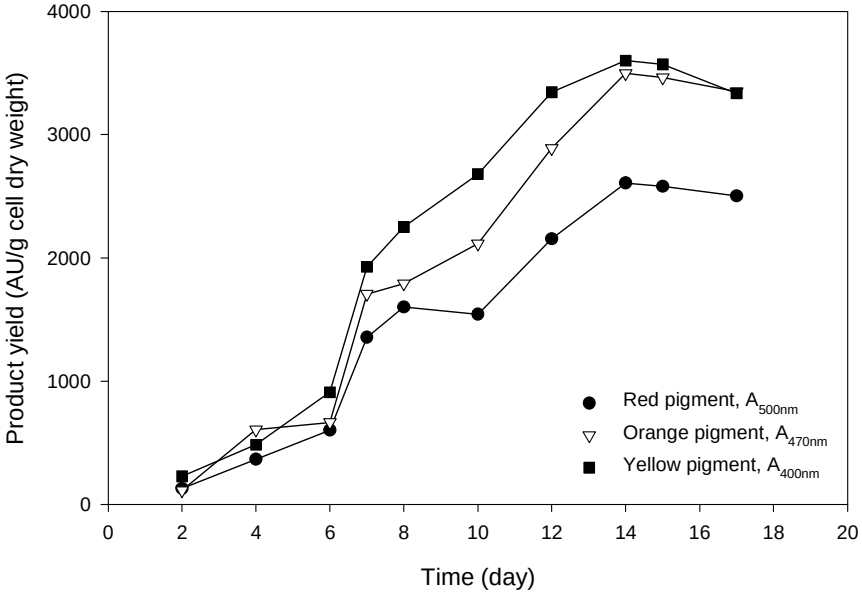

Figure 4.39: Yield of pigments on biomass in Erlenmeyer flasks

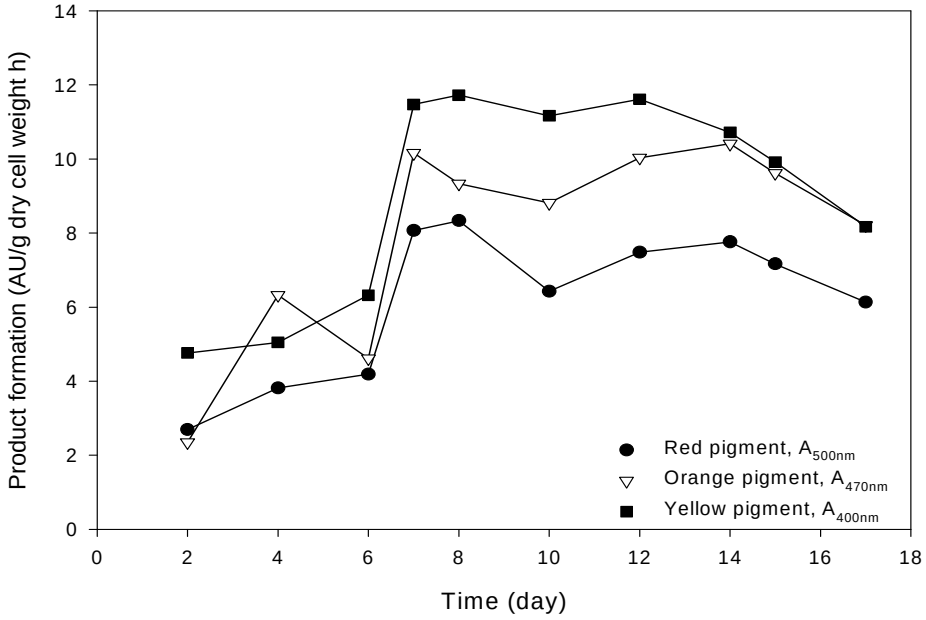

Figure 4.40: Specific rates of products formation in Erlenmeyer flasks

As the main purpose of this study was to maximize the red pigment production, the specific red pigment production rate and productivity of the solid-state and submerged culture methods are compared in Table 4.7. From the data (Table 4.7), the red pigment productivity and specific production rate by *Monascus ruber* ICMP 15220 are within the ranges seen with the other *Monascus* strains, for both solid-state and submerged cultures.

The red pigment productivity and specific production rate for *Monascus ruber* ICMP 15220 were clearly superior in SSC compared to submerged culture (Table 4.7). Apparently, the superiority of solid-state culture for production of *Monascus* pigments is not strain specific. For example, the specific production rate of red pigment by *Monascus purpureus* ATCC 16365 grown in solid-state culture was 268-fold greater than in submerged culture (Table 4.7) (Lee *et al.*, 2001). For *Monascus ruber* ICMP 15220, the solid-state culture showed 32-fold and 18-fold greater productivity and production rate of red pigment, respectively, compared to submerged culture.

Table 4.7: Comparison of red pigment production by different fermentation methods

Fermentation method	Substrate	Organism	Red pigment productivity (AU/g dry matter h or AU/L h)	Specific rate of red pigment production (AU/g cdw h)	Reference
Submerged culture					
	Glucose, Yeast extract	*M. purpureus*	0.007	0.011	Tseng *et al.* (2000)
	Ethanol, $NaNO_3$	*M. purpureus* CCM8152	0.041	0.741	Juzlova *et al*. (1994)
	Glucose, NH_4Cl	*M. purpureus* C322	0.155	0.634	Fenice *et al.* (2000)
	Glucose, MSG	*M. purpureus* ATCC 16365	0.115	1.169	Lee *et al.* (2001)
	Maltose, MSG	*M. purpureus* ATCC 16365	0.061	0.64	Lee *et al.* (2001)
	Glucose, MSG	*M. ruber* ICMP 15220	0.023	0.416	This work
	Maltose, MSG	*M. ruber* ICMP 15220	0.021	0.26	This work
	Ethanol, MSG	*M. ruber* ICMP 15220	0.031	0.463	This work
Solid-state culture					
	Jack fruit seed powder	*M. purpureus* LPB 97	0.097	0.444*	Babitha *et al.* (2007a)
	Long grain rice	*M. purpureus* ATCC 16365	31.542	312.913	Han and Mudgett (1992)
	Rice	*Monascus* sp. ATCC 16434	1.542	-	Tsukahara *et al.* (2009)
	Rice	*M. purpureus* ATCC 16362	17.593	79.167	Lee *et al.* (2002)
	Polished rice meal	*M. kaoliang* R10847	11.807	-	Lin and Iizuka (1982)
	Mantou meal (steamed bread)	*M. kaoliang* R10847	37.727	-	Lin and Iizuka (1982)
	Mantou meal (steamed bread)	*M. kaoliang* F2	0.329	-	Lin and Iizuka (1982)
	Long grain rice (Erlenmeyer flask)	*M. ruber* ICMP 15220	0.980	8.3	This work

Note: * calculated per unit glucosamine

4.3.5 Effect of additional nitrogen source

A few researchers have highlighted the need for nutrients supplementation of solid substrates for improving growth and metabolites production, especially when nutrient-poor agricultural residues are used as substrates (Manpreet *et al.*, 2005; Nimnoi and Lumyong, 2009). As mentioned in an earlier section, the carbon to nitrogen ratio in long grain rice used in this work was 30 : 1, or significantly higher than the ratio of 9 : 1 that had proved to be optimal for producing the red pigment in submerged culture (Section 4.2.5).

To correct for this deficiency, the rice was supplemented with additional nitrogen to adjust the C : N ratio to 9 : 1 (as per submerged culture) prior to sterilization. The nitrogen sources used were MSG, $NaNO_3$, and NH_4NO_3 in separate experiments. The choices of the nitrogen sources were based on their ability to promote red pigment production in submerged culture (Section 4.2.6).

Rice (30 g) with the added nitrogen source was sterilized in a 200 mL Erlenmeyer flask as described in Section 3.3.3.1.1. Rice alone (not supplemented with nitrogen) was also used for control purpose. In all cases, the initial moisture content of the substrate was adjusted to approximately 45% (g water per g wet substrate). The cooled substrate was then inoculated with 10^6 spores per g rice (dry weight) and grown in the dark at 30^oC, as described in Section 3.3.3.3.2. The cultures were grown for 14 days. Glucosamine content, pigments concentration, the final moisture content, water activity, and pH were measured after harvest. The biomass content per g dry matter were estimated from glucosamine measurements.

Figure 4.41 depicts the effect of nitrogen sources on pigment produced. Table 4.8 provides the final values of moisture content, pH, Aw, and biomass content on day 14. Supplementation of rice with MSG and $NaNO_3$ prevented pigments development and biomass growth. This was presumably because of the lower water activity of the supplemented substrate (Table 4.8) and a consequent insufficiency of water for the fungal growth. The final measured moisture contents for the substrates were 47.8, 44.6, 44.4, and

41.4, for the control, and the substrate supplemented with NH_4NO_3, $NaNO_3$, and MSG, respectively. However, a substrate's ability to support growth is controlled by water activity and not by moisture content per se. Moisture level can have other indirect effects, as described later.

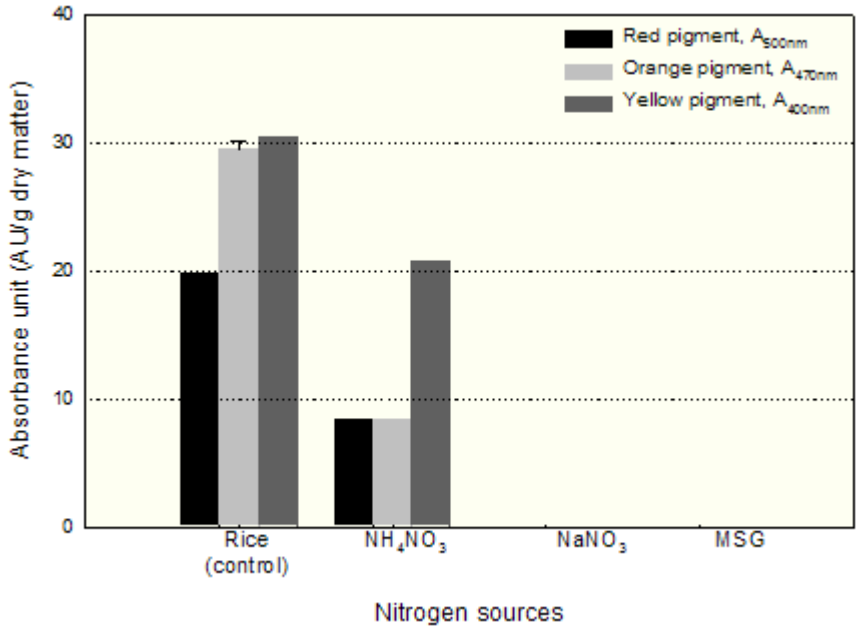

Figure 4.41: Effect of supplementation of nitrogen sources on pigment production at day 14

Table 4.8: Final moisture content, A_w, final pH, and glucosamine content on day 14 of different nitrogen sources

Nitrogen sources	Final moisture content (%)	pH	Aw	Glucosamine content (mg glucosamine/g dry matter)
Rice (control)	47.8	4.8	0.985	17.3
NH_4NO_3	44.6	4.6	0.967	12.4
$NaNO_3$	44.4	5.5	0.929	
MSG	41.4	6.6	0.900	

The rice supplemented with NH_4NO_3 was able to support fungal growth and pigments development. The pigments produced were acceptable, but the production was less than on the control (substrate rice only). The superiority of rice alone as a substrate was presumably because of the many complex nutrients present in rice.

In view of the above results, supplementation of rice with nitrogen was entirely unnecessary for producing the pigments and biomass. Therefore, rice with a naturally occurring C : N ratio of 30 : 1 was used for all further investigations in solid-state fermentation.

4.3.6 Effect of initial moisture content

Water content of the substrate of SSC are one of the critical factors that affect microbial growth and product formation (Pandey, 1992, 2003; Singhania *et al.*, 2009; Yongsmith *et al.*, 2000). Moisture content can influence water activity, but too much water causes water logging of substrates and adversely affects mass transfer of oxygen and carbon dioxide. Generally, the optimal moisture content tends to be in the range of 40 to 70% (Raimbault, 1998). The optimal initial moisture depends on the water holding capacity of the substrate and on the organism used. Therefore, the effect of the initial moisture content of rice substrate on pigments production was examined.

For the experiments, 20 g of rice was placed in a 200 mL Erlenmeyer flask and distilled water (5.5 to 50 mL depending on the desired moisture content) was added. Initial moisture content values of approximately 35, 45, 55, 70, and 75% (g water per g wet substrate) were investigated (Section 3.3.3.1.1). The fermentations ran for 18 days at 30^{o}C in a dark room. Duplicate samples (entire flasks) were taken on day 14 and 18 for analyses. The biomass cell dry weight, pigments production, the final moisture content, the water activity, and pH, were measured as explained in Section 3.4.2.

Figure 4.42 and Figure 4.43 depict the effect of initial moisture content on the production of pigments and biomass on day 14. The initial moisture content of the substrate (rice grain) clearly had a significant effect on the production of pigments and biomass. Maximum pigments and biomass production were obtained at 55% initial moisture content. The maximum biomass value was 117.3 mg cell dry weight/g dry matter. For the pigments, the maximum values were 328.0, 492.0, and 444.9 AU/ g dry matter, for red, orange, and yellow, respectively. A higher or lower initial moisture content than the optimal (55%), adversely affected pigment production and fungal growth. Under optimal moisture conditions, the fermenting solids attained a lower pH-value (pH 3.3) than at non-optimal moisture levels. In solid-state fermentation the moisture and pH levels unavoidably vary (Chisti 1999b; Mitchell *et al*., 2006) and the effects of the variables are nearly impossible to separate.

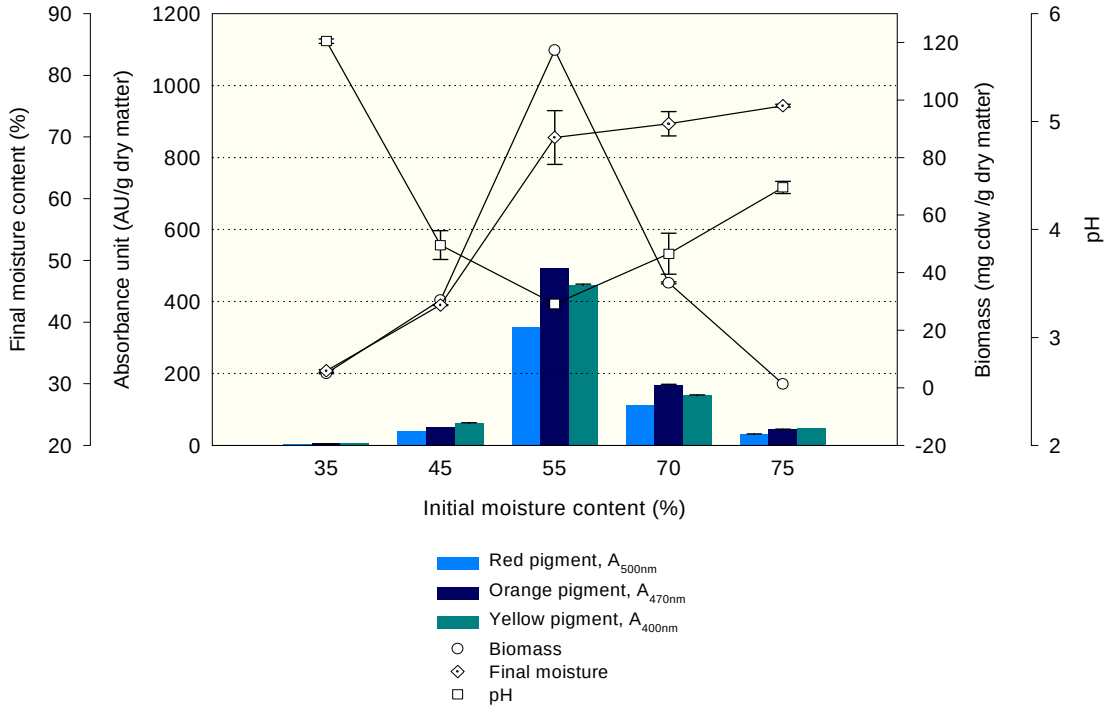

Figure 4.42: Effect of initial moisture content on pigments and biomass production at day 14

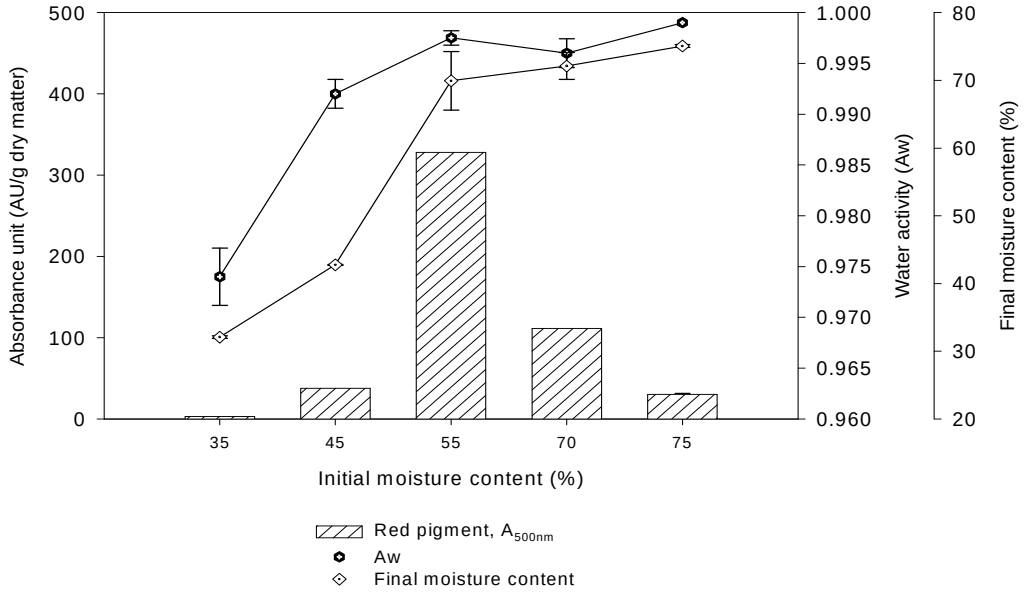

Figure 4.43: Effect of initial moisture content on red pigment production, final moisture content and water activity of the substrate at day 14

The dependence of final moisture content and water activity of the substrate on the initial moisture content is shown in Figure 4.43. Both the water activity and the final moisture content increased with an increase in initial moisture content until the latter attained the optimal values of approximately 55%. Further increase in the initial moisture content did not substantially alter either the water activity or the final moisture content. Water activity is a measure of the accessibility of the substrate water to the microorganism. Therefore, the decline in productivity for an initial moisture content of more than 55% is likely due to excess water affecting the oxygen penetration in the substrate bed.

Figure 4.44 and Figure 4.45 depict the effects of initial moisture content on pigments and biomass production at day 18. Once again, the optimal initial moisture content appears to be at 55%. Beyond an initial moisture content of 55-70%, the pigments production was drastically reduced as was the fungal growth.

It can be concluded that initial moisture content of 55% is the most suitable for producing red pigment in solid-state culture.

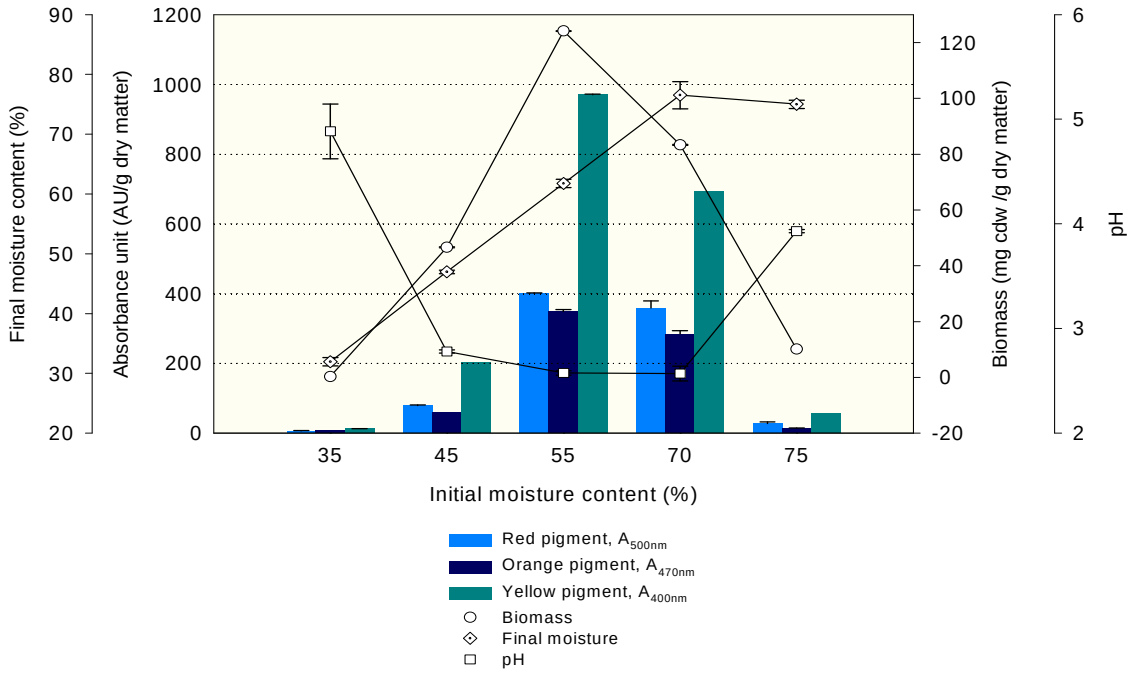

Figure 4.44: Effect of initial moisture content on pigments and biomass production at day 18

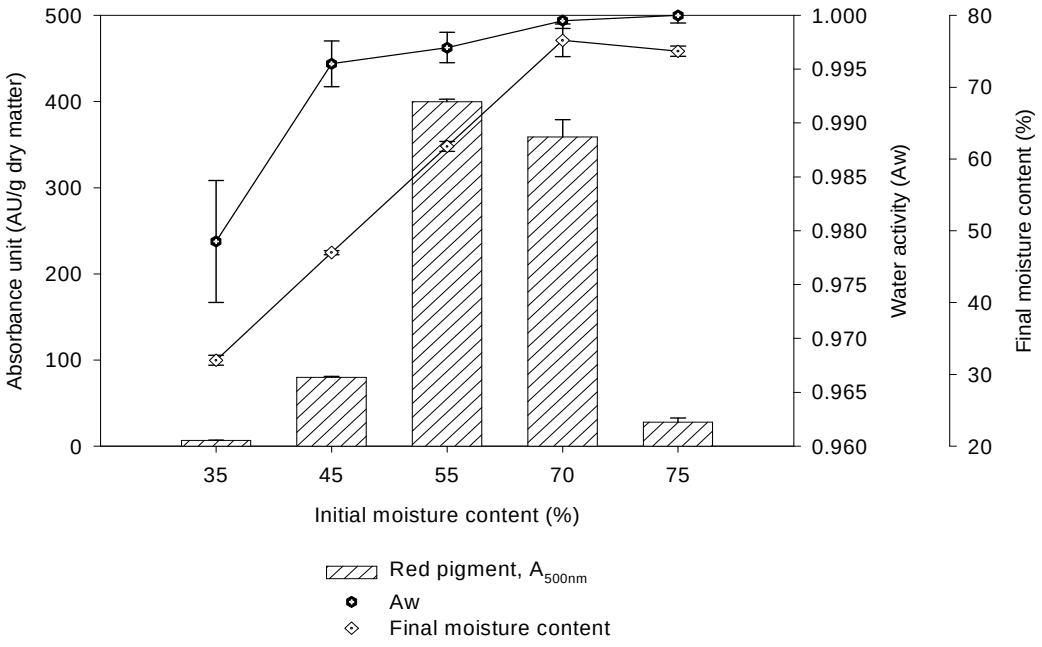

Figure 4.45: Effect of initial moisture content on red pigment production, final moisture content and water activity of the substrate at day 18

Figure 4.46 shows clear visual differences in the bed morphology and pigment production during growth at different initial moisture contents. From the figure, on day 6, there was red pigment produced for an initial moisture content of 35, 45, and 55%. However, only a few spots of red colour were observed for the substrate with the initial moisture contents of 70 and 75%.

Furthermore, at an initial moisture content of 35% on day 6 of fermentation, the fungal growth had covered almost 80-85% of the rice surface. By day 10, the fungal hyphae had started to penetrate into the rice. At this point, the rice looked dry and granular. By day 14, the fungal biomass had covered the entire rice surface and penetrated into the rice. At the same time, the red colour produced had become intense (Figure 4.46).

At an initial moisture content of 45% (Figure 4.46), nearly 80% of the surface of rice had been covered with the fungus by day 6 of the fermentation. The rice grain looked wet at this stage, likely because of moisture produced during a vigorous fermentation. By day 10, all of the rice surface had been covered by the fungus that had penetrated into the rice. At this stage, some of the rice had become orange-yellow in colour. At day 14, the change in colour from orange-yellow to red was obvious and further growth of the fungus was observed. At this stage, fungal spores could be clearly seen especially on the orange-yellow rice. At day 18, the red colour of the fungus became more intense and more spores were observed on the rice surface. In addition, water droplets were observed on the inside of the flask walls.

At an initial moisture content of 55% (Figure 4.46), almost 70% of the rice surface had been covered with the fungus at day 6. The rice looked wet and some of the red rice grain had turned to orange-yellow. At day 10 of fermentation, the entire rice surface had been covered with the fungus, the fungus had penetrated into the rice grain, and the colour had changed from orange-yellow to red. Inside of the flask was foggy. As the fermentation went to day 14, water droplets were observed on the flask wall and almost the entire rice had turned from red to orange-yellow. Many spores could be observed on the rice surface. At day 18 of fermentation, the red rice colour became intense and thick sporulation could be observed on the surface of the rice. Development of orange-yellow coloration prior to the final intense red suggests that some orange-yellow pigments form initially and are later converted to red (Blanc *et al.*, 1994; Juzlova *et al.*, 1996).

In contrast, at the higher initial moisture content of 70% (Figure 4.46), only a small part (approximately 5-10%) of the rice had been covered with the fungus at day 6. The rice was wet because of the water initially added and the grains stuck together. By day 10, more rice surface had been covered with the fungus and the fungus had penetrated into the rice. At day 14, more rice surface became covered with mycelia, but white rice could still be seen at this stage. As the fermentation went to day 18, almost 95% of the rice had been covered with the fungus and spores could be observed on the rice surface. At this stage, about 5% of the white rice was still visible, indicating that the fungal growth had not been completed, presumably because the stickiness of the rice reduced the penetration of oxygen.

At initial moisture content of 75% (Figure 4.46), at day 6 of fermentation, only a very small part of the rice (approximately 1-5%), had become covered with the fungus. As the fermentation went to day 10, the red fungal spots spread to approximately 15-20% of the rice. By day 14, the red spots covered approximately 30% of the rice. Orange-yellow rings were seen within the red spots. The rice was very wet, sticky, and soft. By day 18 of fermentation, more red spots had emerged, but nearly 30% of the rice still remained white at this stage. This indicated that the fungal growth was incomplete likely because of a poor oxygen supply due to water logging of the rice bed. Clearly, too high an initial moisture content adversely affected this fermentation. Similarly, too low a water content led to incomplete and poor fermentation, as the fungus could not completely penetrate into the rice and growth was poor due to a low water activity of the substrate.

Initial moisture content (IMC) (%)	Bed morphology and pigment production during fungal growth			
	Day 6	Day 10	Day 14	Day 18
a) 35				
b) 45				
c) 55				

Initial moisture content (IMC) (%)	Bed morphology and pigment production during fungal growth			
	Day 6	Day 10	Day 14	Day 18
d) 70	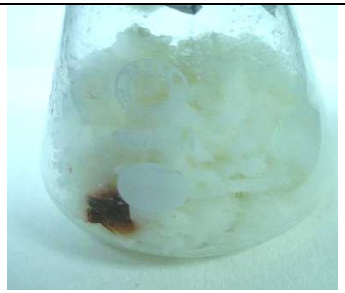			
e) 75	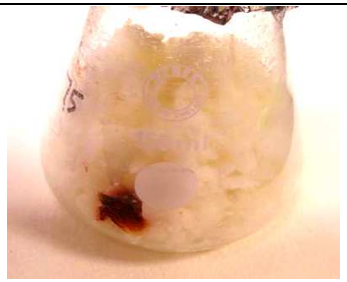	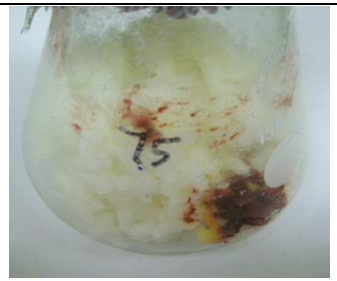		

Figure 4.46: Bed morphology and pigment production during fungal growth at different initial moisture contents

4.3.7 Summary

Solid-state fermentation in Erlenmeyer flasks proved to be superior to submerged culture for pigment production in keeping with similar observations for other *Monascus* strains (Carvalho *et al.*, 2006; Johns and Stuart, 1991; Kaur *et al.*, 2009). Under optimal conditions, the solid substrate fermentation provided a concentrated substrate, sufficient moisture, and oxygen. The SSC environment was comparable to the natural habitat in which fungi are normally found and this may have contributed to the observed high productivity.

Determination of the biomass concentration was based on the indirect method of measuring the glucosamine produced by hydrolysis of the chitin in the fungal cell wall. This method is widely used (Desgranges *et al.*, 1991a; Raimbault, 1998; Roche *et al.*, 1993). A strong correlation between the glucosamine level and cell dry weight was observed, confirming this method to be a good indicator of fungal growth. A conversion factor of 5.91×10^{-2} mg glucosamine/mg cell dry weight, was experimentally established. This conversion factor (*cf*) was comparable to the values reported by Scotti *et al.* (2001) and Han and Mudgett (1992). Different fungi and different strains of the same fungus can have very different *cf* values (Scotti *et al.*, 2001; Sharma *et al.*, 1977). For example, *cf* values of 1.70×10^{-1} and 6.70×10^{-2} mg glucosamine/mg cell dry weight, have been reported for *Caenorhabditis elegans* ATCC 26269 (Scotti *et al.*, 2001) and *Monascus purpureus* ATCC 16365 (Han and Mudgett, 1992), respectively.

Under optimal condition in SSC, rapid growth of fungus occurred after 6 to 7 days of inoculation. The maximum biomass concentration was attained at day 14 and the fermentation slowed down afterwards. A similar trend was observed for the production of pigments, confirming the pigment production to be growth associated, as also seen in submerged culture. This was consistent with reports for pigment production by other *Monascus* strains (Carvalho *et al.*, 2006; Han and Mudgett, 1992; Lee *et al.*, 2002).

Supplementation of rice with nitrogen sources to a C : N ratio of 9 : 1 adversely affected the pigments production as well as biomass growth. $NaNO_3$ and MSG had the most adverse effect on the pigment and biomass production, although both nitrogen sources were found to be good for the red pigment production in submerged culture at a C : N ratio of 9 : 1. Although the C : N ratio of rice was 30 : 1, or higher than the optimal for submerged culture (C : N ratio of 9 : 1), no additional nitrogen was required for pigment and biomass production on rice in solid-state fermentation. This observation was consistent with the report of Lee *et al.* (2002).

Initial moisture content of the substrate significantly affected the pigment production as well as fungal growth. Superior red pigment production and fungal growth were observed at an initial moisture content of 55%. An initial moisture content in the range of 50-56% has been reported to be good for pigment production also with other *Monascus* strains (Babitha *et al.*, 2007b; Johns and Stuart, 1991). High initial moisture content may flood the substrate, reducing porosity and adversely affecting the oxygen supply (Babitha *et al.*, 2007b; Cavalcante *et al.*, 2008; Chisti, 1999b; Gautam *et al.*, 2002; Lee *et al.*, 2002). Too low an initial moisture content may result in a water activity that is too low to support fungal growth (Dufosse *et al.*, 2005; Pandey, 2003). These factors likely explain the adverse effect of moisture levels that were higher or lower than the optimal level.

4.4 Production of red pigment in packed-bed bioreactor

4.4.1 Introduction

In view of the promising results with solid-state fermentation in static rice beds in Erlenmeyer flasks, attempts were made to scale up this fermentation in bioreactors.

Although many different types of bioreactors are available for solid-state culture (Durand, 2003; Mitchell *et al.*, 2006), the packed-bed bioreactor configuration was chosen for this work because of its simplicity, absence of mechanical agitation and ease of aseptic operation (Lonsane *et al.*, 1985; Mudgett, 1986; Pandey, 1991). Although many studies on packed-bed bioreactors have been reported as reviewed in Section 2.6.6.2, barely any work has been done on producing *Monascus* pigments in packed-beds, especially using *Monascus ruber*.

4.4.2 Effect of aeration rate on pigment production

Mycelial fungi are obligate aerobes and therefore a sufficiency of oxygen supply is critical to their successful culture. In a relatively deep bed of static particulate solids, forced aeration provides a relatively simple method of aeration (Chisti, 1999a; Perez-Guerra *et al.*, 2003). Forced aeration is effective in preventing a build up of carbon dioxide that can severely inhibit the productivity of an aerobic fermentation (Chisti, 1999a; Teng and Feldheim, 2000). Furthermore, forced aeration helps to remove the water produced by fermentation. Forced aeration is essential also for temperature control. For *Monascus* species, pigment production has been reported to be more sensitive to aeration than is growth (Juzlova *et al.*, 1996; Lin *et al.*, 2008). In view of its importance, effects of forced aeration on pigment production were examined to establish a suitable aeration regimen for the packed-bed bioreactor.

The packed-beds used were as described in Section 3.3.3.1.2. All the packed-bed glass columns (0.052 m inner diameter, 0.22 m height) were loaded with inoculated rice with a constant initial moisture content of approximately 55-57% wet basis. The glass columns were aerated at aeration rate values of 0.05, 0.2, 0.5, 1.0, and 2.0 L min^{-1} in separate parallel experiments. Aeration was with humidified air (relative humidity of 97-99%) through a 0.22 μm air filter (see Section 3.3.3.1.2). Fermentations were run for 6 days in a dark room at 30^{o}C. During fermentation, the temperature in the beds was measured at the centre line approximately 0.08 m from the bottom of the bed. The entire bed was harvested at the end of the fermentation for various analyses.

Figure 4.47 depicts the effect of aeration rate on pigments production in the packed-bed on day 6. All of the aeration rates used supported pigments production. The yellow pigments were predominantly produced at all the aeration rates. Aeration rates of 0.2 and 0.05 L min^{-1} were the most suitable for pigments production. Higher aeration rates (> 0.2 L min^{-1}) reduced pigment production because high rates promoted some drying of the bed (Figure 4.48), despite the high humidity in the aeration gas. In studies in Erlenmeyer flasks (Section 4.3.6), an initial moisture content of 55% had been found to be optimal for growth and pigment production. In the packed-bed, on day 6 and at an aeration rate of up to 0.5 L min^{-1}, the moisture content was 55% (Figure 4.48), but the biomass growth and pigment production were reduced relative to the values attained at lower aeration rates. This suggests that too much oxygen might adversely impact growth and pigment production, but this affect was not further examined. In preliminary experiment, unaerated bed resulted in little growth and pigment production because of oxygen limitation (Anisha *et al*., 2010; Sangsurasak and Mitchell, 1995; Wu *et al.*, 2000). In a packed bed, multiple factors vary and the overall effect on performance is difficult to assign to an individual factor.

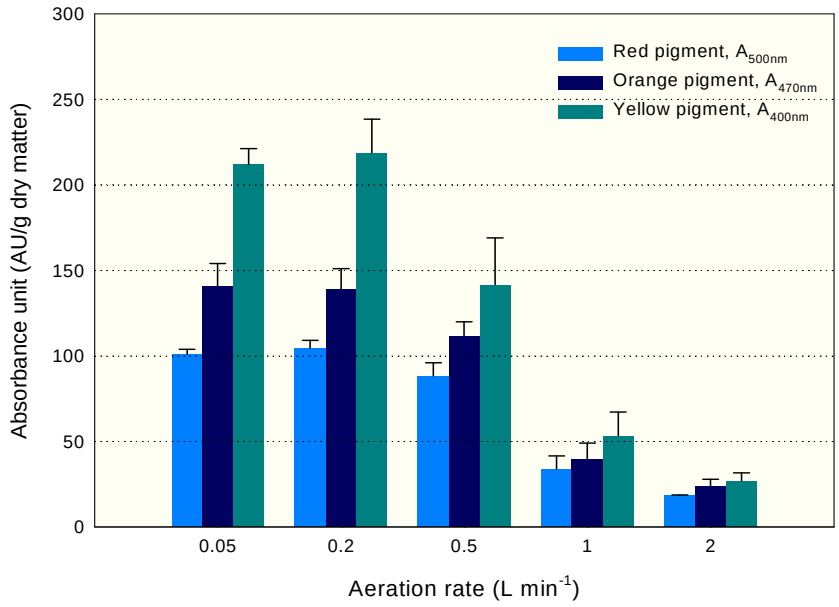

Figure 4.47: Effect of aeration rate on pigments production in packed-bed bioreactor on day 6

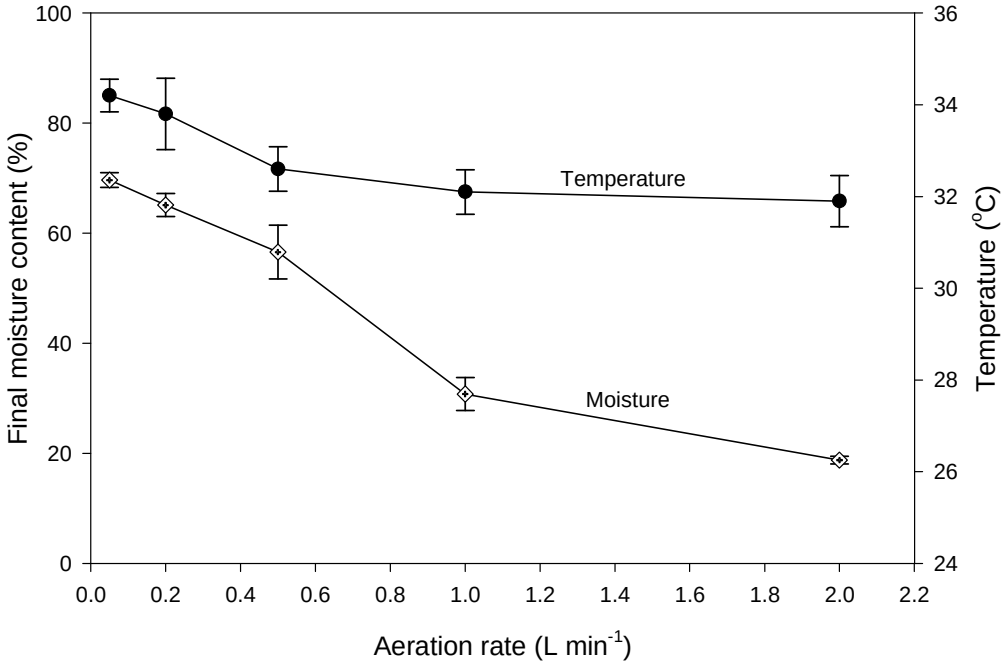

Figure 4.48: Temperature and final moisture content (day 6) at different aeration rates

As shown in Figure 4.48, increasing aeration rate had an increasing cooling effect but the temperature always remained within a range that was satisfactory for growth.

The aeration rate of 0.05 L min^{-1} that most favoured the production of the red pigment also afforded the highest biomass concentration (Figure 4.49), confirming a growth-associated production of the pigment.

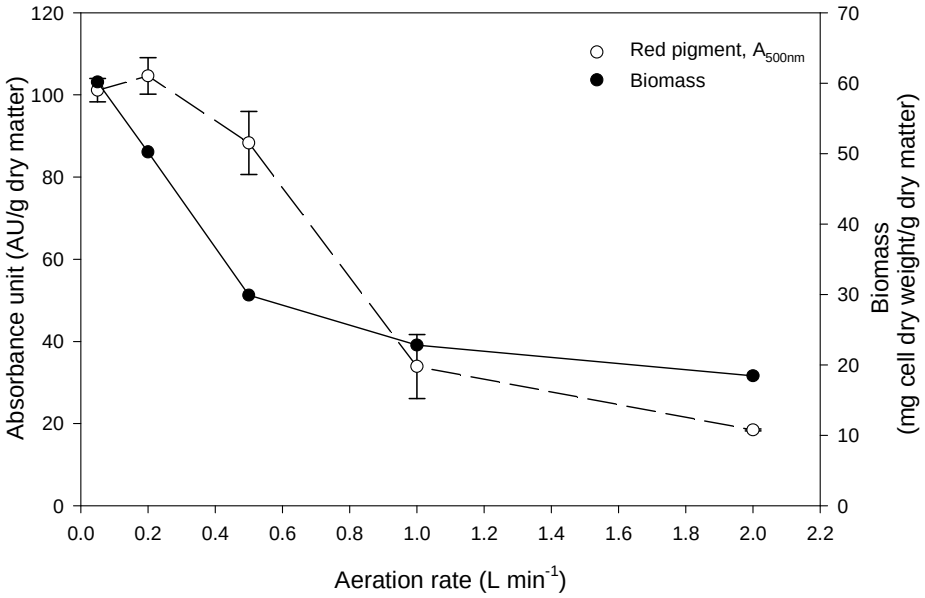

Figure 4.49: Red pigment and biomass production (day 6) at different aeration rates

Figure 4.50 illustrates the observations on the bed morphology and pigmentation during fungal growth in packed-bed bioreactors at different aeration rates. Clearly observable fungal growth commenced at day 2 of the incubation period for all forced aeration rates. At this point, the colour of the rice surface changed from white to slightly pale red. Further incubation resulted in progressively greater fungal growth that eventually covered the entire observable part of the rice bed.

At higher aeration rate of 2.0 L min^{-1}, the colour of the bed surface was lighter than at other aeration rate (1.0, 0.5, 0.2, 0.05 L min^{-1}) at any time (Figure 4.50). Noticeable biomass growth and pigment production occurred at all aeration rate values during the 6 days observation period (Figure 4.50). However, at the relatively low aeration rate values of 0.05 and 0.2 L min^{-1}, on day 3, the intensity of the red colour was

the greatest compared to observation at the other aeration rates (Figure 4.50). After day 3, progression of growth and pigment development were gradually slowed because of possible bed drying at aeration rate values of ≥ 0.5 L min^{-1} (Figure 4.50) compared to the lower aeration rates. At the two lower aeration values, the water produced by fermentation was observed as droplets on the walls of the glass column, by day 5 and 6, especially at the lowest aeration rate (aeration rate ≤ 0.2 L min^{-1}). At high aeration rates (≥ 0.5 L min^{-1}), drying tended to occur in the lower part of the bed where the air entered. Upper parts of the bed were moister as a consequence of the water picked up from the lower parts and fermentation progressed further in the upper parts. This explains the two tone colour (yellow lower portion, redder upper parts) seen in the columns (Figure 4.50), especially at the aeration rate values of ≥ 0.5 L min^{-1}. Some of this effect occurred also at the lower aeration values (0.5 L min^{-1}) and the growth in the upper moister regions of the packed columns tended to be better than in the lower drier region (Figure 4.50).

Therefore, the visual observation of growth and pigmentation were consistent with the quantitative measurements; aeration rates that were too high adversely affected biomass growth and pigment development because of drying of the bed. Aeration rate in the range of 0.05 – 0.2 L min^{-1} were best for biomass growth and pigment development. Thus, further work was confined to an aeration rate value of 0.2 L min^{-1}.

Aeration rate (L min^{-1})	Bed morphology and pigment production during fermentation in the packed-bed bioreactor					
	Day 1	Day 2	Day 3	Day 4	Day 5	Day 6
a) 2.0	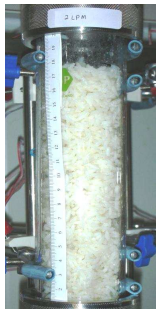	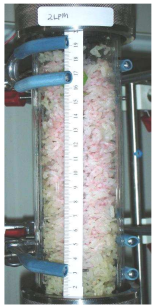	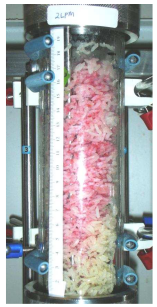	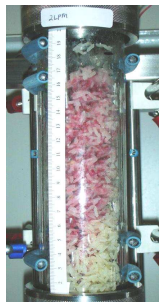		
b) 1.0		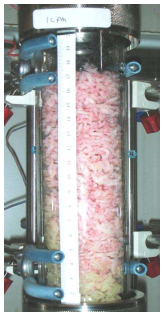	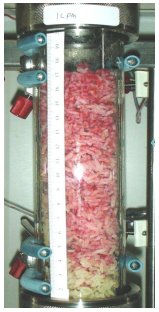	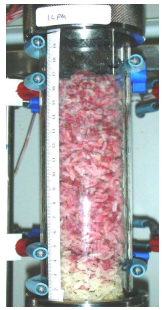		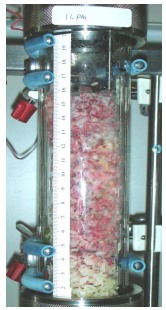
c) 0.5	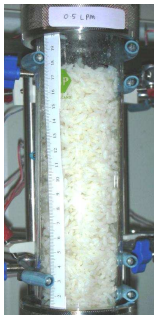					

Aeration rate (L min^{-1})	Bed morphology and pigment production during fermentation in the packed-bed bioreactor					
	Day 1	Day 2	Day 3	Day 4	Day 5	Day 6
d) 0.2	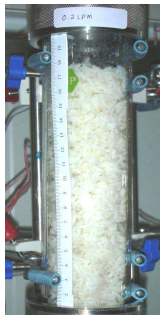		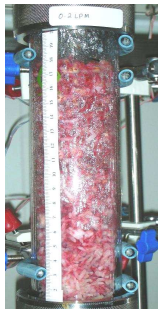	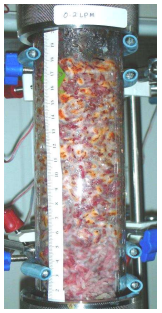	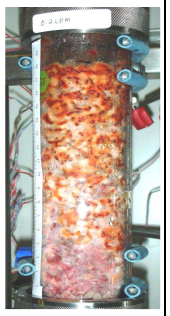	
e) 0.05						

Figure 4.50: Morphology and pigment production in packed-beds bioreactor at different aeration rates

a) 2.0 L min^{-1}, b) 1.0 L min^{-1}, c) 0.5 L min^{-1}, d) 0.2 L min^{-1}, e) 0.05 L min^{-1}

4.4.3 Kinetics of solid-state culture in packed-bed bioreactor

Kinetics of growth and product formation in the packed-bed were examined at a fixed aeration rate of 0.2 L min^{-1}. The geometry of the beds and the other details have been previously described (Figure 3.1). The long grain rice substrate used was pre-treated as follows: Rice (120 g) was placed in a 500 mL beaker and soaked in 132 mL of water mixed with 12 mL of a 0.128 M $ZnSO_4 7H_2O$ solution. Each beaker containing soaked rice was covered with two layers of aluminium foil, and autoclaved (121^oC, 15 min). The empty glass packed-bed columns were autoclaved separately (121^oC, 25 min). When the substrate had cooled it was aseptically inoculated with 12 mL of a spore suspension (approximately 10^7 spores/mL) and mixed well (Section 3.3.3.1.2). The sterile glass columns were filled aseptically with the inoculated substrate to a bed depth of approximately 0.18 m. The approximate initial moisture content of the substrate was 55-57% on wet basis. The glass columns were covered with the aluminium foil and incubated at 30^oC. Columns were aerated continuously with humidified air at a flow rate of 0.2 L min^{-1} for 18 days. Several identical columns were prepared for each run. An entire column was harvested at specified time intervals for various measurements.

Figure 4.51 and Figure 4.52 show the fermentation profile in the packed-bed bioreactor. The biomass growth had the expected profile of a lag phase (day 0 to day 6), an exponential growth phase (day 6 to day 10), and a slower growth phase (day 10 to day 18) leading to the stationary phase. Fermentation was essentially complete by day 18. The maximum biomass produced was 122.2 mg cell dry weight/g dry fermented matter. Red, orange, and yellow pigments were produced simultaneously with growth (Figure 4.51) indicating growth associated production. The highest pigments concentration obtained at day 18 were 890.1, 1285.5, and 1208.0 AU/g dry matter, for red, orange, and yellow pigments, respectively.

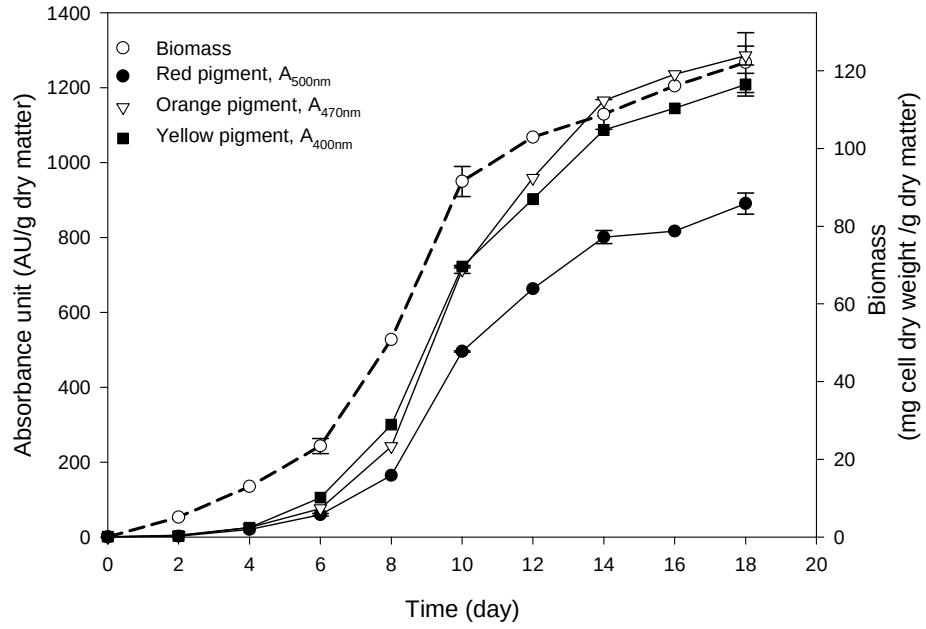

Figure 4.51: Fermentation time course of *Monascus ruber* in packed-bed bioreactor

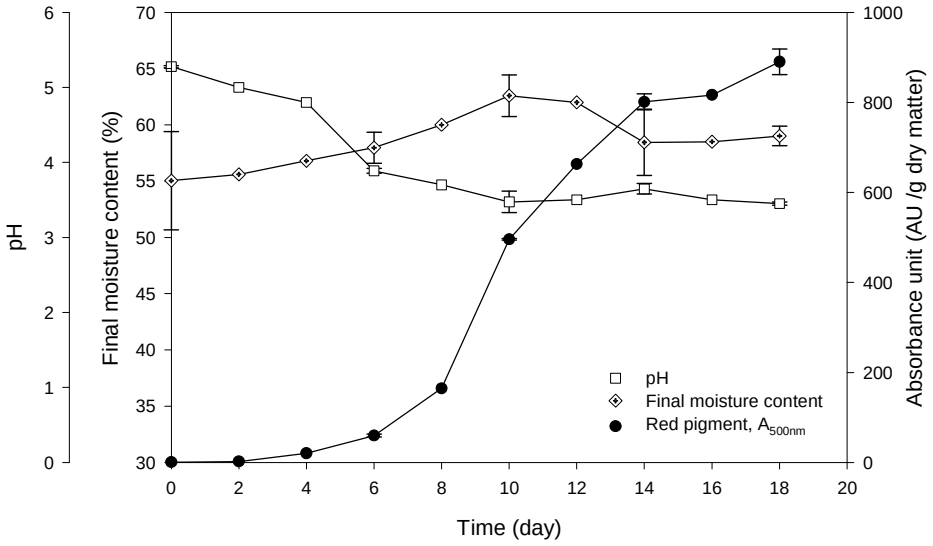

Figure 4.52: Fermentation time course of pH, final moisture content, and red pigment content in packed-bed bioreactor

The final moisture content remained relatively stable at 55 – 63% (Figure 4.52). The slight increase in moisture of the bed during day 0 to day 10 (Figure 4.52) indicated that water production by fermentation during this biomass growth period (Figure 4.51) was slightly greater than water loss by evaporation. Once fermentation and growth had slowed (day > 10 in Figure 4.51), there was some drying of the bed (Figure 4.52, day > 10) as water loss by evaporation was somewhat greater than water generation by fermentation.

The pH of the bed progressively declined to around pH 2.5 (Figure 4.52) probably due to the production of H^+ and consumption of ammonia, which corresponded to the transformation of the orange precursor pigment to the red because of reaction with $-NH_2$. The profiles of specific growth rate, biomass production rate, pigment yield, pigment productivity, and biomass specific rate of product formation are shown in Figures 4.53 to 4.56. The biomass production rate peaked on day 10 with a value of 0.38 mg cell dry weight/g dry matter h (Figure 4.53). However, the instantaneous specific growth rate declined throughout the fermentation process (Figure 4.53). The maximum specific growth rate was 0.034 h^{-1} on day 2.

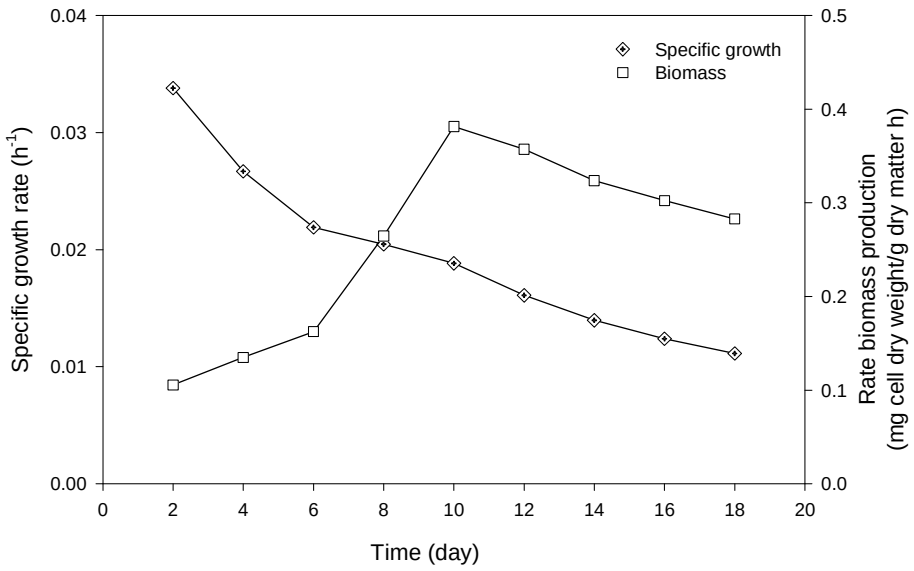

Figure 4.53: Specific growth rate and biomass production rate in packed-bed bioreactor

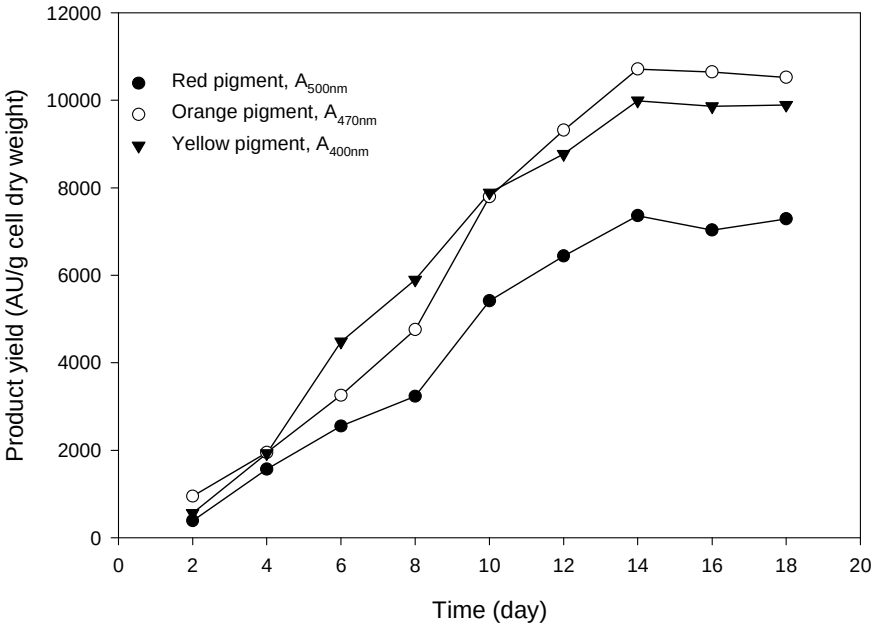

Figure 4.54: Yield of pigments on biomass in the packed-bed bioreactor

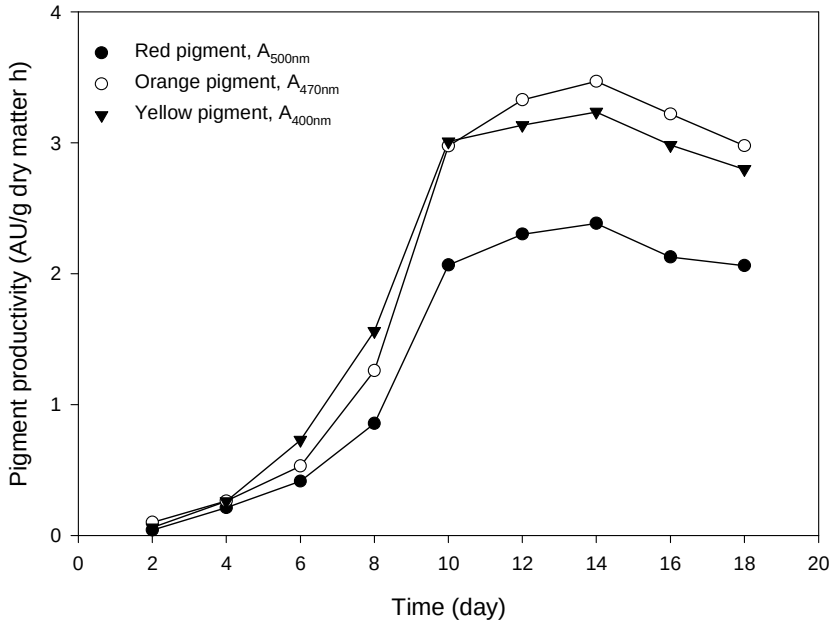

Figure 4.55: Pigments productivity in the packed-bed bioreactor

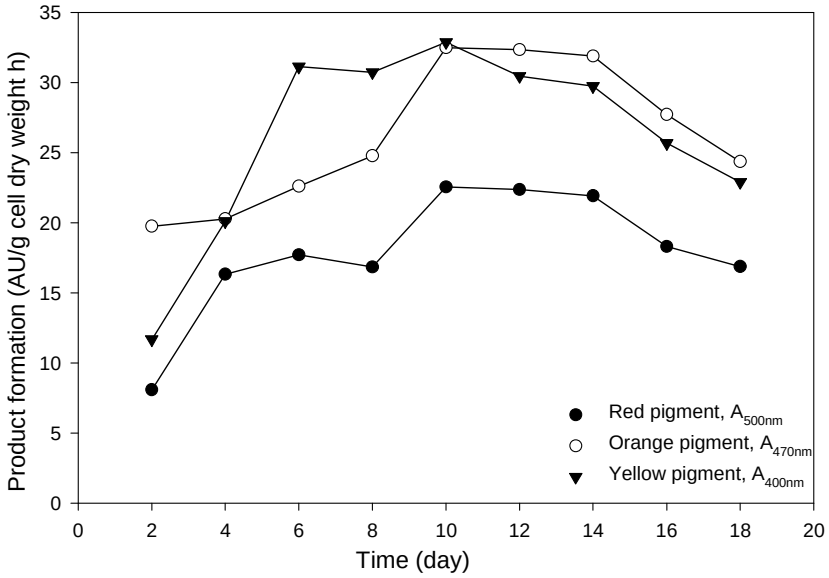

Figure 4.56: Specific rate of products formation in packed-bed bioreactor

The product yield per unit cell mass (Figure 4.54) and pigment productivity (Figure 4.55) generally increased in proportion to the biomass concentration. The values for pigments yields were 7362.4, 10712.6, and 9991.0 AU/g dry cell weight, for red, orange, and yellow pigments, respectively.

Table 4.9 compares the fermentation parameters of the packed-bed bioreactor and Erlenmeyer flask solid-state culture. The maximum biomass production rate in packed-bed bioreactor was quite comparable to that in Erlenmeyer flasks, but in all other respects, the packed-bed bioreactor proved to be greatly superior. For example, the red pigment concentration in the packed-bed was 2.7 times greater than in Erlenmeyer flask. The red pigment productivity in the packed-bed was 2.4-fold greater than in the flasks. The superior performance of the bed was largely explained by its being sparged with humidified air. This not only improved oxygen supply but also prevented an excessive rise in temperature. Forced aeration further ensured a continuous removal of carbon dioxide from the bed. Carbon dioxide is known to be inhibitory to many fungal fermentations (Han and Mudgett, 1992; Teng and Feldheim, 2000).

Table 4.9: Comparison of fermentation parameters of packed-bed bioreactor and Erlenmeyer flask

Parameters	Units	Packed-bed bioreactor	Erlenmeyer flask
Maximum red pigment concentration	AU/g dry matter	890.1	328.1
Maximum red pigment productivity	AU/g dry matter h	2.38	0.98
Maximum yield of red pigment on biomass	AU/g cell dry weight	7362.4	2607.4
Specific rate of red pigment production	AU/g cell dry weight h	21.9	8.3
Maximum biomass concentration	mg cell dry weight/g dry matter	122.18	125.9

4.4.4 Summary

Solid-state fermentation in aerated packed-bed bioreactors proved to be superior to the otherwise identical fermentation in static Erlenmeyer flasks. In the packed-bed, the forced aeration rate value needed to be ≤ 0.2 L min^{-1} to prevent excessive drying and a consequent adverse impact on the fermentation. In preliminary experiments a packed-bed bioreactor without forced aeration afforded little fungal growth and the observed growth remained confined to the upper zone of the bed that received oxygen from the enclosed headspace of the packed-bed column. In unaerated beds, oxygen limitation has been reported to limit growth and metabolite production by various fungi (Anisha *et al.*, 2010; Sangsurasak and Mitchell, 1995; Wu *et al.*, 2000). In *Monascus* sp., pigment production has been found to be more responsive to aeration than biomass growth (Juzlova *et al.*, 1996; Lin *et al.*, 2008; Turner, 1971).

4.5 Spatial characterization and optimization of the packed-bed bioreactor

4.5.1 Introduction

Packed-bed bioreactors lack mixing by design and are invariably operated with a batch loading of the substrate. As a consequence of spatial and temporal variation of environmental conditions, non-uniform growth and product formation occur in packed-beds during a fermentation (Gumbira-Said *et al.*, 1993; Mazutti *et al.*, 2010b; Rao *et al.*, 1993). At the beginning of the fermentation in a freshly inoculated bed, the conditions are fairly uniform in terms of temperature, oxygen concentration, and moisture content. A packed-bed is aerated using humidified air that enters usually at the bottom of the column. As the air moves up the bed, its composition inevitably changes in terms of concentration of oxygen, concentration of carbon dioxide, temperature, and moisture content. This results in a differentiated growth microenvironment up the bed and consequent differences in microbial metabolism. Different metabolic rates in different zones of the bioreactor translate to different rates of biomass growth, moisture production, heat generation, and pigment production (Ghildyal *et al.*, 1994; Mazutti *et al.*, 2010b). Spatial and temporal variations in packed-bed bioreactors need to be characterized to establish limits on acceptable bed height and suitable forced aeration regimens. The overall, or averaged, pigment productivity of the bed could then be used to optimize the bed dimensions and operations.

Traditionally, the optimization of packed-bed bioreactors is done by varying one of the experimental factors at a time and observing the effect on performance (Kumar *et al.*, 2003; Lee *et al.*, 2002; Patidar *et al.*, 2005). Unfortunately, this process is time consuming and expensive if there are too many variables that necessitate a large number of experiments. In addition, this optimization process is unable to account for possible interactive effects of variables on the performance of the bioreactor. This study therefore used a statistical experimental design for the optimization as discussed later.

4.5.2 Characterization of spatial and temporal variations in the packed-bed bioreactor

Spatial heterogeneity of the fermenting substrate occurs almost always in solid-state fermentation. A porous bed of particulate substrate is a poor conductor of heat. Heat produced by metabolism can lead to overheating especially in the middle and top sections of the bed (Saucedo-Castaneda *et al.,* 1990). Temperature gradients further accentuate heterogeneity by affecting the local rates of biomass and metabolite production (Ashley *et al.,* 1999; Chen *et al.,* 2005; Ghildyal *et al.,* 1994; Lonsane *et al.,* 1992; Mazutti *et al.,* 2010a; Oriol *et al.,* 1988).

Forced aeration is known to reduce the unwanted local temperature rise and improve oxygen supply (Saucedo-Castaneda *et al.,* 1990). However, continuous aeration frequently results in evaporative loss of moisture from the bed even if the air is pre-humidified. Some moisture loss is necessary for evaporative cooling, but if moisture loss exceeds water production by fermentation, the bed will become drier and this will adversely affect biomass growth and metabolite production. Therefore, the initial moisture content in the bed and the rate of forced aeration with humidified air are two of the most important variables that influence fermentation. Using prior experiments (Sections 4.3.6 and 4.4.2) as guides a series of experiments were designed to combine an initial moisture contents of 45 to 70% (g water/g wet substrate) and forced aeration rates of 0.05 to 0.2 L/min as in Table 4.9, to study this fermentation.

To obtain the required initial moisture content, long grain rice, distilled water, and 0.128 M $ZnSO_4 7H_2O$ were mixed (Table 4.10) in 500 mL beakers and autoclaved. Once the substrate had cooled, it was inoculated aseptically with a fungal spore suspension of approximately 10^7 spores/mL (Table 4.10) and mixed well (Section 3.3.3.1.2). Separately autoclaved glass columns were filled aseptically with the inoculated substrate to a bed depth of approximately 0.18 m. The glass columns were covered with the aluminium foil and incubated at 30^oC. Humidified aeration rate (at a relative humidity of 97-99%) was set as indicated in Table 4.11. The fermentations were run for 18 days. One column was withdrawn at specified times for various analyses. Care was taken to harvest the whole

bed, without breaking or mixing it. The bed column was cut into six equal 3 cm thick segments for analyses (Section 3.3.3.3.2). The biomass cell dry weight, pigments concentration, the final moisture content, water activity, and pH of each bed section were measured as explained in Section 3.4.2. The bed temperature was continuously monitored during the fermentation by six thermocouples placed at various depths of the bioreactor column.

Table 4.10: Rice substrate preparation and inoculation for various initial moisture contents

Initial moisture content (%)	Rice (g)	Distilled water (mL)	$ZnSO_4 7H_2O$ (0.128 M) (mL)	Spore suspension (mL)
45	130	73.6	13	13
57.5	120	132	12	12
70	110	187	11	11

Table 4.11: Various packed-bed experimental conditions

Run	Initial moisture content (%)	Aeration rate (L/min)
1	45	0.05
2	45	0.2
3	57.5	0.05
4	70	0.05
5	57.5	0.125
6	70	0.125
7	57.5	0.2
8	70	0.2

4.5.2.1 Temperature profiles

During the fermentation, metabolic heat generation led to temperature changes. The axial and temporal temperature gradients depended on the aeration rate and the bed porosity, which depended on the initial moisture content. Figure 4.57 depicts the temperature profiles obtained as functions of time and height of the bed for eight runs (Table 4.11) in the packed-bed bioreactors.

The profile in Figure 4.57 reveals the following:

1. In all runs, the temperature during the first 120 h was relatively low, consistent with the metabolically less active lag phase of the fermentation. During this period, heat removal by aeration generally compensated for metabolic heat generation and the temperature remained at approximately 30^{o}C, i.e at the temperature of the air and the incubation chamber.

2. Runs 1 and 2 with a low initial moisture content of 45% (Table 4.11) did not produce as large a temperature rise at any time as did the other runs. This suggests a generally low metabolic activity and growth in the bed mainly because of a low initial moisture content. The result is consistent with the low biomass growth obtained at 45% initial moisture content in rice beds in Erlenmeyer flasks (Figure 4.44).

3. The maximum rise in temperature at any bed depth generally occurred between 120 h and 150 h in beds with 70% moisture content (i.e. run 4, 6, 8). Compared to the beds with lower moisture contents, the rise in temperature was quite sharp. This not only indicated a high metabolic activity during rapid fungal growth, but also a lack of effective cooling at any of the aeration rates (Table 4.11). For air with the specified humidity level, an increase in the initial moisture content in the bed reduced mass transfer during forced aeration and the evaporative cooling effect. The 120 – 150 h period was the course period of rapid fungal growth.

4. In beds with an intermediate moisture contents of 57.5% (Table 4.11, i.e. runs 3, 5, 7), temperature rose during rapid growth (i.e. 100 – 200 h), but never as rapidly as in the high moisture runs 4, 6, and 8. In runs 3, 5, and 7, the metabolic activity was high but better cooling prevented too rapid a temperature rise.

5. In all fermentations, after the metabolic peak activity, the temperature declined as growth entered the stationary phase and heat removal by aeration exceeded the rate of heat production by metabolism. Temperature declined more rapidly after the peak in beds that had attained a higher temperature during the peak (runs 4, 6, 8). This was likely because of a higher temperature difference during forced aeration (i.e. bed temperature minus cooling air temperature of 30^{o}C) in these beds.

6. Irrespective of the run, at any given time, the temperature at level 1 (bottom of bed) tended to be the lowest (Fanaei and Vaziri, 2009; Mitchell and Von Meien, 2000; Weber *et al.*, 2002). Temperature rose to a peak around the middle and the upper regions of the bed were cooler than the middle but warmer than the lower parts. This suggests that the proximity of the upper zone to the headspace of the bioreactor improved cooling. This was likely because the upper surface of the bed provided some extra cooling area compared the deeper parts of the bed.

7. Temperature gradients within the beds at any given time could be quite pronounced. For example in beds with an initial moisture content of 70% at an aeration rate of 0.2 L/min the temperature gradient in the vicinity of level 5 was 0.73^{o}C cm^{-1} (Figure 4.57, run 4). Nevertheless, the temperature at any time and position never exceeded 40^{o}C. The observed temperature rise was unlikely to have adversely affected fungal growth much as a temperature of up to 45^{o}C is still quite satisfactory for growth of *Monascus* fungi (Pitt and Hocking, 1997).

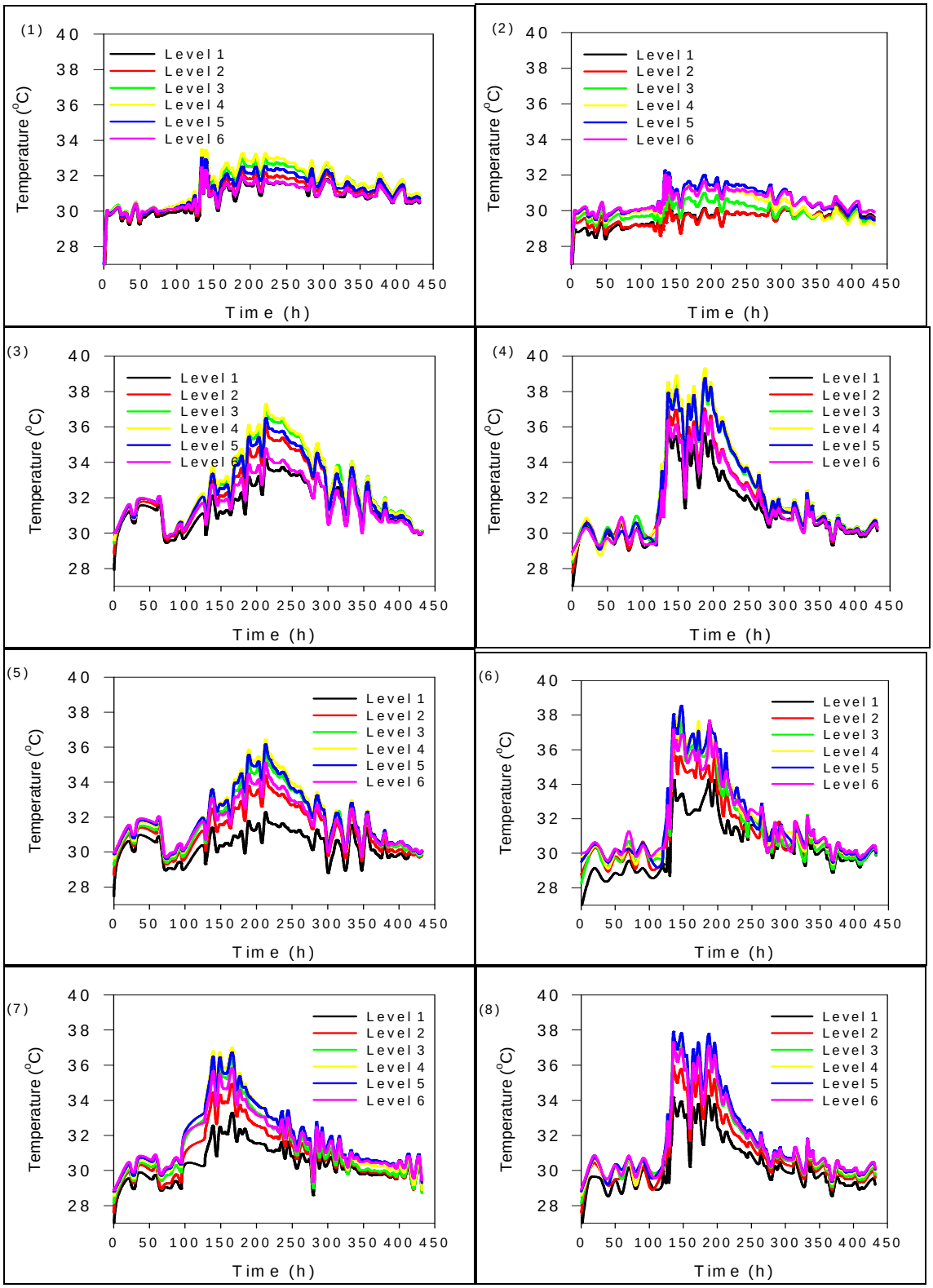

Figure 4.57: Profiles of temperature obtained in eight experiments

(1) run 1, (2) run 2, (3) run 3, (4) run 4, (5) run 5, (6) run 6, (7) run 7, (8) run 8. Measured at centre of bioreactor or column at following depth: Level 1 (3 cm), Level 2 (6 cm), Level 3 (9 cm), Level 4 (12 cm), Level 5 (15 cm), and Level 6 (18 cm). The various runs are as identified in Table 4.11.

4.5.2.2 Red pigment production profiles

The axial and temporal profiles of the red pigment production in packed-bed bioreactors are shown in Figure 4.58 for eight runs (Table 4.11). The generally low level of pigment production in runs 1 and 2 was due to a low initial moisture content of 45% and consequently low level of biomass as explained in Section 4.5.2.1 and directly confirmed in Section 4.5.2.3.

The pigment production varied significantly axially in the bed in all runs, suggesting a non-uniform local environment. In beds with a low (45%) and intermediate initial moisture content, the pigment production was lowest in the bottom of the bed, a zone of low metabolic activity as confirmed also by the temperature profile in Figure 4.57. The pigment concentration generally tended to increase up the bed and was highest at the upper levels (runs 1, 2, 3, 5, 7).

Highest levels of pigment production were generally attained in the beds with the highest initial moisture content (70%) (Babitha *et al.*, 2007b; Chutmanop *et al.*, 2008; Yongsmith *et al.*, 2000). For these beds, the most suitable aeration rate appeared to be 0.05 L/min (run 4), the lowest level tested. These beds generally tended to be most metabolically active as discussed in Section 4.5.2.1. The pigments level varied axial specially after the first 300 h of fermentation, but the pattern of variation did not seem to have a systematic trend.

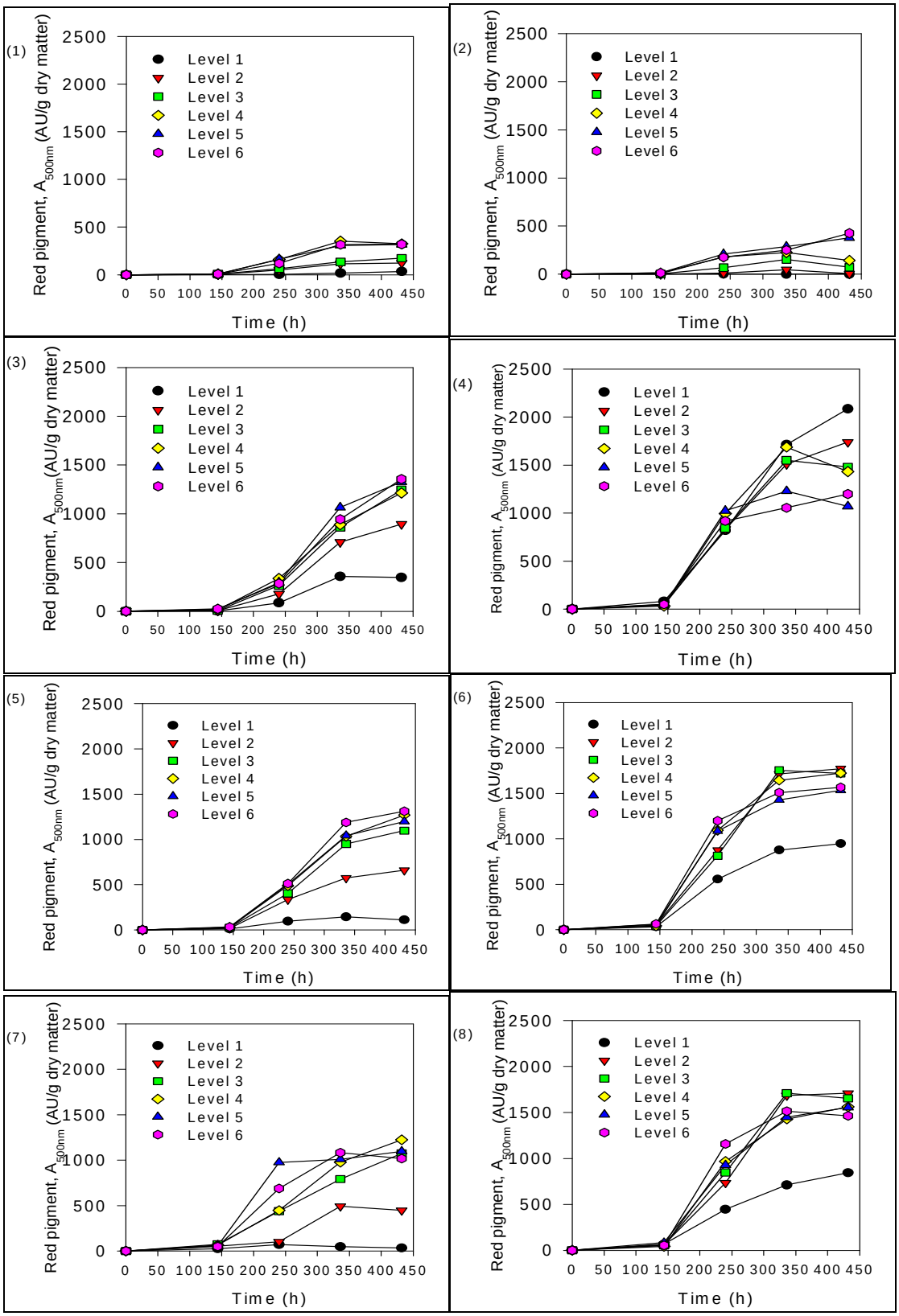

Figure 4.58: Profiles of red pigment production from eight experiments

(1) run 1, (2) run 2, (3) run 3, (4) run 4, (5) run 5, (6) run 6, (7) run 7, (8) run 8. Measured in bed segments harvested at: Level 1 (3 cm), Level 2 (6 cm), Level 3 (9 cm), Level 4 (12 cm), Level 5 (15 cm), and Level 6 (18 cm). The various runs are identified in Table 4.11.

4.5.2.3 Biomass production profiles

The biomass production profiles for runs 1 to 8 (Table 4.11) are shown in Figure 4.59. The profiles are quite comparable to the pigment production profiles discussed in Section 4.5.2.2 for the same runs. This is because pigment production is directly correlated with biomass production. At level 1, the bottom of the bed, near the air entry point, the biomass production was generally low because this is where most moisture loss occurred via evaporation. This tended to dry the bed so much that fungal growth was suppressed.

In general, at any given time the biomass concentration in the bed increased with the bed height. Upper regions of the beds were moister because of a higher metabolic activity and a lower water loss than in the lower zones. As the air moved up the bed, it became progressively poor in oxygen and rich in carbon dioxide. Despite this, the upper parts of the bed may have been better aerated because of the flat surface at the top of the substrate bed.

Surprisingly, in upper regions of the beds the fermentations with an intermediate moisture content of 57.5% (i.e. runs 3, 5, 7) were just as good in terms of biomass production as the higher moisture (70% initial moisture content, i.e. runs 4, 6, and 8) runs. The latter runs had shown a more vigorous metabolic activity in terms of heat generation (Figure 4.57) than the former set of runs. The low moisture runs 1 and 2 showed poor biomass growth, as discussed earlier.

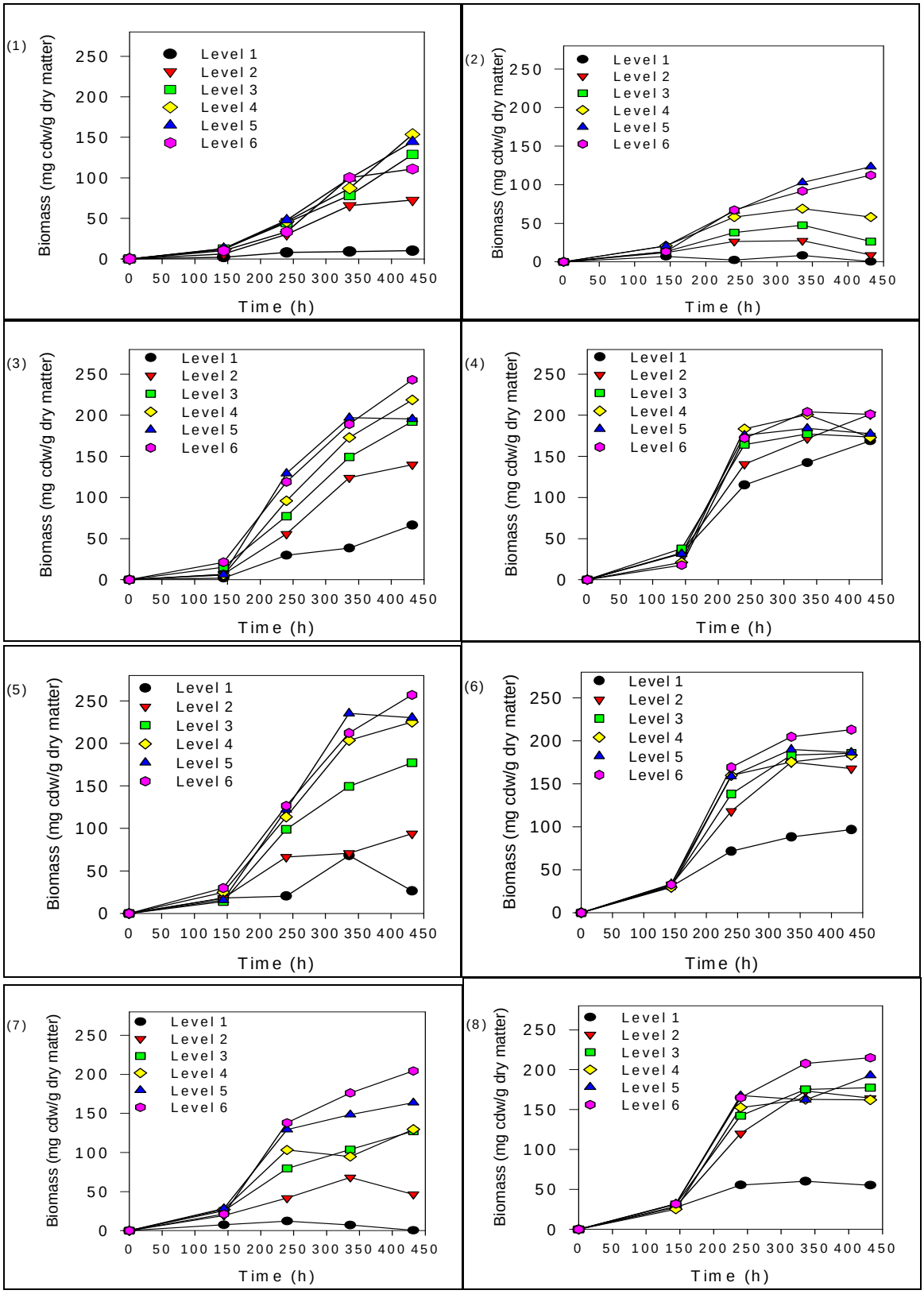

Figure 4.59: Profiles of biomass production from eight experiments

(1) run 1, (2) run 2, (3) run 3, (4) run 4, (5) run 5, (6) run 6, (7) run 7, (8) run 8. Measured in bed segments harvested at: Level 1 (3 cm), Level 2 (6 cm), Level 3 (9 cm), Level 4 (12 cm), Level 5 (15 cm), and Level 6 (18 cm). The various runs are identified in Table 4.11.

4.5.2.4 Moisture content and water activity profiles

As moisture content and water activity profoundly influence microbial growth and are in turn influenced by the fermentation itself and by moisture loss via aeration, the temporal and spatial profiles of moisture content and water activity were measured as shown in Figures 4.60 and 4.61, respectively.

As the fermentation progressed, the moisture content and water activity declined rapidly at the lowest levels of the beds because of drying, as explained earlier. In the upper regions of the beds, the moisture content generally tended to increase a little with time whereas the water activity tended to remain at ≥ 0.98. This was because of a higher level of moisture production and lower rate of moisture loss in the upper zone as explained earlier (Section 4.4.2). In the bed with a low initial moisture content of 45% at the high aeration rate of 0.2 L/min (run 2) most of the lower levels of the beds tended to dry out (Meien *et al.*, 2004). In all bed segments, in which the moisture content rose with time, the rise tended to occur during the period of most rapid biomass growth, or the period of greatest metabolic moisture production. Once growth had ceased, then the moisture content tended to stabilize in bed segments where growth occurred.

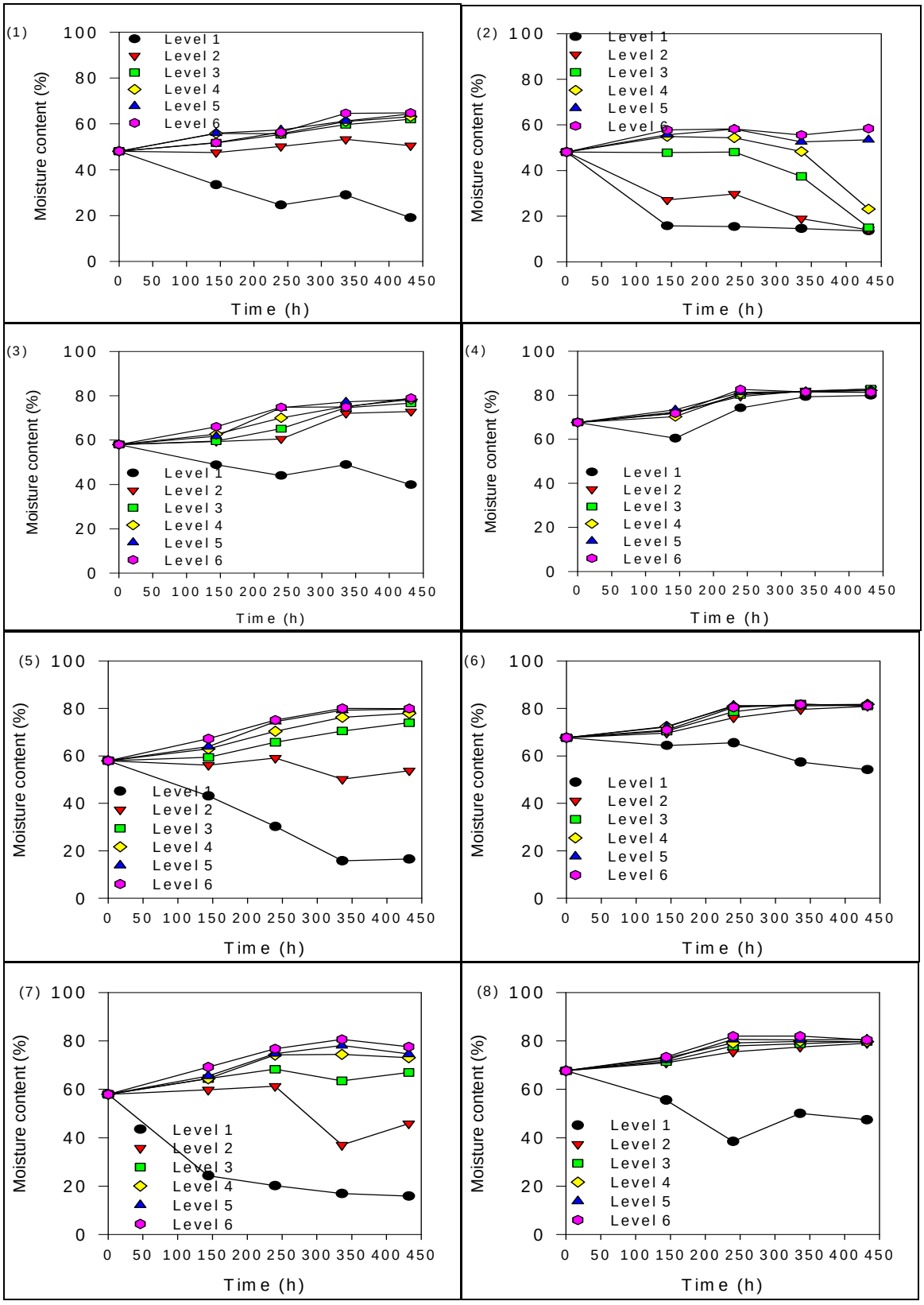

Figure 4.60: Profiles of final moisture content from eight experiments

(1) run 1, (2) run 2, (3) run 3, (4) run 4, (5) run 5, (6) run 6, (7) run 7, (8) run 8. Measured in bed segments harvested at: Level 1 (3 cm), Level 2 (6 cm), Level 3 (9 cm), Level 4 (12 cm), Level 5 (15 cm), and Level 6 (18 cm). The various runs are identified in Table 4.11.

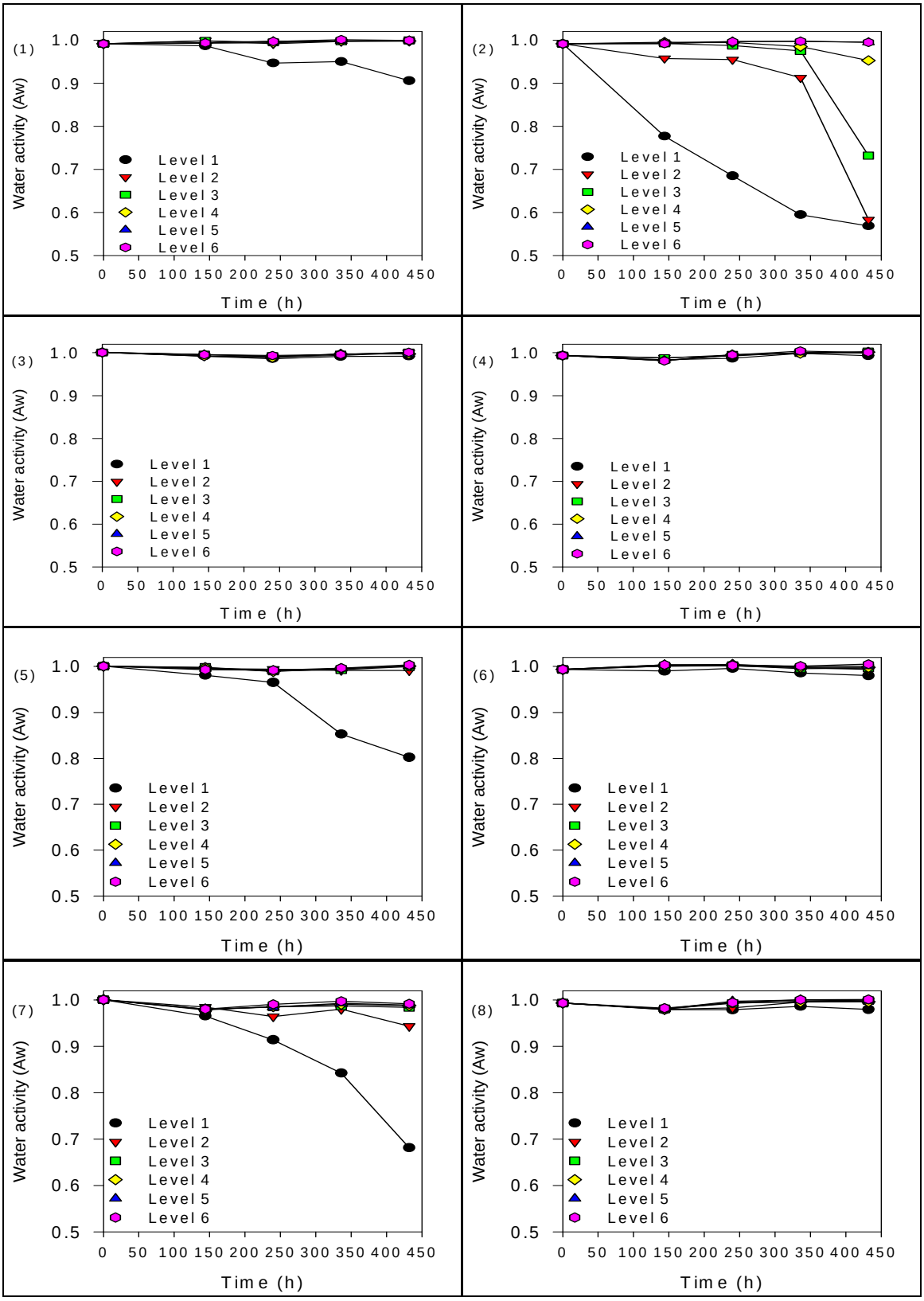

Figure 4.61: Profiles of water activity from eight experiments

(1) run 1, (2) run 2, (3) run 3, (4) run 4, (5) run 5, (6) run 6, (7) run 7, (8) run 8. Measured in bed segments harvested at: Level 1 (3 cm), Level 2 (6 cm), Level 3 (9 cm), Level 4 (12 cm), Level 5 (15 cm), and Level 6 (18 cm). The various runs are identified in Table 4.11.

4.5.2.5 pH profiles

The pH profiles for the fermentations (Table 4.11) are shown in Figure 4.62. In all segments that supported growth, the pH tended to decline with time, a characteristic of this fermentation on rice substrate. pH decline was relatively less in segments that tended to dry out (i.e. run 2, Figure 4.62). The pH may have declined because of production of carbon dioxide and/or organic acids.

Aeration rate and initial moisture contents of the beds affected the development of the pH profiles indirectly by influencing fungal growth and metabolic activity.

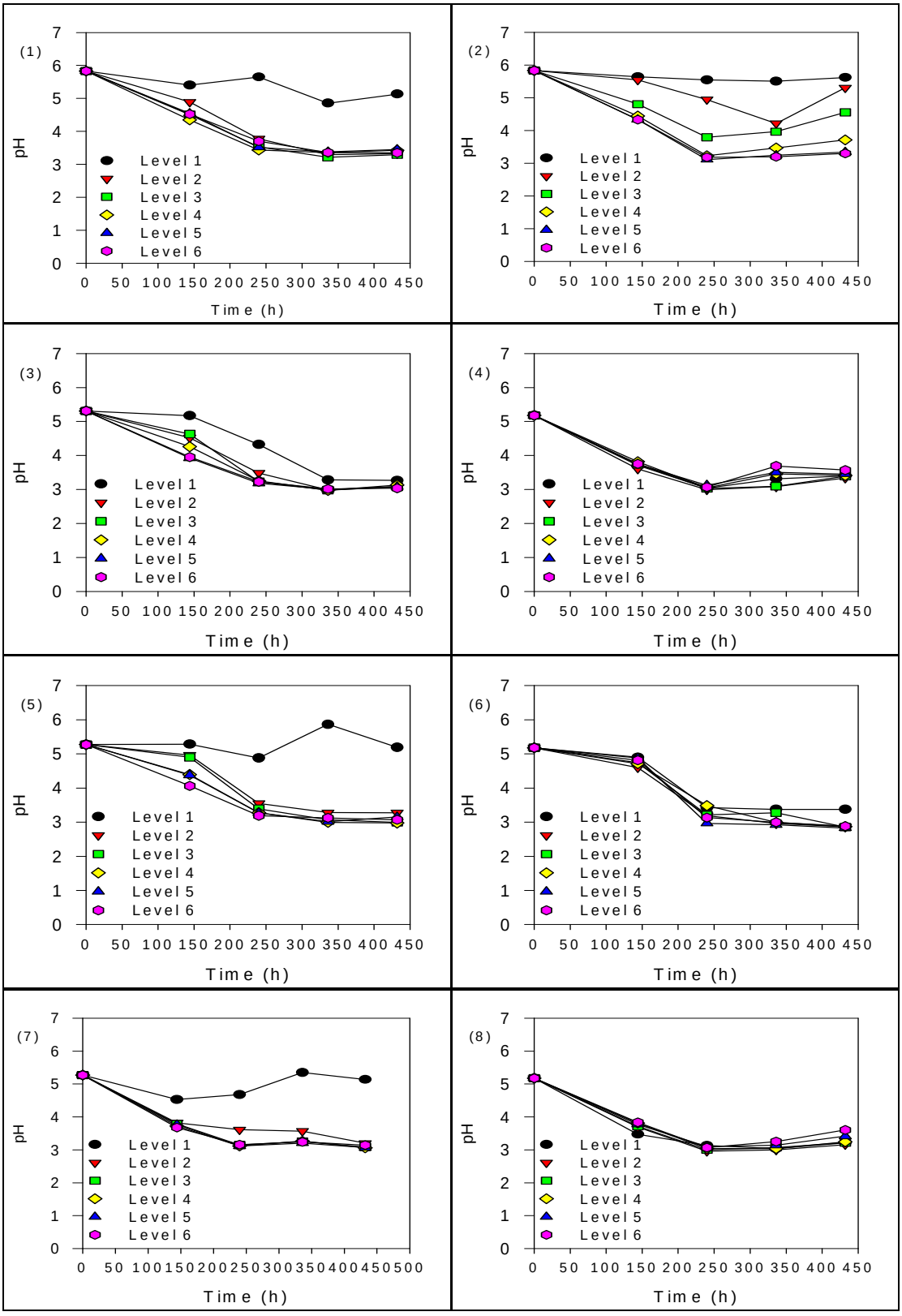

Figure 4.62: Profiles of pH from eight experiments

(a) run 1, (b) run 2, (c) run 3, (d) run 4, (e) run 5, (f) run 6, (g) run 7, (h) run 8. Measured in bed segments harvested at: Level 1 (3 cm), Level 2 (6 cm), Level 3 (9 cm), Level 4 (12 cm), Level 5 (15 cm), and Level 6 (18 cm). The various runs are identified in Table 4.11.

4.5.3 Characterization of the overall performance for red pigment production

The temporal and spatial variations in pigment production in solid-state fermentations carried out under various condition (Table 4.11) were discussed in Section 4.5.2.2. For the same packed-bed bioreactor fermentations, this section discusses the overall performance of the bioreactors in production of the target red pigment. For measuring the overall or averaged pigment production, the contents of the entire bed harvested at a given time were thoroughly mixed and the red pigment concentration was measured as specified in Section 3.4.3.3. The bed-averaged pigment production profile and the overall pigment productivity are shown in Figure 4.63 and Figure 4.64, respectively. The data are for the various combinations of initial moisture content and aeration rates as in Table 4.11.

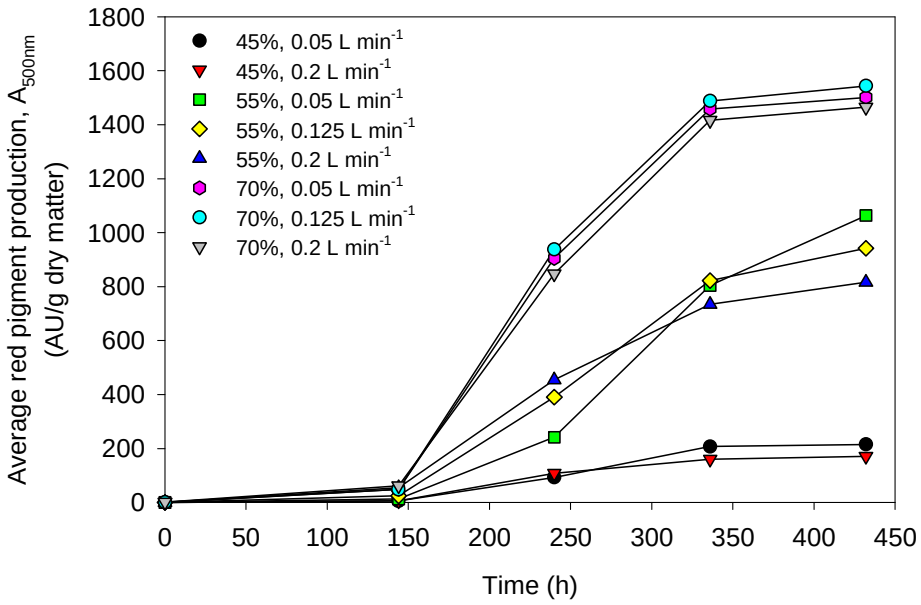

Figure 4.63: Bed-averaged red pigment production for various packed-bed fermentations (Table 4.11)

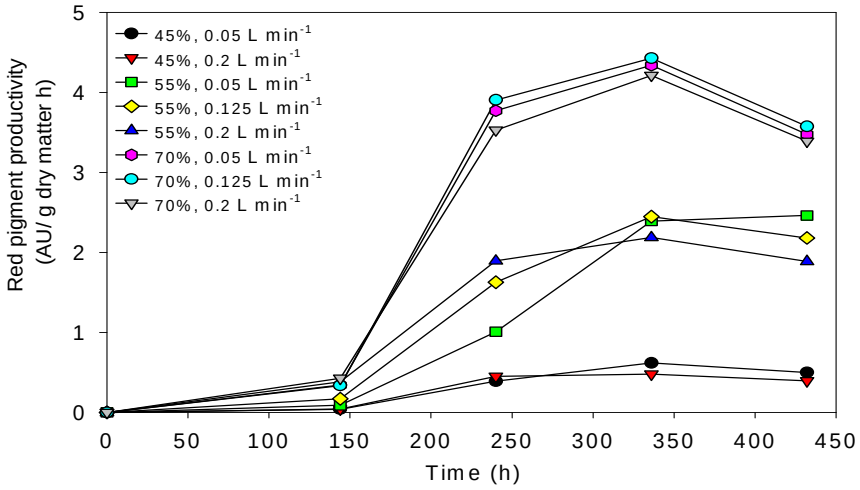

Figure 4.64: Overall red pigment productivity in packed-bed fermentations (Table 4.11)

The pigment concentration and productivity profiles in Figure 4.63 and Figure 4.64 cluster in three groups based on the initial moisture content of the bed. Beds with an initial moisture content of 70%, were clearly the most productive and yielded the most red pigment. Beds with an intermediate moisture content of 57.5% had an intermediate level of pigment productivity whereas the beds that had a low initial moisture content of 45% were the least productive. These differences were previously discussed in the section relating to spatial variations in pigment production (Section 4.5.2.2).

Within a given cluster of data, i.e. for a fixed initial moisture content, the final pigment concentration and productivity were generally highest at the lower aeration rate of 0.05 L/min (Figure 4.63 and Figure 4.64). Although in Figure 4.63 and Figure 4.64 the initial moisture content of 70% and an aeration rate of 0.05 L/min show slightly lower pigment productivity than at an aeration rate of 0.125 L/min, the difference is minimal and therefore the aeration rate of 0.05L/min has been claimed to be generally better for pigment production. This too was explained in Section 4.5.2.2. Under best condition, the pigment productivity peaked around 300 h (Figure 4.64). Compared to differences in aeration rate, differences in the initial moisture contents had by far the most profound impact on the final pigment concentration and productivity. If differences in aeration rate are disregarded, the best final pigment concentration in the bed with an initial moisture content of 70% was nearly 7-fold the level attained in the best case at an initial moisture content of 45%. Compared to the best case pigment production at an initial moisture

content of 57.5%, the best case pigment concentration at the 70% initial moisture content was nearly 45% greater.

4.5.4 Optimization of the red pigment production in the packed-bed

4.5.4.1 Introduction

Pigment production in solid-state fermentations in packed-bed bioreactors was significantly affected by the initial moisture content of the substrate and the forced aeration rate as seen in Section 4.3.6 and Section 4.4.2. Therefore, a statistical optimization of the overall pigment productivity in beds was attempted. The optimization used the initial moisture content and the forced aeration rate as the main influencing factors. The fermentation time was fixed at 336 h as the maximum overall pigment productivity had been attained by this time in earlier experiments (Section 4.5.3).

4.5.4.2 Experimental design

A 2^2 factorial central composite design (CCD) with two factors was used. The design included four axial points and duplicates at the centre point (Kennedy and Krouse, 1999). This corresponded to a total of 10 sets of experiments. All experiments were done in duplicate. The ranges of variation of the factors were 45% to 70% for the initial moisture content and 0.05 to 0.2 L/min for forced aeration rate. The details of the design and the responses are summarized in Table 4.12. Four responses were evaluated for each experiment in packed-bed bioreactors. The responses were the total red pigment production, the red pigment productivity per unit bed volume, the yield of the pigment on biomass, and the total biomass in the bed. The Design Expert (Version 6.0.8, 2002, Minneapolis MN, USA) and Statistica packages (Version 5.5, 1999, Tulsa OK, USA) were used for the statistical design and regression analysis of the experimental data, respectively.

Table 4.12: Coded values, actual values and responses of the central composite design at 336 h of the packed bed bioreactor

Standard order	Run order	Coded value		Actual value		Responses			
		Initial moisture content (x_1) (%)	Aeration rate (x_2) (L/min)	Initial moisture content (x_1) (%)	Aeration rate (x_2) (L/min)	Total pigment (AU)	Pigment productivity (AU/L h)	Pigment yield (AU/g cdw)	Total biomass (g cell dry weight)
1	4	-1	-1	45	0.05	18616.2	144.9	2829.5	6.6
2	1	1	-1	70	0.05	74173.1	577.5	8101.7	9.2
3	3	-1	1	45	0.2	17071.3	132.9	2775.9	6.1
4	5	1	1	70	0.2	86238.9	671.4	9022.2	9.6
5	8	-1	0	45	0.125	21364.1	166.3	2919.5	7.3
6	6	1	0	70	0.125	86822.6	676.0	8778.1	9.9
7	9	0	-1	57.5	0.05	54992.6	428.1	5543.0	9.9
8	7	0	1	57.5	0.2	63099.0	491.3	7362.7	8.6
9	2	0	0	57.5	0.125	68679.7	534.7	5088.6	13.5
10	10	0	0	57.5	0.125	64952.9	505.7	7185.3	9.0

The general response surface model of the selected design is as follows:

$$Y = \beta_o + \beta_1 x_1 + \beta_2 x_2 + \beta_{11} x_1^{\,2} + \beta_{22} x_2^{\,2} + \beta_{12} x_1 x_2 \qquad \text{Equation 4.7}$$

Where, Y = predicted response

β_o = interception coefficient

β_1 and β_2 = coefficients of the linear effect

β_{11} and β_{22} = coefficients of the quadratic effect

β_{12} = coefficient of the interaction effect

x_1 = coded value for the initial moisture content

x_2 = coded value for the forced aeration rate

An analysis of variance (ANOVA) was used to determine the significance of the effect of the independent variables on the response activity (Montgomery, 2001). A “lack of fit” statistic was determined to assess how well the model fit the data. For this, the mean square of the residual error was compared to the mean square of pure error. An insignificant result for lack of fit (p-value > 0.05), shows that a model is a good predictor of the response (Montgomery, 2001). In contrast, a significant lack of fit suggests an unsatisfactory model.

4.5.4.3 Central composite design and response analysis

In assessing a statistical model, ANOVA is performed first to establish the lack of fit of the model. An insignificant result for lack of fit at 95% confidence level (p-value > 0.05) shows that the model is fit. A fit model means that the responses are satisfactorily close to the actual values. If the model fits, further examination is carried out on the statistical coefficients to determine the significance of the model and the responses. However, if the model shows a significant lack of fit at the 95% confidence level (p-value < 0.05), the model is considered unsatisfactory and not examined further. Following sections discuss the model and how well it described the experimental responses of the packed-bed bioreactor system.

4.5.4.4 Response of total red pigment production and red pigment productivity based on the total bed volume

Tables 4.13 to 4.16 show the ANOVA results, regression coefficients, and estimate effects for total red pigment concentration and pigment productivity of the packed-bed bioreactor, respectively. The red pigment contents are expressed as total pigment production in the bed. The pigment productivity is expressed in terms of the total bed volume.

Table 4.13: ANOVA table for the total red pigment in the packed-bed bioreactor

Source	SS	DF	MS	*F*-value	*p*-value
Model	6.581E+09	5	1.316E+09	309.475	< 0.0001*
Residual	1.701E+07	4	4.253E+06		
Lack of fit	1.007E+07	3	3.356E+06	0.483	0.754
Pure error	6.945E+06	1	6.945E+06		
Corrected total	6.598E+09	9			

R^2 = 0.9974, CV = 3.709

Note: SS, sum of squares; DF, degrees of freedom; MS, mean square; CV, coefficient of variation; *, significant at 95% confidence level

Table 4.14: Regression coefficients and estimated effects for total red pigment production

Factor	Regression coefficient	Effect	Standard error	*t*-value	*p*-value
Intercept	-3.127E+05	6.604E+04	1232.456	53.588	7.259E-07*
x_1-moisture	1.031E+04	6.339E+04	1683.855	37.648	2.973E-06*
x_2-aeration	1.094E+05	6.209E+03	1683.855	3.687	0.021*
x_1^2	-71.545	-2.236E+04	2700.175	-8.280	0.001*
x_2^2	-1.107E+06	-1.245E+04	2700.175	-4.612	0.010*
x_1x_2	3.629E+03	6.805E+03	2062.293	3.300	0.030*

Table 4.15: ANOVA table for red pigment productivity based on the total bed volume

Source	SS	DF	MS	*F*-value	*p*-value
Model	3.989E+05	5	79782.770	309.49	< 0.0001*
Residual	1.031E+03	4	257.79		
Lack of fit	610.251	3	203.41	0.483	0.754
Pure error	420.952	1	420.94		
Corrected total	4.000E+05	9			

R^2 = 0.9974, CV = 3.709

Note: SS, sum of squares; DF, degrees of freedom; MS, mean square; CV, coefficient of variation; *, significant at 95% confidence level

Table 4.16: Regression coefficients and estimated effects on red pigment productivity

Factor	Regression coefficient	Effect	Standard error	*t*-value	*p*-value
Intercept	-2434.490	514.194	9.595	53.588	7.259E-07*
x_1-moisture	80.268	493.563	13.110	37.648	2.973E-06*
x_2-aeration	852.962	48.342	13.110	3.687	0.021*
x_1^2	-0.557	-174.069	21.022	-8.280	0.001*
x_2^2	-8618.119	-96.954	21.022	-4.612	0.010*
x_1x_2	28.258	52.984	16.056	3.300	0.030*

From the Tables 4.13 and 4.15, the *p*-values for the lack of fit statistic of both models were 0.754. A lack of fit *p*-value of > 0.05 for a model means a satisfactory fit at the 95% confidence level. Therefore, the models for both responses were satisfactory fit for further evaluations.

For the total red pigment production, the ANOVA result showed that the model developed was highly significant as the *F*-value obtained was very high (*F*-value = 309.49) with the very low *p*-value of < 0.0001 (Table 4.13). The R^2 value was 0.9974, therefore the model explained more than 99.7% of the total variance. In addition, a low value of coefficient of variation (CV), (CV = 3.7) showed that the experiment was precise and reliable. The model for the predicted response was :

$$\text{Total red pigment (AU)} = -3.127\times10^5 + 1.031\times10^4\, x_1 + 1.094\times10^5\, x_2 - 71.545\, x_1^2 - 1.107\times10^6\, x_2^2 + 3.630\times10^3\, x_1x_2 \qquad \text{Equation 4.8}$$

Where, x_1 is the coded variable for initial moisture content, while, x_2 is the coded variable for aeration rate.

The significance of the effect of each variable was validated by *t*-test and *p*-value (Table 4.14). At 95% confidence level, both factors had a significant linear effect (x_1 and x_2), quadratic effect (x_1^2 and x_2^2), and interaction effect (x_1x_2) on the response.

The initial moisture content was found as the most significant factor that affected the total red pigment production, as this factor had the smallest *p*-value of 2.97×10^{-6} and a high coefficient value of 10309.78 (Table 4.14). The significance of the estimated effects of variables on the total red pigment production is shown in Pareto chart in Figure 4.65. The figure clearly shows that initial moisture content was the most significant factor in the production of red pigment in the packed-bed bioreactor.

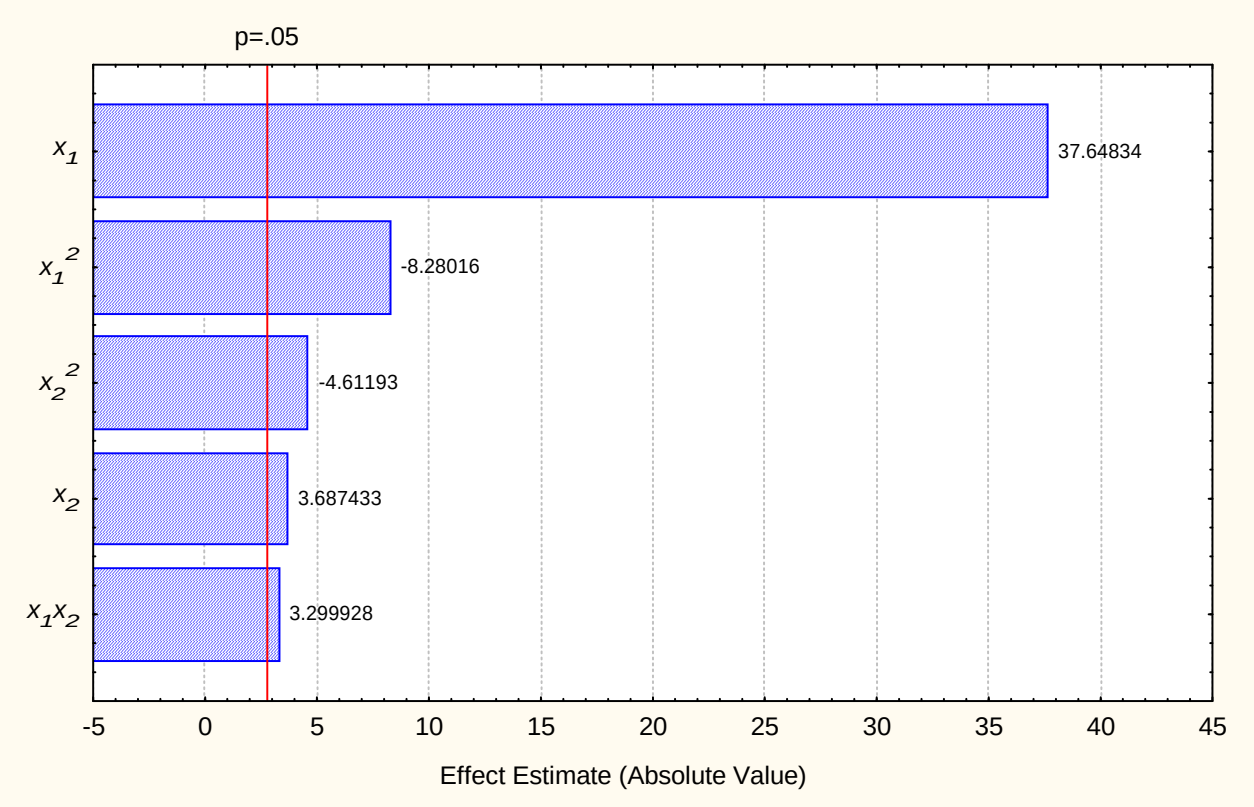

Figure 4.65: Pareto chart of total red pigment production in packed-bed bioreactor

Note: x_1, initial moisture content

x_2, forced aeration rate

The ANOVA results for the red pigment productivity based on the total bed volume also showed the model to be highly significant with a *p*-value of < 0.0001 (Table 4.15). The R^2 value was 0.9974, therefore the model could explain > 99.7% of the variation in the responses. The model was as follows:

$$\text{Red pigment productivity (AU/L h)} = -2.434\times10^{3} + 80.268\,x_1 + 851.96\,x_2 - 0.557\,x_1^{2} - 8.6\times10^{3}\,x_2^{2} + 2.826\times10^{2}\,x_1x_2 \qquad \text{Equation 4.9}$$

Where, x_1 is the coded variable for initial moisture content, while, x_2 is the coded variable for aeration rate.

The estimated effects obtained showed a significant effect at 95% confidence level of all of the factors (*p*-value < 0.05) on the response (Table 4.16). A high *t*-value in combination with low *p*-value indicates a factor to be more significant in affecting the response compared to a factor with lower *t*-value and high *p*-value. Therefore, the initial moisture content also played the most important role in affecting the red pigment productivity. This is clear in the Pareto chart in Figure 4.66.

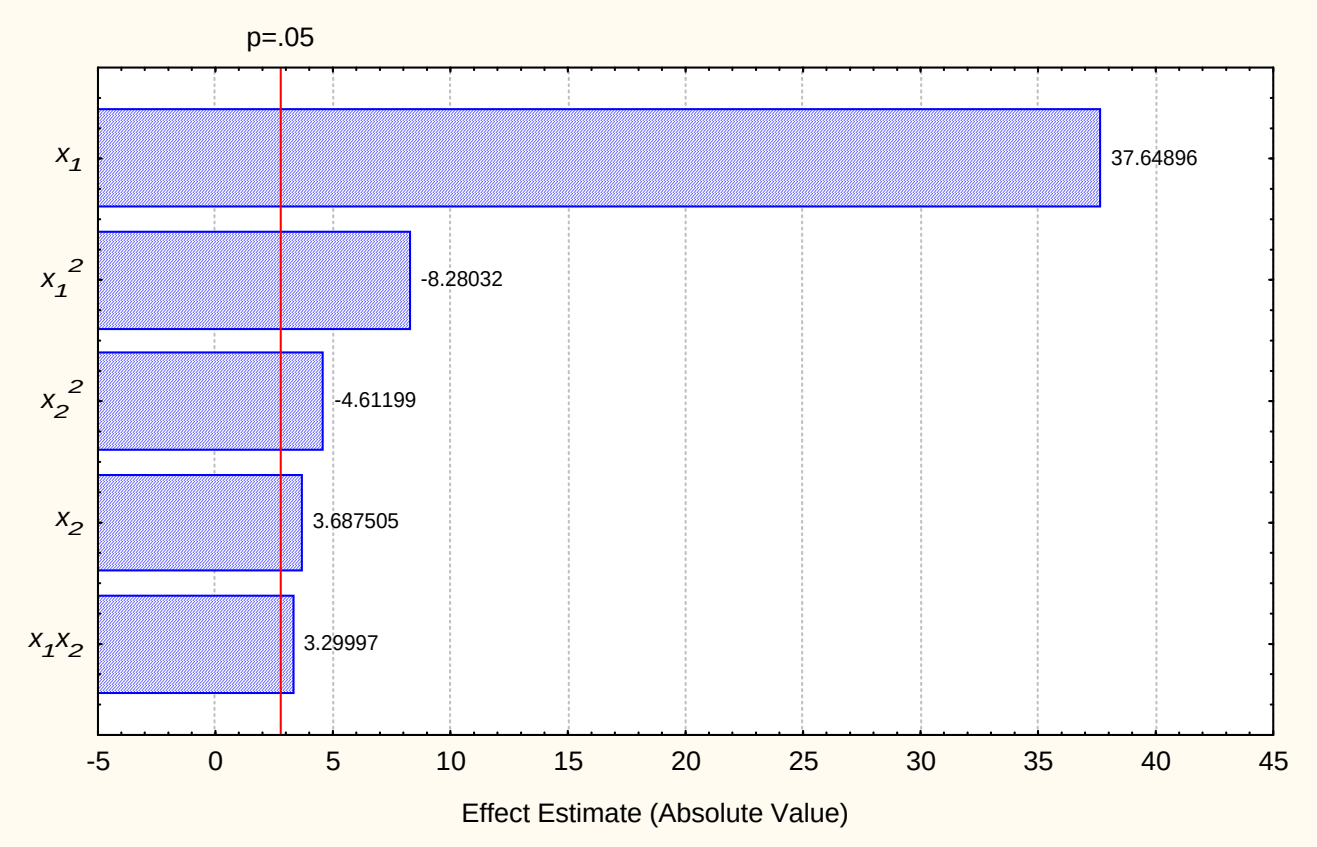

Figure 4.66: Pareto chart of red pigment productivity based on the total bed volume

Note: x_1, initial moisture content

x_2, forced aeration rate

The two Pareto charts (Figure 4.65 and Figure 4.66) are identical because of a direct relationship between the red pigment concentration in the bed and the productivity of the pigment.

The model Equations 4.8 and 4.9 were used to create the three-dimensional surface plots of total red pigment production and productivity, respectively. The plots are shown in Figures 4.67 and 4.68 and help to illustrate the combination of initial moisture content and forced aeration rate that maximize pigment production and productivity.

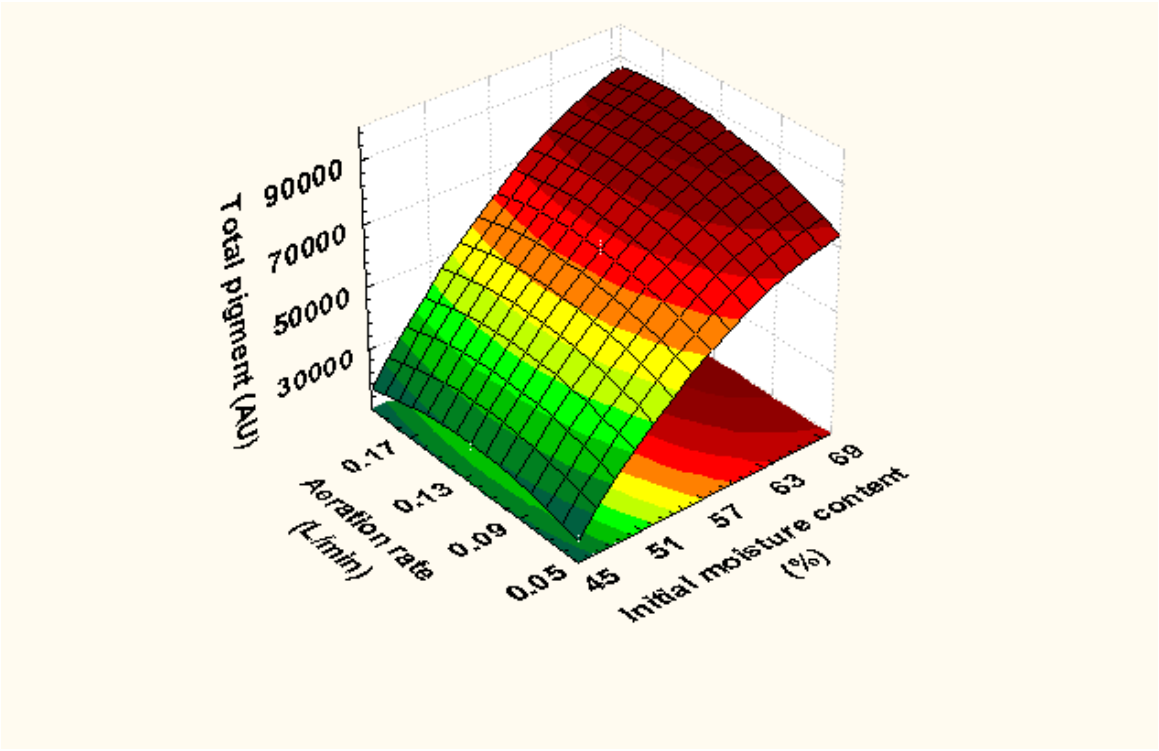

Figure 4.67: Surface response plot of total red pigment production

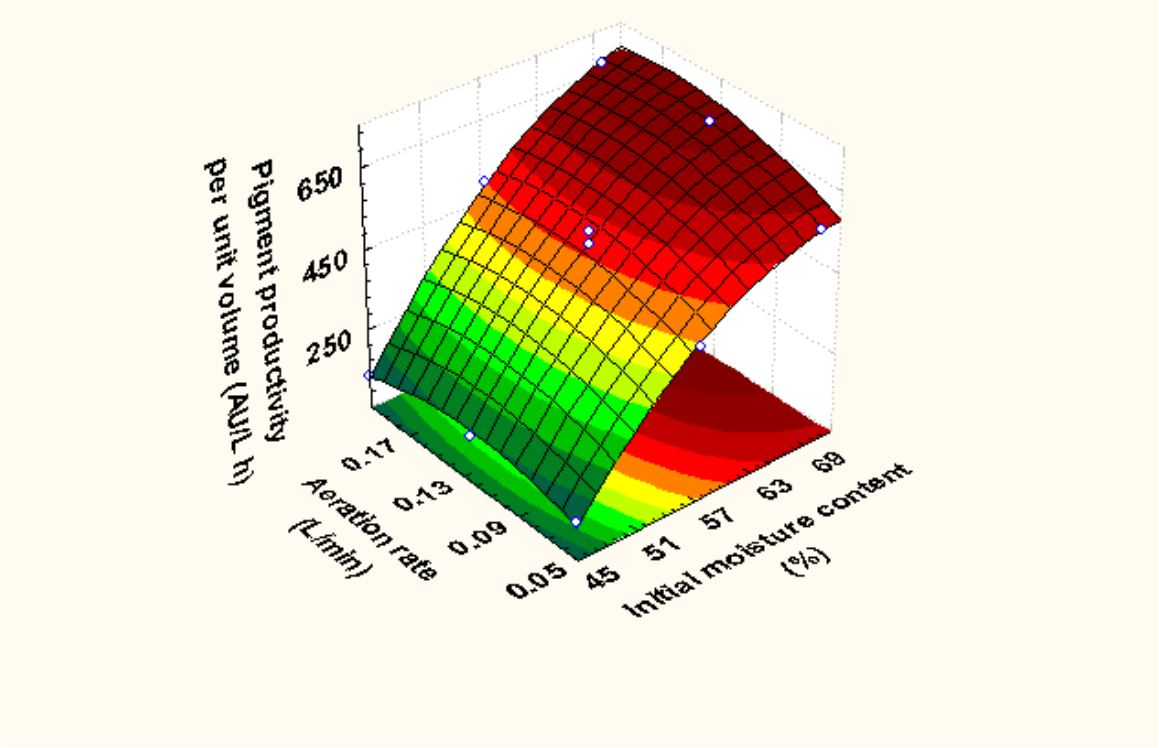

Figure 4.68: Surface response plot of red pigment productivity

4.5.4.5 Response of total biomass in the packed-bed bioreactor

Tables 4.17 and 4.18 show the ANOVA results and regression coefficient for the biomass model (Equation 4.10). The lack of fit value at confidence level of 95% was insignificant (*p*-value = 0.977, Table 4.17) and therefore the model satisfactorily fit the data. The *F*-value (1.921) was relatively low and the *p*-value exceeded 0.05. Hence, the model was insignificant to the biomass production. The coefficient determination, R^2 was 0.706, indicating that the model could explain only 70.6% of the variability in biomass production. The model was developed as follows:

$$\text{Total biomass (g cdw)} = -38.169 + 1.510\,x_1 + 41.58\,x_2 - 0.012\,x_1^2 - 2.298\times10^2\,x_2^2 + 0.222\,x_1x_2 \qquad \text{Equation 4.10}$$

In the above equation, x_1 is the coded variable for initial moisture content and x_2 is the coded variable for forced aeration rate.

Table 4.17: ANOVA table for the total biomass in the packed bed bioreactor

Source	SS	DF	MS	*F*-value	*p*-value
Model	27.66	5	5.53	1.921	0.273
Residual	11.52	4	2.88		
Lack of fit	1.59	3	0.53	0.053	0.977
Pure error	9.93	1	9.93		
Corrected total	39.19	9			

$R^2 = 0.706$

Note: SS, sum of squares; DF, degrees of freedom; MS, mean square; CV, coefficient of variation; *, significant at 95% confidence level

Table 4.18: Regression coefficient and estimated effect for total biomass production

Factor	Regression coefficient	Effect	Standard error	*t*-value	*p*-value
Intercept	-38.169	10.903	1.015	10.749	< 0.001
x_1-moisture	1.510	2.853	1.386	2.058	0.109
x_2-aeration	41.58	-0.459	1.386	-0.331	0.757
x_1^2	-0.012	-3.866	2.223	-1.740	0.157
x_2^2	-229.635	-2.583	2.223	-1.163	0.310
x_1x_2	0.222	0.416	1.697	0.245	0.818

The data in Table 4.18 suggest that there were no significant estimated effects of the factors and their combination on biomass production at the 95% confidence level. This implied a lack of a direct influence of the initial moisture content and the forced aeration rate on the total biomass production. The insignificance of the estimated effects of the factors on the total biomass may be further seen in Pareto chart in Figure 4.69. The results suggest that a more complex model than Equation 4.10 may be necessary for describing the biomass concentration dependence on the initial moisture content and the forced aeration rate.

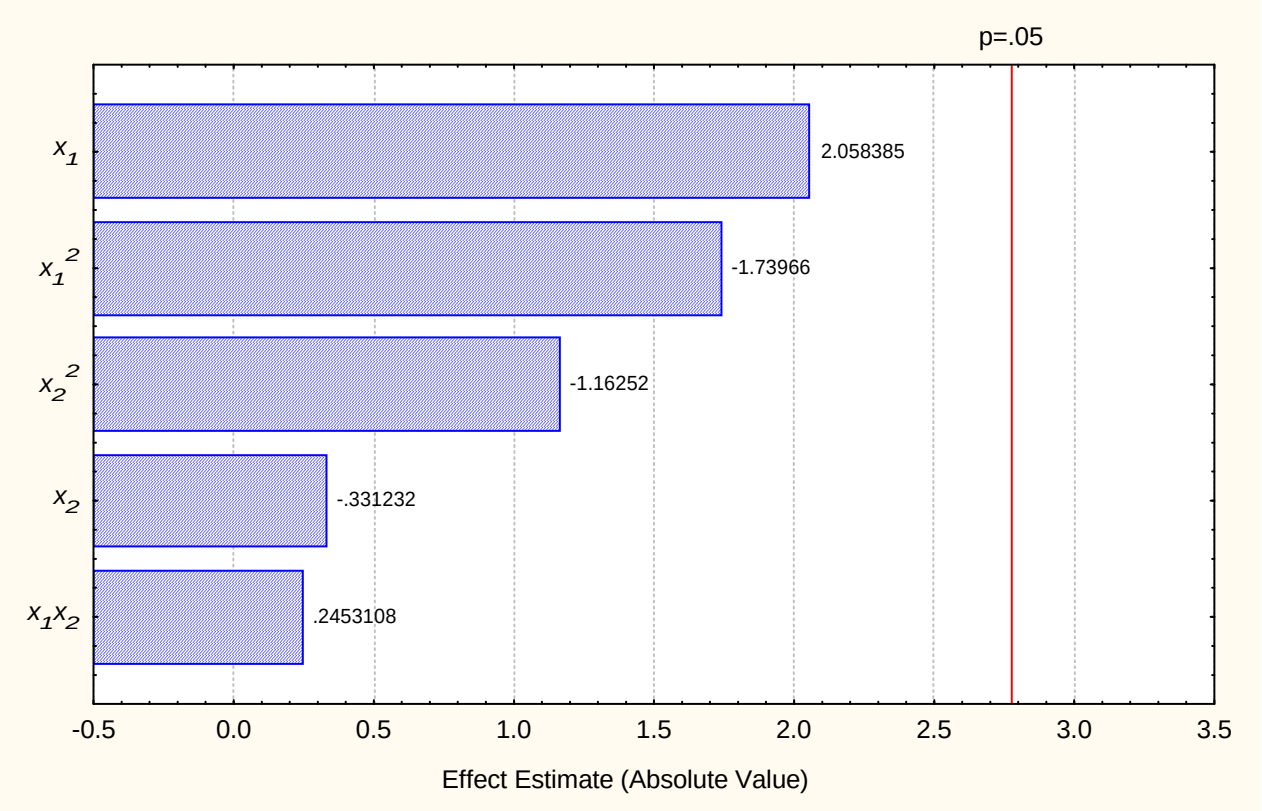

Figure 4.69: Pareto chart for total biomass production

Note: x_1, initial moisture content

x_2, forced aeration rate

4.5.4.6 Response of the yield of red pigment based on biomass in the packed-bed bioreactor

The statistical model obtained for the yield of red pigment based on biomass production was as follows:

$$\text{Yield of red pigment (AU/g cdw)} = -17745.73 + 614.20\,x_1 - 10754.95\,x_2 - 3.609\,x_1^2 + 7.152\times10^3\,x_2^2 + 2.60\times10^2\,x_1x_2 \quad \text{Equation 4.11}$$

where, x_1 is the coded variable for initial moisture content and x_2 is the coded variable for aeration rate

ANOVA result showed that the model adequately fitted the data, as the *p*-value of the lack of fit was 0.9382 at 95% confidence level (Table 4.19). Moreover, ANOVA results showed that the model was significant in correlating the yield of the red pigment and the *p*-value was 0.012 (*p*-value < 0.05). The R^2 value of 0.946 suggests that the model could explain 94.6% of the variation in the data.

Table 4.19: ANOVA table for the yield of red pigment on biomass in the packed-bed

Source	SS	DF	MS	*F*-value	*p*-value
Model	5.25E+07	5	1.05E+07	14.12307	0.0119*
Residual	2.975E+06	4	7.437E+05		
Lack of fit	7.768E+05	3	2.589E+05	0.117855	0.9382
Pure error	2.198E+06	1	2.198E+06		
Corrected total	5.544E+07	9			

$R^2 = 0.946$

Note: SS, sum of squares; DF, degrees of freedom; MS, mean square; CV, coefficient of variation; *, significant at 95% confidence level

The yield of pigment was significantly influenced by only the linear effect of the initial moisture content (*p*-value = 0.0012, Table 4.20). For all the other factors and combinations the *p*-value was > 0.05. The significant effect of the initial moisture content on the yield of red pigment is clearly seen in Pareto chart in Figure 4.70. The model Equation 4.11 was used to create a surface response plot (Figure 4.71) to clearly visualize the influence of the factors on the response.

Table 4.20: Regression coefficient and estimated effect of yield of red pigment on biomass

Factor	Regression coefficient	Effect	Standard error	*t*-value	*p*-value
Intercept	-17745.73	6274.81	515.38	12.175	0.0003
x_1-moisture	614.204	5792.39	704.14	8.226	0.0012
x_2-aeration	-10754.95	895.50	704.14	1.271	0.272
x_1^2	-3.609	-1127.66	1129.14	-0.999	0.374
x_2^2	7152.414	80.465	1129.14	0.071	0.947
x_1x_2	259.772	487.07	862.39	0.565	0.602

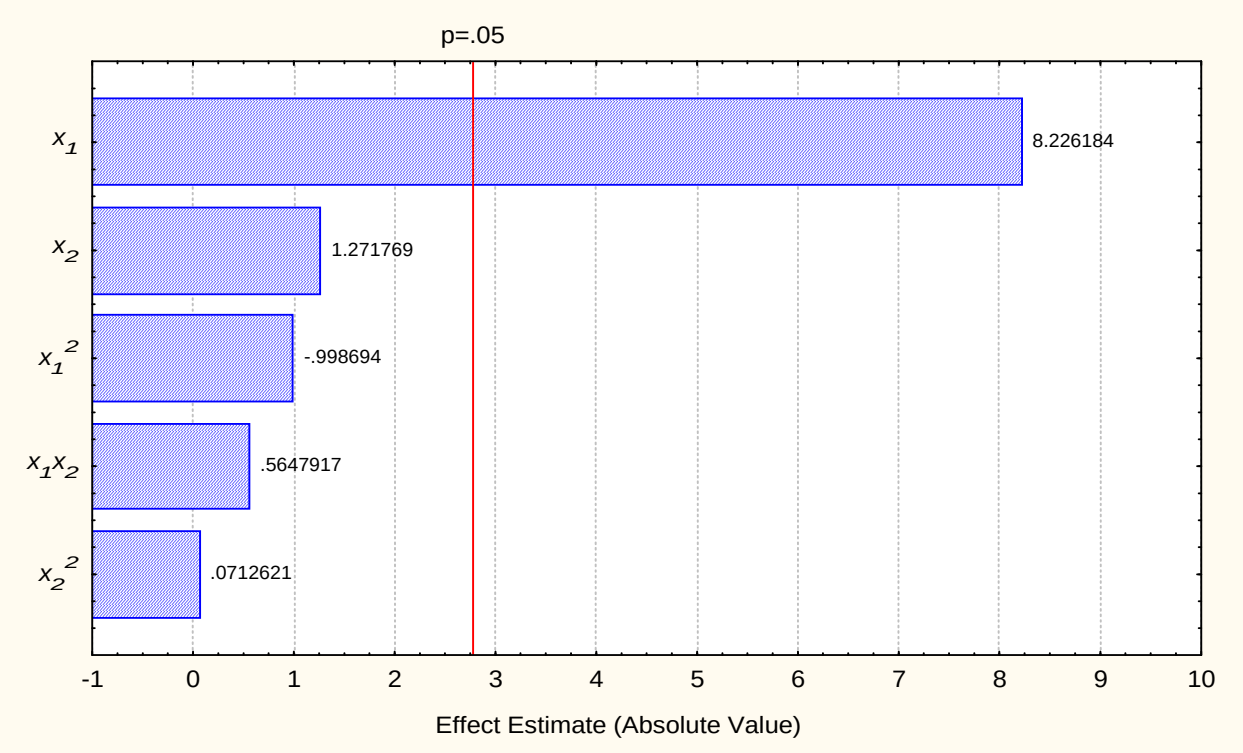

Figure 4.70: Pareto chart for total biomass production

Note: x_1, initial moisture content

x_2, forced aeration rate

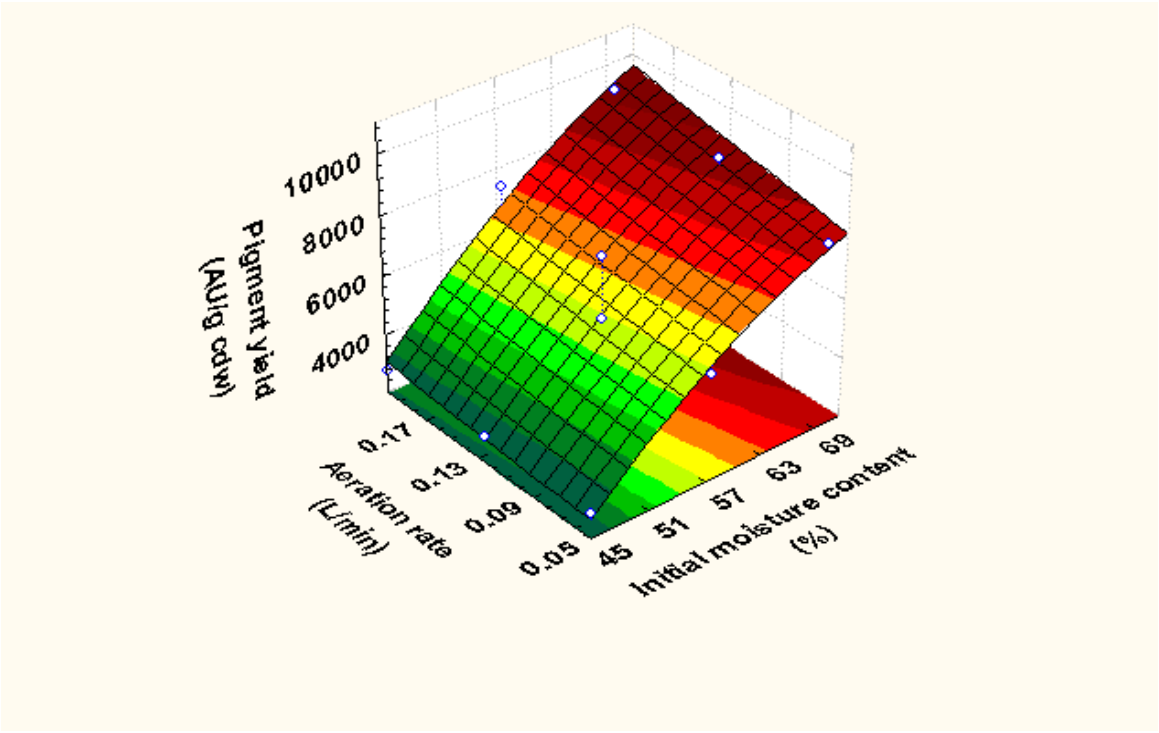

Figure 4.71: Surface response plot of yield red pigment based on biomass

4.5.4.7 Model validation

As the purpose of this study was to maximize the red pigment production and productivity, a validation experiment was performed for the statistical models (Equations 4.8 and 4.9) that were developed in Section 4.5.4.4. The two model equations were used in the Design Expert program to calculate the predicted levels of the two variables (i.e. the initial moisture content and the forced aeration rate) for maximizing the two responses. For both responses, the predicted optimal values of the variables were 70% for initial moisture content and 0.140 L/min for forced aeration rate. For these optimal values, the predicted levels of the total red pigment and its productivity at 336 h were 87555.1 AU and 681.67 AU/L h, respectively.

The validation experiment used packed-beds (duplicate) with the optimum initial moisture content of 70% in combination with continuous aeration (humidified air at relative humidity of 97-99%) at 0.140 L/min. The packed-bed was held in the dark at 30^{o}C for 336 h. At the end of fermentation, the whole bioreactor was harvested and the contents were weighed prior to analysis. The measured values of the total pigment content

and productivity were 86629.86 AU and 674.46 AU/L h, respectively. The measured pigment content were 1.1% lower than the model predicted value of 87555.1 AU. Similarly, the measured productivity was 1.1% lower than the predicted value of 681.67 AU/L h. Therefore, the experimental results agreed well with the model predicted values. The model Equations 4.8 and 4.9 were therefore shown to be quite reliable within the range of condition used in developing them.

4.6 Characterization of red pigment

4.6.1 Introduction

Although *Monascus* pigments have a long history of use in food preparations in East Asia, pure reference standards for red pigments (monascorubramine and rubropunctamine) have proved impossible to obtain commercially. Hence, it is difficult to accurately quantify the production of pigments in a fermentation process.

Spectra (infrared, ultraviolet, NMR, and mass spectra) of the pigments became available relatively recently (Blanc *et al.*, 1994). Hajjaj *et al.* (1997) established the molecular structure of the extracelular pigments (N-glutarylrubropunctamine, N-glutarylmonascorubramine, N-glucosylrubropunctamine, and N-glucosylmonascosubramine). Martinkova *et al. (*1999) and Chatterjee *et al.* (2009) reported on antimicrobial activities of the purified pigments.

This study attempted to purify the pigments for possible use as standards. As purification from the fermented solid substrate was relatively difficult, the purification effort focused on submerged culture. In addition, the effects of light, pH, and temperature on stability of the pigments were measured.

4.6.2 Extraction and purification

Crude pigments were extracted from the submerged culture fermentation broth produced using medium J (Table 3.2). The broth was produced under conditions specified in Section 3.3.2.2.2 and harvested on day 4. The broth was filtered using qualitative filter paper (grade 4, Whatman Schleicher & Schuel) to separate the mycelium and the suspending liquid. The mycelium and the supernatant were separately freeze-dried. The resulting solids were extracted separately as explained in Section 3.4.2.6.1. The crude extracts were filtered and purified initially by silica gel column chromatography (Figure 4.72) (Section 3.4.2.6.1). Isolated fractions were further purified by thin layer chromatography (TLC).

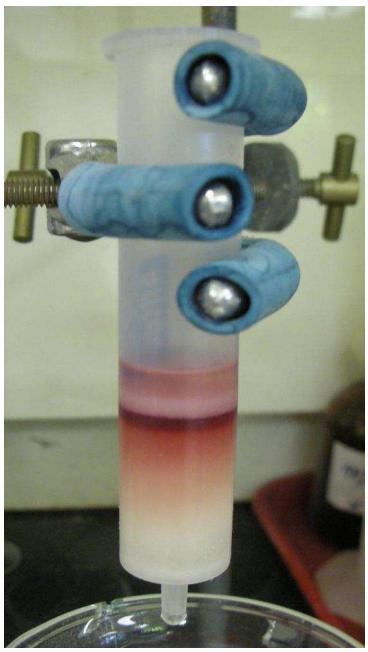

Figure 4.72: Pre-packed column chromatography for purification of pigments

4.6.2.1 Purification by column chromatography

Broth produced using medium J with a C : N ratio of 9 : 1 and glucose of 10 g/L, as described in Table 3.2 and Section 3.3.2.2 was filtered to separate the mycelia and the liquid supernatant. The filtrate and mycelium were then freeze-dried and extracted separately as explained in Section 3.4.2.6.1. The resulting solids (approximately 25 mg each) were dissolved in 2 mL of chloroform:methanol (50:50, vol/vol) and applied to pre-eluted pre-packed SPE chromatography columns, separately (Section 3.4.2.6.1). Different polarities of eluents (chloroform:methanol) were applied to the columns continuously (see Section 3.4.2.6.1). The solvent fractions eluted from the columns were collected in pre-weighed round bottom flasks and evaporated. An accurately weighed amount of the recovered solids was dissolved in 95% ethanol and the UV visible spectra were measured using a scanning spectrophotometer between 350 to 650 nm wavelength ranges (see Section 3.4.2.6.1).

The absorption spectrum of the solids recovered from extraction of the fermentation broth filtrate is shown in Figure 4.74. The spectrum showed two peaks at approximately ~400 nm and ~500 nm, corresponding to yellow and red pigments, respectively (Figure 4.73).

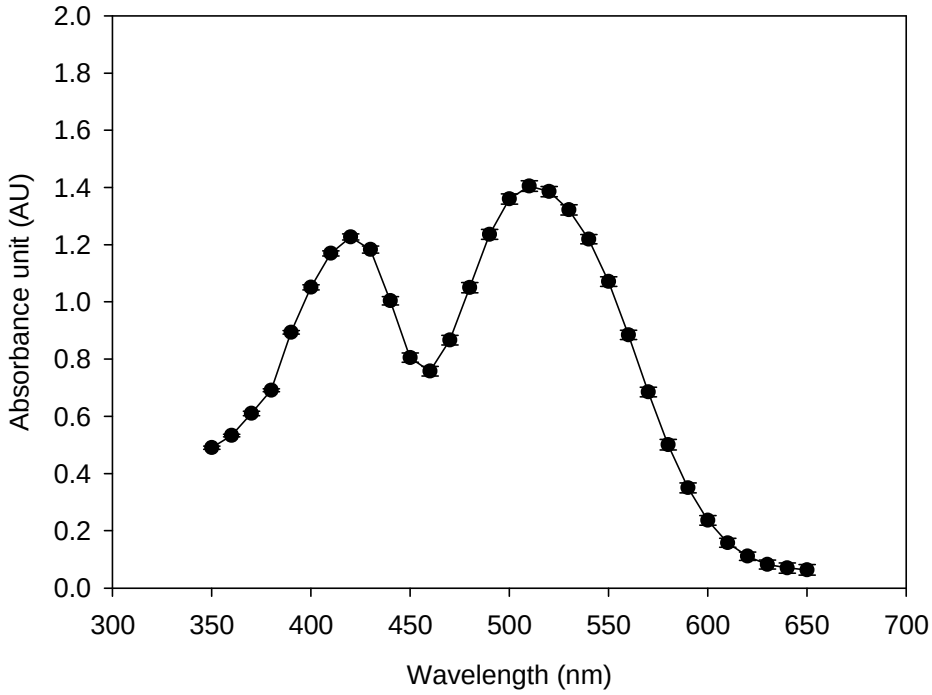

Figure 4.73: Absorption spectrum of solids recovered from extraction of the broth filtrate

Despite many attempts at separating the red and yellow pigments by silica gel column chromatography using solvents (mixture of chloroform and methanol) of different polarities, a clear separation was not achieved. The best case purified red band still contained an absorbance peak corresponding to yellow, as shown in Figure 4.74. In view of the very slight structural differences between the red and the yellow pigments, the polarities of the molecules were quite close and this made purification impossible.

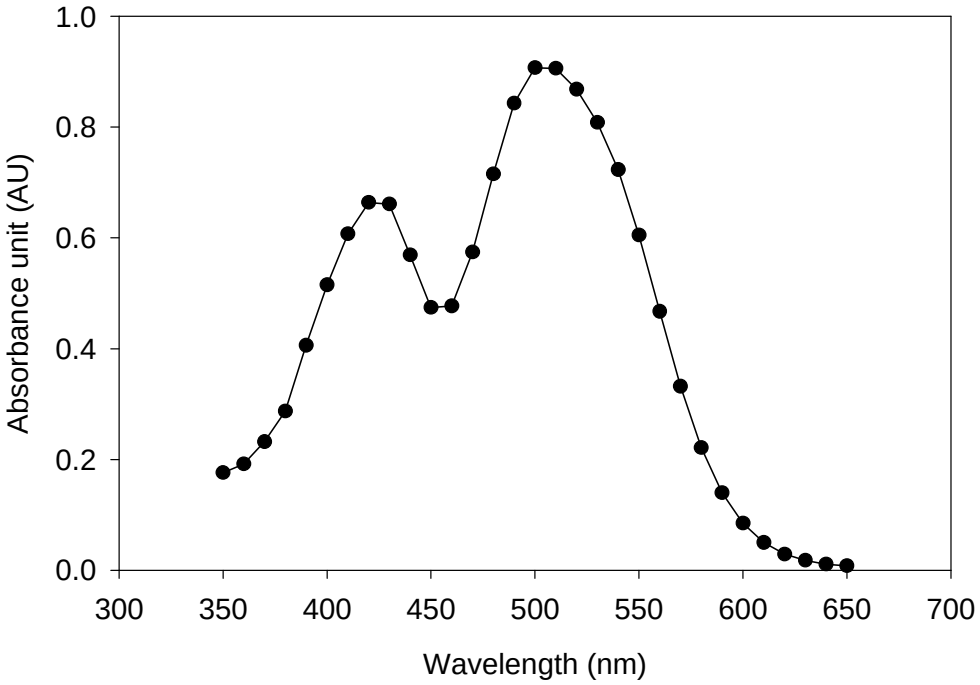

Figure 4.74: Absorption spectrum of purified red band

The absorption spectrum of the filtered extract of the mycelium is shown in Figure 4.75. Once again, two peaks of light absorption are seen. The peak corresponding to the yellow pigment (~400 nm) is much larger than the peak at 500 nm (red pigment). Thus, compared to the extract of the fermentation supernatant (Figure 4.73), the extract of the mycelium is much richer in yellow colour. This suggests that perhaps the red colour is preferentially released from the mycelium into the broth during fermentation.

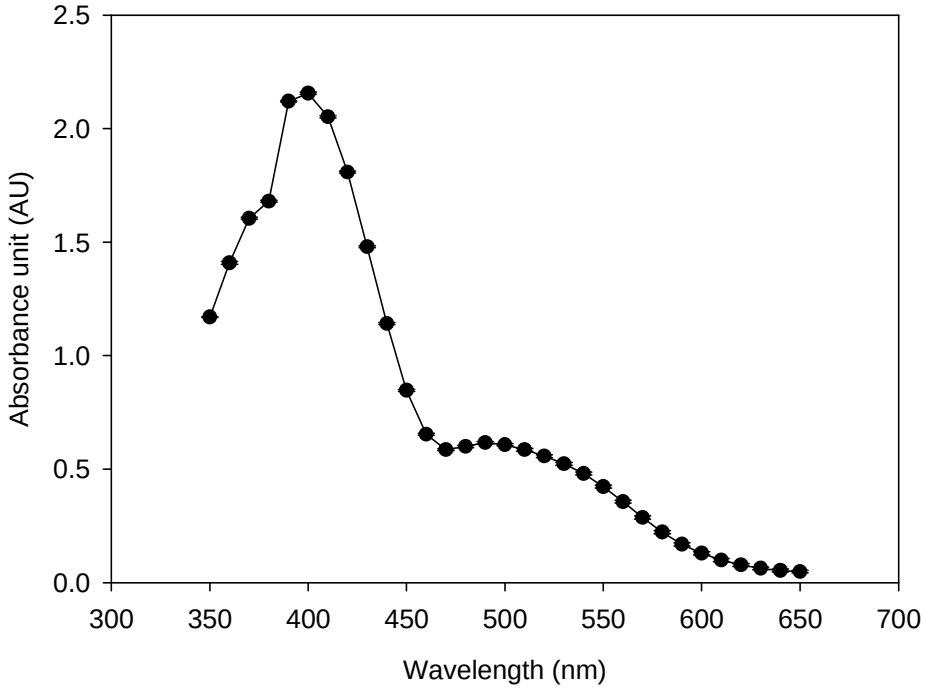

Figure 4.75: Absorption spectrum of extract of mycelia

Attempts were made to separate the red and yellow pigments from the mycelial extracts (Figure 4.75). The expectation was that a purification might be possible as the level of the "contaminating" red pigment in this extract of predominantly yellow pigment was low. Under the best purification conditions (Section 3.4.2.6.1), the "purified" yellow band had the spectrum shown in Figure 4.76. Clearly, some purification was achieved, as the fraction had a single absorption peak at ~ 400 nm, corresponding to yellow pigment, but also a contaminating shoulder at ~ 500 nm due to residual red pigment (Figure 4.76).

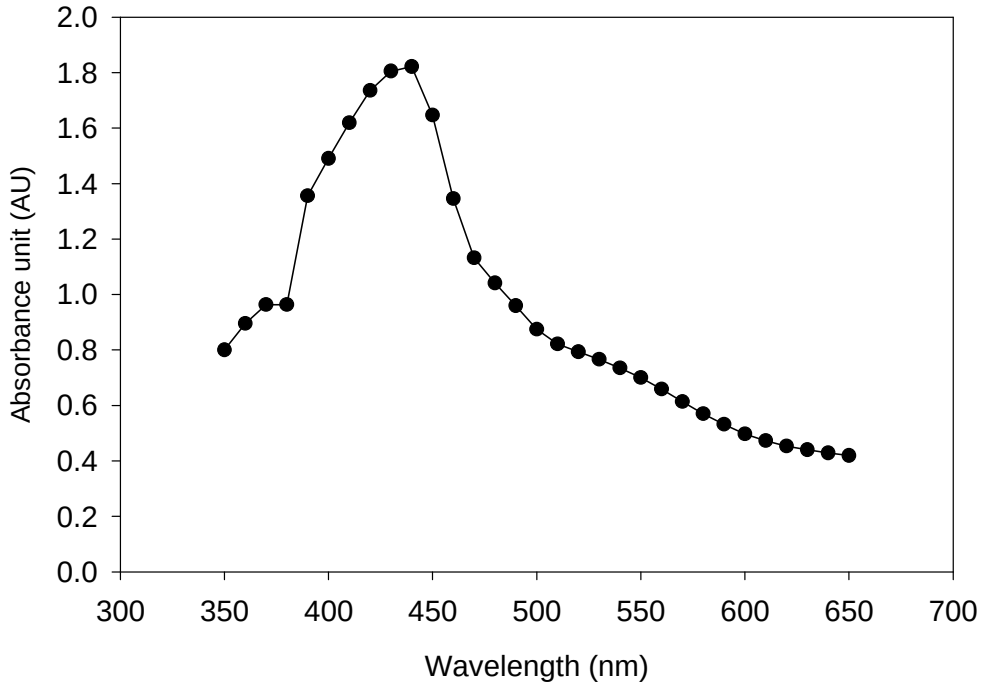

Figure 4.76: Absorption spectrum of purified yellow band from mycelia extraction

4.6.2.2 Thin layer chromatography

As column chromatography was not particularly successful in separating the pigments, further purification was attempted using preparative thin layer chromatography (TLC). The purified red fractions obtained from column chromatography were used for TLC. Approximately 100 µL of purified red fraction (1 mg/mL) from both the broth filtrate and mycelia extracts were applied separately onto the prep-TLC plate using a 10 µL pipette tip. The solvent was allowed to evaporate. Then the spotted TLC plates were placed in a developing chamber (flat-bottomed 20 × 20 cm chamber) that contained the solvent system of chloroform:methanol:water (65:25:4, vol/vol.). After 90 min, the red spot obtained was scrapped off, dissolved in 3 mL of 95% ethanol and subjected to the scanning UV visible spectrophotometer analysis. The retention factor (R_f) values for the various spots on the TLC plate were determined as described in Section 3.4.2.6.2.

Figures 4.77 and 4.78 show the UV visible absorption spectra of purified red spots from the broth supernatant and the mycelia, respectively. Unfortunately, even though a single red spot was recorded from the TLC plates, the absorption spectra showed two absorption peaks in both cases. This suggests either inability to separate or the possibility that the red pigment also absorbs at the wavelength corresponding to yellow. This is consistent with other reports (Broder and Koehler, 1980; Carvalho *et al.*, 2007; Jung *et al.*, 2003; Juzlova *et al.*, 1994; Mapari *et al.*, 2006) that suggest that supposedly purified red pigment has an absorption peak also at 400 nm (yellow).

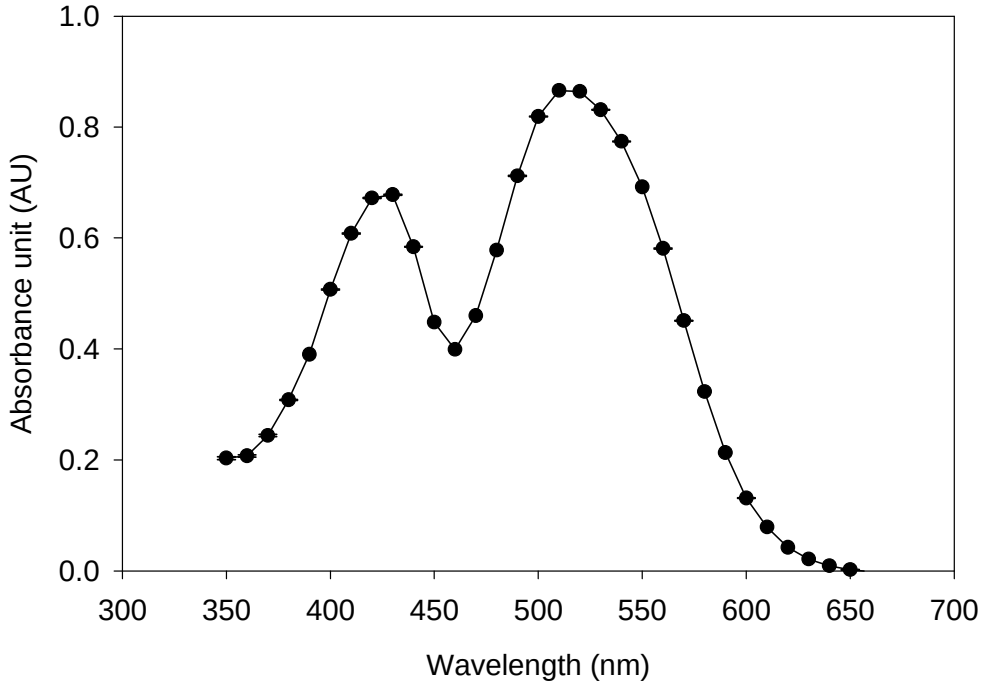

Figure 4.77: Absorption UV-visible spectrum of the TLC purified red spot from the broth filtrate

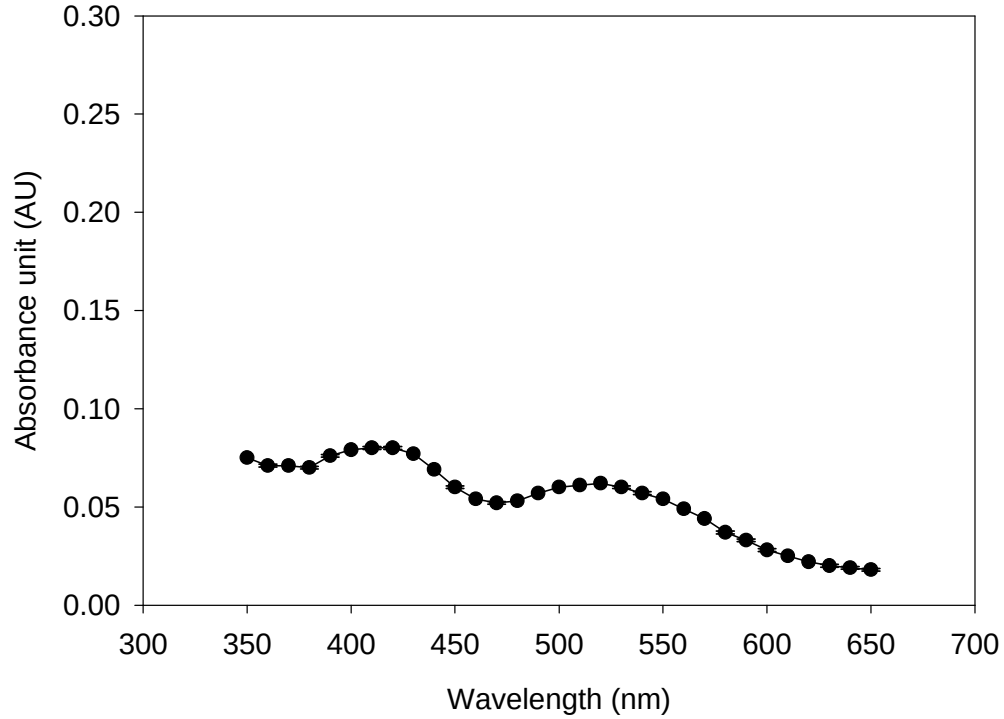

Figure 4.78: Absorption UV-visible spectrum of the TLC purified red spot from the mycelial extraction

A developed TLC plate is shown in Figure 4.79. The plate also shows a lane corresponding to extract of solid-state fermented rice powder. The retention factors (R_f) observed for various compounds on the TLC plate are noted in Table 4.21 and correspond to Figure 4.79. The colour spots developed on the TLC could be classified into three categories: red, yellow, and orange. The TLC plate showed that in submerged culture fermentation, the red pigment occurred mainly in the filtrate (i.e. the hydro soluble pigment), while the yellow pigment was cell bound in the mycelia. The R_f values for the yellow spots were almost similar for all extractions (R_f = 0.95-0.97); however, for the red rice powder, a second yellow spot was observed at R_f of 0.59. This suggests pigment production to be quite complex in solid-state culture. Multiple red spots were observed. The R_f for red varied in the range of 0.01 to 0.86. Again, multiple red pigments appear to be produced. Surprisingly, the orange spot was only observed on the red rice of solid-state fermentation product. This was probably because of all the orange pigment that was produced in submerged culture had been transformed to the hydro soluble red pigment.

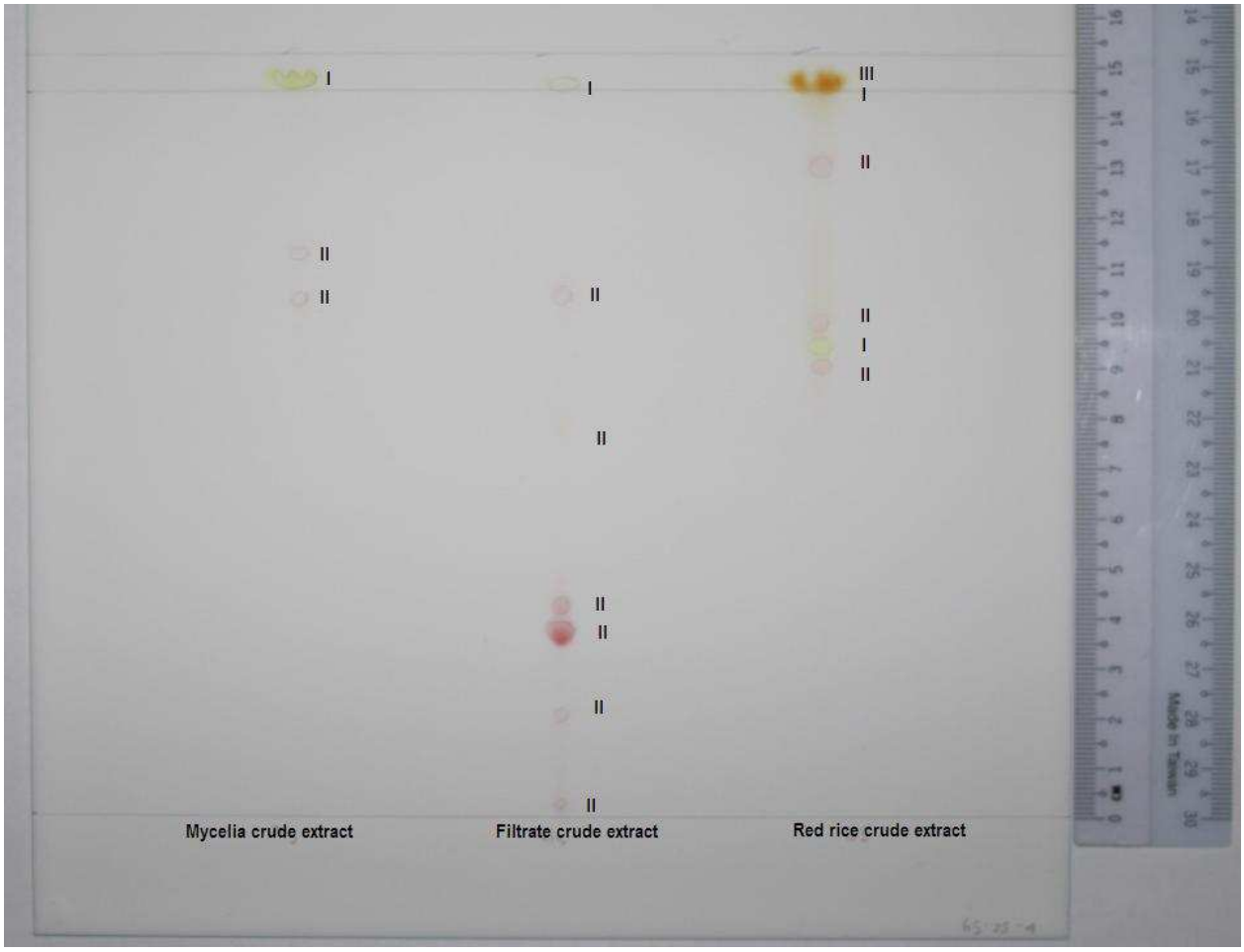

Figure 4.79: Thin layer chromatography (TLC) developed plate of crude mycelia (submerged culture), broth filtrate (submerged culture), and fermented rice powder (solid-state culture)

Note:

I, yellow spots; II, red spots; III, orange spots

Table 4.21: Retention factors (R_f) of colour components separated on TLC plate (with solvent system of chloroform: methanol: water (65:25:4, vol/vol))

Fermentation technique	Sample	Colour component	R_f
Submerged culture[1]	Crude extract of		
(Substrate: Glucose+MSG)	broth filtrate powder	Yellow spot	0.96
		Red spot	0.69
		Red spot	0.55
		Red spot	0.25
		Red spot	0.22
		Red spot	0.12
		Red spot	0.02
	Crude extract of		
	mycelia extract powder	Yellow spot	0.97
		Red spot	0.74
		Red spot	0.68
Solid-state culture[2]	Crude extract of		
	red rice extract powder	Yellow spot	0.95
		Yellow spot	0.59
		Red spot	0.86
		Red spot	0.65
		Red spot	0.55
		Orange spot	0.97

Note:

[1] Submerged culture on medium J with C : N ratio of 9 : 1, glucose concentration of 10 g/L, at 30^{o}C, 250 rpm, run for 4 days

[2] Solid-state culture of packed-bed bioreactor at 0.05 L/min aeration rate and 70% initial moisture content, 30^{o}C, run for 18 days

The yellow pigments produced by *Monascus ruber* in both submerged and solid-state fermentation were likely identical as their R_f values were comparable (R_f 0.95-0.97) in concurrence with other reports (Blanc *et al.*, 1994; Jung *et al.*, 2003; Martinkova *et al.*, 1995). A high value of R_f indicates a high hydrophobicity of a component (Blanc *et al.*, 1994; Jung *et al.*, 2003). A high R_f for the yellow pigment suggests it to be more hydrophobic than the red pigment. This was consistent with the elution pattern observed in column chromatography where the less polar yellow pigment tended to elute before the red band. Water soluble red pigments are known to result through incorporation of nitrogen in the relatively hydrophobic orange pigment (Carvalho *et al.*, 2003).

4.6.3 Stability of the pigment

Monascus pigments are commonly used as food colorants. For industrial applications, it is necessary to understand how the stability of the pigments might be affected by light, pH, and temperature. The intracellular *Monascus* pigments, produced by submerged culture are said to be highly sensitive to heat, pH, and light (Hajjaj *et al.*, 1997; Wong and Koehler, 1983).

Stability of the crude red pigment produced by *Monascus ruber* ICMP 15220 under various fermentation conditions was examined. For this purpose, the submerged culture was first filtered to remove the mycelia. Then, the filtrate samples were again filtered using sterile filters 0.45 μm (Minisart, Sartorius Stedim Biotech) in order to remove any contaminating microorganism and placed in sterile Pyrex tubes (10 mL each). Similarly, the solid-state fermented solids were extracted with 95% ethanol (Section 3.4.3.3), sterile filtered and placed in sterile Pyrex tubes. The tubes were subjected to the various treatments as described in Section 3.4.2.5.

4.6.3.1 Effect of light

The sterile Pyrex tubes containing the filter sterilized fermentation broth (submerged culture, pH 7.3) or ethanol extract of fermented solids (solid-state fermentation, pH 4.0) were held under ambient laboratory lightning for 168 h at 25^{o}C. An identical set of control tubes were kept covered with aluminium foil. Tubes were withdrawn at specified intervals for measurements of absorbance at 500 nm. The results are shown in Figure 4.80. The stability was measured as percentage of the initial absorbance remaining at any time.

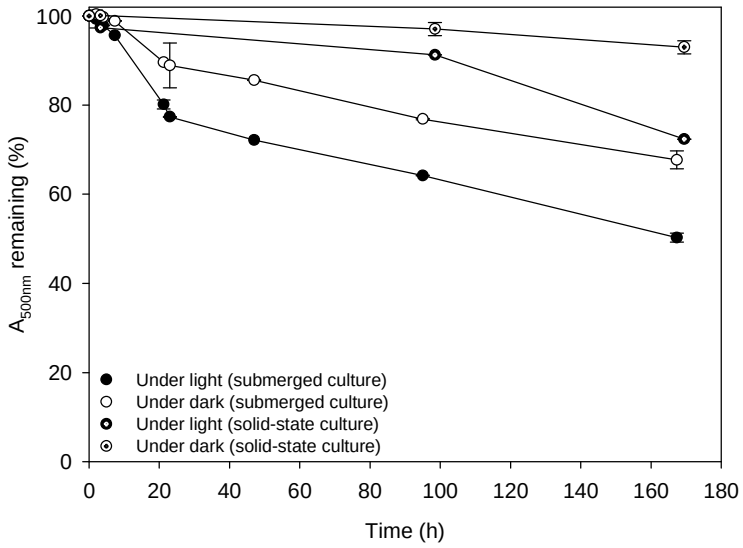

Figure 4.80: The stability of the crude red pigment under light and dark conditions

The pigments were always more stable in the dark than under ambient laboratory lightning. The relatively purer red pigment from the submerged culture was always less stable than the crude pigment extracted from the solid-state culture. For example, after 4 days of exposure, 91% of the red pigment isolated from solid-state culture remained, but only 64% of the red pigment from submerged culture remained. However, these differences in stability of pigments from the different types of fermentation may be due to differences in the solvents used and the pH. Within samples from a given type of fermentation the effects attributed to light are valid.

4.6.3.2 Effect of temperature

The sterile Pyrex tubes (Section 4.6.3) containing the samples were subjected separately to 70^{o}C for 8 h, boiling water bath for 1 min, and autoclave treatment (121^{o}C, 15 min). The results are shown in Figures 4.81 and 4.82. The red pigment was quite stable at 4^{o}C. Some degradation occurred at 70^{o}C for the pigment produced by solid-state culture. In contrast, the pigment produced by submerged culture was quite sensitive to heat at 70^{o}C. At this temperature, the pigment concentration declined to ~ 50% of initial value after 5 h of exposure. A 1 min exposure to 100^{o}C, did damage the pigments (Figure 4.83), but not as much as a 5 h exposure to 70^{o}C. A prolonged exposure to heat tended to discolour the pigment from bright red to brownish red. Autoclaving at 121^{o}C for 15 min caused some damage (Figure 4.82) but not as much as was seen after a prolonged exposure to 70^{o}C. For brief heat treatments, the stability of the pigments from the solid-state culture was comparable to that of the pigment from submerged culture. Clearly, the pigments were relatively stable to quite intense heat so long as the exposure could be kept to < 15 min.

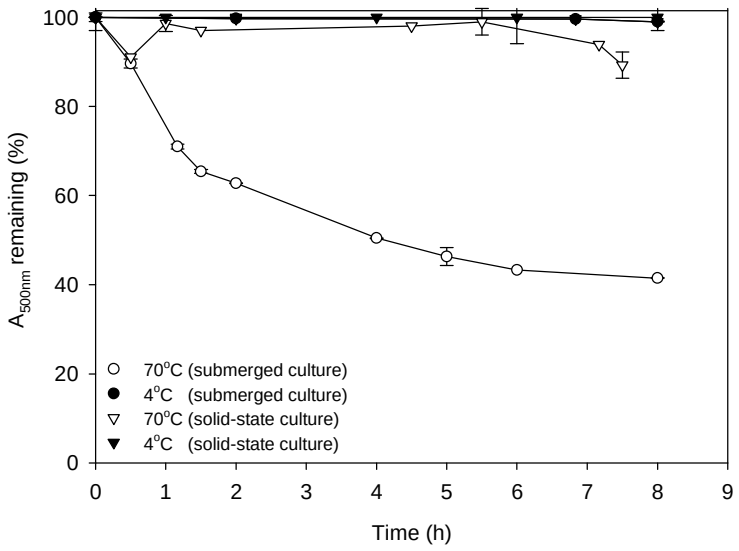

Figure 4.81: The stability of the crude red pigment at different temperatures

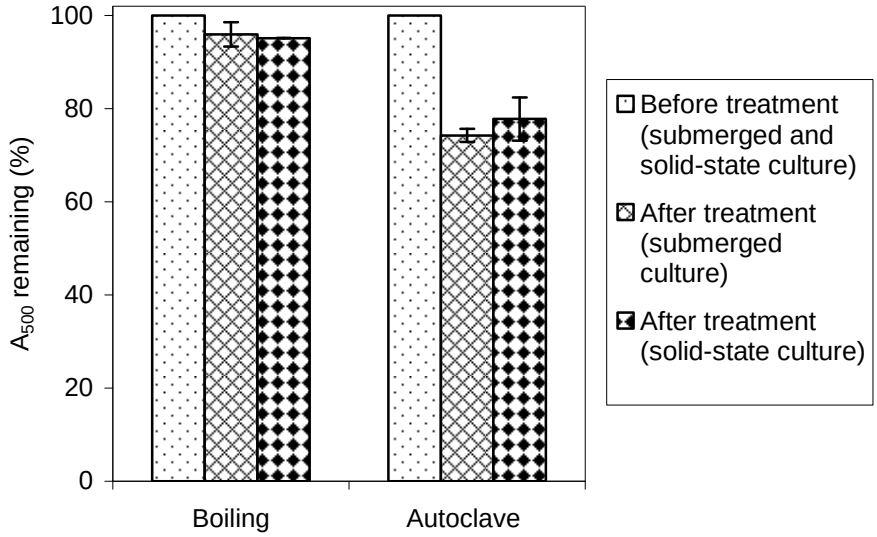

Figure 4.82: The stability of the crude red pigment after boiling and autoclave treatments

4.6.3.3 Effect of pH

The pigment samples in Pyrex tubes (Section 4.6.3) were subjected to pH 4, 7, and 10 for 8 h at room temperature in the dark. Absorbance (500 nm) was measured at specified intervals. The results are shown in Figure 4.83. At pH 4, the pigment from the solid-state fermentation was quite stable in ethanolic solution (Figure 4.83). Similarly, pigments produced in submerged culture were quite stable at neutral pH. Pigments from both types of fermentations were relatively more sensitive to alkaline pH (pH = 10). Addition of a few drops of NaOH to the pigment solution (initially at pH 7), to bring the pH to 10, resulted in a rapid change in colour from red to orange. Subsequently, the absorbance remained stable with time (Figure 4.83).

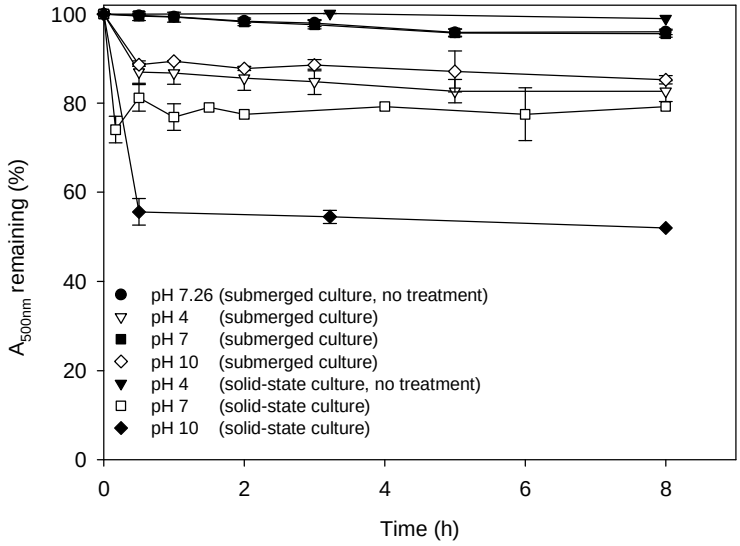

Figure 4.83: The stability the red pigment under different pH

The pigment stability patterns under various conditions were generally consistent with data published for other *Monascus* strains (Babitha *et al.*, 2008; Carvalho *et al.*, 2005; Fabre *et al.*, 1993; Jung *et al.*, 2005; Kaur *et al.*, 2009).

4.7 Comparison of red pigment production by different methods

Like other *Monascus* strains reported in the literature, *Monascus ruber* ICMP 15220 could be grown successfully in both submerged culture and solid-state fermentation. Pigments were produced under both types of fermentations. Table 4.22 compares the two fermentation methods for red pigment. Among the solid-state culture methods tested, Erlenmeyer flask (static culture) were least effective for pigment production. The non-optimized packed-bed bioreactor had nearly 2.4-fold greater pigment productivity compared to the Erlenmeyer flask. Through optimization, the red pigment productivity of the packed-bed could be raised by ~ 78% compared to the non-optimized case.

For various *Monascus* fungi, solid-state culture has been frequently associated with a higher pigment yield compared to submerged culture (Carvalho *et al.*, 2006; Evans and Wang, 1984; Lin, 1973; Soccol and Vandenberghe, 2003). This phenomenon has been attributed to the pigment accumulation within the mycelium in submerged culture due to the low solubility of the pigment in the acidic fermentation medium (Johns and Stuart, 1991). In contrast, in solid-state culture, the fungus penetrates into the rice and the pigment is released into the grains. In addition, a limited oxygen availability in submerged culture has been associated with a low yield of pigment (Oostra *et al.*, 2001). Limitation of oxygen in submerged culture occurs because of the low solubility of oxygen in aqueous solutions.

The higher pigment productivity in the packed-bed bioreactor compared to Erlenmeyer flasks is due to a better oxygen supply by forced aeration of the packed-bed. Forced aeration in packed-beds is known to improve oxygen supply compared to unaerated static beds (Han and Mudgett, 1992).

Table 4.22: Comparison of fermentation methods for the red pigment production

Parameters	Unit	Submerged culture	Solid-state culture		
			Erlenmeyer flask	Packed-bed bioreactor	Packed-bed bioreactor (after optmized)
Maximum yield of red pigment production on biomass	AU/g cell dry weight	24.65	2607.40	7362.40	7709.70
Specific rate of red pigment production	AU/g cell dry weight h	0.41	8.30	21.90	22.95
Maximum red pigment productivity	AU/ L h	0.02	-	491.20	674.50

CHAPTER 5

Summary and conclusions

This work investigated the production of the red pigments of the fungus of *Monascus ruber* ICMP 15220. Both the submerged fermentation and the solid-state fermentation methods were assessed. Solid-state fermentation on steamed rice without supplemented nitrogen, but with supplemented Zn^{2+} proved to be most effective for pigment production.

In both batch submerged culture fermentation and batch solid-state fermentation, the red pigment production was found to be growth associated. The C : N ratio of 9 : 1 that was optimal for red pigment development in submerged culture failed to promote pigment production in solid-state culture. The solid-state fermentation method was optimized for red pigment production in 18 cm deep packed beds of rice at 30^{o}C. The optimal C : N ratio for solid-state fermentation was 30 : 1, as in natural rice. The optimal initial moisture content of solid substrate was 70%. An aeration rate (97 – 99% relative humidity) of 0.14 L/min proved to be optimal. Under the optimal conditions in the packed-bed bioreactor, the red pigment productivity was nearly 674 AU/L h, or nearly 3.4×10^{4}-fold greater than in the best submerged fermentation.

The red pigment produced by solid-state fermentation was more stable to light, high temperature, and acidic pH compared to the red pigment produced by submerged culture.

Pigment productivity of *Monascus ruber* ICMP 15220 was comparable to that of the other *Monascus* fungi. Solid-state fermentation in packed-beds under optimal culture conditions was effective for production of a highly concentrated red pigment. This work shows that yield in commercial production of the red pigments can be significantly improved by the use of solid-state fermentation under the conditions specified above.

References

Abd-Aziz, S., Hung, G., Mohd Ali, H., Mohamed Ismail, A.K. and Noraini, S. (2008) Indirect method for quantification of cell biomass during solid-state fermentation of palm kernel cake based on protein content. Asian Journal of Scientific Research, 1, 385-393

Ahn, J., Jung, J., Hyung, W., Haam, S. and Shin, C. (2006) Enhancement of *Monascus* pigment production by the culture of *Monascus* sp. J101 at low temperature. Biotechnology Progress, 22, 338-340

Akihisa, T., Tokuda, H., Ukiya, M., Kiyota, A., Yasukawa, K., Sakamoto, N., Kimura, Y., Suzuki, T., Takayasu, J. and Nishino, H. (2005) Anti-tumor-initiating effects of monascin, an azaphilonoid pigment from the extract of *Monascus pilosus* fermented rice (red-mold rice). Chemistry and Biodiversity, 2, 1305-1309

Alani, F., Grove, J.A., Anderson, W.A. and Moo-Young, M. (2009) Mycophenolic acid production in solid-state fermentation using a packed-bed bioreactor. Biochemical Engineering Journal, 44, 106-110

Al-Sarrani, A.Q.M. and El-Naggar, M.Y.M. (2006) Application of Plackett-Burman factorial design to improve citrinin production in *Monascus ruber* batch cultures. Botanical Studies, 47, 167-174

Anisha, G.S., John, R.P., Prema, P. and Pandey, A. (2010) Investigation on alpha-galactosidase production by *Streptomyces griseoloalbus* in a forcefully aerated packed-bed bioreactor operating in solid-state fermentation condition. Applied Biochemistry and Biotechnology, 160, 421-427

Anonymous (1993) Precise color communication, color control from feeling to instrumentation. Konika Minolta Sensing, Japan

Anonymous (2007) A guide to understanding color communication. X-Rite Incorporated, Michigan, USA, pp. 1-26

Ashley, V.M., Mitchell, D.A. and Howes, T. (1999) Evaluating strategies for overcoming overheating problems during solid-state fermentation in packed-bed bioreactors. Biochemical Engineering Journal, 3, 141-150

Assamoi, A.A., Destain, J., Delvigne, F., Lognay, G. and Thonart, P. (2008) Solid-state fermentation of xylanase from *Penicillium canescens 10–10c* in a multi-layer-packed bed reactor. Applied Biochemistry and Biotechnology, 145, 87-98

ATCC (American Type Culture Collection) (2007), Online catalog. http://www.atcc.org

Babitha, S., Soccol, C.R. and Pandey, A. (2006) Jackfruit seed - A novel substrate for the production of *Monascus* pigments through solid-state fermentation. Food Technology Biotechnology, 44, 465-471

Babitha, S., Soccol, C.R. and Pandey, A. (2007a) Effect of stress on growth, pigment production and morphology of *Monascus* sp. in solid cultures. Journal of Basic Microbiology, 47, 118-126

Babitha, S., Soccol, C.R. and Pandey, A. (2007b) Solid-state fermentation for the production of *Monascus* pigments from jackfruit seed. Bioresource Technology, 98, 1554-1560

Babitha, S., Carvahlo, J.C., Soccol, C.R. and Pandey, A. (2008) Effect of light on growth, pigment production and culture morphology of *Monascus purpureus* in solid-state fermentation. World Journal of Microbiology and Biotechnology, 24, 2671-2675

Bajracharya, R. and Mudgett, R.E. (1980) Effects of controlled gas environments in solid-substrate fermentations of rice. Biotechnology and Bioengineering, 22, 2219-2235

Barrios-Gonzalez, J., Fernandez, F.J., Tomasini, A. and Mejia, A. (2005) Secondary metabolites production by solid-state fermentation. Malaysian Journal of Microbiology, 1, 1-6

Bau, Y.S. and Wong, H.C. (1979) Zinc effects on growth, pigmentation and antibacterial activity of *Monascus purpureus*. Physiologia Plantarum, 46, 63-67

Blanc, P.J., Loret, M.O., Santerre, A.L., Pareilleux, A., Prome, D., Prome, J.C. and Goma, G. (1994) Pigments of *Monascus*. Journal of Food Science, 59, 862-865

Braun, S. and Vechtlifshitz, S.E. (1991) Mycelial morphology and metabolite production. Trends in Biotechnology, 9, 63-68

Broder, C.U. and Koehler, P.E. (1980) Pigments produced by *Monascus purpureus* with regard to quality and quantity. Journal of Food Science, 45, 567-569

Bull, A.T. and Trinci, A.P.J. (1977) The physiology and metabolic control of fungal growth. Advances in Microbial Physiology, 15, 1-84

Carels, M. and Shepherd, D. (1975) Sexual reproductive cycle of *Monascus* in submerged shaken culture. Journal of Bacteriology, 122, 288-294

Carels, M. and Shepherd, D. (1977) The effect of different nitrogen sources on pigment production and sporulation of *Monascus* species in submerged, shaken culture. Canadian Journal of Microbiology, 23, 1360-1372

Carels, M. and Shepherd, D. (1979) The effect of changes in pH on phosphate and potassium uptake by *Monascus rubiginosus* ATCC 16367 in submerged shaken culture. Canadian Journal of Microbiology, 25, 1484-1488

Carvalho, J.C.D., Pandey, A., Babitha, S. and Soccol, C.R. (2003) Production of *Monascus* biopigments: An overview. Agro Food Industry Hi-Tech, 14, 37-42

Carvalho, J.C.D., Oishi, B.O., Pandey, A. and Soccol, C.R. (2005) Biopigments from *Monascus*: Strains selection, citrinin production and color stability. Brazillian Archives of Biology and Technology an International Journal, 48, 885-894

Carvalho, J.C.D., Pandey, A., Oishi, B.O., Brand, D., Leon, J.A.R. and Soccol, C.R. (2006) Relation between growth, respirometric analysis and biopigments production from *Monascus* by solid-state fermentation. Biochemical Engineering Journal, 29, 262-269

Carvalho, J.C.D., Oishi, B.O., Woiciechowski, A.L., Pandey, A., Babitha, S. and Soccol, C.R. (2007) Effect of substrates on the production of *Monascus* biopigments by solid-state fermentation and pigment extraction using different solvents. Indian Journal of Biotechnology, 6, 194-199

Casas Lopez, J.L., Rodrigues Porcel, E.M., Vilches Ferron, M.A., Sanchez Perez, J.A., Fernandez Sevilla, J.M. and Chisti, Y. (2004) Lovastatin inhibits its own synthesis in *Aspergillus terreus*. Journal of Industrial Microbiology & Biotechnology, 31, 48-50

Cavalcante, R.S., Lima, H.L.S., Pinto, G.A.S., Gava, C.A.T. and Rodrigues, S. (2008) Effect of moisture on *Trichoderma* conidia production on corn and wheat bran by solid state fermentation. Food and Bioprocess Technology, 1, 100-104

Chang, Y.N., Huang, J.C., Lee, C.C., Shih, I.L. and Tzeng, Y.M. (2002) Use of response surface methodology to optimize culture medium for production of lovastatin by *Monascus ruber*. Enzyme and Microbial Technology, 30, 889-894

Chatterjee, S., Maity, S., Chattopadhyay, P., Sarkar, A., Laskar, S. and Sen, S.K. (2009) Characterization of red pigment from *Monascus* in submerged culture red pigment from *Monascus purpureus*. Journal of Applied Sciences Research, 5, 2102-2108

Chen, F.C., Manchand, P.S. and Whalley, W.B. (1971) The structure of monascin: the relative stereochemistry of the azaphilones. Journal of Chemical Society, 21, 3577-3579

Chen, M.H. and Johns, M.R. (1993) Effect of pH and nitrogen source on pigment production by *Monascus purpureus*. Applied Microbiology and Biotechnology, 40, 132-138

Chen, M.H. and Johns, M.R. (1994) Effect of carbon source on ethanol and pigment production by *Monascus purpureus*. Enzyme and Microbial Technology, 16, 584-590

Chen, H.Z., Xu, J. and Li, Z.H. (2005) Temperature control at different bed depths in a novel solid-state fermentation system with two dynamic changes of air. Biochemical Engineering Journal, 23, 117-122

Chisti, Y. (1999a) Fermentation (Industrial): Basic considerations. In Encyclopedia of Food Microbiology, R. Robinson, C. Batt and P. Patel (eds), Acedemic Press, London. pp. 663-674

Chisti, Y. (1999b) Solid substrate fermentations, enzyme production, food enrichment. In Encyclopedia of Bioprocess Technology: Fermentation, Biocatalysis, and Bioseparation, Flickinger, M. C., Drew, S. W., eds, Wiley, New York. pp. 2446-2462

Chiu, S.W. and Poon, Y.K. (1993) Submerged production of *Monascus* pigments. Mycologia, 85, 214-218

Chiu, C.H., Ni, K.H., Guu, Y.K. and Pan, T.M. (2006) Production of red mold rice using a modified Nagata type koji maker. Applied Microbiology and Biotechnology, 73, 297-304

Cho, Y.J., Park, J.P., Hwang, H.J., Kim, S.W., Choi, J.W. and Yun, J.W. (2002) Production of red pigment by submerged culture of *Paecilomyces sinclairii*. Letters in Applied Microbiology, 35, 195-202

Chutmanop, J., Chuichulcherm, S., Chisti, Y. and Sirinophakun, P. (2008) Protease production by *Aspergillus oryzae* in solid-state fermentation using agroindustrial substrates. Journal of Chemical Technology and Biotechnology, 83, 1012-1018

Cochrane, V.W. (1958) Physiology of fungi, John Wiley and Sons, Inc., New York

Couto, S.R. and Sanroman, M.A. (2006) Application of solid-state fermentation to food industry—A review. Journal of Food Engineering, 76, 291-302

Dalla Santa, H.S., Dalla Santa, O.R., Brand, D., Vandenberghe, L.P.D. and Soccol, C.R. (2004) Spore production of *Beauveria bassiana* from agro-industrial residues. In 15th Brazilian Congress of Chemical Engineering, Curitiba, Brazil. pp. 51-60

Desgranges, C., Vergoignan, C., Georges, M. and Durand, A. (1991a) Biomass estimation in solid state fermentation. I. Manual biochemical methods. Applied Microbiology and Biotechnology, 35, 200-205

Desgranges, C., Georges, M., Vergoignan, C. and Durand, A. (1991b) Biomass estimation in solid-state fermentation. II. Online measurements. Applied Microbiology and Biotechnology, 35, 206-209

Dominguez-Espinosa, M., R. and Webb, C. (2003) Submerged fermentation in wheat substrates for production of *Monascus* pigments. World Journal of Microbiology and Biotechnology, 19, 329-336

Downham, A. and Collins, P. (2000) Colouring our foods in the last and next millennium. International Journal of Food Science and Technology, 35, 5-22

Dufosse, L., Galaup, P., Yaron, A., Arad, S.M., Blanc, P., Murthy, K.N.C. and Ravishankar, G.A. (2005) Microorganisms and microalgae as sources of pigments for food use: A scientific oddity or an industrial reality? Trends in Food Science and Technology, 16, 389-406

Durand, A., de la Broise, D. and Blachere, H. (1988) Laboratory scale bioreactor for solid state processes. Journal of Biotechnology, 8, 59-66

Durand, A. (2003) Bioreactor designs for solid-state fermentation. Biochemical Engineering Journal, 13, 113-125

Eduardo, M.P., Costa, J.P.C. and Kilikian, B.V. (2007) Effect of agitation pattern on growth of *Monascus* sp in SSF in drum type bioreactor. Journal of Biotechnology, 131S, S177-S177

Endo, A. (1979) Monacolin K, a new hypocholesterolemic agent that specifically inhibits 3-hydroxy-3-methylglutaryl coenzyme A reductase. Journal of Antibiotics, 33, 334-336

Erdogrul, O. and Azirak, S. (2005) A review on the red yeast rice (*Monascus purpureus*). KSU Journal of Science and Engineering, 8, 10-15

Evans, P.J. and Wang, H.Y. (1984) Pigment production from immobilized *Monascus* sp. utilizing polymeric resin adsorption. Applied and Environmental Microbiology, 47, 1323-1326

Fabre, C.E., Santerre, A.L., Loret, M.O., Baberian, R., Pareilleux, A., Goma, G. and Blanc, P.J. (1993) Production and food applications of the red pigments of *Monascus ruber*. Journal of Food Science, 58, 1099-1102

Fanaei, M.A. and Vaziri, B.M. (2009) Modeling of temperature gradients in packed-bed solid-state bioreactors. Chemical Engineering and Processing, 48, 446-451

Farina, J.I., Tonetti, G.R. and Perotti, N.I. (1997) A mathematical model applied to the fungal colony growth of *Sclerotium rolfsii*. Biotechnology Techniques, 11, 217-219

Favela-Torres, E., Cordova-Lopez, J., Garcia-Rivero, M. and Gutierrez-Rojas, M. (1998) Kinetics of growth of *Aspergillus niger* during submerged, agar surface and solid state fermentations. Process Biochemistry, 33, 103-107

Fenice, M., Federici, F., Selbmann, L. and Petruccioli, M. (2000) Repeated-batch production of pigments by immobilised *Monascus purpureus*. Journal of Biotechnology, 80, 271-276

Fielding, B.C., Holker, J.S.E., Jones, D.F., Powell, A.D.G., Richmond, K.W., Robertson, A. and Whalley, W.B. (1961) The chemistry of fungi. Part XXXIX. The structure of monascin. Journal of Chemical Society, 1961, 4579 - 4589

Francis, F.J. (1987) Lesser-known food colorants. Food Technology, 41, 62-68

Gautam, P., Sabu, A., Pandey, A., Szakacs, G. and Soccol, C.R. (2002) Microbial production of extra-cellular phytase using polystyrene as inert solid support. Bioresource Technology, 83, 229-233

Gervais, P. and Molin, P. (2003) The role of water in solid-state fermentation. Biochemical Engineering Journal, 13, 85-101

Ghildyal, N.P., Gowthaman, M.K., Rao, K.S. and Karanth, N.G. (1994) Interaction of transport resistances with biochemical reaction in packed-bed solid-state fermentors: effect of temperature gradients. Enzyme and Microbial Technology, 16, 253-257

Gumbira-Said, E., Greenfield, P.F., Mitchell, D.A. and Doelle, H.W. (1993) Operational parameters for packed beds in solid-state cultivation. Biotechnology Advances, 11, 599-610

Gunasekaran, S. and Poorniammal, R. (2008) Optimization of fermentation conditions for red pigment production from *Penicillium* sp under submerged cultivation. African Journal of Biotechnology, 7, 1894-1898

GutierrezRojas, M., Hosn, S.A.A., Auria, R., Revah, S. and FavelaTorres, E. (1996) Heat transfer in citric acid production by solid state fermentation. Process Biochemistry, 31, 363-369

Hadfield, J.R., Holker, J.S.E. and Stanway, D.N. (1967) The biosynthesis of fungal metabolites. Part II. The β-oxo-lactone equivalents in rubropunctatin and monascorubrin. Journal of Chemical Society, 19, 751-755

Hajjaj, H., Klaebe, A., Loret, M.O., Tzedakis, T., Goma, G. and Blanc, P.J. (1997) Production and identification of N-Glucosylmonascorubramine from *Monascus ruber* and occurence of electron donor-acceptor complexes in these red pigments. Applied and Environmental Microbiology, 63, 2671-2678

Hajjaj, H., Blanc, P.J., Groussac, E., Goma, G., Uribelarrea, J.L. and Loubiere, P. (1999) Improvement of red pigment / citrinin production ratio as a function of environmental conditions by *Monascus ruber*. Biotechnology and Bioengineering, 64, 497-501

Hajjaj, H., Blanc, P., Groussac, E., Uribelarrea, J.L., Goma, G. and Loubiere, P. (2000a) Kinetic analysis of red pigment and citrinin production by *Monascus ruber* as a function of organic acid accumulation. Enzyme and Microbial Technology, 27, 619-625

Hajjaj, H., Klaebe, A., Goma, G., Blanc, P.J., Barbier, E. and Francois, J. (2000b) Medium-chain fatty acids affect citrinin production in the filamentous fungus *Monascus ruber*. Applied and Environmental Microbiology, 66, 1120-1125

Hamano, P.S., Orozco, S.F. and Kilikian, B.V. (2005) Concentration determination of extracellular and intracellular red pigments produced by *Monascus* sp. Brazillian Archives of Biology and Technology, 48, 43-49

Hamdi, M., Blanc, P.J. and Goma, G. (1996) Effect of aeration conditions on the production of red pigments by *Monascus purpureus* growth on prickly pear juice. Process Biochemistry, 31, 543-547

Hamdi, M., Blanc, P.J., Loret, M.O. and Goma, G. (1997) A new process for red pigment production by submerged culture of *Monascus purpureus*. Bioprocess Engineering, 17, 75-79

Han, O. and Mudgett, R.E. (1992) Effects of oxygen and carbon dioxide partial pressures on *Monascus* growth and pigment production in solid-state fermentations. Biotechnology Progress, 8, 5-10

Hawksworth, D.L. and Pitt, J.I. (1983) A new taxonomy for *Monascus* species based on cultural and microscopical characters. Australian Journal of Botany, 31, 51-61

Hesseltine, C.W. (1965) A millenium of fungi, food and fermentation. Mycologia, 57, 149-197

Holker, U. and Lenz, J. (2005) Solid-state fermentation — are there any biotechnological advantages? Current Opinion in Biotechnology, 8, 301-306

De Hoog, G.S., Guarro, J., Gene, J. and Figueras, M.J. (2004) Atlas of clinical fungi, Centraalbureau voor Schimmelcultures/Universitat Rivora i Virgili, Baarn, The Netherlands

Hoogschagen, M., Zhu, Y., As, H.v., Tramper, J. and Rinzema, A. (2001) Influence of wheat type and pre-treatment on fungal growth in solid state fermentation. Biotechnology Letters, 23, 1183-1187

Hopwood, D.A. and Sherman, D.H. (1990) Molecular genetics of polyketides and its comparison to fatty acid biosynthesis. Annual Review of Genetics, 24, 37-66

Hsu, F.L., Wang, P.M., Lu, S.Y. and Wu, W.T. (2002) A combined solid-state and submerged cultivation integrated with adsorptive product extraction for production of *Monascus* red pigments. Bioprocess Biosystems Engineering, 25, 165-168

Ishiaku, U.S., Pang, K.W., Lee, W.S. and Ishak, Z.A.M. (2002) Mechanical propertis and enzymatic degradation of thermoplastic and granular sago starch filled poly(ε-carpolactone). European Polymer Journal, 38, 393-401

Jiang, Y., Li, H.B., Chen, F. and Hyde, K.D. (2005) Production potential of water-soluble *Monascus* red pigment by a newly isolated *Penicillium* sp. Journal of Agricultural Technology, 113-126

Johns, M.R. and Stuart, D.M. (1991) Production of pigments by *Monascus purpureus* in solid culture. Journal of Industrial Microbiology, 8, 23-28

Johnson, G.T. and McHan, F. (1975) Some effects of zinc on the utilization of carbon sources by *Monascus purpureus*. Mycologia, 67, 806-816

Jung, H., Kim, C., Kim, K. and Shin, C.S. (2003) Color characteristics of *Monascus* pigments derived by fermentation with various amino acids. Journal of Agricultural Food Chemistry, 51, 1302-1306

Jung, H., Kim, C. and Shin, C.S. (2005) Enhanced photostability of *Monascus* pigments derived with various amino acids via fermentation. Journal of Agricultural and Food Chemistry, 53, 7108-7114

Juzlova, P. (1994) Biosynthesis of pigments by the fungus *Monascus purpureus*. PhD thesis, Paraguay Institute of Chemical Technology,

Juzlova, P., Martínkova, L., Lozinski, J. and Machek, F. (1994) Ethanol as substrate for pigment production by the fungus *Monascus purpureus*. Enzyme and Microbial Technology, 16, 996-1001

Juzlova, P., Martinkova, L. and Kren, V. (1996) Secondary metabolites of the fungus *Monascus*: a review. Journal of Industrial Microbiology, 16, 163-170

Kaur, B., Chakraborty, D. and Kaur, H. (2009) Production and evaluation of physicochemical properties of red pigment from *Monascus purpureus* MTCC 410. Internet Journal of Microbiology, 7, 1-7

Kennedy, M. and Krouse, D. (1999) Strategies for improving fermentation medium performance: a review. Journal of Industrial Microbiology and Biotechnology, 23, 456-475

Kim, S.Y., Lee, K.H., Kim, J.H. and Oh, D.K. (1997) Erythritol production by controlling osmotic pressure in *Trigonopsis variabilis*. Biotechnology Letters, 19, 727-729

Kim, C.H., Kim, S.W. and Hong, S.I. (1999) An integrated fermentation–separation process for the production of red pigment by *Serratia* sp. KH-95. Process Biochemistry, 35, 485-490

Kim, H.J., Kim, J.H., Oh, H.J. and Shin, C.S. (2002) Morphology control of *Monascus* cells and scale-up of pigment fermentation. Process Biochemistry, 38, 649-655

Kono, I. and Himeno, K. (1999) Antimicrobial activity of *Monascus pilosus* IFO 4520 against contaminant of *Koji*. Bioscience, Biotechnology, and Biochemistry, 63, 1494-1496

Krishna, C. (2005) Solid-state fermentation systems - An overview. Critical Reviews in Biotechnology, 25, 1-30

Kumar, D., Jain, V.K., Shanker, G. and Srivastava, A. (2003) Citric acid production by solid state fermentation using sugarcane bagasse. Process Biochemistry, 38, 1731-1738

Kuromo, M., Nakanishi, K., Shindo, K. and Tada, M. (1963) Biosynthesis of monascorubrin and monascoflavin. Chemical and Pharmaceutical Bulletin, 11, 358-362

Lambers, H., III, F.S.C. and Pons, T.L. (2008) Plant Physiological Ecology 2nd edition, Springer, New York

Lee, Y.K., Lim, B.L., Ng, A.L. and Chen, D.C. (1994) Production of polyketide pigments by submerged culture of *Monascus*: Effects of substrate limitations. Asia-Pacific Journal of Molecular Biology and Biotechnology, 2, 21-26

Lee, Y.K., Chen, D.C., Chauvatcharin, S., Seki, T. and Yoshida, T. (1995) Production of *Monascus* pigments by a solid-liquid state culture method. Journal of Fermentation and Bioengineering, 79, 516-518

Lee, B.K., Park, N.H., Piao, H.Y. and Chung, W.J. (2001) Production of red pigments by *Monascus purpureus* in submerged culture. Biotechnology and Bioprocess Engineering, 6, 341-346

Lee, B.K., Piao, H.Y. and Chung, W.J. (2002) Production of red pigments by *Monascus purpureus* in solid-state culture. Biotechnology and Bioprocess Engineering, 7, 21-25

Lee, C.L., Hung, H.K., Wang, J.J. and Pan, T.M. (2007) Improving the ratio of monacolin K to citrinin production of *Monascus purpureus* NTU 568 under dioscorea medium through the mediation of pH value and ethanol addition. Journal of Agricultural and Food Chemistry, 55, 6493-6502

Lin, C.F. (1973) Isolation and cultural conditions of *Monascus* sp. for the production of pigments in a submerged shaken culture. Journal of Fermentation Technology, 51, 407-414

Lin, C.F. and Suen, S.J.T. (1973) Isolation of hyperpigment productive mutants of *Monascus* sp F-2. Journal of Fermentation Technology, 51, 757-759

Lin, C.F. and Iizuka, H. (1982) Production of extracellular pigment by a mutant of *Monascus kaoliang* sp. nov. Applied Microbiology and Biotechnology, 43, 671-676

Lin, T.F. (1991) Studies on the formation of *Monascus* red pigments. PhD thesis, Massachusetts Institute of Technology, M.A., USA

Lin, T.F. and Demain, A.L. (1991) Effect of nutrition of *Monascus* sp. on formation of red pigments. Applied Mirobiology and Biotechnology, 36, 70-75

Lin, T.F., Yakushijin, K., Buchi, G.H. and Demain, A.L. (1992) Formation of water-soluble *Monascus* red pigments by biological and semi-synthetic processes. Journal of Industrial Microbiology, 9, 173-179

Lin, T.F. and Demain, A.L. (1993) Resting cell studies on formation of water-soluble red pigments by *Monascus* sp. Journal of Industrial Microbiology and Biotechnology, 12, 361-367

Lin, T.F. and Demain, A.L. (1994) Leucine interference in the production of water-soluble red *Monascus* pigments. Archives of Microbiology, 162, 114-119

Lin, W.Y., Ting, Y.C. and Pan, T.M. (2007) Proteomic response to intracellular proteins of *Monascus pilosus* grown under phosphate-limited complex medium with different growth rates and pigment production Journal of Agricultural Food Chemistry, 55, 467 - 474

Lin, Y.L., Wang, T.H., Lee, M.H. and Su, N.W. (2008) Biologically active components and nutraceuticals in the *Monascus*-fermented rice: a review. Applied Microbiology and Biotechnology, 77, 965-973

Liu, B.L. and Tzeng, Y.M. (1999) Water content and water activity for the production of cyclodepsipeptides in solid-state fermentation by *Metarhizium anisopliae*. Biotechnology Letters, 21, 657-661

Lonsane, B.K., Ghildyal, N.P., Budiatman, S. and Ramakrishna, S.V. (1985) Engineering aspects of solid state fermentation. Enzyme Microbial Technology, 7, 258-265

Lonsane, B.K., Saucedo-Castaneda, G., Raimbault, M., Roussos, S., Viniegra-Gonzalez, G., Ghildyal, N.P., Ramakrishna, M. and Krishnaiah, M.M. (1992) Scale-up strategies for solid-state fermentation systems. Process Biochemistry, 27, 259-273

Lotong, N. and Suwanarit, P. (1990) Fermentation of ang-kak in plastic bags and regulation of pigmentation by initial moisture content. Journal of Applied Bacteriology, 68, 565-570

Mak, N.K., Fong, W.F. and Wong-Leung, Y.L. (1990) Improved fermentative production of *Monascus* pigments in roller bottle culture. Enzyme and Microbial Technology, 12, 965-968

Makhmur Ahmad, M., Nomani, M.S. and Panda, B.P. (2009) Screening of nutrient parameters for red pigment production by *Monascus purpureus* MTCC 369 under submerged fermentation using Plackett-Burman design. Chiang Mai Journal of Science, 36, 104-109

Manpreet, S., Sawraj, S., Sachin, D., Pankaj, S. and Banerjee, U.C. (2005) Review article: Influence of process parameters on the production of metabolites in solid-state fermentation. Malaysian Journal of Microbiology, 1, 1-9

Mao, X.B., Eksriwong, T., Chauvatcharin, S. and Zhong, J.J. (2005) Optimization of carbon source and carbon/nitrogen ratio for cordycepin production by submerged cultivation of medicinal mushroom *Cordyceps militaris*. Process Biochemistry, 40, 1667-1672

Mapari, S.A.S., Meyer, A.S. and Thrane, U. (2006) Colorimetric characterization for comparative analysis of fungal pigments and natural food colorants. Journal of Agricultural Food Chemistry, 54, 7027-7035

Mapari, S.A.S., Thrane, U. and Meyer, A.S. (2010) Fungal polyketide azaphilone pigments as future natural food colorants? Trends in Biotechnology, 28, 300-307

Martin, S. and Edward, J. (1990) Production of crystalline pigments from monascus during fermentation. US Patent 4927760

Martinkova, L., Juzlova, P. and Vesely, D. (1995) Biological activity of polyketide pigments produced by the fungus *Monascus*. Journal of Applied Bacteriology, 79, 609-616

Martinkova, L. and Patakova, P. (1999) *Monascus*. In Encyclopedia of Food Microbiology, R.K. Robinson, C. Batt and P. Patel (eds), Academic Press, London. pp. 1481-1487

Mazutti, M.A., Zabot, G., Boni, G., Skovronski, A., De Oliveira, D., Di Luccio, M., Rodrigues, M.I., Treichel, H. and Maugeri, F. (2010a) Kinetics of inulinase production by solid-state fermentation in a packed-bed bioreactor. Food Chemistry, 120, 163-173

Mazutti, M.A., Zabot, G., Boni, G., Skovronski, A., De Oliveira, D., Di Luccio, M., Rodrigues, M.I., Treichel, H. and Maugeri, F. (2010b) Optimization of inulinase production by solid-state fermentation in a packed-bed bioreactor. Journal of Chemical Technology and Biotechnology, 85, 109-114

Mazutti, M.A., Zabot, G., Boni, G., Skovronski, A., Oliveira, D.D., Luccio, M.D., Rodrigues, M.I., Maugeri, F. and Treichel, H. (2010c) Mathematical modeling of *Kluyveromyces marxianus* growth in solid-state fermentation using a packed-bed bioreactor. Journal of Industrial Microbiology and Biotechnology, 37, 391-400

McGuire, R.G. (1992) Reporting of objective color measurements. Hortscience, 27, 1254-1255

McHan, F. and Johnson, G.T. (1970) Zinc and amino acids: Important components of a medium promoting growth of *Monascus purpureus*. Mycologia, 62, 1018-1031

Meien, O.F.V., Luz, L.F.L., Mitchell, D.A., Correa, J.R.P., Agosin, E., Fernandez, M.F. and Arcas, J.A. (2004) Control strategies for intermittently mixed, forcefully aerated solid-state fermentation bioreactors based on the analysis of a distributed parameter model. Chemical Engineering Science, 59, 4493-4504

Metz, B. and Kossen, N.W.F. (1977) The growth of molds in the form of pellets-a literature review. Biotechnology and Bioengineering, 19, 781-799

Miller, G.L. (1959) Use of dinitrosalicylic acid reagent for determination of reducing sugar. Analytical Chemistry, 31, 426-428

Mitchell, D.A. (1989) Development of a model system and a mathematical model for solid state fermentation. PhD Thesis, University of Queensland, Australia

Mitchell, D.A. (1992) Biomass determination in solid-state cultivation. In Solid substrate cultivation, H.W. Doelle, D.A. Mitchelle and C.E. Rolz (eds), Elsevier Science publishers, England, pp. 53-63

Mitchell, D.A. and Lonsane, B.K. (1992) Definition, characteristics and potential. In Solid substrate cultivation, H.W. Doelle, D.A. Mitchell and C.E. Rolz (eds), Elsevier, England, pp. 1-16

Mitchell, D.A., Z.Targonski, J.Rogalski and Leonowicz, A. (1992a) Substrates for processes. In Solid substrate cultivation, H.W. Doelle, D.A. Mitchell and C.E. Rolz (eds), Elsevier, England, pp. 29-52

Mitchell, D.A., Lonsane, B.K., Durand, A., Renaud, R., Almanza, S., Maratray, J., Desgranjes, C., Crooke, P.S., Hong, K., Tanner, R.D. and Malaney, G.W. (1992b) General principles of reactor design and operation for SSC. In Solid substrate cultivation, H.W. Doelle, D.A. Mitchell and C.E. Rolz (eds), Elsevier, England, pp. 115-139

Mitchell, D.A. and Von Meien, O.F. (2000) Mathematical modeling as a tool to investigate the design and operation of the *Zymotis* packed-bed bioreactor for solid-state fermentation. Biotechnology and Bioengineering, 68, 127-135

Mitchell, D.A., Meien, O.F.V. and Krieger, N. (2003) Recent developments in modeling of solid-state fermentation: heat and mass transfer in bioreactors. Biochemical Engineering Journal, 13, 137-147

Mitchell, D.A., Krieger, N. and Berovic, M. (2006) Solid-state fermentation bioreactors: fundamentals of design and operation, Springer-Verlag, Berlin

Montgomery, D.C. (2001) Design and Analysis of Experiments, John Wiley and Sons, New York

Mudgett, R.E. (1986) Solid state fermentations, ASM Press, Washington, D. C.

Najafpour, G.D., Tajallipour, M., Komeili, M. and Mohammadi, M. (2009) Kinetic model for an up-flow anaerobic packed bed bioreactor: Dairy wastewater treatment. African Journal of Biotechnology, 8, 3590-3596

Nilsson, K. and Bjurman, J. (1998) Chitin as an indicator of the biomass of two wood-decay fungi in relation to temperature, incubation time, and media composition. Canadian Journal of Microbiology, 44, 575-581

Nimnoi, P. and Lumyong, S. (2009) Improving solid-state fermentation of *Monascus purpureus* on agricultural products for pigment production. Food and Bioprocess Technology, DOI no.: 10.1007/s11947-009-0233-8, 1-7, 9 August 2009

Oostra, J., Comte, E.P.L., Heuvel, J.C.V.D., Tramper, J. and Rinzema, A. (2001) Intra-particle oxygen diffusion limitation in solid-state fermentation. Biotechnology and Bioengineering, 75, 13-24

Oriol, E., Raimbault, M., Roussos, S. and Viniegragonzales, G. (1988) Water and water activity in the solid state fermentation of cassava starch by *Aspergillus niger*. Applied Microbiology and Biotechnology, 27, 498-503

Orozco, S.F.B. and Kilikian, B.V. (2008) Effect of pH on citrinin and red pigments production by *Monascus purpureus* CCT3802. World Journal of Microbiology and Biotechnology, 24, 263-268

Ozkan, M., Kirca, A. and Cemeroglu, B. (2003) Effect of moisture content on CIE color values in dried apricots. European Food Research Technology, 216, 217-219

Pandey, A. (1991) Aspects of fermenter design for solid state fermentations. Process Biochemistry, 26, 355-361

Pandey, A. (1992) Recent process developments in solid-state fermentation. Process Biochemistry, 27, 109-117

Pandey, A. (1994) Solid state fermentation, Wiley Eastern Limited, New Delhi

Pandey, A., Soccol, C.R. and Mitchell, D. (2000) New developments in solid state fermentation: I-bioprocesses and products. Process Biochemistry, 35, 1153-1169

Pandey, A. (2003) Solid-state fermentation. Biochemical Engineering Journal, 13, 81-84

Pastrana, L., Blanc, P.J., Santerre, A.L., Loret, M.O. and Goma, G. (1995) Production of red pigments by *Monascus ruber* in synthetic media with a strictly controlled nitrogen source. Process Biochemistry, 30, 333-341

Patakova-Juzlova, P., Rezanka, T. and Viden, I. (1998) Identification of volatile metabolites from rice fermented by the fungus *Monascus purpureus* (ang-kak). Folia Microbiologica, 43, 407-410

Patidar, P., Agrawal, D., Banerjee, T. and Patil, S. (2005) Chitinase production by *Beauveria felina* RD 101: optimization of parameters under solid substrate fermentation conditions. World Journal of Microbiology and Biotechnology, 21, 93-95

Pattanagul, P., Pinthong, R., Phianmongkhol, A. and Leksawasdi, N. (2007) Review of angkak production (*Monascus purpureus*). Chiang Mai Journal of Science, 34, 319-328

Perez-Guerra, N., Torrado-Agrasar, A., Lopez-Macias, C. and Pastrana, L. (2003) Main characteristics and applications of solid substrate fermentation. Electronic Journal of Environmental Agricultural Food Chemistry, 2, 343-350

Phoolphundh, S., Wongwicharn, A. and Terasawat, A. (2007) Effect of C:N ratio on *Monascus* pigment production in fermentor using cassava decanter wastewater as substrate. In The 2nd International Conference on Fermentation Technology for Value Added Agricultural Products, Khon Kaen, Thailand. pp. 3-5

Pirt, S.J. (1985) Principles of microbe and cell cultivation, Blackwell Scientific Publications, London

Pitt, J.I. and Hocking, A.D. (1997) Fungi and food spoilage, Chapman and Hall, London

Prabhakar, A., Krishnaiah, K., Janaun, J. and Bono, A. (2005) An overview of engineering aspects of solid state fermentation. Malaysian Journal of Microbiology, 1, 10-16

Prado, F.C., Vandenberghe, L.P.D. and Soccol, C.R. (2004) Relation between citric acid production by solid-state fermentation from cassava bagasse and respiration of *Aspergillus niger* LPB 21 in semi-pilot scale. In 15th Brazilian Congress of Chemical Engineering, Curitiba, Brazil. pp. 29-36

Prior, B.A. and Preez, J.C.D. (1992) Environmental parameters. In Solid substrate cultivation, H.W. Doelle, D.A. Mitchelle and C.E. Rolz (eds), Elsevier, London, pp. 65-85

Prosser, J.I. and Tough, A.J. (1991) Growth mechanisms and growth-kinetics of filamentous microorganisms. Critical Reviews in Biotechnology, 10, 253-274

Raghavarao, K.S.M.S., Ranganathan, T.V. and Karanth, N.G. (2003) Some engineering aspects of solid-state fermentation. Biochemical Engineering Journal, 13, 127-135

Raimbault, M. and Alazard, D. (1980) Culture method to study fungal growth in solid fermentation. European Journal of Applied Microbiology and Biotechnology, 9, 199-209

Raimbault, M. (1998) General and microbiological aspects of solid state fermentation. Electronic Journal of Biotechnology, 1, 174-188

Rao, K., Gowthaman, M.K., Ghildyal, N.P. and Karanth, N.G. (1993) A mathematical-model for solid-state fermentation in tray bioreactors. Bioprocess Engineering, 8, 255-262

Rasheva, T., Hallet, J.N. and Kujumdzieva, A. (1997-1998) Taxonomic investigation of *Monascus purpureus* 94-25 strain. Journal of Culture Collections, 2, 51-59

Robinson, J.A. (1991) Polyketide synthase complexes: their structure and function in antibiotic biosynthesis. Philosophical Transactions: Biological Sciences, 332, 107-114

Roche, N., Venague, A., Desgranges, C. and Durand, A. (1993) Use of chitin measurement to estimate fungal biomass in solid state fermentation. Biotechnology Advances, 11, 677-683

Rondle, C.J.M. and Morgan, W.T.J. (1955) The determination of glucosamine and galactosamine. Biochemical Journal, 61, 586-589

Roopesh, K., Ramachandran, S., Nampoothiri, K.M., Szakacs, G. and Pandey, A. (2006) Comparison of phytase production on wheat bran and oilcakes in solid state fermentation by *Mucor racemosus*. Bioresource Technology, 97, 506-511

Rosenblitt, A., Agosin, E., Delgado, J. and Correa, R.P. (2000) Solid substrate fermentation of *Monascus purpureus*: Growth, carbon balance, and consistency analysis. Biotechnology Progress, 16, 152-162

Sabater-Vilar, M., Maas, R.F.M. and Fink-Gremmels, J. (1999) Mutagenicity of commercial *Monascus* fermentation products and the role of citrinin contamination. Mutation Research-Genetic Toxicology and Environmental Mutagenesis, 444, 7-16

Sakurai, Y., Lee, T.H. and Shiota, H. (1977) On the convenient method for glucosamine estimation in koji. Agricultural and Biological Chemistry, 41, 619-624

Sangsurasak, P. and Mitchell, D.A. (1995) The investigation of transient multidimensional heat transfer in solid state fermentation. Chemical Engineering Journal and the Biochemical Engineering Journal, 60, 199-204

Santerre, A.L., Queinnec, I. and Blanc, P.J. (1995) A fedbatch strategy for optimal red pigment production by *Monascus ruber*. Bioprocess Engineering, 13, 245-250

Saucedo-Castaneda, G., Rojas, M.G., G. Bacquet, M.R. and Viniegra-Gonzalez, G. (1990) Heat transfer simulation in solid substrate fermentation. Biotechnology and Bioengineering, 35, 802-808

Scotti, C.T., Vergoignan, C., Feron, G. and Durand, A. (2001) Glucosamine measurement as indirect method for biomass estimation of *Cunninghamella elegans* grown in solid state cultivation conditions. Biochemical Engineering Journal, 7, 1-5

Sharma, P.D., Fisher, P.J. and Webster, J. (1977) Critique of the chitin essay technique for estimation of fungal biomass. Transactions of the British Mycological Society, 69, 479-483

Shepherd, D. (1977) The relationship between pigment production and sporulation on *Monascus*. In Biotechnology and Fungal Differentiation, FEMS Symposium No. 4, J. Meyrath and J.D. Bullock (eds), Academic Press, London. pp. 103-118

Shih, C.N. and Marth, E.H. (1974) Aflatoxin formation, lipid synthesis, and glucose metabolism by *Aspergillus parasiticus* during incubation with and without agitation Biochimica et Biophysica Acta (BBA), 338, 286-296

Shojaosadati, S.A. and Babaeipour, V. (2002) Citric acid production from apple pomace in multi-layer packed bed solid-state bioreactor. Process Biochemistry, 37, 909-914

Shuler, M.L. and Kargi, F. (2002) Bioprocess Engineering Basics Concepts, Prentice Hall, USA

Sinegani, A.A.S. and Emtiazi, G. (2006) The relative effects of some elements on the DNS method in cellulase assay. Journal of Applied Sciences and Environmental Management, 10, 93-96

Silveira, S.T., Daroita, D.J. and Brandelli, A. (2008) Pigment production by *Monascus purpureus* in grape waste using factorial design. Food Science and Technology, 41, 170-174

Singhania, R.R., Patel, A.K., Soccol, C.R. and Pandey, A. (2009) Recent advances in solid-state fermentation. Biochemical Engineering Journal, 44, 13-18

Soccol, C.R. and Vandenberghe, L.P.S. (2003) Overview of applied solid-state fermentation in Brazil. Biochemical Engineering Journal, 13, 205-218

Stanbury, P.F. and Whitaker, A. (1984) Principles of fermentation technology, Pergamon Press, London

Stuart, D.M., Mitchell, D.A., Johns, M.R. and Litster, J.D. (1999) Solid-state fermentation in rotating drum bioreactors: Operating variables affect performance through their effects on transport phenomena. Biotechnology and Bioengineering, 63, 383-391

Stuart, D.M. and Mitchell, D.A. (2003) Mathematical model of heat transfer during solid-state fermentation in well-mixed rotating drum bioreactors. Journal of Chemical Technology and Biotechnology, 78, 1180-1192

Su, Y.C. and Huang, J.H. (1980) Fermentation production of anka pigment. Proceedings National Science Council, R. China, 4, 201-215

Sweeny, J.G., Estrada-Valdes, M.C., Lacobucci, G.A., Sato, H. and Sakamura, S. (1981) Photoprotection of the red pigments of *Monascus anka* in aqueous media by 1,4,6-tryhydroxynaphthalene. Journal of Agricultural and Food Chemistry, 29, 1189-1193

Swift, M.J. (1973) The estimation of mycelial biomass by determination of the hexosamine content of wood tissue decayed by fungi. Soil Biology Biochemestry, 55, 321-332

Teng, S.S. and Feldheim, W. (1998) Analysis of anka pigments by liquid chromatography with diode array detection and tandem mass spectrometry. Chromatographia, 47, 529-536

Teng, S.S. and Feldheim, W. (2000) The fermentation of rice for anka pigment production. Journal of Industrial Microbiology and Biotechnology, 25, 141-146

Teng, S.S. and Feldheim, W. (2001) Anka and anka pigment production. Journal of Industrial Microbiology and Biotechnology, 26, 280-282

Terebiznik, M.R. and Pilosof, A.M.R. (1999) Biomass estimation in solid state fermentation by modeling dry matter weight loss. Biotechnology Techniques, 13, 215-219

Tezuka, T. and Kashino, M. (1979) Heat-stable food-coloring agent. Japan Patent Kokai 79086669

Tseng, Y.Y., Chen, M.T. and Lin, C.F. (2000) Growth, pigment production and protease activity of *Monascus purpureus* as affected by salt, sodium nitrite, polyphosphate and various sugars. Journal of Applied Microbiology, 88, 31-37

Tsukahara, M., Shinzato, N., Tamaki, Y., Namihira, T. and Matsui, T. (2009) Red yeast rice fermentation by selected *Monascus* sp with deep-red color, lovastatin production but no citrinin, and effect of temperature-shift cultivation on lovastatin production. Applied Biochemistry and Biotechnology, 158, 476-482

Turner, W.B. (1971) Fungal metabolites, Academic Press, London

Vidyalakshmi, R., Paranthaman, R., Murugesh, S. and Singaravadivel, K. (2009) Stimulation of *Monascus* pigments by intervention of different nitrogen sources. Global Journal of Biotechnology and Biochemistry, 4, 25-28

Viniegra-Gonzalez, G. (1996) Solid state fermentation: Definition, characteristics, limitations and monitoring. In Advances in solid state fermentaion, S. Roussos, B.K. Lonsane, M. Raimbault and G. Viniegraz Gonzalez (eds), Kluwer Academic Publishers, Dordrecht, pp. 5-22

Weber, F.J., Oostra, J., Tramper, J. and Rinzema, A. (2002) Validation of a model for process development and scale-up of packed-bed solid-state Bioreactors. Biotechnology and Bioengineering, 77, 381-393

Weinberg, E.D. (1989) Roles of micronutrients in secondary metabolism in actinomycetes. In Regulation of secondary metabolism in actinomycetes, S. Shapiro (ed), CRC Press, Boca Raton, pp. 239-261

Wissgott, U. and Bortlik, K. (1996) Prospects for new natural food colorants. Trends in Food Science and Technology, 7, 298-302

Wong, H.C. and Bau, Y.S. (1977) Pigmentation and antibacterial activity of fast neutron- and xray-induced strains of *Monascus purpureus* Went. Plant Physiology, 60, 578-581

Wong, H.C., Lin, Y.C. and Koehler, P.E. (1981) Regulation of growth and pigmentation of *Monascus purpureus* by carbon and nitrogen concentrations. Mycologia, 73, 649-654

Wong, H.C. (1982) Antibiotic and pigment production by *Monascus purpureus*. Ph.D. Thesis, University of Georgia, G.A., USA

Wong, H.C. and Koehler, P.E. (1983) Production of red water-soluble *Monascus* pigments. Journal of Food Science, 48, 1200-1203

Wongwicharn, A., Phoolphundh, S., Suksud, K. and Nimsiri, A. (2006) *Monascus* pigment formation in cassava liquid waste under various agitation speeds. KMITL Science Journal, 6, 692-698

Wu, W.T., Wang, P.M., Chang, Y.Y., Huang, T.K. and Chien, Y.H. (2000) Suspended rice particles for cultivation of *Monascus purpureus* in a tower-type bioreactor. Applied Microbiology and Biotechnology, 53, 542-544

Xu, B.J., Wang, Q.J., Jia, X.Q. and Sung, C.K. (2005) Enhanced lovastatin production by solid-state fermentation of *Monascus ruber*. Biotechnology and Bioprocess Engineering, 10, 78-84

Yang, S., Zhang, H., Li, Y., Qian, J. and Wang, W. (2005) The ultrasonic effect on biological characteristics of *Monascus* sp. Enzyme and Microbial Technology, 37, 139-144

Yongsmith, B., Tabloka, W., Yongmanitchai, W. and Bavavoda, R. (1993) Culture conditions for yellow pigment formation by *Monascus* sp. KB 10 grown on cassava medium. World Journal of Microbiology and Biotechnology, 9, 85-90

Yongsmith, B., Krairak, S. and Bavavoda, R. (1994) Production of yellow pigments in submerged culture of a mutant of *Monascus* sp. Journal of Fermentation and Bioengineering, 78, 223-228

Yongsmith, B., Kitprechavanicha, V., Chitradona, L., Chaisrisooka, C. and Budda, N. (2000) Color mutants of *Monascus* sp. KB9 and their comparative glucoamylases on rice solid culture. Journal of Molecular Catalysis B: Enzymatic, 10, 263-272

Yoshimura, M., Yamanaka, S., Mitsugi, K. and Hirose, Y. (1975) Production of *Monascus* pigment in a submerged culture. Agricultural and Biological Chemistry, 39, 1789-1795

Young, M.M., Moreira, A.R. and Tengerdy, R.E. (1983) Principles of solid-substrate fermentation. In The Filamentous Fungi, J.E. Smith, D.R. Berry and B. Kristiansen (eds), Edward Arnold, London, pp. 117-144

Zadrazil, F. and Puniya, A.K. (1995) Studies on the effect of particle size on solid-state fermentation of sugarcane bagasse into animal feed using white-rot fungi. Bioresource Technology, 54, 85-87

Zheng, Z. and Shetty, K. (1998) Solid-state production of beneficial fungi on apple processing wastes using glucosamine as the indicator of growth. Journal of Agricultural Food Chemistry, 46, 783-787

Appendix I

Calibration curve of glucose by dinitrosalicylic acid (DNS) method.

Reagents:
A = The DNS reagent (g L^{-1}) : 10.0 dinitrosalicylic acid (DNS), 2.0 phenol, 0.5 sodium sulphite, and 10.0 sodium hydroxide.

B = Rochelle salt (40% (g/100 mL)) : potassium sodium tartrate in deionized water

C = 1 mg/mL of standard aqueous glucose solution (0.1 g of glucose in deionized water in 100 mL volumetric flask).

Procedure:
Part A:
Measurement of the standard glucose calibration curve

1. (0, 0.4, 0.6, 0.8, 1.0, and 1.2 mL) of 1 mg/mL of standard aqueous glucose solution was added to a clean test tube for each volume. Deionized water (3.0, 2.6, 2.4, 2.2, 2, and 1.8) was added to each test tube, respectively and mixed well.
2. 3.0 ml of reagent A was added and mixed well.
3. The tubes were allowed to heat in a boiling water bath for 15 min.
4. Then 1 mL of reagent B was added to each of the test tubes. The test tubes were allowed to cool to room temperature.
5. Absorbance at 575 nm was measured. The blank was prepared exactly as above, but using deionized water in place of the glucose solution.

Results:

Standard glucose solution, 1mg/mL (mL)	Deonizied water (mL)	Reagent DNS (mL)	Rochelle salt (mL)	Standard glucose concentration (μg /mL)	A_{575nm}			
					I	II	Average	sd
0.0	3.0	3.0	1.0	0.000	0.000	0.000	0.000	0.000
0.4	2.6	3.0	1.0	57.143	0.230	0.246	0.238	0.011
0.6	2.4	3.0	1.0	85.714	0.371	0.390	0.381	0.013
0.8	2.2	3.0	1.0	114.286	0.526	0.528	0.527	0.001
1.0	2.0	3.0	1.0	142.857	0.712	0.723	0.718	0.008
1.2	1.8	3.0	1.0	171.429	0.891	0.909	0.900	0.013

Standard glucose concentration in each tube is:

$$\text{Glucose concentration } (\mu g/mL) = \frac{\text{volume of glucose solution } (mL) \times \text{C}}{\text{Total volume in tube } (mL)} \times 1000 \mu g/mg$$

$$= \frac{0.4mL \times 1mg/mL}{7mL} \times 1000 \mu g/mg$$

$$= 57.14 \mu g/mL$$

where, C is a reagent “C”

Linear regression on absorbance at 575 nm (A_{575nm}):

$A_{575} = 0.0049 * x$ ($\mu g/mL$); $R^2 = 0.9846$

Where x is the glucose concentration

Part B

Measurement of the glucose concentration of the sample:

1. 3.0 mL of filtrate sample was added to a clean test tube.
2. 3.0 mL of reagent A was added and mixed well.
3. The tube was allowed to heat in a boiling water bath for 15 min.
4. Then 1 mL of reagent B was added to the test tube and was allowed to cool to room temperature.
5. Absorbance at 575 nm was read. The blank was prepared exactly as above, but using deionized water in place of the sample solution.

The glucose content of the samples was calculated as follows:

$$\text{Glucose content } (g\ L^{-1})$$

$$= \frac{Abs_{575}}{0.0049(mL/\mu g)} \times \frac{\text{total volume of mixture } (mL)}{\text{sample volume } (mL)} \times df \times 10^{3} mL/L \times \frac{1}{10^{6}} g/\mu g$$

$$= \frac{Abs_{575}}{0.0049} \times \frac{\text{total volume of mixture } (mL)}{\text{sample volume } (mL)} \times df \times 10^{-3} g/L$$

$$= \frac{Abs_{575}}{0.0049} \times \frac{7\ (mL)}{3\ (mL)} \times df \times 10^{-3} g/L$$

Appendix II

Determination of *N*-acetyl-D-glucosamine for determination of conversion factor (*cf*) to biomass in solid-state culture sample.

Data on calibration curve of *N*-acetyl-D-glucosamine content by UV visible spectrophotometer method.

Reagents:

A = 60% (vol/vol) sulfuric acid

B = 5N NaOH

C = acetyl acetone reagent : (2% (vol/vol) of acetyl acetone in 1N Na_2CO_3

D = 95% ethanol

E = Ehrlich reagent : (2.67% (w/v) of p-dimethylaminobenzaldehyde in 1:1 mixture of ethanol and concentrated HCl

F = 1 mg/mL of standard aqueous *N*-acetyl-D-glucosamine solution (0.1 g of *N*-acetyl-D-glucosamine in deionized water in 100 mL volumetric flask).

Procedure:

Part A: Measurement of the standard *N*-acetyl-D-glucosamine calibration curve

1. Add (0, 20, 40, 60, 80, and 100 μL) of 1 mg/mL of standard *N*-acetyl-D-glucosamine solution to a clean stopper test tube.
2. Add deionized water (980, 960, 940, 920, and 900 μL) to each test tube, respectively, mix well.
3. Add 1.0 mL of regent C and properly stopper the test tubes.
4. Heat in a boiling water bath for 20 min.
5. Leave to cool and add 6.0 mL of reagent D, followed by 1 mL of reagent E. Mix.
6. Heat at 65^{o}C for 10 min.
7. Allow test tubes to cool to room temperature and develop colour for 45 min to 1 h.
8. Read absorbance at 530 nm. The blank was prepared exactly as above, but using deionized water in place of the standard *N*-acetyl-D-glucosamine solution.

Results:

Standard N-acetyl-D-glucosamine solution, 1mg/mL (mL)	Deonizied water (mL)	Reagent acetyl acetone (mL)	95% ethanol (mL)	Ehrlich reagent (mL)	Standard N-acetyl-D-glucosamine concentration (μg /mL)	A_{530nm}			
						I	II	Average	sd
0	1.00	1.00	6.00	1.00	0.000	0.000	0.000	0.000	0.000
0.02	0.98	1.00	6.00	1.00	2.222	0.132	0.129	0.131	0.002
0.04	0.96	1.00	6.00	1.00	4.444	0.314	0.320	0.317	0.004
0.06	0.94	1.00	6.00	1.00	6.667	0.456	0.454	0.455	0.001
0.08	0.92	1.00	6.00	1.00	8.889	0.596	0.610	0.603	0.010
0.1	0.90	1.00	6.00	1.00	11.111	0.733	0.726	0.730	0.005

To calculate standard *N*-acetyl-D-glucosamine concentration in each tube:

$$\text{N-acetyl-D-glucosamine concentration } (\mu g / mL)$$

$$= \frac{\text{volume N-acetyl-D-glucosamine solution } (mL) \times \text{F}}{\text{Total volume in tube } (mL)} \times 1000 \mu g / mg$$

$$= \frac{0.02 mL \times 1 mg / mL}{9 mL} \times 1000 \mu g / mg$$

$$= 2.22 \mu g / mL$$

Where, F is a reagent “F”

Linear regression on absorbance at 530 nm (A_{530nm}):

$A_{575} = 0.067\ x\ (\mu g / mL)$; $R^2 = 0.9973$

Where, *x* is the concentration of the *N*-acetyl-D-glucosamine

Part B

Measurement of *N*-acetyl-D-glucosamine concentration of the sample

1. Add 2 mL of reagent A to 0.5 g freeze-dried fermented substrate in 100 mL Erlenmeyer flask and incubate at 25^{o}C for 24 h.
2. Dilute the mixture of no. 1 (as above) with deionized water to make a concentration of 1 N sulphuric acid. Autoclave at 121^{o}C for 1 h.
3. Allow the autoclaved mixture to cool to room temperature and neutralize with 5N NaOH to pH 7.
4. Make the final volume of the mixture to 60 mL with deionized water.
5. Filter the mixture, add 1 mL of the filtrate to a clean stopper test tube.
6. Add 1.0 mL of reagent C and properly apply the stopper to the test tube.
7. Heat in a boiling water bath for 20 min.
8. Leave to cool and add 6.0 mL of reagent D, followed by 1 mL of reagent E. Gently mix.
9. Heat at 65^{o}C for 10 min.
10. Let test tubes cool to room temperature and develop colour for 45 min to 1 h.
11. Read absorbance at 530 against blank. The blank was prepared exactly as above, but using unfermented substrate in place of the fermented substrate.

The *N*-acetyl-D-glucosamine content of the samples was calculated as follows:

Glucosamine content per g of dry matter fermented substrate ($mg\ g^{-1}$)

$$= \frac{Abs_{530}}{0.067(mL/\mu g)} \times \frac{\text{total volume of mixture } (mL)}{\text{sample volume } (mL)} \times \frac{\text{total volume in Erlenmeyer flask } (mL)}{\text{fermented substrate } (g)} df \times \frac{1}{10^3} mg/\mu g$$

$$= \frac{Abs_{530}}{0.067(mL/\mu g)} \times \frac{9mL}{1mL} \times \frac{60mL}{0.5g} df \times \frac{1}{10^3} mg/\mu g$$

Part C

Glucosamine content of the fermented substrate was corrected to a biomass concentration using a conversion factor (*cf*). The relevant conversion factor had been measured in a submerged fermentation that used only dissolved substrate. The condition of submerged culture used was comparable to the medium in solid-state culture especially in terms of the mass ratio of carbon to nitrogen (C : N, 30 : 1) and the trace elements added.

Medium:

A = Medium for biomass production in submerged culture: glucose 10g/L, NH_4NO_3 0.379 g/L (C : N ratio of 30 : 1), $ZnSO_47H_2O$ 0.038 g/L added to the liquid medium at the same ratio of $ZnSO_47H_2O$ to carbon (as in solid-state culture).

B = Medium for inoculumn contained (g L^{-1}): yeast extract (3.0); malt extract (3.0); peptone from soymeal (5.0); and glucose (20.0) . The medium was autoclaved at 121^oC for 15 min.

Results of mycelial cell dry weight and glucosamine content of submerged culture

Time (h)	Mycelial cell dry weight (mg/mL)	Glucosamine content (mg/mL)
0	0.770 ± 0.071	0.039 ± 0.026
24	0.793 ± 0.053	0.043 ± 0.012
48	1.090 ± 0.120	0.065 ± 0.000
72	1.333 ± 0.124	0.074 ± 0.004
88	1.523 ± 0.166	0.085 ± 0.023
96	1.788 ± 0.270	0.092 ± 0.018
112	1.678 ± 0.293	0.098 ± 0.023
120	1.833 ± 0.202	0.108 ± 0.020
135	2.188 ± 0.315	0.134 ± 0.016
144	2.425 ± 0.337	0.149 ± 0.028
167	2.628 ± 0.341	0.164 ± 0.023

The mycelium was analyzed and the glucosamine content was expressed in mg per g dry mycelial weight (Section 4.3.3).

Part D

Determination of mycelial weight in solid-state fermentation.

The mycelial weight in solid-state fermentation medium was calculated by dividing the measurement of glucosamine content (mg/g) of the fermented dry solids by the factor (*cf* = 59.1 mg glucosamine/g cell dry weight) found in submerged culture:

$$X = \frac{P}{cf}$$

Where, X = g biomass per g dry matter, P = mg glucosamine per g dry matter, cf = mg glucosamine/g biomass cell dry weight

Appendix III

Data for figures

For Figures 4.1 and 4.2: Growth profiles of *M. ruber* ICMP 15220 and colony radius on different media.

Variables	Diameter (mm)					
Day/ Formulations	Day 2	Day 3	Day 4	Day 5	Day 6	Day 7
A	14.50± 0.71	21.50± 0.71	27.50± 0.71	32.50± 0.71	38.00± 1.41	42.50± 0.71
B	11.50± 2.12	17.00± 1.41	21.50± 2.12	26.00± 1.41	31.50± 2.12	38.00± 1.41
C	12.50± 0.71	20.00± 1.41	25.00± 1.41	29.50± 2.12	34.50± 2.12	39.00± 1.41
D	8.50± 0.71	15.00± 0.00	20.50± 0.71	26.50± 0.71	31.50± 0.71	37.00± 0.00
E	10.50± 2.12	19.00± 1.41	24.50± 2.12	31.50± 2.12	38.00± 1.41	43.50± 2.12
F	3.00± 0.00	7.00± 1.41	14.50± 2.12	20.50± 0.71	26.00± 0.00	30.00± 0.00
G	8.00± 0.00	22.00± 0.00	31.50± 0.71	40.00± 1.41	48.00± 0.00	55.00± 0.00
H	5.50± 0.71	11.00± 0.00	16.00± 0.00	21.50± 0.71	25.00± 1.41	28.50± 0.71
I	9.50± 0.71	20.00± 0.00	26.50± 0.71	33.00± 1.41	39.00± 0.00	46.50± 2.12
J	7.00± 0.00	13.00± 0.00	19.00± 0.00	24.50± 2.12	30.00± 2.83	34.00± 1.41

To calculate colony radius;

$$\text{Colony radius } (mm) = \frac{\text{Diameter of the colony } (mm)}{2}$$

For Figures 4.5 to 4.8: L*, a*, b*, h^o, and C* colour values of fungal colony on different media compositions

	Day 2			Day 3			Day 4			Day 5			Day 6			Day 7		
Formulations	L*	a*	b*	L*	a*	b*	L*	a*	b*	L*	a*	b*	L*	a*	b*	L*	a*	b*
A	51.29	6.17	20.68	43.39	17.73	19.72	39.47	18.54	14.86	34.04	19.17	8.22	32.73	19.26	6.85	32.72	19.13	6.38
standard deviation	0.69	0.16	0.31	0.36	0.64	0.40	0.06	0.61	0.33	0.16	0.20	0.09	0.16	0.01	0.24	0.13	0.04	0.28
B	43.99	6.78	8.62	35.51	18.47	7.81	34.64	18.77	6.63	33.22	16.98	5.01	30.61	11.03	2.03	30.29	9.27	1.35
standard deviation	0.42	1.06	0.44	0.59	0.69	1.29	0.01	0.93	0.37	0.18	1.45	0.50	0.05	1.46	0.35	0.11	0.77	0.17
C	47.25	5.52	7.80	43.95	18.78	12.43	41.56	22.50	11.52	39.24	23.57	10.93	38.55	23.56	10.90	38.44	23.43	10.59
standard deviation	0.72	0.66	1.01	0.89	0.14	0.88	2.20	0.79	0.14	3.17	1.03	1.39	2.88	0.45	1.78	2.66	0.52	1.87
D	39.60	0.17	-0.33	38.74	5.62	3.96	43.13	12.88	11.14	42.68	24.36	17.59	38.10	26.45	13.39	37.81	25.41	11.83
standard deviation	0.21	0.37	0.38	0.42	2.40	2.46	0.37	4.21	3.04	0.89	0.65	1.08	0.47	0.81	0.76	0.79	0.68	0.37
E	45.59	5.63	10.97	39.38	19.45	13.81	31.66	16.84	4.73	30.46	13.67	2.93	30.12	13.44	2.86	30.18	13.14	2.51
standard deviation	8.12	8.79	15.00	9.11	0.75	9.96	1.32	1.91	1.64	0.21	0.34	0.00	0.06	0.36	0.06	0.08	0.22	0.08
F	40.01	-0.26	-1.88	39.94	0.62	-1.20	37.49	6.65	3.39	35.27	19.49	8.29	33.01	21.44	6.49	31.05	16.08	3.62
standard deviation	1.05	0.00	0.64	0.44	0.59	0.66	0.97	1.45	0.82	0.15	2.57	0.57	0.89	1.32	1.29	0.91	3.88	1.32
G	48.79	2.47	8.73	34.03	17.23	6.35	31.90	13.62	3.80	30.49	10.49	2.68	29.94	8.76	2.35	30.05	8.52	1.80
standard deviation	0.27	0.57	0.78	0.59	0.76	0.50	1.21	0.45	0.70	1.16	0.23	0.11	0.79	0.23	0.09	0.60	0.32	0.33
H	39.21	-0.03	-1.29	38.29	1.19	0.42	38.60	2.92	2.96	40.62	10.64	10.94	38.14	18.26	13.22	36.63	17.28	10.48
standard deviation	0.35	0.01	0.13	1.32	0.16	0.16	0.68	0.40	0.68	0.22	0.64	1.05	0.23	0.64	1.14	0.18	0.51	0.78
I	53.22	8.27	15.87	36.84	20.04	10.31	34.35	12.22	3.78	35.27	6.54	1.67	35.84	5.66	1.64	42.16	13.26	6.87
standard deviation	0.55	0.97	0.40	1.68	0.30	1.77	3.23	4.00	1.25	1.29	0.36	0.65	0.92	0.83	0.38	0.52	0.11	0.45
J	40.19	0.54	-0.78	36.97	14.36	9.33	36.10	25.51	11.88	34.63	26.27	9.71	35.46	26.62	10.67	36.96	26.31	11.74
standard deviation	0.63	0.28	0.05	0.60	0.37	0.62	0.74	0.23	1.33	0.23	0.98	0.68	0.40	0.93	1.02	1.07	1.15	1.97

To calculate hue angle, h^o and chroma, C*:

$$\text{Hue angle, } h^o = \left(\tan^{-1}\left(\frac{b^*}{a^*} \right) \right)$$

$$\text{Chroma, } C^* = \left(\sqrt{\left(a^*\right)^2 + \left(b^*\right)^2} \right)$$

For Figures 4.10 and 4.11: Fermentation time course for *Monascus ruber* growing on medium D

Time (h)/ Responses	Biomass (g/L)	pH	Glucose concentration (g/L)	Red pigment (A_{500nm})	Orange pigment (A_{470nm})	Yellow pigment (A_{400nm})
0	1.837± 0.024	6.39± 0.00	19.118± 1.096	0.689± 0.091	0.578± 0.083	1.931± 0.452
24	2.110± 0.354	6.42± 0.00	15.143± 0.600	1.074± 0.098	0.867± 0.098	3.013± 0.301
35.5	2.513± 0.396	6.56± 0.01	14.214± 0.400	1.229± 0.095	0.951± 0.093	2.347± 0.358
48	3.870± 0.382	6.63± 0.02	10.024± 0.200	1.328± 0.015	1.019± 0.011	2.565± 0.004
59.5	6.340± 1.117	6.76± 0.01	6.762± 0.404	1.347± 0.021	1.026± 0.021	2.298± 0.038
72	9.255± 0.502	6.85± 0.02	0.400± 0.162	1.416± 0.030	1.079± 0.023	2.271± 0.081
83.5	9.770± 0.170	6.96± 0.01	0.031± 0.014	1.520± 0.087	1.167± 0.085	2.374± 0.264
96	10.405± 0.766	6.96± 0.01	0.244± 0.016	1.457± 0.002	1.127± 0.006	2.285± 0.045
107.5	9.630± 0.240	7.09± 0.03	0.259± 0.005	1.434± 0.030	1.121± 0.032	2.241± 0.127
120	9.802± 0.309	7.04± 0.01	0.227± 0.015	1.428± 0.030	1.133± 0.023	2.486± 0.019
144	8.920± 0.207	7.04± 0.01	0.207± 0.025	1.407± 0.051	1.118± 0.053	2.277± 0.327

For Figures 4.12 and 4.13: Fermentation time course for *Monascus ruber* growing on medium J

Time (h)/ Responses	Biomass (g/L)	pH	Glucose concentration (g/L)	Red pigment (A_{500nm})	Orange pigment (A_{470nm})	Yellow pigment (A_{400nm})
0	1.155± 0.219	6.53± 0.00	4.491± 0.084	0.549± 0.034	0.447± 0.038	1.470± 0.284
24	2.288± 0.214	6.57± 0.00	0.958± 0.530	0.860± 0.002	0.645± 0.004	1.652± 0.049
35.5	3.877± 0.005	6.68± 0.00	0.036± 0.000	1.022± 0.006	0.764± 0.006	1.793± 0.049
48	3.852± 0.059	6.96± 0.00	0.012± 0.012	1.038± 0.030	0.770± 0.015	1.652± 0.062
59.5	4.313± 0.033	7.11± 0.00	0.027± 0.004	1.032± 0.064	0.773± 0.053	1.613± 0.070
72	3.930± 0.042	7.24± 0.00	0.035± 0.001	1.065± 0.030	0.816± 0.008	1.686± 0.051
83.5	3.825± 0.177	7.27± 0.00	0.066± 0.007	1.017± 0.017	0.777± 0.030	1.649± 0.030
96	3.597± 0.005	7.42± 0.00	0.095± 0.007	0.969± 0.055	0.737± 0.053	1.259± 0.015
107.5	3.340± 0.085	7.45± 0.02	0.088± 0.018	0.996± 0.068	0.768± 0.059	1.359± 0.072
120	3.598± 0.002	7.50± 0.00	0.100± 0.012	0.935± 0.049	0.708± 0.034	1.167± 0.098
144	3.322± 0.130	7.50± 0.01	0.185± 0.011	0.938± 0.057	0.734± 0.045	1.215± 0.025

For Figure 4.14: Absorption spectra of the extracellular pigment produced by *Monascus ruber* at different incubation temperatures

Temperature (^{o}C)	23-25^{o}C				30^{o}C			
Wavelength (nm)	I	II	average	std	I	II	average	std
700	-0.011	-0.015	-0.013	0.003	-0.007	-0.010	-0.009	0.002
690	-0.010	-0.014	-0.012	0.003	-0.008	-0.010	-0.009	0.001
680	-0.009	-0.013	-0.011	0.003	-0.008	-0.010	-0.009	0.001
670	-0.008	-0.012	-0.010	0.003	-0.008	-0.011	-0.010	0.002
660	-0.007	-0.011	-0.009	0.003	-0.008	-0.010	-0.009	0.001
650	-0.007	-0.010	-0.009	0.002	-0.008	-0.010	-0.009	0.001
640	-0.004	-0.009	-0.007	0.004	-0.006	-0.008	-0.007	0.001
630	-0.003	-0.007	-0.005	0.003	-0.004	-0.005	-0.005	0.001
620	-0.001	-0.004	-0.003	0.002	0.001	0.000	0.001	0.001
610	0.003	-0.002	0.001	0.004	0.009	0.008	0.009	0.001
600	0.009	0.006	0.008	0.002	0.025	0.025	0.025	0.000
590	0.015	0.012	0.014	0.002	0.046	0.046	0.046	0.000
580	0.023	0.020	0.022	0.002	0.076	0.076	0.076	0.000
570	0.035	0.032	0.034	0.002	0.118	0.119	0.119	0.001
560	0.050	0.046	0.048	0.003	0.170	0.170	0.170	0.000
550	0.066	0.062	0.064	0.003	0.229	0.229	0.229	0.000
540	0.084	0.080	0.082	0.003	0.289	0.290	0.290	0.001
530	0.099	0.095	0.097	0.003	0.343	0.343	0.343	0.000
520	0.112	0.108	0.110	0.003	0.385	0.385	0.385	0.000
510	0.124	0.120	0.122	0.003	0.416	0.416	0.416	0.000
500	0.136	0.132	0.134	0.003	0.438	0.439	0.439	0.001
490	0.149	0.144	0.147	0.004	0.445	0.445	0.445	0.000
480	0.155	0.150	0.153	0.004	0.419	0.419	0.419	0.000
470	0.148	0.143	0.146	0.004	0.360	0.360	0.360	0.000
460	0.133	0.129	0.131	0.003	0.294	0.294	0.294	0.000
450	0.122	0.118	0.120	0.003	0.249	0.249	0.249	0.000
440	0.119	0.114	0.117	0.004	0.239	0.238	0.239	0.001
430	0.119	0.115	0.117	0.003	0.253	0.251	0.252	0.001
420	0.124	0.119	0.122	0.004	0.274	0.272	0.273	0.001
410	0.129	0.124	0.127	0.004	0.286	0.284	0.285	0.001
400	0.126	0.122	0.124	0.003	0.267	0.266	0.267	0.001
390	0.128	0.124	0.126	0.003	0.219	0.217	0.218	0.001
380	0.118	0.113	0.116	0.004	0.151	0.149	0.150	0.001
370	0.122	0.116	0.119	0.004	0.103	0.102	0.103	0.001
360	0.107	0.101	0.104	0.004	0.048	0.046	0.047	0.001
350	0.112	0.106	0.109	0.004	0.029	0.028	0.028	0.001

For Figures 4.15 to 4.18: Effect of initial glucose concentration on the *Monascus ruber*

a) Initial glucose of 0.5%

Time (h)/ Responses	Biomass (g/L)	pH	Glucose concentration (g/L)	Red pigment (A_{500nm})	Orange pigment (A_{470nm})	Yellow pigment (A_{400nm})
0	1.155 ± 0.219	6.53 ± 0.00	4.491 ± 0.084	0.549 ± 0.034	0.447 ± 0.038	1.470 ± 0.284
24	2.288 ± 0.214	6.57 ± 0.00	0.958 ± 0.530	0.860 ± 0.002	0.645 ± 0.004	1.652 ± 0.049
35.5	3.877 ± 0.005	6.68 ± 0.00	0.036 ± 0.000	1.022 ± 0.006	0.764 ± 0.006	1.793 ± 0.049
48	3.852 ± 0.059	6.96 ± 0.00	0.012 ± 0.012	1.038 ± 0.030	0.770 ± 0.015	1.652 ± 0.062
59.5	4.313 ± 0.033	7.11 ± 0.00	0.027 ± 0.004	1.032 ± 0.064	0.773 ± 0.053	1.613 ± 0.070
72	3.930 ± 0.042	7.24 ± 0.00	0.035 ± 0.001	1.065 ± 0.030	0.816 ± 0.008	1.686 ± 0.051
83.5	3.825 ± 0.177	7.27 ± 0.00	0.066 ± 0.007	1.017 ± 0.017	0.777 ± 0.030	1.649 ± 0.030
96	3.597 ± 0.005	7.42 ± 0.00	0.095 ± 0.007	0.969 ± 0.055	0.737 ± 0.053	1.259 ± 0.015
107.5	3.340 ± 0.085	7.45 ± 0.02	0.088 ± 0.018	0.996 ± 0.068	0.768 ± 0.059	1.359 ± 0.072
120	3.598 ± 0.002	7.50 ± 0.00	0.100 ± 0.012	0.935 ± 0.049	0.708 ± 0.034	1.167 ± 0.098
144	3.322 ± 0.130	7.50 ± 0.01	0.185 ± 0.011	0.938 ± 0.057	0.734 ± 0.045	1.215 ± 0.025

b) Initial glucose of 1.0%

Time (h)/ Responses	Biomass (g/L)	pH	Glucose concentration (g/L)	Red pigment (A_{500nm})	Orange pigment (A_{470nm})	Yellow pigment (A_{400nm})
0	1.127 ± 0.009	6.64 ± 0.01	8.980 ± 0.572	0.575 ± 0.002	0.483 ± 0.000	1.485 ± 0.004
24	3.037 ± 0.066	6.72 ± 0.04	2.238 ± 0.337	1.419 ± 0.021	1.035 ± 0.017	2.085 ± 0.119
35.5	5.268 ± 0.097	6.83 ± 0.01	1.220 ± 0.261	1.731 ± 0.030	1.245 ± 0.021	2.223 ± 0.115
48	6.307 ± 0.066	7.15 ± 0.05	0.079 ± 0.051	1.899 ± 0.030	1.373 ± 0.053	2.336 ± 0.316
59.5	6.658 ± 0.082	7.49 ± 0.04	0.250 ± 0.008	1.938 ± 0.115	1.413 ± 0.093	2.201 ± 0.189
72	6.402 ± 0.073	7.79 ± 0.05	0.246 ± 0.006	1.812 ± 0.098	1.313 ± 0.078	1.748 ± 0.142
83.5	6.003 ± 0.146	7.83 ± 0.06	0.339 ± 0.012	1.761 ± 0.115	1.293 ± 0.098	1.727 ± 0.176
96	5.808 ± 0.073	8.07 ± 0.05	0.360 ± 0.000	1.695 ± 0.004	1.266 ± 0.021	1.803 ± 0.238
107.5	5.683 ± 0.118	8.10 ± 0.01	0.365 ± 0.006	1.635 ± 0.047	1.238 ± 0.028	1.635 ± 0.034
120	5.225 ± 0.064	8.24 ± 0.01	0.434 ± 0.094	1.575 ± 0.047	1.215 ± 0.030	1.653 ± 0.081
144	5.038 ± 0.054	8.28 ± 0.00	0.482 ± 0.020	1.380 ± 0.025	1.083 ± 0.013	1.458 ± 0.042

c) Initial glucose of 1.5%

Time (h)/ Responses	Biomass (g/L)	pH	Glucose concentration (g/L)	Red pigment (A_{500nm})	Orange pigment (A_{470nm})	Yellow pigment (A_{400nm})
0	1.305 ± 0.186	6.27 ± 0.00	13.291 ± 0.707	0.861 ± 0.000	0.890 ± 0.002	2.589 ± 0.081
24	3.195 ± 0.285	6.43 ± 0.01	4.548 ± 0.101	1.272 ± 0.144	1.181 ± 0.125	3.020 ± 0.503
35.5	4.290 ± 0.269	6.59 ± 0.01	2.232 ± 1.288	1.476 ± 0.055	1.311 ± 0.042	3.086 ± 0.015
48	6.958 ± 0.224	6.70 ± 0.04	0.143 ± 0.040	1.641 ± 0.106	1.412 ± 0.074	2.874 ± 0.025
59.5	8.345 ± 0.295	6.85 ± 0.15	0.122 ± 0.000	1.794 ± 0.013	1.524 ± 0.000	2.954 ± 0.231
72	8.973 ± 0.104	7.43 ± 0.13	0.114 ± 0.054	1.886 ± 0.019	1.616 ± 0.045	3.230 ± 0.452
83.5	7.907 ± 0.283	7.76 ± 0.06	0.211 ± 0.076	1.781 ± 0.019	1.530 ± 0.017	2.678 ± 0.057
96	8.210 ± 0.198	7.86 ± 0.11	0.571 ± 0.256	1.794 ± 0.017	1.569 ± 0.017	2.901 ± 0.004
107.5	8.343 ± 0.217	8.14 ± 0.06	0.448 ± 0.088	1.755 ± 0.025	1.560 ± 0.021	2.834 ± 0.104
120	7.768 ± 0.139	8.25 ± 0.01	0.668 ± 0.051	1.652 ± 0.040	1.491 ± 0.030	2.691 ± 0.144
144	6.567 ± 0.217	8.36 ± 0.24	0.507 ± 0.000	1.550 ± 0.023	1.448 ± 0.049	2.637 ± 0.076

d) Initial glucose of 2.0%

Time (h)/ Responses	Biomass (g/L)	pH	Glucose concentration (g/L)	Red pigment (A_{500nm})	Orange pigment (A_{470nm})	Yellow pigment (A_{400nm})
0	1.062 ± 0.040	6.31 ± 0.01	18.863 ± 0.798	0.682 ± 0.015	0.408 ± 0.072	0.509 ± 0.078
24	2.523 ± 0.061	6.48 ± 0.04	12.975 ± 0.955	0.952 ± 0.093	0.557 ± 0.134	0.564 ± 0.352
35.5	4.975 ± 0.186	6.58 ± 0.04	6.946 ± 0.447	1.088 ± 0.136	0.675 ± 0.165	0.684 ± 0.373
48	7.592 ± 0.554	6.77 ± 0.04	1.755 ± 0.644	1.144 ± 0.098	0.692 ± 0.138	0.624 ± 0.403
59.5	10.070 ± 0.240	6.95 ± 0.01	0.221 ± 0.072	1.192 ± 0.138	0.723 ± 0.178	0.624 ± 0.484
72	11.057 ± 0.080	7.57 ± 0.06	0.167 ± 0.067	1.080 ± 0.113	0.566 ± 0.303	0.539 ± 0.541
83.5	10.088 ± 0.266	7.90 ± 0.00	0.667 ± 0.393	1.055 ± 0.093	0.699 ± 0.136	0.630 ± 0.378
96	9.790 ± 0.410	8.06 ± 0.04	1.753 ± 0.438	1.066 ± 0.134	0.737 ± 0.180	0.749 ± 0.460
107.5	9.677 ± 0.391	8.14 ± 0.14	1.649 ± 0.319	0.959 ± 0.119	0.731 ± 0.172	0.764 ± 0.452
120	9.212 ± 0.299	8.22 ± 0.01	1.555 ± 0.279	0.986 ± 0.098	0.704 ± 0.159	0.761 ± 0.439
144	7.333 ± 0.825	8.40 ± 0.02	1.488 ± 0.354	0.839 ± 0.161	0.605 ± 0.193	0.657 ± 0.484

e) Initial glucose of 2.5%

Time (h)/ Responses	Biomass (g/L)	pH	Glucose concentration (g/L)	Red pigment (A_{500nm})	Orange pigment (A_{470nm})	Yellow pigment (A_{400nm})
0	1.353 ± 0.047	6.27 ± 0.03	22.905 ± 1.414	0.686 ± 0.011	0.474 ± 0.004	0.606 ± 0.034
24	2.690 ± 0.090	6.46 ± 0.00	19.024 ± 0.909	0.879 ± 0.038	0.590 ± 0.045	0.689 ± 0.112
35.5	5.305 ± 0.210	6.58 ± 0.01	11.143 ± 0.269	1.029 ± 0.008	0.708 ± 0.017	0.818 ± 0.032
48	7.472 ± 0.243	6.71 ± 0.02	7.460 ± 0.617	1.088 ± 0.015	0.767 ± 0.019	0.836 ± 0.019
59.5	10.263 ± 0.141	6.80 ± 0.01	1.448 ± 0.365	1.178 ± 0.040	0.840 ± 0.064	0.981 ± 0.182
72	11.783 ± 0.349	7.20 ± 0.01	0.556 ± 0.045	1.047 ± 0.030	0.777 ± 0.030	0.863 ± 0.015
83.5	12.168 ± 0.144	7.75 ± 0.01	0.958 ± 0.025	1.056 ± 0.008	0.798 ± 0.017	0.960 ± 0.000
96	10.988 ± 0.695	7.98 ± 0.01	2.670 ± 0.023	1.011 ± 0.047	0.783 ± 0.034	0.990 ± 0.110
107.5	11.260 ± 0.170	8.08 ± 0.03	2.550 ± 0.237	1.034 ± 0.049	0.821 ± 0.032	1.088 ± 0.078
120	10.653 ± 0.471	8.13 ± 0.03	2.477 ± 0.523	0.944 ± 0.002	0.755 ± 0.011	1.011 ± 0.013
144	10.003 ± 0.094	8.34 ± 0.01	1.870 ± 0.301	0.849 ± 0.008	0.699 ± 0.034	0.986 ± 0.023

For figures 4.19 to 4.23: : Effect of carbon to nitrogen ratio on the *Monascus ruber*

a) Ratio 6:1

Time (h)/ Responses	Biomass (g/L)	pH	Red pigment (A_{500nm})
0	3.02 ± 1.0271	6.32 ± 0.0318	0.2915 ± 0.0775
24	3.135 ± 0	6.49 ± 0	0.368 ± 0
48	6.85 ± 0.9983	6.82 ± 0.1131	0.5455 ± 0.0257
72	7.36 ± 0.5056	7.33 ± 0.1909	0.7537 ± 0.0534
96	7.675 ± 0.1043	7.92 ± 0.2192	0.48819 ± 0.1231
120	7.43 ± 0.1556	8.29 ± 0.2386	0.4955 ± 0.0671

b) Ratio 9:1

Time (h)/ Responses	Biomass (g/L)	pH	Red pigment (A_{500nm})
0	2.85 ± 0.3986	6.47 ± 0.0212	0.313 ± 0.0718
24	3.145 ± 0	6.49 ± 0	0.5965 ± 0
48	6.055 ± 0.6877	6.53 ± 0.0141	1.15 ± 0.0555
72	7.24 ± 0.4322	6.83 ± 0.0018	1.2724 ± 0.1269
96	8 ± 0.1653	7.44 ± 0.0495	0.8832 ± 0.0013
120	7.555 ± 0.4667	8.01 ± 0.1467	0.7022 ± 0.0478

c) Ratio 14:1

Time (h)/ Responses	Biomass (g/L)	pH	Red pigment (A_{500nm})
0	2.86 ± 0.3465	6.49 ± 0.0053	0.3315 ± 0.0753
24	3.27 ± 0	6.49 ± 0	0.645 ± 0
48	4.415 ± 0.0619	6.63 ± 0.0398	1.1 ± 0.1098
72	7.14 ± 0.4419	6.66 ± 0.0778	1.2011 ± 0.1723
96	7.2 ± 0.122	7 ± 0.0672	0.7564 ± 0.0176
120	7 ± 0.2599	7.25 ± 0.0725	0.6401 ± 0.0292

d) Ratio 20:1

Time (h)/ Responses	Biomass (g/L)	pH	Red pigment (A_{500nm})
0	2.575 ± 0.4959	6.49 ± 0.0194	0.328 ± 0.0788
24	2.64 ± 0	6.48 ± 0	0.5675 ± 0
48	4.315 ± 0.6479	6.64 ± 0.0398	0.9 ± 0.0468
72	6.36 ± 0.9608	6.8 ± 0.0672	0.9236 ± 0.0611
96	6.525 ± 0.0256	7 ± 0.0442	0.8069 ± 0.0308
120	6.28 ± 0.0027	7.01 ± 0.0106	0.7018 ± 0.0486

For Figures 4.24 to 4.28: Effect of nitrogen sources on *Monascus ruber* fermentation

a) $NaNO_3$

Time (h)/ Responses	Biomass (g/L)	pH	Glucose concentration (g/L)	Red pigment (A_{500nm})	Orange pigment (A_{470nm})	Yellow pigment (A_{400nm})
0	1.32 ± 0.0141	6.44 ± 0	9.4048 ± 0.40406	0.271 ± 0.0057	0.2175 ± 0.0049	0.20925 ± 0.0039
24	1.94 ± 0.1202	6.395 ± 0.02	6.5 ± 0.60609	0.326 ± 0.024	0.262 ± 0.0191	0.275 ± 0.0396
48	3.36 ± 0.0071	6.415 ± 0.01	4.3857 ± 0.70711	0.4148 ± 0.0074	0.3418 ± 0.0039	0.44725 ± 0.0216
59.5	4.0025 ± 0.0389	6.455 ± 0.02	1.5786 ± 1.02025	0.4615 ± 0.0049	0.3845 ± 0.0064	0.503 ± 0.024
72	4.93 ± 0.3536	6.54 ± 0.03	0.0107 ± 0.08586	0.6238 ± 0.1609	0.436 ± 0.0106	0.689 ± 0.0955
83.5	5.1125 ± 0.0672	6.505 ± 0.02	-0.0429 ± 0.00673	0.812 ± 0.0665	0.4863 ± 0.0449	0.72975 ± 0.187
96	4.7175 ± 0.0601	6.735 ± 0.01	0.0173 ± 0.00589	0.8393 ± 0.0555	0.5055 ± 0.0403	0.7505 ± 0.1824
120	4.635 ± 0.0212	6.8 ± 0.01	0.0854 ± 0.00354	0.805 ± 0.0615	0.4908 ± 0.0407	0.68525 ± 0.1397

b) NH_4NO_3

Time (h)/ Responses	Biomass (g/L)	pH	Glucose concentration (g/L)	Red pigment (A_{500nm})	Orange pigment (A_{470nm})	Yellow pigment (A_{400nm})
0	1.43 ± 0.0212	6.495 ± 0.01	10.155 ± 0.35355	0.2758 ± 0.0166	0.2203 ± 0.0145	0.21 ± 0.0134
24	1.425 ± 0.7354	6.365 ± 0.04	8.0595 ± 0.11785	0.2863 ± 0.0265	0.235 ± 0.0212	0.23375 ± 0.0237
48	3.31 ± 0.1556	6.18 ± 0.07	4.3714 ± 0.26264	0.3365 ± 0.0212	0.2858 ± 0.0166	0.41425 ± 0.0173
59.5	4.45 ± 0.0707	6.085 ± 0.06	2.5357 ± 0.34345	0.3355 ± 0.0134	0.2895 ± 0.0078	0.45875 ± 0.0711
72	5.5525 ± 0.2934	5.93 ± 0.01	-0.0095 ± 0.02694	0.3448 ± 0.0322	0.3028 ± 0.0279	0.60075 ± 0.0654
83.5	5.41 ± 0.1131	5.88 ± 0.01	-0.0429 ± 0.00673	0.3273 ± 0.0152	0.291 ± 0.0134	0.57325 ± 0.0124
96	5.2025 ± 0.1308	6.125 ± 0.02	0.0143 ± 0.00505	0.3298 ± 0.0421	0.2965 ± 0.0354	0.62125 ± 0.088
120	5.165 ± 0	6.16 ± 0.03	0.0629 ± 0.01919	0.3578 ± 0.0979	0.3218 ± 0.0817	0.6535 ± 0.1676

c) NH_4Cl

Time (h)/ Responses	Biomass (g/L)	pH	Glucose concentration (g/L)	Red pigment (A_{500nm})	Orange pigment (A_{470nm})	Yellow pigment (A_{400nm})
0	1.435 ± 0.099	6.395 ± 0.01	10.702 ± 0.48824	0.2708 ± 0.0092	0.2659 ± 0.0083	0.4245 ± 0.0573
48	4.985 ± 0.2616	5.66 ± 0.08	0.4345 ± 0.58757	0.34 ± 0.0127	0.3348 ± 0.0138	0.5855 ± 0.0357
59.5	5.4975 ± 0.0601	5.71 ± 0.01	0.0224 ± 0.01549	0.3225 ± 0.0141	0.3195 ± 0.0148	0.5245 ± 0.0873
72	5.5875 ± 0.6753	5.84 ± 0.03	0.0161 ± 0.00253	0.322 ± 0.0113	0.3203 ± 0.0124	0.52975 ± 0.0573
83.5	4.59875 ± 0.076	5.88 ± 0	0.0161 ± 0.00859	0.323 ± 0.012	0.323 ± 0.012	0.5765 ± 0.0477
96	4.865 ± 0.0707	5.92 ± 0	0.0205 ± 0.01894	0.3275 ± 0.0014	0.328 ± 0.0021	0.605 ± 0.0025
120	4.9825 ± 0.6258	5.97 ± 0	0.0149 ± 0.00926	0.32 ± 0.0212	0.322 ± 0.0219	0.56513 ± 0.113

d) $(NH_4)_2SO_4$

Time (h)/ Responses	Biomass (g/L)	pH	Glucose concentration (g/L)	Red pigment (A_{500nm})	Orange pigment (A_{470nm})	Yellow pigment (A_{400nm})
0	0.81 ± 0.0801	6.52 ± 0.01	7.3571 ± 0.26937	0.3438 ± 0.006	0.282 ± 0.0057	0.3135 ± 0.0071
24	1.535 ± 0.3559	6.455 ± 0.04	5.8452 ± 0.21887	0.3175 ± 0.0049	0.2615 ± 0.0148	0.294 ± 0.0396
48	2.815 ± 0.3088	6.27 ± 0.08	4.65 ± 0.83843	0.3168 ± 0.0088	0.2695 ± 0.0035	0.35675 ± 0.0187
59.5	4.105 ± 1.1196	6.06 ± 0.13	2.9393 ± 0.06566	0.3105 ± 0.0028	0.261 ± 0.0035	0.34575 ± 0.006
72	5.11167 ± 0.1155	5.95 ± 0.03	0.1745 ± 0.22223	0.3044 ± 0.0044	0.2601 ± 0.0058	0.32338 ± 0.0405
83.5	5.28167 ± 0.3229	5.925 ± 0.04	0.0143 ± 0	0.2868 ± 0.0071	0.2443 ± 0.0053	0.32025 ± 0.0028
96	4.91333 ± 0.264	6.075 ± 0.01	0.0127 ± 0	0.299 ± 0.0021	0.2553 ± 0.0011	0.32675 ± 0.0004
120	4.99167 ± 0.3041	6.07 ± 0.03	0.0222 ± 0	0.3165 ± 0.0057	0.273 ± 0.0049	0.342 ± 0.0035

For Figures 4.36 to 4.40: Fermentation time profile of *Monascus ruber* in Erlenmeyer flasks

Time (day)	Moisture content (%)	pH	Biomass (mg cdw/gids)	Red pigment (A_{500nm})	Orange pigment (A_{470nm})	Yellow pigment (A_{400nm})
0	50.256 ± 0.651	5.10 ±	0.000 ± 0.000	0.000 ±	0.000 ±	0.000 ±
2	52.700 ± 0.778	5.05 ± 0.01	2.189 ± 0.200	0.283 ± 0.000	0.247 ± 0.070	0.500 ± 0.100
4	53.500 ± 0.212	4.70 ± 0.20	8.091 ± 0.400	2.963 ± 0.100	4.911 ± 0.300	3.921 ± 0.500
6	55.000 ± 0.658	4.55 ± 0.21	17.633 ± 7.955	10.631 ± 0.214	11.711 ± 3.524	16.051 ± 3.844
7	56.213 ± 0.165	4.18 ± 0.03	43.068 ± 5.539	58.379 ± 3.310	73.479 ± 2.029	82.996 ± 7.581
8	56.000 ± 0.636	3.84 ± 0.03	58.958 ± 3.000	94.345 ± 4.000	105.632 ± 2.000	132.712 ± 4.000
10	55.700 ± 1.556	3.53 ± 0.37	92.612 ± 5.329	142.809 ± 8.206	195.855 ± 13.261	248.168 ± 11.748
12	55.000 ± 0.849	3.27 ± 0.06	119.811 ± 2.512	258.127 ± 10.000	346.084 ± 5.000	400.714 ± 2.000
14	56.770 ± 2.308	3.14 ± 0.03	125.849 ± 10.410	328.140 ± 5.339	440.031 ± 3.630	453.172 ± 1.922
15	53.435 ± 0.658	3.35 ± 0.03	126.577 ± 5.056	326.529 ± 15.498	438.279 ± 26.553	451.882 ± 21.001
17	52.988 ± 1.414	3.40 ± 0.00	120.041 ± 5.000	300.298 ± 10.000	402.000 ± 3.000	400.140 ± 3.000

For Figures 4.51 to 4.56: Fermentation time course of *Monascus ruber* in packed-bed bioreactor

Time (day)	Moisture content (%)	pH	Biomass (mg cdw/gids)	Red pigment (A_{500nm})	Orange pigment (A_{470nm})	Yellow pigment (A_{400nm})
0	55.036 ± 4.370	5.28 ± 0.01	0.000 ± 0.000	0.393 ± 0.000	0.393 ± 0.000	0.524 ± 0.020
2	55.600 ± 0.600	5.00 ± 0.20	5.066 ± 0.300	1.964 ± 0.300	4.800 ± 0.340	2.836 ± 0.000
4	56.800 ± 0.700	4.80 ± 0.05	12.955 ± 0.800	20.291 ± 1.200	25.200 ± 1.400	24.982 ± 1.200
6	57.964 ± 1.394	3.89 ± 0.03	23.403 ± 1.932	59.658 ± 3.338	76.138 ± 2.400	104.844 ± 3.400
8	60.000 ± 0.300	3.70 ± 0.40	50.822 ± 4.000	164.291 ± 4.700	241.636 ± 3.600	299.673 ± 4.530
10	62.587 ± 1.842	3.47 ± 0.14	91.575 ± 3.865	495.499 ± 1.768	713.639 ± 10.013	722.091 ± 3.338
12	62.000 ± 0.600	3.50 ± 0.10	102.947 ± 2.000	662.727 ± 5.700	958.473 ± 12.650	902.400 ± 12.760
14	58.443 ± 2.941	3.65 ± 0.07	108.817 ± 3.865	800.806 ± 17.678	1165.207 ± 24.200	1086.713 ± 22.540
16	58.500 ± 0.500	3.50 ± 0.20	116.155 ± 4.000	816.327 ± 23.600	1235.891 ± 3.320	1144.691 ± 21.300
18	59.013 ± 0.855	3.45 ± 0.02	122.183 ± 7.730	890.050 ± 28.284	1285.458 ± 25.284	1208.036 ± 30.284

For Figures 4.42 and 4.43: Effect of initial moisture content on pigments and biomass production at day 14

Initial Moisture Content (%)	Biomass (mg cdw/g dry matter)	pH	Final moisture (%)	Aw	Red pigment (A_{500nm})	Orange pigment (A_{470nm})	Yellow pigment (A_{400nm})
35.0	5.036 ± 0.183	5.75 ± 0.02	32.091 ± 0.205	0.974 ± 0.003	3.240 ± 0.000	3.940 ± 0.028	6.160 ± 0.000
45.0	30.475 ± 0.000	3.86 ± 0.13	42.750 ± 0.081	0.992 ± 0.001	37.720 ± 0.000	50.840 ± 0.000	60.680 ± 2.319
55.0	117.252 ± 0.000	3.31 ± 0.03	69.916 ± 4.348	0.998 ± 0.001	328.000 ± 0.000	492.000 ± 0.000	444.850 ± 2.899
70.0	36.415 ± 0.365	3.78 ± 0.19	72.114 ± 1.977	0.996 ± 0.001	111.520 ± 0.000	168.100 ± 1.160	137.760 ± 2.319
75.0	1.291 ± 0.000	4.39 ± 0.06	75.058 ± 0.213	0.999 ± 0.000	30.340 ± 1.160	43.460 ± 1.160	45.920 ± 0.000

For Figures 4.44 and 4.45: Effect of initial moisture content on pigments and biomass production at day 18

Initial Moisture Content (%)	Biomass (mg cdw/g dry matter)	pH	Final moisture (%)	Aw	Red pigment (A_{500nm})	Orange pigment (A_{470nm})	Yellow pigment (A_{400nm})
35.0	0.258264 ± 0	4.885 ± 0.262	31.946 ± 0.688	0.979 ± 0.006	6.78 ± 0.085	7.2 ± 0	12.68 ± 0.0566
45.0	46.61674 ± 0.183	2.78 ± 0.014	46.956 ± 0.298	0.9955 ± 0.002	79.54 ± 1.16	59.04 ± 0	201.72 ± 0
55.0	124.0961 ± 0.183	2.575 ± 0.021	61.751 ± 0.704	0.997 ± 0.001	399.75 ± 2.899	348.5 ± 5.798	969.65 ± 2.8991
70.0	83.29029 ± 0.183	2.57 ± 0.071	76.512 ± 2.272	0.9995 ± 7E-04	358.75 ± 20.29	284.95 ± 8.697	692.9 ± 0
75.0	10.07231 ± 0	3.93 ± 0.014	75.005 ± 0.701	1 ± 7E-04	27.88 ± 4.639	13.94 ± 1.16	57.4 ± 0

For Figures 4.47 to 4.49: Effect of aeration rate on pigments production in packed-bed bioreactor on day 6

Aeration rate (L/min)	Biomass (mg cdw/g dry matter)	Final temperature (^{o}C)	Final moisture (%)	Red pigment (A_{500nm})	Orange pigment (A_{470nm})	Yellow pigment (A_{400nm})
0.05	60.142 ± 4.900	34.20 ± 0.35	69.644 ± 1.353	101.122 ± 2.849	140.732 ± 13.387	211.954 ± 9.301
0.2	50.217 ± 4.800	33.80 ± 0.78	65.105 ± 2.120	104.601 ± 4.419	139.323 ± 11.825	218.849 ± 19.692
0.5	29.877 ± 2.500	32.60 ± 0.48	56.563 ± 4.892	88.289 ± 7.685	111.733 ± 8.226	141.700 ± 27.361
1	22.785 ± 2.120	32.10 ± 0.48	30.769 ± 2.978	33.867 ± 7.800	39.833 ± 9.240	53.333 ± 13.895
2	18.442 ± 0.890	31.90 ± 0.56	18.783 ± 0.690	18.433 ± 0.257	23.600 ± 4.266	26.933 ± 4.659

For Figures 4.58, 4.63, and 4.64: Profiles of red pigment production (AU/g dry matter) of packed-bed bioreactor

Aeration (mL/min)		50					125					200				
(day)/Initial moisture conter		0	144	240	336	432	0	144	240	336	432	0	144	240	336	432
	level 1	0.0	0.8	2.9	17.4	34.1	0.24	2	3.92	20.4	17.7	0.0	0.2	1.8	0.6	0.2
	level 2	0.0	2.5	49.2	114.8	123.0	0.24	3.7	60.1	106.7	94.2	0.0	0.3	11.5	47.6	4.8
	level 3	0.0	6.6	64.0	136.1	173.8	0.24	7.5	74.9	150.6	161.9	0.0	2.9	67.2	152.5	72.2
	level 4	0.0	9.7	159.9	352.6	323.9	0.24	8.5	190.3	372.6	367	0.0	6.8	180.4	225.5	143.5
	level 5	0.0	6.2	164.0	307.5	315.7	0.24	9.7	209.6	340.8	327.2	0.0	13.5	209.1	287.0	377.2
45%	level 6	0.0	7.6	118.9	315.7	319.8	0.24	12.5	163.1	314.2	350.7	0.0	13.1	176.3	250.1	426.4
	level 1	0.2	3.8	87.7	357.0	346.8	0.3	11.0	95.8	144.1	111.9	0.4	24.4	72.5	47.9	33.3
	level 2	0.2	7.6	178.5	708.9	892.5	0.3	18.4	336.2	574.7	659.5	0.4	53.8	102.4	494.0	447.5
	level 3	0.2	7.9	265.2	861.9	1244.4	0.3	24.5	405.2	949.8	1097.5	0.4	74.0	440.0	792.5	1075.0
	level 4	0.2	14.0	336.6	887.4	1213.8	0.3	29.0	489.6	1034.7	1269.6	0.4	66.0	447.4	977.5	1224.0
	level 5	0.2	19.1	295.8	1065.9	1326.0	0.3	30.4	504.6	1041.8	1199.0	0.4	60.0	975.0	1010.5	1098.0
57.50%	level 6	0.2	24.5	285.6	943.5	1356.6	0.3	33.2	511.4	1188.2	1312.0	0.4	50.0	688.0	1082.0	1017.5
	level 1	0.8	81.5	819.0	1713.6	2085.9	0.24	32.8	745.9	1426.9	1407.6	0.8	68.3	445.9	711.7	844.8
	level 2	0.8	46.9	831.3	1509.6	1739.1	0.24	51.2	946.1	1713.8	1672.1	0.8	63.2	734.4	1683.0	1708.5
	level 3	0.8	42.8	841.5	1550.4	1479.0	0.24	40.5	953.8	1675.3	1654.9	0.8	55.1	846.6	1708.5	1652.4
	level 4	0.8	32.6	994.5	1688.1	1433.1	0.24	42.1	1104	1704.2	1673.9	0.8	42.8	969.0	1428.0	1560.6
	level 5	0.8	40.8	1025.1	1229.1	1071.0	0.24	58.3	1045.6	1728.6	1734.2	0.8	83.6	928.2	1448.4	1555.5
70%	level 6	0.8	49.9	918.0	1055.7	1198.5	0.24	64.3	1068.8	1698.4	1677	0.8	55.1	1157.7	1514.7	1463.7

A		125				
		0	144	240	336	432
	level 1	0.2	1.8	30.6	32.6	36.7
	level 2	0.2	3.2	219.3	275.4	459.0
	level 3	0.2	5.1	326.4	943.5	1071.0
	level 4	0.2	9.9	413.1	1137.3	1489.2
	level 5	0.2	18.7	413.1	1147.5	1326.0
57.50%	level 6	0.2	24.5	392.7	1244.4	1269.9

B		125				
		0	6	10	14	18
	level 1	0.36	20.32	160.952	255.588	187
	level 2	0.36	33.63	453.12	874	860
	level 3	0.36	44	484	956	1124
	level 4	0.36	48	566	932	1050
	level 5	0.36	42	596	936	1072
57.50%	level 6	0.36	42	630	1132	1354

To calculate the overall pigment production on the packed-bed, following equation was used:

$$\left(AU\ g^{-1}\right) = \frac{\left(AU\ g^{-1}\right)_{level1} + \left(AU\ g^{-1}\right)_{level2} + \ldots\ldots\ldots + \left(AU\ g^{-1}\right)_{level6}}{6}$$

Where, pigment for each level was added and the sum was devided into total level in the bed (which was 6 levels).

For Figure 4.59: Profiles of biomass production (g cdw/g dry matter) of packed-bed bioreactor

Aeration (mLPM)		50					125					200				
(day)/Initial moisture conter		0	144	240	336	432	0	144	240	336	432	0	144	240	336	432
	level 1	0	0.002059	0.007925	0.009018	0.010111	0	0.001366	0.009547	0.010111	0.009601	0	0.006832	0.002186	0.008199	0.000273
	level 2	0	0.006286	0.030334	0.065861	0.072693	0	0.008836	0.024322	0.056023	0.053311	0	0.012024	0.026509	0.027328	0.009018
	level 3	0	0.012298	0.044819	0.078159	0.12899	0	0.011259	0.051997	0.083734	0.094957	0	0.013391	0.037986	0.047551	0.026235
	level 4	0	0.011881	0.046458	0.087178	0.153585	0	0.014101	0.046258	0.088817	0.116729	0	0.02077	0.058209	0.069141	0.057936
	level 5	0	0.012844	0.047825	0.099475	0.144544	0	0.012863	0.05544	0.104303	0.112702	0	0.020496	0.066135	0.103028	0.123524
45%	level 6	0	0.010111	0.033341	0.100295	0.110953	0	0.010476	0.049118	0.104303	0.130028	0	0.013118	0.067228	0.091823	0.11232
	level 1	0	0.001975	0.029597	0.038424	0.06623	0	0.010558	0.016488	0.05025	0.023911	0	0.007379	0.012024	0.007105	0.000273
	level 2	0	0.006583	0.055604	0.123962	0.140031	0	0.01729	0.067592	0.09257	0.095167	0	0.019403	0.041539	0.068048	0.046458
	level 3	0	0.015188	0.077285	0.149281	0.192319	0	0.017531	0.088972	0.146495	0.167093	0	0.025415	0.079526	0.103848	0.12735
	level 4	0	0.00567	0.095989	0.172934	0.218591	0	0.023985	0.102117	0.167906	0.208534	0	0.027055	0.103301	0.094829	0.12981
	level 5	0	0.006118	0.129186	0.196901	0.19538	0	0.022391	0.129409	0.190837	0.189904	0	0.028422	0.129263	0.148393	0.163697
57.50%	level 6	0	0.02117	0.118906	0.189263	0.243188	0	0.029253	0.127118	0.175931	0.211494	0	0.021043	0.138008	0.176268	0.204416
	level 1	0	0.032065	0.115235	0.14229	0.168844	0	0.030579	0.106566	0.113278	0.109673	0	0.027556	0.055613	0.060163	0.055363
	level 2	0	0.03261	0.140536	0.171643	0.200966	0	0.032599	0.138217	0.175069	0.16793	0	0.028822	0.120179	0.173412	0.164585
	level 3	0	0.037827	0.164335	0.17727	0.173665	0	0.031407	0.158238	0.183557	0.1756	0	0.031118	0.142319	0.175435	0.177612
	level 4	0	0.021043	0.183524	0.200736	0.173102	0	0.029681	0.159897	0.200626	0.193691	0	0.025279	0.152784	0.162795	0.162331
	level 5	0	0.031564	0.175858	0.184157	0.177457	0	0.033475	0.159013	0.190156	0.186377	0	0.031933	0.167578	0.16229	0.192893
70%	level 6	0	0.017695	0.172148	0.204	0.201246	0	0.032744	0.169239	0.214736	0.21313	0	0.031883	0.165027	0.207791	0.215122

A		125				
		0	144	240	336	432
	level 1	0	0.01811	0.020405	0.068253	0.026506
	level 2	0	0.017948	0.066317	0.070908	0.093864
	level 3	0	0.014019	0.098965	0.149516	0.17732
	level 4	0	0.024741	0.113504	0.203542	0.225222
	level 5	0	0.015814	0.122176	0.235468	0.230321
57.50%	level 6	0	0.029811	0.126612	0.212214	0.257105

B		125				
		0	6	10	14	18
	level 1	0	0.003006	0.012571	0.032247	0.021316
	level 2	0	0.016632	0.068868	0.114233	0.096469
	level 3	0	0.021043	0.078979	0.143474	0.156865
	level 4	0	0.023229	0.09073	0.132269	0.191845
	level 5	0	0.028968	0.136642	0.146207	0.149486
57.50%	level 6	0	0.028695	0.127624	0.139648	0.165883

For Figure 4.60: Profiles of moisture content (%) of packed-bed bioreactor

Aeration (mLPM)		50					125					200				
(day)/Initial moisture conter		0	6	10	14	18	0	6	10	14	18	0	6	10	14	18
	level 1	48.1115	33.45567	24.63426	29.02629	19.13585	48.1115	24.74154	31.03614	17.6605	15.12243	48.1115	15.78806	15.42497	14.58674	13.52277
	level 2	48.1115	47.51779	50.24232	53.31065	50.51654	48.1115	43.59194	47.61227	38.67179	23.02016	48.1115	27.09749	29.74496	18.88269	14.03522
	level 3	48.1115	51.74278	55.43144	59.70423	62.04453	48.1115	49.67142	49.4413	50.40607	46.07828	48.1115	47.81214	48.11816	36.51211	15.01253
	level 4	48.1115	55.81269	55.7718	61.08424	63.18139	48.1115	48.66646	48.02868	56.87157	53.8165	48.1115	54.90143	54.31812	44.33287	23.10343
	level 5	48.1115	56.00045	57.32756	61.26817	64.43002	48.1115	49.57262	48.91334	54.94432	57.80318	48.1115	55.70806	58.1601	52.61107	53.49157
45%	level 6	48.1115	51.84287	56.38939	64.62073	64.79172	48.1115	49.56741	49.74996	56.47227	57.89421	48.1115	57.77055	58.24272	55.59505	58.41621
	level 1	59.96798	48.82496	43.95988	48.90729	39.82586	59.96798	43.1088	30.19388	15.7815	16.49818	55.03562	24.32146	20.16461	16.90976	15.88656
	level 2	59.96798	59.33635	60.53948	72.03092	72.87619	59.96798	56.10642	59.14316	50.20832	53.80839	55.03562	59.82156	61.30951	36.9895	45.88749
	level 3	59.96798	59.56473	65.125	74.57381	76.6346	59.96798	59.38497	65.77539	70.51314	73.98171	55.03562	64.45127	68.29928	63.50385	67.00749
	level 4	59.96798	62.6257	70.06646	75.14587	78.32245	59.96798	62.96963	70.37554	76.27006	77.97085	55.03562	64.42637	74.1771	74.43655	73.05443
	level 5	59.96798	61.70606	74.51834	77.21215	78.35967	59.96798	63.90922	74.50959	79.27204	79.71356	55.03562	65.50232	74.78798	78.12707	74.6091
57.50%	level 6	59.96798	66.01777	74.8032	74.86961	78.9696	59.96798	67.24543	75.13757	80.03413	79.93316	55.03562	69.25993	76.78614	80.69368	77.63281
	level 1	67.69594	60.43806	74.24301	79.27162	79.88132	67.69594	53.5807	46.7167	43.46336	33.52876	67.69594	55.55735	38.45508	50.04397	47.40571
	level 2	67.69594	72.35522	79.4451	81.98868	82.78347	67.69594	68.0072	68.86474	71.01587	73.39562	67.69594	70.9851	75.49197	77.54706	79.09958
	level 3	67.69594	71.90451	80.20909	81.68554	82.86909	67.69594	68.3328	69.89262	71.55123	76.16219	67.69594	71.52312	77.91434	78.89374	79.83364
	level 4	67.69594	70.32068	80.75649	81.62554	82.21346	67.69594	68.37776	70.31309	73.46098	77.60575	67.69594	72.98256	79.15174	79.86757	79.70818
	level 5	67.69594	73.34267	81.22665	81.69503	82.0548	67.69594	68.67894	71.19076	75.79353	80.16109	67.69594	72.15564	80.68446	80.44304	80.6192
70%	level 6	67.69594	71.7526	82.66212	81.49801	81.32269	67.69594	68.56252	70.72832	84.49744	78.58903	67.69594	73.38713	81.96507	81.98549	80.47181

		125				
	A	0	6	10	14	18
	level 1	59.96798	43.1088	30.19388	15.7815	16.49818
	level 2	59.96798	56.10642	59.14316	50.20832	53.80839
	level 3	59.96798	59.38497	65.77539	70.51314	73.98171
	level 4	59.96798	62.96963	70.37554	76.27006	77.97085
	level 5	59.96798	63.90922	74.50959	79.27204	79.71356
57.50%	level 6	59.96798	67.24543	75.13757	80.03413	79.93316

		125				
	B	0	6	10	14	18
	level 1	55.03562	37.33787	21.91647	24.53678	18.23564
	level 2	55.03562	59.75414	63.00779	70.22245	66.83621
	level 3	55.03562	65.35241	69.08609	72.96404	74.9372
	level 4	55.03562	64.32245	72.98777	75.07128	76.06829
	level 5	55.03562	67.61844	75.73893	78.02804	76.71464
57.50%	level 6	55.03562	65.41469	76.9693	76.54547	79.06555

For Figure 4.61: Profiles of water activity (Aw) of packed-bed bioreactor

Aeration (mLPM)		50					125					200				
(day)/Initial moisture conter		0	144	240	336	432	0	144	240	336	432	0	144	240	336	432
	level 1	0.9915	0.987	0.947	0.95	0.906	0.9915	0.953	0.951	0.8365	0.673	0.9915	0.777	0.685	0.595	0.569
	level 2	0.9915	0.999	0.9915	0.997	0.9975	0.9915	0.993	0.997	0.9805	0.951	0.9915	0.9575	0.955	0.913	0.5835
	level 3	0.9915	0.9985	0.995	0.9975	0.9995	0.9915	1.0005	0.997	0.994	0.9885	0.9915	0.9925	0.9875	0.975	0.732
	level 4	0.9915	0.993	0.994	0.9985	0.998	0.9915	1.0005	0.997	0.997	0.9955	0.9915	0.9955	0.9945	0.985	0.953
	level 5	0.9915	0.994	0.9975	0.9985	0.999	0.9915	1.0015	0.998	0.9965	0.9965	0.9915	0.9935	0.997	0.997	0.995
45%	level 6	0.9915	0.994	0.997	1.0015	0.9995	0.9915	1.0005	1	1.001	0.9955	0.9915	0.992	0.9965	0.9975	0.995
	level 1	1.0005	0.992	0.986	0.991	0.992	0.997	0.98025	0.955	0.9155	0.827875	1.0005	0.9655	0.914	0.8425	0.6815
	level 2	1.0005	0.9925	0.99	0.994	1	0.997	0.99275	0.982	0.99	0.969625	1.0005	0.9845	0.9645	0.9805	0.9435
	level 3	1.0005	0.996	0.992	0.996	1.0005	0.997	0.98975	0.993375	0.99275	0.99225	1.0005	0.9795	0.985	0.9875	0.984
	level 4	1.0005	0.992	0.9885	0.997	0.997	0.997	0.990625	0.99425	0.99475	0.99325	1.0005	0.9785	0.9855	0.9905	0.988
	level 5	1.0005	0.9955	0.9905	0.997	0.997	0.997	0.991375	0.994	0.996625	0.9945	1.0005	0.9805	0.9845	0.993	0.989
57.50%	level 6	1.0005	0.9955	0.9935	0.996	1.001	0.997	0.991625	0.996	0.999125	0.997625	1.0005	0.9805	0.9905	0.9975	0.992
	level 1	0.9935	0.9835	0.987	0.9985	0.993	0.9935	0.995	0.996	0.9885	0.97425	0.9935	0.979	0.979	0.9865	0.9795
	level 2	0.9935	0.9885	0.9925	1	1.001	0.9935	1.001	0.9995	0.9995	0.99575	0.9935	0.9795	0.983	0.9955	0.997
	level 3	0.9935	0.9875	0.995	0.9995	1.0025	0.9935	1	1.00175	0.998	1.0005	0.9935	0.981	0.9925	0.997	0.9985
	level 4	0.9935	0.982	0.9955	0.998	1.0015	0.9935	1.00275	1.003	0.999	0.9985	0.9935	0.9805	0.9945	0.9955	0.996
	level 5	0.9935	0.982	0.994	1	0.999	0.9935	1.00225	1.0035	1.00025	1	0.9935	0.981	0.997	1	0.998
70%	level 6	0.9935	0.981	0.995	1.004	1.001	0.9935	1.00275	1.0015	1.00075	1.00325	0.9935	0.9825	0.9945	1.0005	1.001

		125				
	A	0	6	10	14	18
	level 1	0.9935	0.995	0.996	0.9885	0.97425
	level 2	0.9935	1.001	0.9995	0.9995	0.99575
	level 3	0.9935	1	1.00175	0.998	1.0005
	level 4	0.9935	1.00275	1.003	0.999	0.9985
	level 5	0.9935	1.00225	1.0035	1.00025	1
57.50%	level 6	0.9935	1.00275	1.0015	1.00075	1.00325

		125				
	B	0	6	10	14	18
	level 1	1.0005	0.971	0.931	0.9495	0.9465
	level 2	1.0005	0.983	0.984	0.987	0.9905
	level 3	1.0005	0.9825	0.9865	0.989	0.9915
	level 4	1.0005	0.9805	0.986	0.985	0.9905
	level 5	1.0005	0.9775	0.992	0.9915	0.991
57.50%	level 6	1.0005	0.9805	0.989	0.9935	0.998

For Figure 4.62: pH profiles of packed-bed bioreactor

Aeration (mLPM)		50					125					200				
(day)/Initial moisture conter		0	144	240	336	432	0	144	240	336	432	0	144	240	336	432
	level 1	5.83	5.405	5.65	4.855	5.13	5.83	5.805	4.305	5.705	5.425	5.83	5.64	5.545	5.505	5.62
	level 2	5.83	4.89	3.775	3.29	3.32	5.83	5.335	3.79	4.07	4.4	5.83	5.545	4.945	4.215	5.305
	level 3	5.83	4.51	3.525	3.215	3.29	5.83	5.255	3.65	3.6	3.36	5.83	4.805	3.795	3.965	4.555
	level 4	5.83	4.35	3.435	3.36	3.43	5.83	5.025	3.635	3.57	3.215	5.83	4.445	3.23	3.47	3.715
	level 5	5.83	4.545	3.515	3.38	3.45	5.83	5.005	3.55	3.36	3.095	5.83	4.335	3.11	3.245	3.345
45%	level 6	5.83	4.525	3.7	3.36	3.35	5.83	4.78	3.53	3.265	3.03	5.83	4.33	3.185	3.195	3.3
	level 1	5.31	5.17	4.325	3.28	3.265	5.31	4.9075	4.7125	4.8	4.415	5.275	4.53	4.68	5.35	5.14
	level 2	5.31	4.525	3.485	2.985	3.065	5.31	4.425	3.4	3.2575	3.18	5.275	3.825	3.615	3.57	3.205
	level 3	5.31	4.63	3.225	2.98	3.08	5.31	4.365	3.295	3.15	3.06	5.275	3.785	3.15	3.255	3.085
	level 4	5.31	4.26	3.25	2.975	3.13	5.31	4.1	3.23	3.105	3.035	5.275	3.73	3.12	3.265	3.06
	level 5	5.31	3.925	3.185	3	3.08	5.31	4.0675	3.2125	3.11	3.1425	5.275	3.77	3.115	3.205	3.07
57.50%	level 6	5.31	3.955	3.23	3.015	3.035	5.31	3.925	3.19	3.175	3.12	5.275	3.68	3.16	3.24	3.145
	level 1	5.18	3.71	3.04	3.315	3.4	5.18	4.9	3.425	3.375	3.375	5.18	3.475	3.13	3.035	3.215
	level 2	5.18	3.605	2.995	3.08	3.335	5.18	4.6	3.19	2.96	2.865	5.18	3.69	2.96	3	3.16
	level 3	5.18	3.74	3.03	3.095	3.39	5.18	4.74	3.21	3.275	2.855	5.18	3.715	3.005	3.075	3.22
	level 4	5.18	3.82	3.045	3.46	3.41	5.18	4.715	3.485	2.99	2.87	5.18	3.81	3.035	3.04	3.245
	level 5	5.18	3.745	3.125	3.505	3.455	5.18	4.88	2.965	2.92	2.83	5.18	3.775	3.1	3.14	3.415
70%	level 6	5.18	3.755	3.07	3.69	3.57	5.18	4.81	3.135	2.995	2.885	5.18	3.84	3.07	3.255	3.605

		125				
	A	0	144	240	336	432
	level 1	5.275	5.285	4.88	5.865	5.19
	level 2	5.275	4.965	3.55	3.28	3.275
	level 3	5.275	4.9	3.39	3.07	2.995
	level 4	5.275	4.395	3.275	2.995	2.975
	level 5	5.275	4.38	3.27	3.015	3.15
57.50%	level 6	5.275	4.065	3.19	3.125	3.07

		125			
	B	0	6	10	14
	level 1	6.06	4.53	4.545	3.735
	level 2	6.06	3.885	3.25	3.235
	level 3	6.06	3.83	3.2	3.23
	level 4	6.06	3.805	3.185	3.215
	level 5	6.06	3.755	3.155	3.205
57.50%	level 6	6.06	3.785	3.19	3.225

For Figures 4.65 to 4.71: Variables and responses of the central composite design at 336 h of the packed bed bioreactor

Standard order	Run order	Variables		Responses			
		Initial moisture content (x_1) (%)	Aeration rate (x_2) (L/min)	Total pigment (AU)	Pigment productivity (AU/L h)	Pigment yield (AU/g cdw)	Total biomass (g cell dry weight)
1	4	45	0.05	18616.2	144.9	2829.5	6.6
2	1	70	0.05	74173.1	577.5	8101.7	9.2
3	3	45	0.2	17071.3	132.9	2775.9	6.1
4	5	70	0.2	86238.9	671.4	9022.2	9.6
5	8	45	0.125	21364.1	166.3	2919.5	7.3
6	6	70	0.125	86822.6	676.0	8778.1	9.9
7	9	57.5	0.05	54992.6	428.1	5543.0	9.9
8	7	57.5	0.2	63099.0	491.3	7362.7	8.6
9	2	57.5	0.125	68679.7	534.7	5088.6	13.5
10	10	57.5	0.125	64952.9	505.7	7185.3	9.0

For Figures 4.74 to 4.77: Absorption UV-visible spectrum of the extracted and purified pigment from submerged culture (filtrate and mycelia)

Wavelength (nm)	Absorbance value			
	Extraction of filtrate sample	Purified red band of filtrate sample	Extraction of mycelia	Purified yellow band of mycelia
650	0.063 ± 0.018	0.008 ± 0.003	0.049 ± 0.006	0.419 ± 0.003
640	0.070 ± 0.018	0.011 ± 0.003	0.054 ± 0.006	0.428 ± 0.003
630	0.082 ± 0.016	0.018 ± 0.003	0.064 ± 0.006	0.440 ± 0.003
620	0.111 ± 0.015	0.029 ± 0.003	0.079 ± 0.006	0.453 ± 0.003
610	0.158 ± 0.016	0.050 ± 0.003	0.100 ± 0.007	0.473 ± 0.003
600	0.236 ± 0.017	0.085 ± 0.002	0.130 ± 0.007	0.497 ± 0.002
590	0.350 ± 0.017	0.140 ± 0.004	0.170 ± 0.007	0.532 ± 0.004
580	0.501 ± 0.018	0.221 ± 0.003	0.223 ± 0.007	0.570 ± 0.003
570	0.685 ± 0.017	0.332 ± 0.002	0.287 ± 0.007	0.613 ± 0.002
560	0.885 ± 0.016	0.467 ± 0.004	0.357 ± 0.006	0.659 ± 0.004
550	1.071 ± 0.016	0.605 ± 0.002	0.423 ± 0.006	0.700 ± 0.002
540	1.219 ± 0.016	0.723 ± 0.002	0.481 ± 0.006	0.735 ± 0.002
530	1.322 ± 0.018	0.808 ± 0.002	0.524 ± 0.006	0.766 ± 0.002
520	1.386 ± 0.018	0.868 ± 0.002	0.558 ± 0.006	0.793 ± 0.002
510	1.405 ± 0.018	0.906 ± 0.003	0.586 ± 0.006	0.821 ± 0.003
500	1.360 ± 0.018	0.907 ± 0.003	0.608 ± 0.005	0.874 ± 0.003
490	1.236 ± 0.017	0.843 ± 0.003	0.617 ± 0.005	0.959 ± 0.003
480	1.050 ± 0.018	0.715 ± 0.003	0.600 ± 0.005	1.041 ± 0.003
470	0.866 ± 0.017	0.574 ± 0.003	0.586 ± 0.004	1.132 ± 0.003
460	0.758 ± 0.017	0.477 ± 0.003	0.654 ± 0.004	1.345 ± 0.003
450	0.805 ± 0.016	0.474 ± 0.003	0.848 ± 0.004	1.646 ± 0.003
440	1.004 ± 0.015	0.569 ± 0.004	1.141 ± 0.004	1.821 ± 0.004
430	1.183 ± 0.012	0.661 ± 0.004	1.480 ± 0.004	1.805 ± 0.004
420	1.227 ± 0.011	0.664 ± 0.004	1.808 ± 0.004	1.735 ± 0.004
410	1.170 ± 0.009	0.607 ± 0.003	2.052 ± 0.005	1.619 ± 0.003
400	1.051 ± 0.008	0.515 ± 0.003	2.156 ± 0.005	1.490 ± 0.003
390	0.894 ± 0.006	0.406 ± 0.004	2.121 ± 0.003	1.355 ± 0.004
380	0.691 ± 0.005	0.287 ± 0.003	1.680 ± 0.004	0.963 ± 0.003
370	0.610 ± 0.008	0.232 ± 0.004	1.605 ± 0.004	0.963 ± 0.004
360	0.533 ± 0.005	0.192 ± 0.004	1.409 ± 0.006	0.895 ± 0.004
350	0.490 ± 0.006	0.176 ± 0.003	1.170 ± 0.001	0.800 ± 0.003

For Figures 4.78 and 4.79: Absorption UV-visible spectrum of the purified pigment from submerged culture (filtrate and mycelia) isolated from TLC plate

Wavelength (nm)	Absorbance value	
	Purified red spot of TLC from filtrate	Purified red spot of TLC from mycelia
650	0.002 ± 0.001	0.018 ± 0.001
640	0.009 ± 0.000	0.019 ± 0.001
630	0.021 ± 0.000	0.020 ± 0.001
620	0.042 ± 0.000	0.022 ± 0.000
610	0.079 ± 0.000	0.025 ± 0.000
600	0.131 ± 0.001	0.028 ± 0.001
590	0.213 ± 0.000	0.033 ± 0.001
580	0.323 ± 0.000	0.037 ± 0.001
570	0.451 ± 0.001	0.044 ± 0.000
560	0.581 ± 0.001	0.049 ± 0.000
550	0.692 ± 0.000	0.054 ± 0.000
540	0.774 ± 0.001	0.057 ± 0.001
530	0.831 ± 0.001	0.060 ± 0.001
520	0.864 ± 0.000	0.062 ± 0.000
510	0.866 ± 0.000	0.061 ± 0.000
500	0.819 ± 0.001	0.060 ± 0.000
490	0.712 ± 0.001	0.057 ± 0.000
480	0.578 ± 0.000	0.053 ± 0.000
470	0.460 ± 0.000	0.052 ± 0.001
460	0.399 ± 0.000	0.054 ± 0.000
450	0.448 ± 0.000	0.060 ± 0.001
440	0.584 ± 0.001	0.069 ± 0.000
430	0.678 ± 0.001	0.077 ± 0.000
420	0.672 ± 0.001	0.080 ± 0.001
410	0.608 ± 0.001	0.080 ± 0.001
400	0.507 ± 0.001	0.079 ± 0.000
390	0.390 ± 0.000	0.076 ± 0.001
380	0.308 ± 0.001	0.070 ± 0.001
370	0.244 ± 0.002	0.071 ± 0.000
360	0.207 ± 0.002	0.071 ± 0.001
350	0.203 ± 0.003	0.075 ± 0.000

For Figure 4.81: The stability of the crude red pigment under light and dark condition

Time (h)/ Condition	Treatment	
	Light	Dark
0.00	100.00 ± 0.00	100.00 ± 0.00
2.00	99.32 ± 2.00	100.41 ± 0.00
4.00	97.89 ± 0.07	99.73 ± 0.30
7.33	95.65 ± 0.00	98.85 ± 0.07
21.25	80.16 ± 1.00	89.59 ± 0.00
23.00	77.38 ± 0.07	88.92 ± 5.00
47.00	72.15 ± 0.00	85.61 ± 0.07
95.00	64.20 ± 0.07	76.89 ± 0.14
167.35	50.27 ± 1.00	67.70 ± 2.00

For Figures 4.82 and 4.83: The stability of the crude red pigment at different temperatures

a) Temperature of 70^{o}C

Time (h)	% A_{500} Remaining	
	Submerged culture	Solid-state culture
0	100.00 ± 0.99	100.00 ± 2.97
0.5	89.62 ± 1.00	91.05 ± 0.00
1.17	70.98 ± 0.57	98.61 ± 1.78
1.5	65.39 ± 0.42	97.02 ± 0.00
4	50.44 ± 0.07	98.00 ± 0.00
5	46.32 ± 2.00	99.00 ± 2.97
6	43.30 ± 0.00	93.84 ± 0.00
8	41.48 ± 0.07	89.26 ± 2.97

b) Temperature of 4^{o}C

Time (h)	% A_{500} Remaining	
	Submerged culture	Solid-state culture
0.0	100.00 ± 0.07	100.00 ± 0.00
2.0	99.71 ± 0.00	100.00 ± 1.30
6.8	99.59 ± 0.00	100.00 ± 0.50
8.0	99.00 ± 0.07	100.00 ± 0.20

c) Temperatures of 100°C and 121°C

Treatment	Before treatment	After treatment (submerged culture)	
		Submerged culture	Solid-state culture
Boiling	100	95.93 ± 2.62	95.15 ± 0.02
Autoclave	100	74.25 ± 1.41	77.78 ± 4.67

For Figure 4.84:

a) Under submerged culture

Time (h)	% A_{500} Remaining			
	pH 7.26 (without treatment)	pH 4	pH 7	pH 10
0	100.00 ± 0.00	100.00 ± 0.00	100.00 ± 0.00	100.00 ± 0.00
0.5	99.65 ± 0.07	86.97 ± 2.55	99.51 ± 0.99	88.60 ± 0.35
1	99.41 ± 0.00	86.77 ± 2.55	99.31 ± 1.13	89.44 ± 0.14
2	98.42 ± 0.42	85.59 ± 2.69	98.22 ± 0.85	87.76 ± 0.42
3	97.98 ± 0.78	84.80 ± 2.83	97.58 ± 0.92	88.55 ± 1.27
5	95.85 ± 0.85	82.68 ± 2.62	95.76 ± 0.85	87.12 ± 4.60
8	96.00 ± 0.64	82.68 ± 2.33	95.61 ± 0.78	85.24 ± 0.92

b) Under solid-state culture pH 7

Time (h)	% A_{500} Remaining
	pH 7
0	100 ± 0
0.166667	74.0741 ± 0.5
0.5	81.1861 ± 2.97
1	76.8758 ± 2.97
1.5	79.031 ± 2.97
2	77.5223 ± 0.9
4	79.2465 ± 1.3
6	77.5223 ± 0.7
8	79.2465 ± 5.94

c) Under solid-state culture pH 9.85 and without treatment

Time (h)	% A_{500} Remaining	
	pH 4.04 (without treatment)	pH 9.85
0	100.00 ± 0.03	100.00 ± 0.00
0.5	100.00 ± 0.03	55.62 ± 2.97
3.22	100.10 ± 0.01	54.51 ± 1.48
8	99.00 ± 0.00	52.00 ± 0.00